Effects Of Diet, Exercise And Anti-Obesity Treatment On Adult Neural Stem Cells And Neurogenesis

Sara Jörgensen

The dissertation is submitted to Cardiff University with the requirements for the degree of

Doctor of Philosophy

School of Biosciences

Cardiff University

September 2024

Acknowledgements

I would first like to express my gratitude to my supervisor, Dr. David Petrik, for all his support and invaluable advice throughout my doctoral studies. I have truly learned so much from you on this journey. I also wish to extend my thanks to Professor Yves-Alain Barde and my co-supervisor, Dr. Isabel Martinez Garay, for providing helpful suggestions during our numerous lab meetings. Additionally, I want to thank Professor Nick Allen and Dr. Kim Jones for kindly sharing their expertise on growing stem cells and for providing the hiPS cell lines. I am also thankful to my co-supervisor Professor Meng Li for generously sharing the i900 cell line. Furthermore, I want to thank the UK Academy of Medical Sciences for helping to support this PhD. I also want to express my gratitude to all the past and current members of our shared lab space. Thank you for your helpful advice, coffee breaks, all the laughter and encouragement - you have truly been the best colleagues throughout this journey. A special thanks also goes to Dr. Andrew Want for his constant kindness and willingness to offer advice with the running experiments, as well as for sharing his running cages.

I want to thank my parents, Lena and Michael for inspiring me to always strive to be the best I can be and for always letting me know how proud you are of me. Your love, and belief in me has made me the person I am today, and I truly owe you everything. I want to thank my grandma and grandpa, Ingrid and Bosse, for being my biggest supporters and always reminding me to enjoy the journey. Finally, I am deeply grateful to my partner Beth for being by my side throughout this journey, supporting me unconditionally through both the happy and the stressful times and for always reminding me of what truly matters. I feel incredibly fortunate to have all of you in my life, and I thank you for always being there for me.

Summary

Obesity is a growing global health issue characterised by poor diet and reduced physical activity. Hypothalamic adult neurogenesis plays a dual role in obesity and energy homeostasis, contributing to its development through appetite and metabolic dysregulation, yet also offering a compensatory mechanism in response to over-nutrition and metabolic dysfunction. To elucidate the role of hypothalamic neurogenesis in energy homeostasis, this work determined how obesity, voluntary exercise, and anti-obesity compounds affect neural stem cells and adult-generated neurons. We used diet-induced obesity, and exposure to running wheels or anti-obesity compounds, Lipidized Prolactin Releasing Peptide (LiPrRP) and Glucagon-like Peptide-1 (GLP-1) agonists, to elucidate how they influence stem cell renewal and proliferation and neuronal differentiation and maturation in the Medial Basal Hypothalamus (MBH). In addition, we utilized the human induced Pluripotent Stem Cell-derived hypothalamic neurons to model the effects of anti-obesity compounds on human hypothalamus. Our results suggest that high fat diet initially elicits a neurogenic response, but over time reduces the survival and generation of adult-born neurons. Treatment with LiPrRP was shown to act cell-intrinsically and directly on the cell populations in the hypothalamus, potentially having long-lasting effects by prolonging the ability of the stem cell population to respond to the high fat diet, and also improving the long-term survival of adult-generated neurons. Meanwhile, exercise exhibited beneficial effects by reversing the High Fat Diet (HFD)-induced neurogenesis and by promoting long term neurogenesis in the physiological conditions. Our results provide new insights into how hypothalamic adult neurogenesis responds to physiological and pharmacological interventions. This establishes a promising foundation for future research pursuing the development of novel treatments and improved lifestyle regimens for individuals living with obesity.

Abbreviations

°C	Degree Celsius
3V	Third Ventricle
AC3	Activated Caspase 3
AD	Alzheimer's Disease
AgRP	Agouti-Related Peptide
Akt	Protein Kinase B
aNSCs	Adult Neural Stem Cells
AraC	Cytosine Arabinoside
ArcN	Arcuate Nucleus
BBB	Blood Brain Barrier
BDNF	Brain-Derived Neurotrophic Factor
BLBP	Brain Lipid-Binding Protein
BMP	Bone Morphogenetic Protein
bp	Base Pairs
BrdU	Bromodeoxyuridine (5-bromo-2'-deoxyuridine)
BSA	Bovine Serum Albumin
CART	Cocaine- And Amphetamine-Regulated Transcript
cDNA	Complementary DNA
cm	Centimetres
CNS	Central Nervous System
CNTF	Ciliary Neurotrophic Factor
CNTF	Ciliary Neurotrophic Factor
Cre	Cyclic Recombinase

CRH	Corticotropin-Releasing Hormone
CTIP2	Chicken Ovalbumin Upstream Promotor Transcription Factor-Interacting Protein 2
CVO	Circumventricular Organs
DAPI	4’,6-Diamidino-2-Phenylindole
DCX	Doublecortin
DEPC	Dimethyl Pyrocarbonate
DG	Dentate Gyrus
DIO	Diet Induced Obesity
DMEM/F12	Dulbecco’s Modified Eagle Medium/Nutrient Mixture F12
DMN	Dorsomedial Nucleus
DPBS	Dulbecco's Phosphate-Buffered Saline
EGF	Epidermal Growth Factor
ES	Embryonic Stem Cells
EtBr	Ethidium Bromide
EtOH	Ethanol
FFA	Free Fatty Acid
FGF	Fibroblast Growth Factor
Foxg1	Forkhead box protein G1 (Mouse gene)
FOXG1	Forkhead box protein G1(Human gene)
Fwd	Forward
GABA	Gaba-Aminobutyric Acid
GFAP	Glial Fibrillary Acidic Protein
GLAST	The Glia High Affinity Glutamate Transporter
GLP-1	Glucagon-Like Peptide-1

GPR10	G-Protein-Coupled Receptor 10
GSK-3β	Glycogen Synthase Kinase 3β
hAN	Hypothalamic Adult Neurogenesis
HBSS	Hanks' Balanced Salt Solution
HCl	Hydrochloric Acid
HFD	High Fat Diet
hiCTNs	Cortical-Like Neurons
hiHTNs	Human Induced Pluripotent Stem Cell Derived Hypothalamic-Like Neurons
hiPSC	Human-Derived Induced Pluripotent Stem Cell
htNPCs	Hypothalamic Neural Progenitor Cells
htNSCs	Hypothalamic Neural Stem Cells
HuC/D	Human Neuronal Protein C And D
HVZ	Hypothalamic Ventricular Zone
i.c.v.	Intracerebroventricular
i.p.	Intraperitoneal
i.v.	Intravenous
ICC	Immunocytochemical Staining
IGF-1	Insulin-Like Growth Factor 1
IHC	Immunohistochemistry
IQR	Interquartile Range
IRS-1	Insulin Receptor Substrate-1
JNK	c-Jun N-terminal kinase
KSR	Knockout Serum Replacement
LepRs	Leptin Receptors

LH	Lateral Hypothalamus
LHA	Lateral Hypothalamic Area
LiPrRP	Lipidized Prolactin Releasing Peptide
LIRA	Liraglutide
Map2	Microtubule - Associated Protein 2
MBH	Medial Basal Hypothalamus
MC4R	Melanocortin-4 Receptors
MCH	Melanin-Concentrating Hormone
ME	Median Eminence
mg	Milligram (s)
mM	Millimolar
Msi1	Musashi-1
n.s.	Not Significant
NaCl	Sodium Chloride
NaN_3	Sodium Azide
NF-κB	Nuclear Factor-Kappa B
Nkx	Nk2 Homeobox 1 (Mouse Gene)
NKX2.1	NK2 homeobox 1 (Human gene)
NPCs	Neural Progenitor Cells
NPFFR2	Neuropeptide FF receptor 2
NPY	Neuropeptide Y
NTS	Nucleus Of The Solitary Tract
PACAP	Pituitary Adenylate Cyclase-Activating Peptide
PBS	Phosphate-Buffered Saline
PCR	Polymerase Chain Reaction

PDK1	3-Phosphoinositide-Dependent Kinase 1
PFA	Paraformaldehyde
pH	Potential of Hydrogen
PI3K	Phosphatidylinositol-4,5-Bisphosphate 3-Kinase
PMD	Postmortem Delay
POA	Preoptic Area
POMC	Pro-Opiomelanocortin
PrRP	Prolactin-Releasing Peptide
pSTAT3	Signal Transducer And Activator Of Transcription 3 Phosphorylation
PVN	Paraventricular Nucleus
PYY	Peptide YY
Rax	Retina And Anterior Neural Fold Homeobox Transcription Factor
Rev.	Reverse
RNA	Ribonucleic Acid
rpm	Revolutions per minute
RT	Room Temperature
RT-qPCR	Real-Time Quantitative PCR
s.b.	Scale bar
s.c.	Subcutaneous
SEM	Standard Error Of The Mean
SGZ	Subgranular Zone
Shh	Sonic hedgehog
SHRSP	Stroke-prone spontaneously hypertensive
SVZ	Subventricular Zone
T2DM	Type-2 Diabetes Mellitus

TBR1	T-Box Brain 1
TRH	Thyrotropin-Releasing Hormone
TUNEL	Terminal Deoxynucleotidyl Transferase dUTP Nick End Labelling
UK	United Kingdom
VMN	Ventromedial Nucleus
VTN	Vitronectin
Wnt	Wingless-Related Integration Site
WT	Wild Type
αMSH	A-Melanocyte-Stimulating Hormone
µg	Microgram (s)
µl	Microlitre (s)
µM	Micromolar

Contents

Figures and Tables

Chapter 1: General Introduction

1.1. Obesity is a global epidemic

Obesity is a growing global health concern, affecting 60% of adults in Europe (Sonnefeld et al., 2023) and in its current trajectory, around 18% of adults worldwide will be obese by 2025 (O'Brien et al., 2017). Although genetic background does predispose certain individuals/ethnicities to developing obesity, the current pandemic can be largely attributed to contemporary lifestyles characterised by overconsumption of energy-dense food and reduced physical activity (Klein et al., 2016). Obesity is also a risk factor that triggers many other severe medical conditions.

Individuals who are overweight or obese have been associated with a persistent, low-level inflammatory state (Jin et al., 2023). This chronic low-grade inflammation is closely linked to the pathophysiology of adipose tissue and is a common characteristic across a range of obesity-related diseases (Lionetti et al., 2009), including metabolic syndrome, Type 2 Diabetes Mellitus (T2DM), insulin resistance, fatty liver disease, arteriosclerosis, and various cancers (Neto et al., 2023; Pergola & Silvestris, 2013; Özcan et al., 2004). Furthermore, this persistent inflammatory condition has also been connected to several mental disorders, dementia, and neurodegenerative diseases such as Alzheimer's disease (AD) (Tronieri et al., 2017; Anstey et al., 2011; Profenno et al., 2010; Neto et al., 2023).

1.1.1. Obesity, neuroinflammation, and brain pathology

Obesity triggers widespread inflammation throughout the body, including the Central Nervous System (CNS). This chronic inflammation, stemming from adipose tissue dysfunction can lead to altered brain metabolism, disruption of the Blood Brain Barrier (BBB), neuroinflammation, neuronal dysfunction, brain atrophy, mood impairments, and cognitive decline (Luppino et al., 2010; Gustafson, 2012). The excessive release of pro-inflammatory adipokines and cytokines into the bloodstream may facilitate the infiltration of leukocytes into the CNS through the disrupted BBB, thereby promoting the development of neurodegenerative diseases (Buckman et al., 2013; Neto et al., 2023; Davanzo et al., 2023). Indeed, the persistent overconsumption of energy dense, high carbohydrate and saturated fat foods by individuals with obesity can significantly impact cerebral glucose metabolism, influencing insulin secretion, which has been

identified as a contributing factor in the pathogenesis of neurodegenerative disorders (Biessels et al., 2006; de la Monte, 2012).

Furthermore, Diet-induced obesity (DIO) rodent models also show impairment in working memory, memory performance and learning (Alford et al., 2018; Lindqvist et al., 2006; Klein et al., 2016; Robison et al., 2020; Park et al., 2010; Ho-yin Lee & Yau, 2020). These deficits are primarily due to brain inflammation originating from the increased levels of inflammatory cytokines from the periphery or from local microglia (De Felice & Ferreira, 2014). The induced inflammation impairs insulin signalling in the brain, which has an important role in neural health through many downstream pathways including the phosphatidylinositol-4,5-bisphosphate 3-kinase (PI3)/Akt cascade. This disruption appears to also promote the accumulation of amyloid-beta and hyperphosphorylated tau proteins, hallmarks of Alzheimer's pathology (Alford et al., 2018). All together contributing to reduced synaptic plasticity and impaired neurogenesis (Zheng et al., 2016; Alford et al., 2018).

Moreover, the hormone leptin, produced by adipose tissue, has been implicated in the association between obesity and cognitive dysfunction (Blüher & Mantzoros, 2015; Farr et al., 2015). Leptin is produced in proportion to fat stores (Casado et al., 2023), and functions as a satiety signal within the brain, particularly in the hypothalamus. Initially, elevated leptin should suppress appetite and enhance energy expenditure. However, over time, the brain may become less responsive to leptin, despite its high levels, a phenomenon known as "leptin resistance." Indeed, despite elevated peripheral leptin levels in obesity, cerebrospinal fluid leptin concentrations appear to be lower, suggesting impaired transport of leptin across the BBB and a potential mechanism for leptin resistance (Farr et al., 2015). Leptin has also been implicated in the regulation of adult neurogenesis and neuroprotection, and central leptin resistance has been associated with the pathology of certain neurological disorders, such as Parkinson's disease and Alzheimer's disease (Casado et al., 2023). In contrast, (Pérez-González et al., 2011) showed that intracerebroventricular infusion (i.c.v.) gene delivery of leptin increased the proliferation of new neurons in the DG and reduced Aβ-induced neuronal degeneration in a mouse model of amyloidosis, suggesting that restoring central leptin signalling can restore neurogenesis (Pérez-González et al., 2011). While obesity does not directly cause leptin resistance, it creates a physiological environment that strongly favours its development. The chronic hyperleptinemia observed in obesity, combined with other factors like inflammation and impaired BBB transport, leads to a diminished response to leptin in the brain, contributing to the maintenance of obesity and possibly the associated neurodegenerative effects.

1.2. Adult neurogenesis

Adult neurogenesis refers to the process of generating new neurons from adult neural stem cells (aNSCs). Historically, it was widely accepted that mammalian neurogenesis was restricted to embryonic and postnatal development (Kuhn et al., 2018; Owji & Shoja, 2019; Yoo & Blackshaw, 2018). However, over the past two decades, a substantial body of research has established that neurogenesis persists in the hippocampus of the majority of mammalian species throughout adult life.

In 1996, Kuhn et al. (1996) published a seminal paper that described the generation of new neurons in the adult rat brain and the decline of hippocampal neurogenesis with aging. This work, along with several other studies, established adult neurogenesis as a cellular process in the mammalian brain (Kuhn et al., 1996; Kuhn et al., 2018). This established adult neurogenesis as a novel research area, although these reports was merely re-discoveries of the same phenomenon described years earlier by Altman (Altman & Das, 1965), Bayer (Bayer, 1982), Kaplan (Kaplan & Hinds, 1977), and Nottenbohm (Nottebohm & Arnold, 1976; Kuhn et al., 2018; Owji & Shoja, 2019). Altman's groundbreaking findings laid the foundation for extensive neuroscience research exploring the adult brain's capacity to generate new neurons, which was previously thought impossible. Later, in the 1970s and 1980s, the work of Kaplan (Kaplan & Hinds, 1977) and Nottebohm (Nottebohm & Arnold, 1976) further expanded the understanding of adult neurogenesis, demonstrating its occurrence in the mammalian neocortex of primates and avian brain, respectively (Kuhn et al., 2018). Today, over half a century since Altman's discovery, the field of adult neurogenesis continues to grow rapidly, offering promising potential for revolutionising treatments for neurodegenerative disorders and brain injuries (Owji & Shoja, 2019).

The early work on adult neurogenesis in the 1960s faced significant methodological challenges. The lack of robust techniques for definitively identifying, quantifying, and analysing newly generated neurons in adult brain tissue made the findings vulnerable to criticism (Kuhn et al., 2018). The limitations of ^{3}H-thymidine labelling and the scarcity of specific neuronal markers, due to the underdevelopment of immunohistochemical analyses, hampered these early studies. However, conceptual and technological advancements over the subsequent decades were thus crucial in establishing adult mammalian neurogenesis as a biological concept, leading to a steep increase of research in this field (Kuhn et al., 2018).

In adult rodents, the most extensively studied regions of active neurogenesis are the subventricular zone (SVZ) of the lateral ventricles and the Subgranular zone (SGZ) of the Dentate Gyrus (DG) in the hippocampus (Yoo & Blackshaw, 2018; Kokoeva et al., 2007). The SVZ generates immature neurons that migrate along the rostral migratory stream (RMS) to the olfactory bulb, where they mature into neurons that process olfactory input (Lim & Alvarez-Buylla, 2016). Meanwhile, the SGZ gives rise to granule cells of the DG, which process information crucial for learning and memory (Song et al., 2012).

The first evidence of adult hippocampal neurogenesis in the human brain was provided by the study of Eriksson et al. (1998). They used the proliferative lineage tracer Bromodeoxyuridine (BrdU) labelling to identify dividing cells, which they then co-labelled with neuronal and astrocyte specific markers, allowing them to detect BrdU-labelled adult born neurons using confocal microscopy (Eriksson et al., 1998; Kuhn et al., 2018). Since then, several labs have found evidence of adult neurogenesis in the DG of the human hippocampus (Boldrini et al., 2018; Mathews et al., 2017; Dennis et al., 2016; Palmer et al., 2001; Palmer et al., 2001), as well as in nonhuman primates (Gould et al., 1999; Kornack & Rakić, 1999; Leuner et al., 2007; Kuhn et al., 2018).

The advancement of increasingly sophisticated techniques for labelling and tracing newly generated neurons in the recent years has now made it evident that several brain regions in adult mammals exhibit substantial levels of neurogenesis (Kokoeva et al., 2007) including the hypothalamus. One of the earliest studies to report findings of hypothalamic neurogenesis was (Pencea et al., 2001), which described a series of experiments where co-intraventricular infusion of brain derived neurotrophic factor (BDNF) and BrdU led to increased BrdU labelling, not only in the SGZ and SVZ, but also in the hypothalamus, striatum, and other forebrain regions (Pencea et al., 2001). The notion of adult neurogenesis in brain regions previously considered non-neurogenic is still met with scepticism. Some studies have failed to validate these findings, while others have only detected new cell generation following brain injury or pharmacological interventions (Migaud et al., 2010). The evidence for adult neurogenesis in the striatum is less conclusive and often associated with injury or disease models (Jurkowski et al., 2020). Whether it occurs under normal physiological conditions remains unclear. The neocortex is another contentious area, as while some early studies reported neurogenesis, later investigations have challenged these observations (Jurkowski et al., 2020). Consequently, the existence, extent, and functional significance of adult neurogenesis beyond the hippocampus and olfactory bulb remains a topic of ongoing debate

and research. As an illustration, no new dopaminergic neurons were detected in the adult rat substantia nigra (BrdU; Frielingsdorf et al., 2004; Lie et al., 2002), although using a different proliferation marker provided evidence for neurogenesis in the mouse substantia nigra (^{3}H-thymidine; Migaud et al., 2010; Zhao et al., 2003). Furthermore, the adult primate neocortex exhibited cell proliferation but no new neuron production or only transiently surviving neurons (Gould et al., 2001; Koketsu et al., 2003; Migaud et al., 2010). Subsequent studies used BrdU incorporation to demonstrate Fibroblast growth factor (FGF) and Ciliary neurotrophic factor (CNTF) induced neurogenesis in the adult hypothalamus (Kokoeva et al., 2005; Pérez-Martín et al., 2010; Xu et al., 2005). However, the high levels of growth factors employed in these experiments raised uncertainty about the extent of basal adult hypothalamic neurogenesis (Lee & Blackshaw, 2012). The hypothalamus is still termed a site of "low level" adult neurogenesis as the proportion of newborn neurons among newborn cells in the adult rodent is normally around 1-37% (Migaud et al., 2010) compared to 70-100% in the SGZ of DG and SVZ of lateral ventricles (Lledo et al., 2006).

While adult hypothalamic neurogenesis in rodents has recently become more extensively researched, our understanding of hypothalamic neurogenesis in humans or primates remains limited. Investigating hypothalamic neurogenesis in humans is extremely challenging due to methodological limitations. Unlike in rodents, techniques such as lineage-tracing and pulse-chase labelling cannot be readily applied in human studies (Sharif et al., 2021). Instead, researchers must rely on postmortem analyses, which are hindered by issues like the preservation of neuronal markers (Sharif et al., 2021). Overall, there is a significant gap in our understanding of Hypothalamic Ventricular Zone (HVZ) neurogenesis in the human brain compared to animal models. Evidence for adult neurogenesis in the human hypothalamus relies primarily on the detection of Doublecortin (DCX), a marker of immature neurons, in postmortem samples. DCX-positive cells have been observed in the tuberal region of the hypothalamus from three individuals, aged 20-, 72-, and 79-year-old (Batailler et al., 2014), suggesting the presence of new neurons in specific hypothalamic nuclei, where neurogenesis has been consistently described also in rodents (Li et al., 2012; McNay et al., 2012; Haan et al., 2013; Robins et al., 2013; Chaker et al., 2016). However, the detection of DCX-positive cells in human hypothalamic specimens may not accurately reflect the actual morphology of these cells in the living brain. Postmortem delay (PMD) can affect DCX immunoreactivity, leading to loss of dendritic staining, an effect that has been observed even in rodent brains (Boekhoorn et al., 2006). For example, a lack of DCX staining was also observed in human

hippocampal samples collected after PMDs of over 48 hours (Sorrells et al., 2018). Additionally, the relationship between factors like temperature, tissue cooling, and proximity to ventricles, and DCX protein breakdown is not well understood. This suggests that DCX immunoreactivity in human hypothalamic samples with postmortem delays of 24-36 hours may not be representative of the true *in vivo* morphology of the DCX-positive cells (Sharif et al., 2021). Additionally, the duration of DCX expression in the human brain is unknown and may differ from the 3 to 14 days observed in the rodent hippocampus (Couillard-Despres et al., 2005). This limits the ability to reliably estimate the birth date and relative age of DCX-positive cells in postmortem human brain samples. Furthermore, adult-born hippocampal granule neurons in macaque monkeys were shown to take over 6 months to mature (Kohler et al., 2011), significantly longer than the 3-14 days observed in rodents. This suggests the maturation of adult generated neurons in humans may also occur over a protracted period of several months, compared to the faster timeline in rodents (Kempermann et al., 2018). The limited knowledge of hypothalamic neurogenesis in humans highlights the need for further research to fully understand its potential functions and implications for human health and disease.

Additionally, the reliance on DCX and PSA-NCAM expression as the primary indicators of neurogenesis may pose challenges in human studies. In humans, we may observe a relative temporal disconnection between precursor cell proliferation, which establishes the potential for neurogenesis, and the actual recruitment or differentiation of these cells into mature new neurons (Kempermann et al., 2018). The activation and integration of newly generated neurons into functional neural circuits is contingent upon the availability of a pool of postmitotic cells that can be recruited, rather than the proliferation of progenitor cells per se (Kempermann et al., 2018). DCX is commonly employed as an indirect measure of this population of "immature" neurons. However, the relationship between cell proliferation, the number of DCX-positive cells, and the actual extent of net neurogenesis is not straightforward (Kempermann et al., 2018). While DCX expression can serve as a marker for adult neurogenesis, it alone is likely not a comprehensive indicator of the functional potential of neurogenesis (Kempermann et al., 2018). Indeed, new neurons in mice do not maintain DCX expression throughout their entire postmitotic maturation phase. Furthermore, rats exhibit fewer DCX-positive cells compared to mice, despite demonstrating higher rates of neurogenesis, due to the faster maturation of their newly formed neurons (Snyder et al., 2009). While the expression of the calcium-binding protein Calretinin (CR) appears to be a more suitable proxy marker for this period in mice, this pattern of expression does not seem to be as evident in the rat brain. Paradoxically, CR has

nonetheless been employed as a marker to investigate adult neurogenesis in at least one study examining the human brain (Galán et al., 2017; Kempermann et al., 2018). To study dividing cells, researchers (Eriksson et al., 1998) used BrdU in combination with calbindin and NeuN to investigate neurogenesis in the adult human hippocampus, while others (Urbán et al., 2002) examined CR containing interneurons in the human hippocampus.

Significant methodological challenges exist in studying this phenomenon directly in humans, and our current understanding is predominantly extrapolated from findings in rodent models. In summary, while animal studies have provided insights into hypothalamic neurogenesis, the evidence for adult neurogenesis in the human hypothalamus remains limited and inconclusive.

1.2.1. Hypothalamic role in energy homeostasis

Current research has indicated that the mammalian hypothalamus, both during the postnatal period and in adulthood, harbours a neurogenic niche where neural progenitor cells (NPCs) that can proliferate and differentiate into neurons, astrocytes and oligodendrocytes, as well as become incorporated into the pre-existing neural circuits (Yoo & Blackshaw, 2018; Sharif et al., 2021). The current evidence of hypothalamic neurogenesis predominantly stems from investigations in animal models focusing on the Mediobasal Hypothalamus (MBH) due its pivotal role in regulating feeding behaviour and energy metabolism (Lee et al., 2014; Kokoeva et al., 2005). Indeed, the hypothalamus serves as a central homeostatic regulator, orchestrating a range of physiological processes including sleep, circadian rhythms, temperature regulation, and appetite control (Lee et al., 2014). Compared to the well-studied neurogenic niches of the SVZ and SGZ, the hypothalamus exhibits relatively low levels of adult neurogenesis (Klein et al., 2019; Kokoeva et al., 2007). However, this characterisation may be an oversimplification, as numerous studies have identified considerable cellular turnover within the MBH. While the hypothalamus exhibits relatively low levels of adult neurogenesis overall, the distribution of neurogenesis varies across different hypothalamic regions. Specifically, the hypothalamic Median Eminence (ME) shows 5-fold greater levels of relative neurogenesis compared to other areas, exhibiting a robust cellular turnover (Lee et al., 2012). Along similar lines, a study (McNay et al., 2012) found that a substantial portion of the BrdU-retaining neurons in the Arcuate Nucleus (ArcN) were subsequently replaced over the first three postnatal months (McNay et al., 2012). This indicates a substantial cell turnover within the MBH. Which means that the hypothalamus, particularly the medio-basal region, exhibits an underappreciated degree of structural plasticity maintained by persistent adult neurogenesis (Lee et al., 2012; Gage, 2002; Yoo et al., 2021).

The understanding of organisation and characteristics of the adult hypothalamic neurogenic niche, including the identity, lineage relations, and spatial distribution of distinct hypothalamic neural progenitor cells and their progeny, as well as the functional significance of hypothalamic neurogenesis, remain relatively underdeveloped compared to the existing knowledge of the SVZ and SGZ (Sharif et al., 2021; Kokoeva et al., 2007).

The hypothalamus occupies a privileged position, as it is partially located outside the BBB. Hence, this neurogenic niche is a key site in the brain that can sense changes of circulating metabolites and hormones, used to modulate behaviour (Klein et al., 2019; Langlet, 2014; Schwartz et al., 2000). Given this, even very low levels of neurogenesis, adding just a small number of specific neuronal subtypes to the existing neural circuits, could have an outsized effect on physiology and behaviour, helping to maintain energy homeostasis (Yoo et al., 2021; Yoo & Blackshaw, 2018). Making this neurogenic niche very interesting for not only understanding the mechanism behind the control of our energy homeostasis but also how we can modulate it to treat disease including obesity.

1.2.2. Stem cells in the hypothalamus

While the cellular origins of adult hypothalamic neurogenesis remains a topic of debate, evidence suggests that it arises from slowly dividing neural stem/progenitor cells residing in the 3rd ventricular walls (Robins et al., 2013; Bolborea & Dale, 2013). These stem cells are termed tanycytes and are believed to give rise to various neuronal subtypes that play crucial roles in energy homeostasis, encompassing populations that express critical neuropeptides involved in appetite regulation and metabolic processes (Robins et al., 2013; Lee et al., 2012). At the heart of this regulation are the anorexigenic and orexigenic neurons, which are distinguished by their expression of the neurotransmitters pro-opiomelanocortin (POMC), Neuropeptide Y (NPY), and agouti-related peptide (AgRP), among other minor neurotransmitters(Goodman & Hajihosseini, 2015).

Tanycytes are specialised radial glial-like cells that line the dorsal portion of the 3rd Ventricle (3V). Unlike the majority of multi-ciliated ependymal cells lining the ventricles of the brain, tanycytes project one or two apical cilia into the ventricle and extend a basal process into the hypothalamic parenchyma or towards the pial surface (Miranda-Angulo et al., 2014). These processes serve as a substrate for the radial migration of newly post-mitotic neurons (Yoo & Blackshaw, 2018).

Tanycytes express various markers including transcription factors including Retina and anterior neural fold homeobox transcription factor (Rax) (Miranda-Angulo et al., 2014), Sox2 and Sox9 (Lee et al., 2012; Robins et al., 2013); intermediate filament proteins such as Nestin, Vimentin and glial fibrillary acidic protein (GFAP) (Prevot et al., 2018; Yoo & Blackshaw, 2018); growth factors such as Fgf10 and Fgf18 (Haan et al., 2013); and membrane-bound proteins such as glutamate-aspartate transporter (GLAST)(Robins et al., 2013; Haan et al., 2013). Studies have demonstrated that tanycytes can proliferate, self-renew, and differentiate into neurons and GFAP-positive astrocytes *in vivo* (Robins et al., 2013). *In vitro*, some tanycytes can generate neuropsheres. Indeed, tanycytes show heterogenous NPC marker expression, proliferative properties and progeny fate (Robins et al., 2013; Prevot et al., 2018).

Tanycytes are traditionally divided into four subtypes termed α-1, α2-, β1- and β2-tanycytes. The subtypes are based on their location, morphology and gene expression profile (Rodriguez et al., 2005). The dorsal tanycytes that are located close to the Dorsomedial- (DMN) and Ventromedial Nuclei (VMN) of the hypothalamus and are referred to as α-1 and α2-tanycytes (Robins et al., 2013), while the more ventrally located tanycytes, near the ArcN and ME, are referred to as β1- and β2-tanycytes (Rodriguez et al., 2005) (Figure 1.1A). Notably, the β2-tanycytes differ from the other subtypes due to their direct access to circulating plasma, as the BBB is fenestrated at the ME (Bolborea & Dale, 2013; Rodriguez et al., 2005; Yoo & Blackshaw, 2018). This privileged access to signals from the periphery enables tanycytes to detect hormonal, nutritional and mitogenic changes (Yoo & Blackshaw, 2018).

In the adult brain, tanycytes primarily generate neurons, and to a lesser extent, glial cells that populate more distant hypothalamic regions, including the ArcN, VMN, and DMN (Chaker et al., 2016). β-tanycytes located in the ME-ventromedial ArcN has been shown to co-express Sox2, brain lipid-binding protein (BLBP) and Musashi-1 (Msi1), but do not express GFAP or GLAST (Prevot et al., 2018). These tanycytes generate neurons that populate the ArcN and VMN but do not produce GFAP-positive NPCs (Haan et al., 2013). Dorsally, closer to the dorsomedial ArcN and VMN, a subpopulation of GLAST-positive α-tanycytes both have gliogenic and neurogenic potential and gives rise to astrocytes and a few neurons within and around the VMN (Robins et al., 2013). GLAST-positive α-tanycytes also have the capacity to generate β1-tanycytes located in the ventromedial ArcN. In addition, α-tanycytes can generate neuropsheres *in vitro*, but β-tanycytes cannot (Robins et al., 2013), suggesting that β-tanycytes are mainly neurogenic and may represent a more committed type of neural progeny (Prevot et al., 2018).

Fgf10 is selectively expressed in a subpopulation of β-tanycytes (Haan et al., 2013). Lineage tracing using Fgf10-CreER^{T2} revealed that β-tanycytes generate more neurons during the early post-weaning period, unlike α-tanycytes (Robins et al., 2013), and their progeny primarily is predominantly neurons that integrate into the ArcN and VMN (Haan et al., 2013). Other lineage tracing studies using the Nestin-CreER^{T2} mouse line (Lee et al., 2012) also showed that in young and early postnatal stages, the β2-tanycyte subtype is the most proliferative and neurogenic (Lee et al., 2012), with the newly generated neurons mainly remaining within the ME (Lee et al., 2012). In addition, Goodman et al. (2020) has recently suggested a different stem cell model to that of Robins et al. (2013) where the β-tanycytes give rise to α-tanycytes. Their study suggest that Fgf10-positive β-tanycytes give rise to a proliferative population of α-tanycytes, which may act as transient amplifying or intermediate progenitor cells (Goodman et al., 2020). This was supported by evidence that β-tanycytes have a slower rate of BrdU incorporation compared to α-tanycytes *in vivo*, can generate fast-dividing α-tanycyte descendants and generate all three neural cell lineages *in vivo* (Goodman et al., 2020).

The findings suggests that different tanycyte subsets have distinct functional characteristics in terms of their neural stem cell potential. While directly comparing lineage tracing studies using diverse drivers can be challenging, it appears that tanycyte subtypes vary significantly in their potential and contribution to hypothalamic cell turnover. Additionally, a parenchymal neural stem cell population has been proposed to exist in the hypothalamus (Robins et al., 2013; Li et al., 2012). Regardless of their ventricular or parenchymal origin, the newly generated neurons seem to be predominantly associated with the regulation of feeding behaviour (Rizzoti & Lovell-Badge, 2017). This notion of functionally distinct neural stem cell properties within the tanycyte subsets may help explain the markedly different effects on body weight observed when the function of each subset is compromised in HFD conditions (Li et al., 2012; Bolborea & Dale, 2013; Lee et al., 2012; Robins et al., 2013).

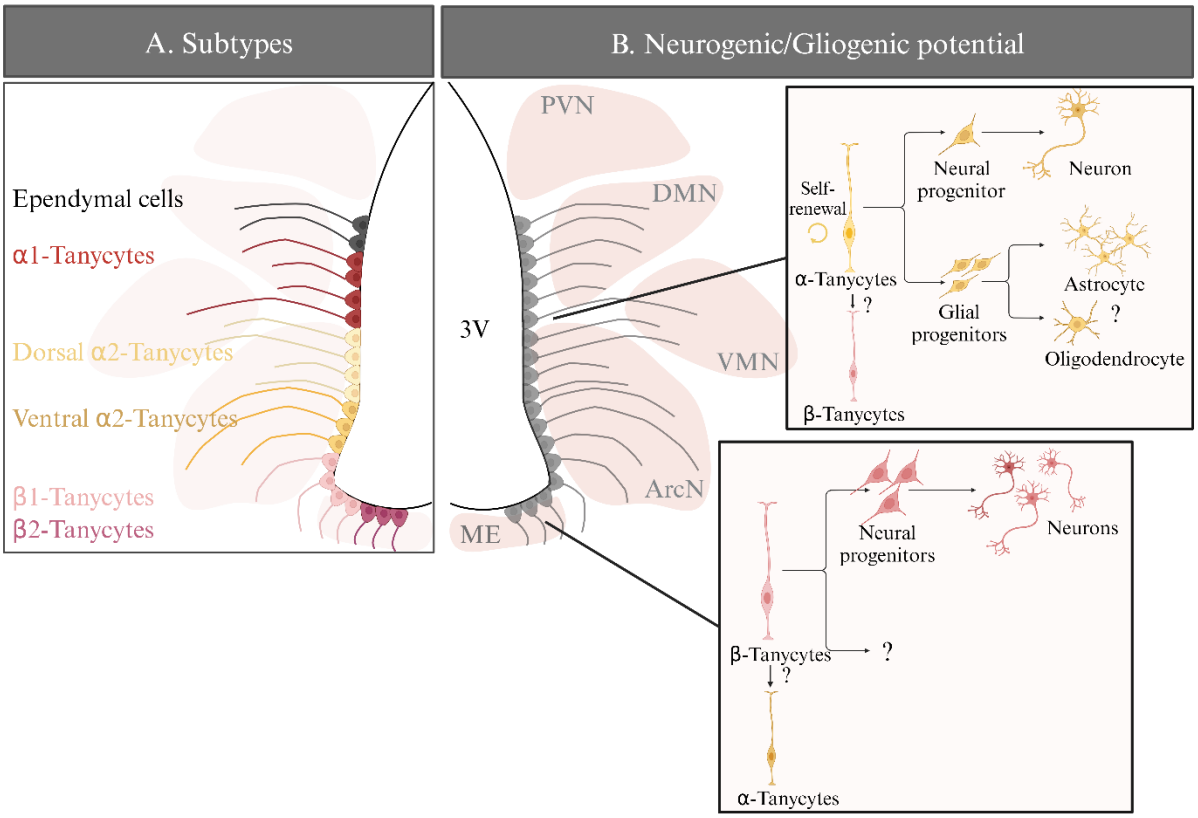

Figure 1.1. Tanycyte subtypes and neurogenic/gliogenic potential. A) Illustration of tanycyte subtypes. Ependymal cells in black, α1-tanycytes in dark red, dorsal α2-tanycytes in light yellow, ventral α2-tanycytes in dark yellow, β1-tanycytes in light pink and β2-tanycytes in plumb. B) Neurogenic and Gliogenic potential of tanycyte subtypes. Top square: α2-tanycytes undergo symmetric self-renewal, give rise to β-tanycytes (debated), and divide asymmetrically to give rise to neurons, astrocytes and rarely oligodendrocytes. Bottom square: β-tanycytes divide symmetrically and asymmetrically, mostly generating neurons. β-tanycytes also give rise to other uncharacterized cells types in the ME and have recently been hypothesized to give rise to α-tanycytes (debated). Figure made in BioRender (Biorender.com) and is modified from Yoo & Blackshaw (2018).

1.2.3. Tanycytes liaises between the periphery of the organism and the CNS

The hypothalamus mediates the connection between the periphery of the body and the CNS through the circumventricular organs (CVOs). These specialised structures allow for the regulated passage of selected metabolic, inflammatory, and autonomic signals, which may subsequently modulate hypothalamic neurogenesis. Therefore, modulation of peripheral signals might be a means of influencing hypothalamic neurogenesis (Makrygianni & Chrousos, 2022; Zhang et al., 2013; Zhang et al., 2017).

The CVOs are specialised structures situated along the midline or near the midline around the 3rd or 4th ventricle. These organs exhibit a unique architectural composition comprising

neurons, glial cells, blood vessels, and leptomeningeal components (Benarroch, 2011). The capillaries at the CVOs are fenestrated, and the perivascular spaces are large, leading to an incomplete BBB in these regions (Morita & Miyata, 2012; Hicks et al., 2021; Okamoto et al., 2022). At the CVOs, modified ependymal cells, including tanycytes, line the ventricular wall (Hicks et al., 2021). The tight junctions between the cell bodies of CVO tanycytes create a diffusion barrier, thereby shifting the BBB function from the capillary to the ventricular wall. The CVOs can be broadly classified into sensory and secretory. Where the ME, is a secretory CVO, consisting mainly of axons and nerve terminals that release bioactive peptides into the systemic circulation (Makrygianni & Chrousos, 2023; Okamoto et al., 2022).

Low molecular weight molecules from the systemic circulation can readily diffuse into the CVOs through the fenestrated capillaries (Hicks et al., 2021). However, high molecular weight molecules, such as various protein hormones and cytokines, are unable to freely enter the CVOs and instead rely on transcytosis systems to cross the BBB (Okamoto et al., 2022; Ayloo & Gu, 2019). At baseline, the transcytosis systems are inhibited by CNS specific genetic programs, maintaining the functional barrier. For example, the high molecular weight biomolecule leptin enters the CNS through transcytosis. Leptin does so exclusively via the activation of Leptin receptors in ME tanycytes (Balland et al., 2014).

1.2.4. Subpopulations of hypothalamic neurons and their role in energy homeostasis

The hypothalamus contains two distinct subpopulations of neurons that play a critical role in the regulation of energy homeostasis: anorexigenic and orexigenic neurons. Anorexigenic neurons suppress food intake, while orexigenic neurons stimulate food intake (Balthasar et al., 2005; Korf & Moller, 2021).

Anorexigenic neurons exert their effects through the Pro-opiomelanocortin (POMC) and Cocaine- and Amphetamine-Regulated Transcript (CART) neuropeptides (Korf & Moller, 2021). Peripheral release of satiety signals, such as insulin from the pancreas, Glucagon-Like Peptide-1 (GLP-1) from the gastrointestinal tract, and leptin from adipose tissue, reach the POMC-expressing neurons in the ArcN via the ME (Varela & Horváth, 2012; Singh et al., 2022). Activation of POMC neurons leads to the cleavage of POMC into α-Melanocyte-Stimulating Hormone (αMSH) (Korf & Moller, 2021), but also adrenocorticotrophin (ACTH), and β-endorphin (Millington, 2007). POMC-derived products regulates appetite, but also play critical roles in the skin, stress response, immune function, and sexual function. The melanocortin receptors (MCRs), a family of five G-protein coupled receptors, bind the MSHs

and ACTH. The MC3R and MC4R subtypes exhibit widespread expression in the CNS, while the MC1R and MC5R subtypes show relatively lower levels of expression (Millington, 2007). When αMSH is released from the POMC neurons in the ArcN that projects to the Paraventricular Nucleus (PVN), it activates MC4R (Korf & Moller, 2021; Garfield et al., 2015). The activation of MC4R-expressing PVN neurons is in turn involved in the regulation of satiety and energy expenditure (Figure 1.2; Garfield et al., 2015; Makrygianni & Chrousos, 2023).

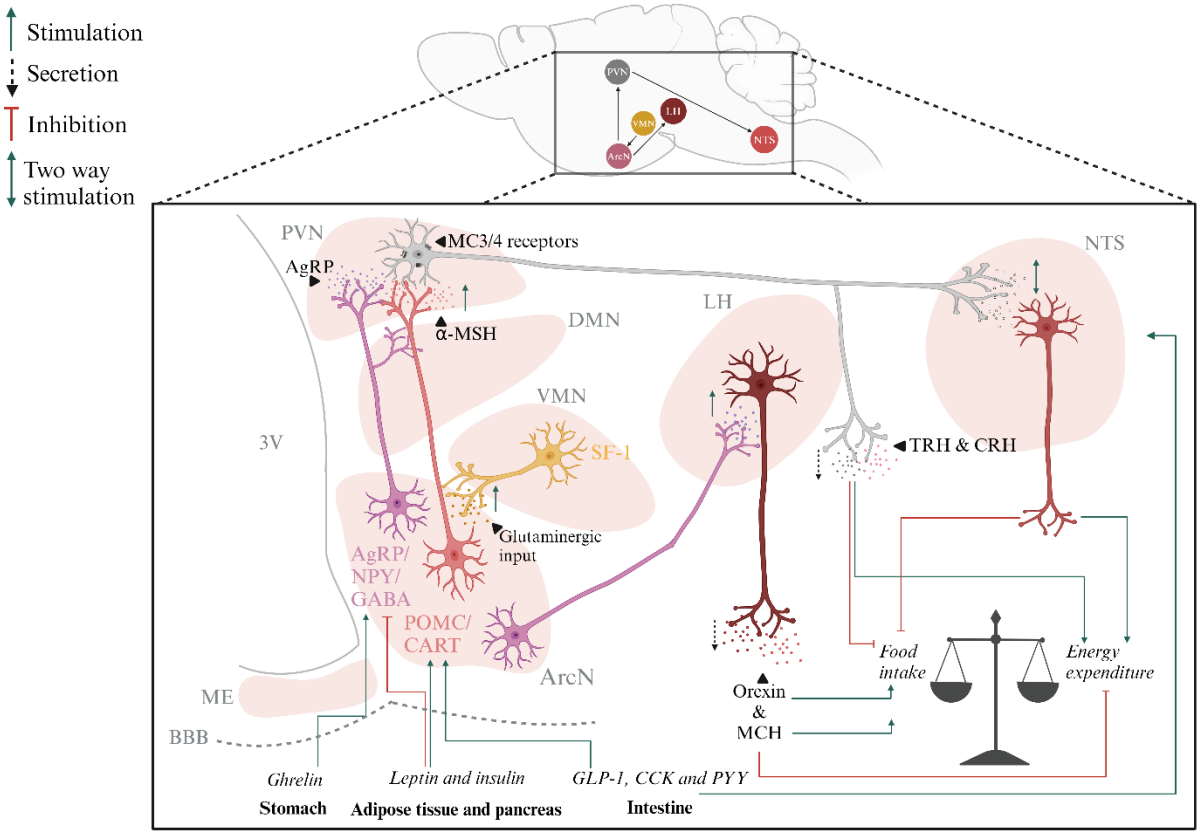

Figure 1.2. Neuronal connections in the regulation of energy homeostasis.
An overview of signalling in the healthy hypothalamus. Peripheral signals from adipocytes, pancreas, intestine and stomach activates the first order neurons, POMC/CART and AgRP/NPY in the ArcN, to secrete orexigenic AgRP and anorexigenic αMSH to the second order neurons in the PVN. The MC3/4 receptors are activated either by AgRP or αMSH and the integrated signals are delivered to the NTS to modulate feeding behaviour. PVN neurons additionally secrete thermogenic neurohormones thyrotropin-releasing hormone (TRH) and corticotropin-releasing hormone (CRH), inhibiting food intake and increase energy expenditure. SF-1 neurons in the VMN enhance POMC/CART anorexigenic action via glutaminergic input. AgRP/NPY neurons additionally project to the lateral hypothalamus (LH) and stimulates LH neurons that secrete orexin and MCH, two orexigenic and anti-thermogenic neurohormones that are directly involved in feeding behaviour. In the periphery, leptin increases GLP-1 and cholecystokinin (CCK) produced by the intestine. Adapted from Seong et al. (2019) and Sonnefeld et al. (2023).

Orexigenic neurons co-express neuropeptide Y (NPY) and Agouti-Related Peptide (AgRP) and the neurotransmitter gamma-aminobutyric acid (GABA)(Korf & Moller, 2021; Deem et al., 2021). Peripheral release of hunger signals such as ghrelin activates AgRP/NPY neurons in the ArcN, while the release of satiety signals like leptin, insulin, GLP-1, and peptide YY (PYY) inhibits them (Makrygianni & Chrousos, 2023). Upon activation, AgRP/NPY neurons in the ArcN release AgRP, which in turn inhibits MC4Rs in the PVN, thereby preventing the satiety signal (Deem et al., 2021). AgRP acts as an antagonist of MC4R, preventing the anorexigenic effects of MSH on second order neurons (Figure 1.2.) (Garfield et al., 2015; Deem et al., 2021). Additionally, activation of AgRP/NPY neurons induces insulin resistance and increased locomotor activity in the absence of food. The neuropeptide NPY mediates a subset of the physiological actions of AgRP neurons, including the stimulation of rapid food intake and regulation of glucose metabolism (Engström et al., 2020). Specifically, NPY signalling is essential for maintaining the long-term effects of AgRP neurons on feeding behaviour, particularly for sustaining hunger during the period between food discovery and consumption (Chen et al., 2019). Furthermore, AgRP/NPY neurons in the ArcN directly inhibit anorexigenic POMC neurons in the ArcN through the co-release of the inhibitory neurotransmitter GABA (Korf & Moller, 2021; Deem et al., 2021).

Notably, these two groups of ArcN-residing neurons are the best-characterised hypothalamic glucose-sensing neurons. They alter their firing rate in response to changes in extracellular glucose levels, with POMC neurons being glucose-excited and NPY/AgRP neurons being glucose-inhibited (Sohn et al., 2013; Makrygianni & Chrousos, 2023).

1.3. The connection between hypothalamic neurogenesis and obesity

Changes in metabolic conditions, including dietary factors and diet regulated cytokines have been shown to modify proliferation of neuronal precursors and neurogenesis in the hypothalamus. Research indicates that hypothalamic neurogenesis can play a dual role in obesity, potentially contributing to its onset through dysregulation of appetite and metabolic control, whilst also offering a mechanism for compensation in response to over nutrition and metabolic dysregulation.

The first study to link adult hypothalamic neurogenesis and energy homeostasis was conducted by Kokoeva et al. (2005), who investigated the effects of i.c.v. of CNTF, a neuro-cytokine that had been shown to lead to long-lasting reductions in body weight in obese rodents (Kokoeva et al., 2005). Notably, the researchers found that co-infusion with CNTF and BrdU for one

week increased the number of BrdU-labelled cells in the hypothalamic parenchyma five-fold. Furthermore, they observed a two-fold increase in BrdU-labelled neurons 42 days after treatment, some of which expressed POMC or NPY markers (Kokoeva et al., 2005). Interestingly, the researchers also demonstrated that simultaneous infusion of the anti-mitotic drug Cytosine Arabinoside (AraC) blocked BrdU incorporation and counteracted the long-term anorexigenic effect of CNTF (Kokoeva et al., 2005). Unfortunately, some concerns arose from this study. Firstly, since AraC globally blocks cell division in the whole brain, questions were raised about whether the observed behavioural effects were a result of disrupted hypothalamic neurogenesis. Secondly, the lack of a behavioural phenotype in animals treated with AraC alone raised questions about whether baseline levels of neurogenesis play any role in regulating body weight (Yoo & Blackshaw, 2018). A concern, McNay et al. (2012) further investigated by employing BrdU labelling to trace neurons generated during embryonic development, and then quantified the BrdU-negative neurons during postnatal maturation as an indirect assessment of ongoing neurogenesis. This revealed that over 50% of BrdU-positive neurons in the ArcN lost their BrdU label (although only 3% of POMC- and 5% of NPY-positive neurons) between 4 and 12 weeks of age (P28 and P84). Interestingly, the loss of BrdU labelling became less pronounced at later time points. Importantly, both leptin deficient mice and those maintained on a HFD displayed a dramatic retention of BrdU labelled cells, indicating a reduction in the loss of BrdU labelling. These findings were interpreted as substantial neurogenesis occurs in the ArcN under normal conditions, but that this process is markedly diminished by both advancing age and obesity induced by chronic HFD feeding or leptin deficiency (McNay et al., 2012). The same study also reported that neurospheres grown from primary stem cells from mice fed HFD for two months formed both more (350%) and larger neurospheres from the same number of seeded cells compared to controls, as if they had been stimulated with the purpose to replace lost progeny (McNay et al., 2012).

Indeed, Li et al. (2012) then reported that long-term HFD feeding (4 months) inhibited BrdU labelling (i.c.v infusion) of neurons in the hypothalamic parenchyma. This effect was mediated by an Nuclear Factor-κB (NF-κB) dependent response to inflammatory cytokines (Li et al., 2012). Furthermore, the activation of NF-κB signalling in Sox2-positive hypothalamic cells was found to lead to prediabetes and obesity (Li et al., 2012). In contrast to the study conducted by McNay et al. (2012), this study reported that neurospheres grown from stem-like cells cultured from mice on 4 months HFD were both smaller and fewer than controls (Li et al., 2012).

Both of these studies reported that HFD reduced BrdU labelling, but they primarily observed a reduction in BrdU labelling of non-neuronal cells in the parenchyma. Although a reduced number of BrdU labelled neurons were observed, both anorexigenic and orexigenic subtypes were equally affected. Additionally the contrasting results in neurosphere size and numbers *in vitro* raises questions about how exactly HFD dependent changes in general cell proliferation and neurogenesis regulate body weight. The discrepancies may be reflected in the differences of length in HFD protocols and the precise location of dissected tissue used to generate the neurospheres.

In contrast to the long-term HFD protocols reported above short-term HFD has been shown to induce cell proliferation in the HVZ and give rise to neurons. For example, Gouazé et al. (2013) observed an increased proliferation of BrdU labelled cells within three days of HFD treatment. This led to an increase in both POMC expressing neurons and glial cells after three weeks (Gouazé et al., 2013). Additionally they reported that i.c.v. of AraC blocked cell proliferation and led to weight gain in mice fed HFD (Gouazé et al., 2013). This may suggest a mechanism whereby increased hypothalamic neurogenesis following short-term HFD exposure could serve as a compensatory response to counterbalance the elevated caloric intake by reducing food intake, a response typically observed in mice fed HFD for one week (Williams et al., 2014).

Another group have also shown that HFD stimulates neurogenesis, as measured by BrdU labelling using intraperitoneal (i.p.) injection, specifically in the ME (Lee et al., 2014; Lee et al., 2012). The effects were observed in both sexes during early post weaning, but were only seen in females during pubescence. Furthermore, they reported that focal X-irradiation of the ME in P45 females fed HFD blocked cell proliferation and reduced their weight gain, despite no change in food intake. Importantly, the HFD induced increase in BrdU-positive cells was confined to the ME. They also confirmed observations from other studies (McNay et al., 2012; Li et al., 2012) where long-term HFD feeding (one month) reduced neurogenesis in the ArcN.

While the studies suggest that a HFD may regulate hypothalamic neurogenesis, the link between the observed phenotypes and the generated neuronal subtypes is not obvious. The fraction of newly generated neurons that express anorexigenic or orexigenic markers is quite small and is not always correlated with the observed behavioural phenotypes. For example, Li et al. (2012) reported that only 10% of the newborn neurons were expressing POMC, and only 4% expressed NPY. Similarly (Gouazé et al., 2013) reported that 6% of the newborn cells were POMC-positive in mice fed HFD.

1.4. Anti-obesity compounds

1.4.1. Liraglutide (LIRA)

T2DM is a significant global health concern closely associated with obesity (He et al., 2019). The identification of the gut-brain axis's role in regulating appetite has opened up new avenues for drug development, particularly nutrient stimulated, hormone based medications that mimic the metabolic effects of naturally occurring entero-pancreatic hormones, including glucagon-like peptide-1 (GLP-1; Gudzune & Kushner, 2024). GLP-1 is an incretin hormone primarily secreted by intestinal L-cells in response to glucose intake. It induces insulin secretion through its receptor, GLP-1R, in a glucose-regulated manner (Kjems et al., 2003; Peyot et al., 2009). Moreover, GLP-1 modulates feeding behaviour by relaying meal related information on nutritional status to the CNS. Consequently, GLP-1 receptor agonists have been widely utilised for the management of T2DM and chronic weight management (He et al., 2019). GLP-1 is produced endogenously in pancreatic alpha cells (Imbernon et al., 2022; Chambers et al., 2017) and neurons in the NTS, which project to the hypothalamus (Holt et al., 2019). However, the rapid degradation of native GLP-1 limits its therapeutic potential. This has led to the development of GLP-1R agonists with longer half-lives, which has been shown to provide a range of benefits, including reduced food intake, increased weight loss, and improved glycaemic control. Some of these agonists, such as LIRA, have been approved for the treatment of obesity and T2DM (Drucker et al., 2017). Originally developed for the treatment of T2DM, LIRA has also demonstrated potent dose-dependent anti-obesity properties. In 2010, the United States Food and Drug Administration (FDA) approved LIRA as an injectable GLP-1 receptor agonist, for the management of T2DM (Myšková et al., 2023). Subsequently, in 2013, the FDA approved LIRA for the treatment of obesity (Myšková et al., 2023). There are six GLP-1 receptor agonists approved for the treatment of T2DM, but only Liraglutide (Saxenda; here called LIRA) and Semaglutide (Ozempic) are approved as an anti-obesity treatment (Gabery et al., 2020; FDA, 2024). Extensive research has shown that LIRA regulates energy homeostasis by acting on the CNS, particularly the hypothalamus (Adams et al., 2018; Secher et al., 2014; Sisley et al., 2014; Imbernon et al., 2022) and the brainstem (Fortin et al., 2020).

LIRA, differs from the native GLP-1 through specific structural modifications. These include the acylation of the lysine residue at position 26 with a hexadecanoyl-glutamyl side chain and a single amino acid substitution from lysine to arginine at position 34 (Jacobsen et al., 2015). These subtle changes, along with the acylation, contribute to LIRA's prolonged pharmacokinetic profile. Following injection, LIRA exhibits high non-covalent binding to the

predominant plasma protein, human serum albumin, likely mediated through a fatty acid-binding site (Jacobsen et al., 2015). The extended action of LIRA is attributed to two key mechanisms: delayed absorption from the s.c. injection and reduced elimination rate due to slower metabolism and renal filtration (Jacobsen et al., 2015). This GLP-1 analogue also exhibits a significantly slower degradation rate by the enzyme dipeptidyl peptidase-4 (DPP-4) compared to endogenous GLP-1 (Soudahome et al., 2018). As a result, LIRA has a prolonged plasma half-life of 11-15 hours, compared to the half-life of native GLP-1 is only 2 to 3 minutes due to the rapid degradation by DPP-4 (Gudzune & Kushner, 2024). The slower degradation enables a once-daily subcutaneous administration. Similar to native GLP-1, LIRA stimulates insulin secretion, suppresses postprandial glucagon release, slows gastric emptying, and enhances feelings of satiety through its actions on the brain (Soudahome et al., 2018).

Extensive evidence from rodent and mammalian studies indicates that LIRA's effects on satiety and weight involve activity within the CNS (Adams et al., 2018; Cork et al., 2015; Richards et al., 2014; Sisley et al., 2014; Tornehave et al., 2008). GLP-1 receptors are widely expressed in the CNS and GLP-1 receptors expressed in CNS glutamatergic neurons are essential for LIRA's physiological effects (Adams et al., 2018; He et al., 2019). Within the hypothalamus, ArcN residing POMC and NPY/AgRP neurons play a crucial role in regulating energy balance and glucose homeostasis. Notably, Arcuate POMC neurons are glutamatergic (Dicken et al., 2012; Jones et al., 2019; Mercer et al., 2013; Wittmann et al., 2013) and GLP-1 receptors in POMC neurons are required for weight regulation on a HFD. Peripheral and central administration of LIRA have been shown to modulate the activity of Arcuate POMC and NPY/AgRP neurons, ultimately influencing food intake and body weight (Kanoski et al., 2011; Secher et al., 2014). These findings underscore the crucial role of GLP-1 signalling within the central nervous system, particularly in the regulation of metabolism through melanocortin neurons (He et al., 2019).

Nutrient stimulated, hormone based therapies, including LIRA and Semaglutide, mimic the actions of enteropancreatic hormones that modify central appetite regulation and provide multiple cardiometabolic weight loss benefits (Gudzune & Kushner, 2024). The relative efficacy of adult obesity medications has been evaluated through meta analyses showing that compared to placebo, LIRA was associated with 4.7% greater weight loss, and Semaglutide with 11.4% greater weight loss. Although there are many benefits of these therapies, adverse effects of these drugs include nausea (28%-44%), diarrhoea (21%-30%), and constipation (11%-24%; Gudzune & Kushner, 2024). Although clinical trials have shown that these

medications can result in significant weight reductions relatively soon after initiation (Tak & Lee, 2021), the rate of loss typically decelerates as the body adapts (Ryan et al., 2024). This plateau effect is characteristic of most weight loss interventions (Ryan et al., 2024). Studies have also found that most individuals regain weight after discontinuing LIRA and Semaglutide, suggesting the need for sustained treatment to maintain the weight loss benefits (Holst, 2024). Randomised trials have shown that participants who stopped taking the active compounds and switched to placebo quickly reverted to their initial weight (Holst, 2024). Thus, the existing evidence indicates that the weight loss effects of LIRA and Semaglutide are largely contingent on continued administration of these therapies. While GLP-1 agonists remains a valuable tool in the fight against obesity, the need for continuous treatment and possible adverse effects underscore the need for continued research and development of novel therapeutic strategies. A new anti-obesity compound that can induce long-term changes in neurocircuitry, leading to sustained weight management after treatment discontinuation, represents a significant advancement in addressing this complex health challenge.

1.4.2. Prolactin releasing peptide: PrRP

Neuropeptides are peptides synthesised and released by different neuronal populations within the nervous system, where they exert regulatory functions (Strnadová et al., 2024). Neuropeptides produced in the ArcN influence the activity of other hypothalamic regions, such as the PVN, VMN, DMN, and lateral hypothalamic area (LHA). This influences the release of other neuropeptides that are both orexigenic, like galanin, Melanin-Concentrating Hormone (MCH), and orexins, as well as anorexigenic, including Corticotropin-Releasing Hormone (CRH), Pituitary Adenylate Cyclase-Activating Peptide (PACAP), Prolactin-Releasing Peptide (PrRP), and Thyrotropin-Releasing Hormone (TRH). The impulses from these hypothalamic areas are then projected to the thalamus and integrated with inputs from the brainstem, primarily the nucleus of the solitary tract (NTS; See Figure 1.2.; Strnadová et al., 2024).

PrRP is a hypothalamic neuropeptide from the RF-amide family with a misleading name (Hinum et al., 1998). Although PrRP was originally named for its apparent ability to stimulate prolactin release, this function was later called into question. Despite the misleading nomenclature, the name PrRP has persisted (Dodd & Luckman, 2013). *In vivo*, there are two equally active isoforms of PrRP: PrRP31 with 31 amino acids, or its shorter analogue PrRP20 with an identical C-terminal sequence. The last two amino acids at the C-terminus, Arg-Phe-amide, are crucial for preserving PrRP's binding affinity to its receptor and ensuring its proper biological activity (Maletínská et al., 2011). PrRP acts as an endogenous ligand for the G-

protein-coupled receptor 10 (GPR10), and its signalling may play diverse roles in neuroendocrinology, including regulation of energy homeostasis, stress responses, cardiovascular function, and circadian rhythms (Dodd & Luckman, 2013). It also displays high affinity for the receptor for neuropeptide FF (NPFFR2), another neuropeptide from the RF-amide family (Strnadová et al., 2024). Both PrRP and GPR10 have been found to be expressed in brain regions implicated in the regulation of food intake, including the DMN, VMN, PVN and the NTS (Lawrence et al., 2000; Pražienková et al., 2019).

Interestingly, studies using i.c.v. injections of PrRP showed that food intake and body weight was reduced in free fed rats (Seal et al., 2001; Lawrence et al., 2000; Maletínská et al., 2011). The weight loss observed with PrRP administration appears to be greater than that attributable solely to reduced food intake, suggesting that increased energy expenditure also contributes to the weight loss effects (Ellacott et al., 2003). The crucial role of PrRP in regulating food intake and energy balance is highlighted by evidence that its expression is directly stimulated by leptin, the primary regulator of energy homeostasis (Ellacott et al., 2002). Additionally, mice deficient in either PrRP (Takayanagi et al., 2008) or its receptor GPR10 (Bjursell et al., 2007; Pražienková et al., 2021) develop late-onset obesity accompanied by reduced energy expenditure.

1.4.3. The lipidized analogue of PrRP: LiPrRP

As described above, PrRP regulates feeding behaviour and energy balance directly in the hypothalamus (Pražienková et al., 2019), and has been described to work in synergistic action with the anti-hunger hormone leptin (Kuneš et al., 2016). PrRP is therefore a suitable candidate as a new anti-obesity compound that acts directly on the brain regions that regulates our feeding behaviour. While anorexigenic neuropeptides administered directly into the CNS have been shown to effectively reduce food intake and body weight, their peripheral administration fails to elicit a comparable response. This is due to the inability of these neuropeptides to cross the BBB and access their receptors, where they are primarily expressed (Strnadová et al., 2024). To achieve the same beneficial effects as when administered centrally, it is necessary to modify neuropeptides to enhance their stability and bioavailability.

The development of long-lasting receptor agonists of GLP-1, which is approved for treating diabetes and obesity, demonstrated the enhanced properties achievable through peptide modification (Cummings et al., 2023; Hölscher, 2018). Since PrRP is a suitable candidate as a new anti-obesity compound, recent work at the Maletínská Lab at the Institute of Organic

Chemistry and Biochemistry in Prague therefore lipidized PrRP. However, therapeutically targeting the central neuropeptide system poses a significant challenge, as peripherally administered neuropeptides must access the brain while avoiding undesirable side effects. The Maletínská lab has therefore extensively studied the functional properties of the PrRP analogues.

The two isoforms of PrRP share an identical C-terminal sequence and exhibit similar *in vitro* activity (Hinuma et al., 1998). Previous research by Roland et al. (1999) revealed that N-terminal deletions of PrRP20 slightly diminished the analogues' affinity for the GPR10 receptor (Roland et al., 1999) The shortest PrRP fragments retaining the highest GPR10 binding affinity were PrRP20 and PrRP31, which exhibited nanomolar-range affinity. Conversely, replacing the C-terminal amide group with an acid completely abolished binding affinity (Hinuma et al., 1998; Roland et al., 1999). Furthermore, the arginine at positions 26 and 30 were found to be crucial for receptor binding, and their modification resulted in a loss of affinity (Roland et al., 1999).

PrRP could be shortened to a tridecapeptide without losing *in vitro* activity, retain binding affinity and agonist properties (Figure 1.3; Boyle et al., 2004). A structure-activity relationship study found that replacing amino acids at positions 21-31, particularly phenylalanine at position 31 (Phe31), with bulky side chains like His(Bzl), Trp, Cys(Bzl), Glu(Obzl), norleucine (Nle) or a halogenated aromatic ring (Phe(4-Cl)) maintained or improved binding affinity and agonist activity (Figure 1.3). Subsequent studies by Maletínská et al. (2011) showed that PrRP20 analogues with Phe31 replaced by different aromatic amino acids with different aromatic rings like (3,4-dichlor)phenylalanine ($PheCl_2$), (4-nitro)phenylalanine ($PheNO_2$), pentafluoro-phenylalanine ($PheF_3$), napthylalanine (1-Nal, 2-Nal), or Tyr retained high binding affinity and increased ERK and CREB phosphorylation in rat RC-4B/C pituitary cells (Figure 1.3; Maletínská et al., 2011).

Lipidization, involving the attachment of fatty acids to peptides via ester or amide bonds, is a valuable strategy for developing novel peptide based therapeutics. One recent example is LIRA that is palmitoylated at position 26 through a γ-glutamyl linker (Knudsen et al., 2000). This lipidization can enhance potency, selectivity, and therapeutic efficacy by increasing peptide stability and prolonging the half-life in the organism. Additionally, lipidization may facilitate delivery across the BBB (Gault et al., 2011). Consequently, the lipidization of neuropeptides involved in the regulation of food intake represents a potential avenue for the development of anti-obesity drugs (Kuneš et al., 2016).

Maletínská et al. therefore developed novel lipidized analogues of PrRP, with various fatty acid lengths attached to the N-terminus (Maletínská et al., 2015). All PrRP20 and PrRP31 analogues lipidized with octanoic, decanoic, dodecanoic, myristic, palmitic, and stearic acids exhibited agonist characteristics and maintained high binding affinity to the GPR10 receptor, comparable to native PrRP20 or PrRP31 (Figure 1.3; Maletínská et al., 2015). Furthermore, lipidized PrRP31 analogues incorporating noncoded amino acids such as 1-Nal, $PheCl_2$, $PheNO_2$, $PheF_5$, or Tyr at position 31, when myristoylated or palmitoylated at the N-terminus, demonstrated potent binding to GPR10. The original methionine at position 8 was substituted with the more stable Nle to prevent Met oxidation, without compromising binding and signalling activity (Figure 1.3; Prazienkova et al., 2016).

The studies evaluated analogues of PrRP31 where palmitic acid was attached either through a γ-glutamyl linker or a short polyethylene glycol chain at the Lys11 position, as well as an analogue with two palmitic acids - one at Lys11 and one at the N-terminus. These analogues were tested in both *in vitro* and *in vivo* experiments. Binding and signalling assays demonstrated that the analogues maintained binding affinity to the GPR10 receptor, although the analogue with two palmitic acids was less potent. Additionally, the single palmitic acid attachment could be made at various positions along the peptide chain without compromising the binding affinity (Pražienková et al., 2017). The C-terminal 20 amino acids of PrRP are essential for maintaining the full anorexigenic effect.

ICV administration of PrRP20 analogues incorporating various aromatic amino acids at position 31, such as $PheCl_2$, $PheNO_2$, $PheF_5$, 1-Nal, 2-Nal, or Tyr, resulted in decreased food intake in fasted mice (Maletínská et al., 2011). Specifically, PrRP20 analogues (PheNO231)PrRP20, (1-Nal31)PrRP20, (2-Nal31)PrRP20, and (Tyr31)PrRP20 with these bulky aromatic substitutions at the C-terminus exhibited the most significant and prolonged anorexigenic response after ICV injection in fasted lean mice. This study demonstrated that a bulky aromatic ring, not necessarily phenylalanine, at the C-terminus enables the full anorexigenic activity of PrRP20 (Maletínská et al., 2011).

The administration of PrRP can reduce food intake, but this effect depends on the PrRP analogues reaching the brain receptors and eliciting the central mechanism of action. As mentioned, Maletínská et al., (2015) demonstrated that lipidization of PrRP did not affect the binding to the GPR10 receptor but also that the analogues demonstrated increased affinity for the NPFFR2 receptor (Maletínská et al., 2015). Among the analogues with various fatty acid lengths attached to the N-terminus of PrRP, only the myristoylated PrRP20 (myr-PrRP20),

palmitoylated (palm-PrRP31), and stearoylated PrRP31 (stear-PrRP31) significantly decreased food intake in fasted or freely fed lean mice after s.c. administration (Maletínská et al., 2015). These lipidized analogues were suggested to cross the BBB and thus produce the central effect after peripheral administration. In contrast, analogues containing shorter fatty acids did not impact food intake. Thereafter, a subsequent study found that administering palm-PrRP31 to free-fed mice for three consecutive days via s.c. or intraperitoneal (i.p.) injections at a dose of 5 mg/kg reduced food intake. A comparable effect was observed after intravenous (i.v.) administration at a lower dose of 0.1 mg/kg (Mikulaskova et al., 2016). Furthermore, the palm-PrRP31 and myr-PrRP20 analogues, but not the unmodified PrRP20, PrRP31, or octanoylated PrRP31, exhibited enhanced stability in rat plasma and significantly increased c-Fos immunoreactivity in hypothalamic and brainstem nuclei involved in the regulation of food intake, such as the PVN, ArcN, and NTS. Administration of palm-PrRP31 via s.c. injection elicited a significant elevation in c-Fos immunoreactivity within the PVN, ArcN, NTS, and DMN regions of the hypothalamus. Furthermore, palm-PrRP31 treatment substantially increased c-Fos expression specifically in the hypocretin neurons of the LHA and the oxytocin neurons of the PVN (Pirník et al., 2015).

Among the lipidized PrRP analogues, PrRP31 palmitoylated or myristoylated at the N-terminus demonstrated the most potent and long lasting anorexigenic effects in fasted mice (Prazienkova et al., 2016). Furthermore, in DIO mice, a two week s.c. administration of palm-PrRP31 and myr-PrRP20 significantly reduced food intake, body weight, and improved metabolic parameters such as plasma insulin and leptin levels, as well as attenuated lipogenesis, compared to lean control mice (Maletínská et al., 2015).

Repeated administration of PrRP analogues palmitoylated through various linkers to Lys11, decreased body weight, liver weight, and levels of plasma insulin, leptin, triglycerides, cholesterol, and free fatty acids in DIO mice. Furthermore, enhanced energy expenditure shown by increased expression of uncoupling protein 1 (UCP-1) in brown adipose tissue (BAT; Pražienková et al., 2017). A single dose of PrRP31 palmitoylated at the Lys11 position through a γ-glutamyl linker (palm11-PrRP31; Figure 1.3) again triggered neuronal activation and reduced food intake, indicating its central effects after peripheral administration (Pražienková et al., 2017). This lipidized analogue, palm11-PrRP31, increased neural activity, as evidenced by elevated FosB immunostaining, specifically within the DMN and in VMN (Pirník et al., 2018). Pražienková et al. (2019) also found that palm11-PrRP31 had improved bioavailability (Pražienková et al., 2019).

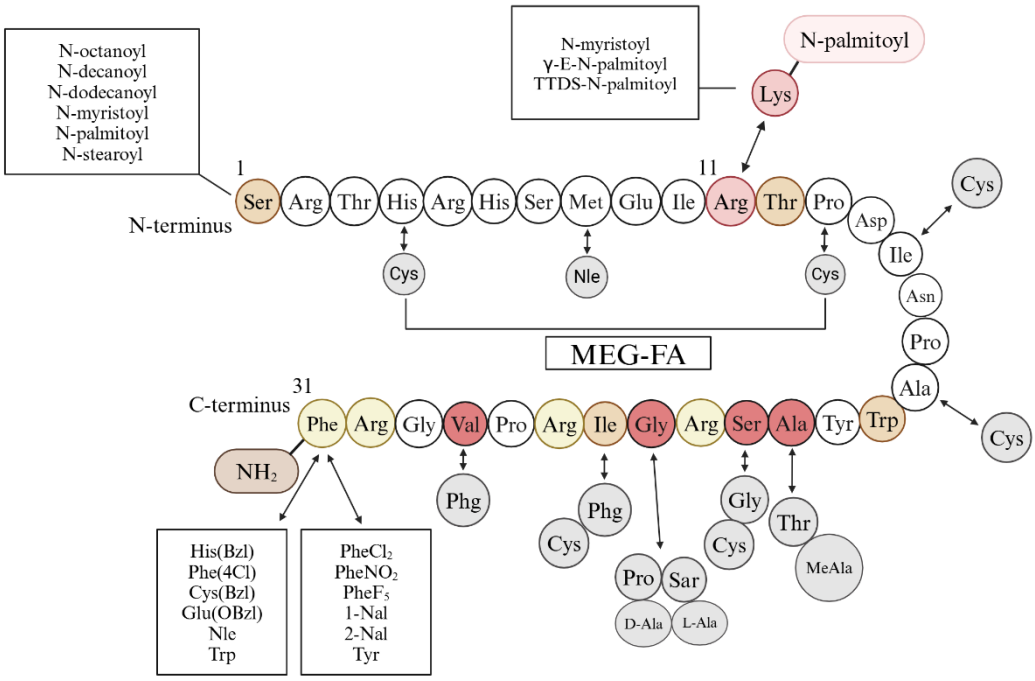

Figure 1.3. Structure of PrRP20 and PrRP31 and its analogues. Amino acid sequence of PrRP analogues. Orange marked Ser marks the beginning of PrRP31 from the N-terminus. Orange-Thr marks the beginning of shorter isoform PrRP20. Orange-Trp marks tridecapeptide PrRP, and orange-Ile marks the shortest fragment heptapeptide PrRP as previously described by Pražienková et al. (2019). Beige amide group NH_2 and yellow marked Arg23, Arg26, Arg30, and Phe31 are essential for the peptide functionality. The yellow marked amino acids represent the amino acids that can be changed and yet preserved good functional activity. Pink marked Arg11 could be substituted by Lys11 and its secondary amino group, fatty acids, were attached through different linkers. γ-E: γ-glutamic acid, MEG-FA: multiple ethylene glycol-fatty acid (four ethylene glycol units attached to octadecanedioic acid via lysine linker incorporating carboxylated moiety), PheCl2: (3,4-dichlor)phenylalanine, PheNO2: (4-nitro)phenylalanine, PheF5: pentafluoro-phenylalanine, 1-Nal, 2-Nal: napthylalanine, Phg: phenylglycine, TTDS: short chain of polyethylene glycol (1,13-diamino-4,7,10-trioxadecan-succinamic acid). Orange-Lys with pink N-palmitoyl (N-γ-E) shows the LiPrRP (palm11-PrRP31) changed structure used in the experiments in this study. Figure and legend modified from Pražienková et al. (2019). Figure made in BioRender (Biorender.com).

A subsequent study examined the potential rebound effect after discontinuation of chronic subcutaneous administration of palm1-PrRP31 (Holubová et al., 2018). In the study, one group of DIO mice received s.c. injections of palm11-PrRP31 for 28 days, while another group was administered palm11-PrRP31 for 14 days, followed by saline injections for the subsequent 14 days. As anticipated, prolonged administration of the treatment for 28 days substantially reduced the body weight of the mice. Notably, a comparable reduction in body weight was

observed in the mice that received the palm11-PrRP31 analogue for 14 days, followed by saline injections for the subsequent 14 days. Interestingly, there was no subsequent weight gain during the 14 days saline administration (Holubová et al., 2018). Holubová et al. (2018) here further revealed that prolonged administration of the lipidized PrRP analogue, palm11-PrRP31, for 28 days did not elicit significantly greater weight loss compared to the 14 day treatment regimen. Notably, withdrawal of palm11-PrRP31 after 14 days of treatment did not result in a rebound weight gain, as the reduction in body weight and subcutaneous adipose tissue to body weight ratio was comparable to that seen with the 28 day continuous treatment (Holubová et al., 2018). This showed promising and long-lasting anti-obesity potential after two weeks administration.

Similarly, several rat DIO models exhibited comparable trends, demonstrating reductions in food intake, body weight, and improvements in metabolic markers such as decreased glucose, leptin, and insulin levels. Furthermore, the degradation of palm-PrRP31 was examined in rat plasma, revealing its stability was prolonged to 24 hours compared to the 10-20 minute half-life of native PrRP31 (Maletínská et al., 2015). This enhanced stability may account for the long-lasting anorexigenic effects of the compound. The prolonged stability is likely due to the compound's association with circulating plasma proteins, facilitated by the attached fatty acid moieties, similar to the mechanism seen with the GLP-1 analogue, LIRA (Maletínská et al., 2015).

All suggesting that the lipidized form of PrRP, palm11-PrRP31 (LiPrRP), has an increased stability, increased half-life, increased affinity to its receptor, slower biodegradation, elicit responses after peripheral administration, and has shown therapeutic potential as it decreased body weight by 15% compared to controls after subcutaneous administration for 14 days in DIO mice (Maletínská et al., 2015; Pražienková et al., 2019).

Although direct evidence is lacking, some indirect evidence suggests that the lipidized form of PrRP, palm-PrRP31, may be able to cross the BBB and exert its effects directly within the brain (Figure 1.4. shows the proposed actions of palm-PrRP31/LiPrRP; Maletínská et al., 2015). Firstly, the pattern of neuronal activation (as measured by c-Fos) observed after peripheral administration of palm-PrRP31 was similar to that seen with i.c.v. administered natural PrRP into the brain at a dose causing an anorexigenic effect (Lawrence et al., 2000). Secondly, the anorexigenic effects were only observed with peripherally administered lipidized PrRP, not the unmodified peptide (Maletínská et al., 2015). Finally, the anorexigenic effects of lipidized PrRP were associated with increased neuronal activation in specific brain regions involved in regulating food intake and energy balance, including those containing GPR10 and NPFF2

receptors (Maletínská et al., 2015). Overall, these indirect lines of evidence suggest that the lipidized PrRP can after peripheral administration act within the CNS. The only direct way to show that LiPrRP can cross BBB would be by labelling it via a short hemaglutinin (HA)-tag, flourophore or by isotopes and thereafter detecting it in the MBH after peripheral administration.

Importantly, peripheral administration of LiPrRP did not cause any side effects such as sedation (open field test), analgesia (hot plate test) or anxiety (elevated plus maze). The behavioural tests were performed at the time and the doses of the maximal anorexigenic effect of LiPrRP (Maletínská et al., 2015; Prazienkova et al., 2016). Suggesting that LiPrRP is an efficacious and safe potential anti-obesity treatment (Maletínská et al., 2015).

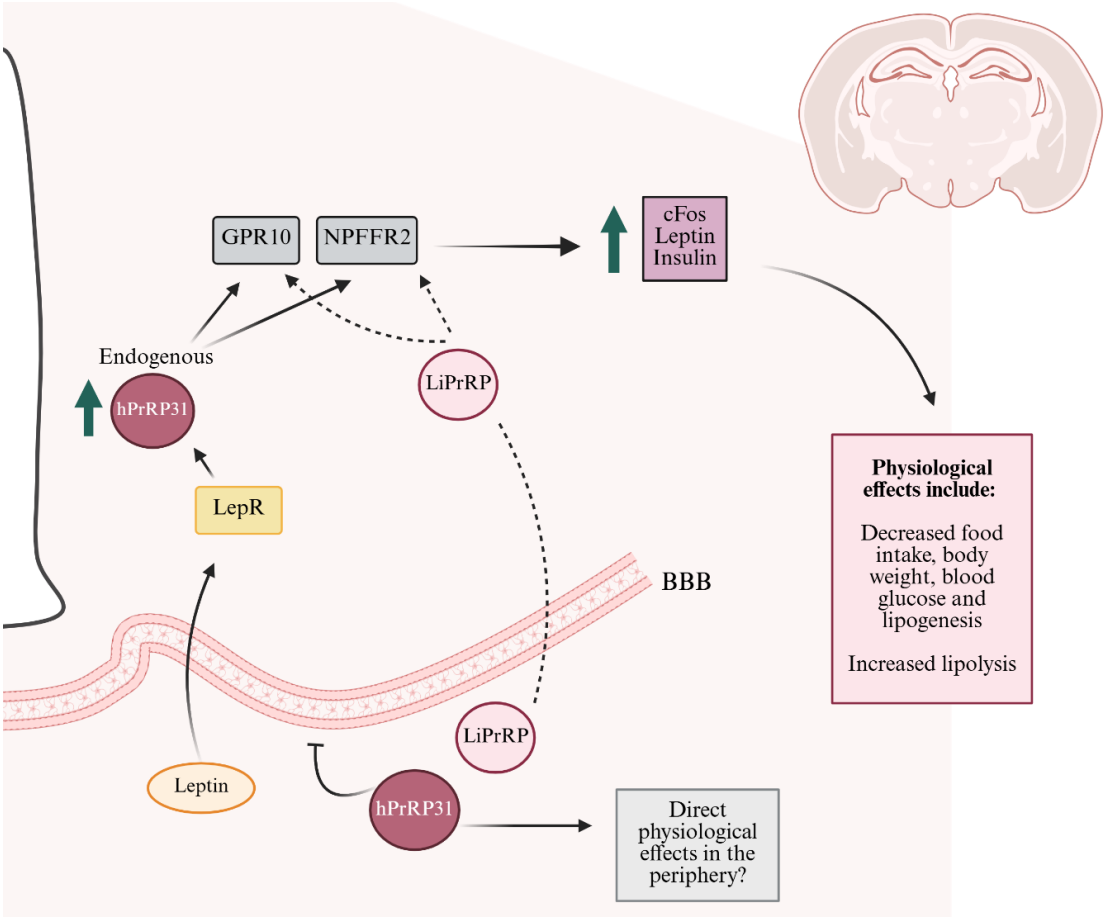

Figure 1.4. Proposed actions of the lipidized analogue of PrRP. Central and peripheral actions of natural PrRP31 and the palmitoylated analogue. Natural PrRP cannot act centrally after peripheral administration. LiPrRP stimulates anorexigenic pathways in the hypothalamus. LiPrRP has been described to work in synergistic action with the anti-hunger hormone leptin. Figure adapted from Mráziková et al. (2021). Figure made in BioRender (Biorender.com).

1.5. Exercise and adult neurogenesis

1.5.1. Impact of exercise on adult neurogenesis in the hippocampus

In the DG of the hippocampus new neurons are generated from neural stem cells. Around 9,000 new cells are generated daily in the rodent hippocampus, with approximately 80%–90% of these differentiating into neurons (Cameron & McKay, 2001). This process of adult hippocampal neurogenesis involves three key developmental stages over 4 to 6 weeks: cell proliferation, differentiation, and functional maturation. The newborn neurons then migrate from the SGZ to the granule cell layer of the DG, where they become integrated into the local neural circuitry as mature granule cells (Duan et al., 2008; Baek, 2016).

Exercise has been demonstrated to markedly enhance adult hippocampal neurogenesis, doubling the generation of new neurons (Praag et al., 1999; Clark et al., 2009). This effect may represent a critical mechanism by which exercise elicits improvements in various brain functions. Exercise positively influences multiple stages of new neuronal maturation, including stimulating cell proliferation, improving survival, and promoting differentiation in the DG. Furthermore, the exercise-induced increase in adult hippocampal neurogenesis plays a crucial role in learning, memory, and neural plasticity (Praag et al., 1999). In rodents, voluntary exercise increases the generation of new cells in the SGZ of the hippocampus in both young and older animals (Praag et al., 1999). Furthermore, voluntary exercise for a duration of three weeks enhances the survival of newly developed neurons within the hippocampus (Praag, 2008).

Multiple studies have demonstrated that 10 days of voluntary wheel running enhanced cell genesis in individually housed rodents (Allen et al., 2001; Borght et al., 2006). Furthermore, Kronenberg et al. (2006) reported that cell proliferation peaked after 3 days of running and remained significantly elevated at 10 days, although the pro-proliferative effect had returned to baseline by 32 days of running. This suggests that prolonged running leads to a transient peak in cell proliferation. Notably, the number of immature neurons continued to increase at the 32-day time point (Kronenberg et al., 2006). Early work by Praag et al. (1999) examined the potential relationship between running distance and hippocampal neurogenesis in mice. In their studies using individually housed C57Bl/6 mice, which displayed minimal variation in running activity, no clear correlation was observed. However, a subsequent investigation by (Allen et al., 2001) utilising a different mouse strain, the 129SvEv, revealed a wide range of individual differences in wheel running behaviour and a significant positive association was identified between cell proliferation/survival and the distance run by the animals (Praag, 2008).

This suggests that the extent of the effects of exercise on hippocampal neurogenesis can vary depending on the mouse strain and large individual differences in running behaviour.

Although adult neurogenesis is well established in laboratory mice and rats (Kempermann et al., 1998; Praag et al., 1999; Praag et al., 2005; Kronenberg et al., 2006; Praag et al., 1999; Meshi et al., 2006), one study on wild long-tailed wood mice have shown that voluntary running and environmental changes did not influence hippocampal neurogenesis in these wild rodents (Häuser et al., 2009). While adult hippocampal neurogenesis has been linked to improved spatial learning and memory, the complete elimination of adult hippocampal neurogenesis has also been shown to have minimal or no effects on a wide range of behavioural measures in mice (Meshi et al., 2006). Importantly, wild wood mice exhibited no changes in hippocampal cell proliferation, neurogenesis, or apoptosis with voluntary running, suggesting their neurogenesis is resistant to environmental influences. This implies that running may only enhance neurogenesis when mice are kept in confined, sedentary conditions. However, the lab mice may indeed represent a good model for the current sedentary lifestyle of our society.

1.5.2. The effect of HFD and running in the hippocampus

High fat diets and metabolic disorders, including obesity and T2DM, have been shown to suppress adult hippocampal neurogenesis (Robison et al., 2020). A study by Park et al., (2010) revealed that HFD feeding for 7 weeks substantially reduced the generation of new cells in the DG region of the hippocampus, without any neuronal loss in rodents. This was attributed to elevated lipid peroxidation and diminished levels of BDNF (Park et al., 2010). Another study by Robison et al. (2020) revealed that in control conditions, female mice exhibited higher levels of cell proliferation (Ki67) and neuroblast/immature neuron (DCX) generation within the hippocampus compared to male counterparts. However, prolonged exposure to a HFD reduced these measures in females to levels comparable to males. Interestingly, the HFD did not impact neurogenesis in male mice. Furthermore, the number of proliferating cells and immature neurons was inversely associated with weight gain and glucose intolerance, but only in the female mice. Notably, these effects were most pronounced in the dorsal hippocampus, a region integral to cognitive functioning (Robison et al., 2020). Similarly, Lindqvist et al. (2006) showed that just 4 weeks HFD feeding decreased hippocampal neurogenesis in male, but not female, rats (Lindqvist et al., 2006).

Crucially, exercise has been shown to reverse the negative effects of HFD on adult hippocampal neurogenesis. The study by Klein et al. (2016) explored the effects of various

HFD and exercise regimes in the hippocampus of female mice. They discovered that 12 weeks of HFD impaired flexible memory expression when initiated in adolescent sedentary mice, but not in young adult mice. However, this impairment was successfully prevented by concurrent exercise. Furthermore, long-term physical exercise (12 weeks) led to accelerated spatial learning during the acquisition period, which was accompanied by increased numbers of newborn mature neurons in both HFD and control diet runners. The researchers concluded that adolescent mice are specifically susceptible to the detrimental effects of HFD. Therefore, physical exercise, by modulating adult neurogenesis in the hippocampus, may represent a potential preventive approach for treating cognitive impairments associated with adolescent obesity (Klein et al., 2016). Additionally, a study (Han et al., 2019) also revealed that a 23-week HFD regimen led to substantial increases in weight gain and hepatic triglyceride levels, which were subsequently reversed by 23 weeks of treadmill exercise. Furthermore, the exercise intervention enhanced hippocampal neurogenesis in the HFD fed mice and improved their memory function, as assessed in a water maze test (Han et al., 2019).

1.5.3. The effect of HFD and running in the hypothalamus

The hypothalamus demonstrates a high degree of plasticity and can respond to peripheral changes. As such, exercise may influence adult neurogenesis within this brain region. Indeed, one study by Klein et al. (2019) found that 12 weeks of a HFD increased the number of new neurons in the ArcN and their rate of maturation into POMC-expressing neurons. These results aligned with those of another study (Gouazé et al., 2013) that reported an increased number of POMC-expressing neurons in response to HFD. Furthermore, Klein et al. (2019) showed that while diet alone had no effect on general cell proliferation (Ki67+) in the ArcN, exercise specifically increased the number of Ki67-positive cells in HFD-fed mice, but not in controls. However, they found no change in long-term cell survival as measured by BrdU labelling. This analysis may have been hampered by the BrdU being administered at the start of the 12-week period, resulting in a pool of cells of mixed ages. Moreover, in other hypothalamic nuclei, the number of newly generated cells was significantly reduced by exercise in control conditions (Klein et al., 2019). This suggests that the influence of running on cell proliferation may be specific to different hypothalamic regions. Another study by Niwa et al. (2015) showed 5-7 weeks of voluntary running led to beneficial effects in stroke-prone spontaneously hypertensive (SHRSP) rats. Exercise markedly increased both overall cell proliferation (BrdU+ cells) and adult neurogenesis in the ArcN and ME of both wild-type and SHRSP rats, compared to Sedentary controls (Niwa et al., 2015). Notably, even in the sedentary state, SHRSP rats

displayed increased levels of cell proliferation and neurogenesis relative to their wild type counterparts (Niwa et al., 2015). Furthermore, Laing et al. (2016) demonstrated that a 12-week HFD significantly reduced the number of POMC expressing neurons in male mice, but this detrimental effect was effectively reversed by exercise. Additionally, HFD administration substantially diminished leptin-induced signal transducer and activator of transcription 3 phosphorylation (pSTAT3) signals in the ArcN and VMN, that was improved by voluntary exercise training, indicating that running improved central leptin signalling (Laing et al., 2016). The HFD group exhibited a significant reduction in Ki67-positive proliferating cells within the MBH, but this was reversed by voluntary exercise. Furthermore, TUNEL assay analysis revealed increased apoptosis in the ArcN of the hypothalamus in the HFD group. Notably, voluntary exercise significantly mitigated this diet-induced neuronal cell death, suggesting a protective mechanism by which exercise can ameliorate the detrimental effects of a HFD (Laing et al., 2016). According to a study by Borg et al. (2014), 7 days of forced running led to a 3.5-fold increase in hypothalamic cell proliferation compared to sedentary mice, and this effect was maintained even in DIO mice. However, blocking cell proliferation through AraC administration did not affect food intake, insulin action, or body mass in obese mice, suggesting that the proliferation of new neurons is not required for exercise training to maintain whole-body homeostasis (Borg et al., 2014).

The studies reviewed indicate that the hypothalamus exhibits a high degree of plasticity and can respond to peripheral changes, such as diet and exercise. A HFD has been shown to increase the number of new neurons and their maturation into POMC-expressing neurons in the ArcN. However, prolonged HFD exposure can also reduce the number of POMC neurons and cell proliferation in the hypothalamus. Importantly, voluntary exercise appears to have a protective effect, reversing the detrimental impacts of HFD on hypothalamic neurogenesis, cell proliferation, and neuronal survival. These findings suggest that exercise can ameliorate the negative effects of DIO on hypothalamic neuronal function and energy homeostasis.

However, there is a gap in our knowledge regarding the effects of short-term voluntary running on hypothalamic neurogenesis in control and HFD conditions. The only current study examining the impact of short-term exercise on hypothalamic neurogenesis utilised forced running (Borg et al., 2014), which is a stressful paradigm for mice (Leasure & Jones, 2008) and could therefore influence the outcomes. Moreover, surprisingly, no studies have employed lineage tracing techniques to investigate the origin and fate of newly generated neurons in the context of running.

1.6. Aims:

The hypothalamus is a crucial brain region for regulating energy homeostasis, as neurons within the MBH sense metabolic and hormonal signals to control appetite and body weight. Anti-obesity compounds can reduce appetite and body weight by targeting these MBH neurons (Tak & Lee, 2021). However, several anti-obesity drugs previously approved for clinical use have been later rejected due to severe side effects such as foetal toxicity, nausea, or depression (Patel & Stanford, 2018; Saunders et al., 2016). Additionally, approved drugs for obesity act only acutely, with patients rapidly regaining weight after terminating treatment, highlighting the need for novel neuroactive anti-obesity compounds. Lipidized analogues of prolactin-releasing peptide, LiPrRP, represent a promising new class of anti-obesity agents with potent appetite-suppressing and weight-lowering effects. Given the importance of adult neurogenesis in the hypothalamus for energy balance regulation, this study hypothesised that anti-obesity compounds like LiPrRP may exert their effects, at least partially, by influencing the cellular and molecular processes of hypothalamic adult neurogenesis, similar to the mechanisms of antidepressants (Eisch & Petřík, 2012; Malberg et al., 2000; Santarelli et al., 2003). To test this, LiPrRP and the GLP-1 receptor agonist LIRA was administered to mice on a HFD to examine the impact on hypothalamic adult neurogenesis.

In contrast to anti-obesity compounds, we also explored the effects of physical exercise, as a physiological intervention, on hypothalamic adult neurogenesis. Only a handful of studies have previously investigated the role of exercise on the hypothalamus and none have reported the effects of short-term voluntary running or lineage traced hypothalamic stem cells. Given the importance of adult neurogenesis in the hypothalamus for energy balance regulation, this study hypothesised that exercise ameliorate HFD induced obesity by influencing cellular and molecular processes of hypothalamic adult neurogenesis, similar to the mechanism by which it reverse HFD induced impaired neurogenesis in the hippocampus (Han et al., 2019; Klein et al., 2016). By examining the impact of voluntary exercise on hypothalamic neurogenesis in both short-term and long-term protocols, using BrdU labelling in combination with inducible GLAST-CreER^{T2} mouse line this study aimed to examine the impact of exercise on hypothalamic adult neurogenesis.

To elucidate the effects of DIO, voluntary exercise, and anti-obesity treatment on hypothalamic neuronal stem cells, this study exposed adult mice to a HFD, together with LiPrRP, or voluntary wheel running. The influence on proliferation and self-renewal of adult neural stem cells, as well as the effects on differentiation, specification, and survival of adult-generated neurons was

assessed. Additionally, human induced Pluripotent Stem Cells were used to study neuronal specification after exposure to LiPrRP.

This study aimed to: 1) investigate how LiPrRP influenced adult neurogenesis in the hypothalamus and hippocampus under short- and long-term exposure to an obesity-inducing diet; 2) determine how LiPrRP affected the fate specification of hypothalamic-like neurons generated from human induced pluripotent stem cells; and 3) elucidated the effects of short-term and long-term voluntary running, in the context of diet-induced obesity, on neurogenesis in the hypothalamus compared to the hippocampus.

Chapter 2: Material and Methods

2.1. Animals

2.1.1. Husbandry

Animal experiments were performed either in the United Kingdom (UK) or in the Czech Republic. All experimental procedures in the in UK were performed in accordance with the local ethical and Home Office approval under the UK Animals (Scientific Procedures) Act 1986 (ASPA). All animals were housed in diurnal light conditions (12 hours light, 12 hours dark) and received food and water *ad libitum*. Mice were weaned 4 weeks post birth and kept in cages of no more than five animals per cage. All mice were 6-8 weeks old at the start of the regulated procedures. All C57BL/6J mice were purchased from Charles River Laboratories, UK. In the Czech Republic, all animal experiments followed the ethical guidelines for animal experiments and the Act of the Czech Republic Nr. 246/1992 and were approved by the Committee for Experiments with Laboratory Animals of the Academy of Sciences of the Czech Republic. C57BL/6 male mice that were 4 weeks old were obtained from Charles River Laboratories (Sulzfeld, Germany). Mice used for all running experiments, and *in vitro* experiments using LiPrRP, including time lapse imaging and RNAseq were treated in the UK. Mice used for the 7-day (7d), 21-day (21d), and 4-month (4mo) protocols with BrdU treatment were conducted in the Czech Republic.

2.1.2. GLAST-CreER^{T2} x R26-tdTomato mouse line

The GLAST-CreER^{T2} transgenic mice were developed in Magdalena Götz lab (Mori et al., 2006) and the R26-tdTomato transgenic mice were developed in Hongkui Zeng lab (Madisen et al., 2010). GLAST-CreER^{T2} x R26-tdTomato breeders were generously provided by the lab of Dr. Florian Siebzehnrubl. This mouse line was used to label adult neural stem cells with tdTomato fluorophore to enable lineage tracing of adult born cells. The Glia High Affinity Glutamate Transporter (GLAST), encoded by the Slc1A3 gene, is expressed in Type-1 radial-glia-like cells in the hippocampus, tanycytes in the hypothalamus, and astrocytes residing in the brain. The GLAST-CreER^{T2} knock-in construct in these mice has a partial Slc1A3 gene promoter that drives the expression of the bacteriophage Cre recombinase fused with a modified Estrogen Receptor T2 (Cre-ER^{T2}) in GLAST expressing cells only. The mice also have an ubiquitous Rosa26 (R26) promoter that drives the expression of a modified, red light emitting GFP called tdTomato. However, a stop codon in the DNA sequence between the R26 promoter and the tdTomato cDNA cassette prevents tdTomato expression normally. This stop

codon is floxed by two loxP sites (and can therefore be knocked out) that the Cre recombinase recognizes. When the Cre recombinase enters the cell nucleus, it removes one of the loxP sites, along with the stop codon, allowing the R26 to drive tdTomato expression. But just like the endogenous Estrogen receptor, the Cre-ER^{T2} fusion protein can only move to the nucleus when bound to its ligand. The modified ER^{T2} receptor is not sensitive to Estrogen but to a chemical analogue to Estrogen known as Tamoxifen. So, when Tamoxifen is administered intraperitoneally to mice, the Cre-ER^{T2} can move from the cytoplasm to the nucleus and remove the stop codon from the R26 construct. This, in turn, drives tdTomato expression in GLAST positive stem cells and astrocytes, as well as all daughter cells from tdTomato positive stem cells.

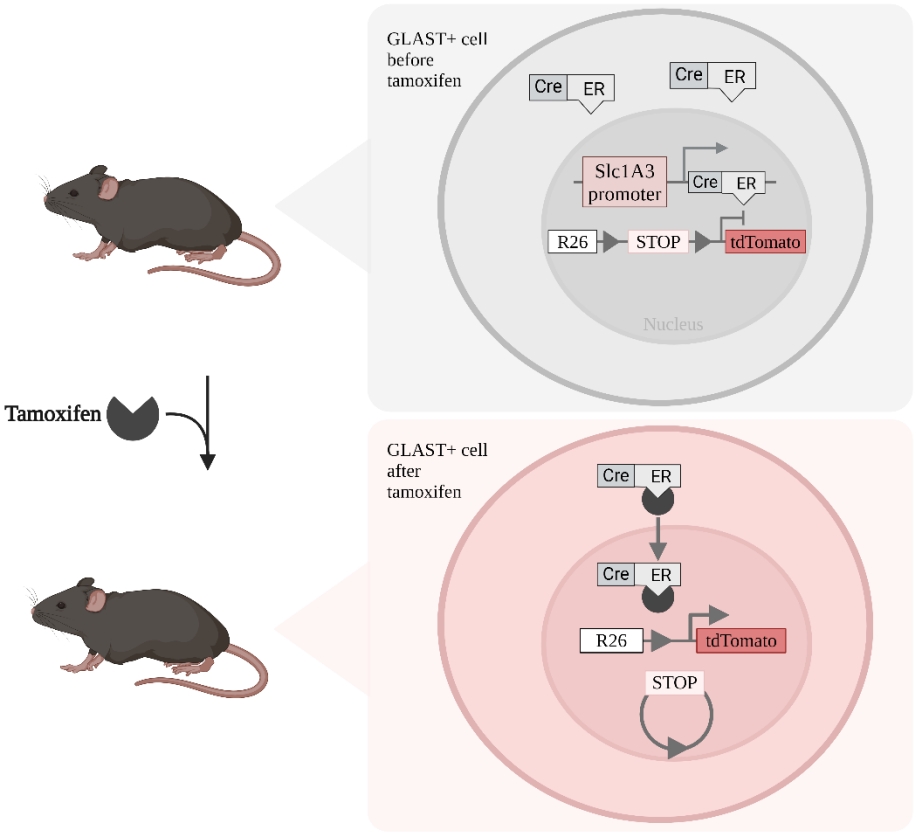

Figure 2.1. Schematic of the GLAST-CreER^{T2} x R26-tdTomato mouse line before and after tamoxifen administration. Grey cell represent GLAST expressing cells before tamoxifen and the pink cell represent GLAST expressing cells and the events in the nucleus after tamoxifen administration. Figure made in BioRender (BioRender.com).

2.1.3. Genotyping

Ear notches from adult mice were obtained and stored at -20°C for genotyping. Genotyping for wild type (WT) and mutant GLAST and R26-tdTomato was conducted. Genomic DNA was extracted from the samples using the MyTaq™ Extract-PCR Kit (Bioline, cat no. BIO-21126). First, a lysis buffer master mix of 5 µl Buffer A, 2.5 µl Buffer B, and 17.5 µl dimethyl pyrocarbonate (DEPC)-treated H_2O were made for each sample. Then, 25 µl lysis buffer master mix was added to each sample. The samples were incubated at 75°C on a heat block for 30 minutes and vortexed in 10 minute intervals. The samples were then incubated at 95°C for 10 minutes to inactivate the protease. The digested solution was spun down for 5 minutes at 10,000 rpm and put on ice. The supernatant was then used directly as the DNA template for the polymerase chain reaction (PCR) using 2x M-PCR OPTI™ mix which includes an optimized Taq Polymerase from the Mouse Direct PCR Kit (Selleckchem). For the PCR reaction, a solution containing 10 µl 2x M-PCR OPTI™ mix, 7.5 µl DEPC-treated H_2O, 0.5 µl specific primers (10 µM), and 1 µl of the extracted DNA template, were combined for a final volume of 20 µl and loaded into a T100 Thermal Cycler (BIORAD). The following cycling program was used:

GLAST:

Lid: 105°C

Step	Degrees	Time
1	95°C	5 minutes
2	95°C	20 seconds
3	60°C	30 seconds
4	72°C	1 minute
	GOTO Step 2, 36x	
5	72°C	5 minutes
6	4°C	Hold

Table 2.1. Cycling program for GLAST.

tdTomato

Lid: 105°C

Step	Degrees	Time
1	95°C	5 minutes
2	95°C	20 seconds
3	50°C	30 seconds
4	72°C	30 seconds
	GOTO Step 2, 36x	
5	72°C	5 minutes
6	12°C	Hold

Table 2.2. Cycling program for tdTomato.

Primer pairs are shown in Table 2.3. PCR products were then separated on a 1-2% agarose gel and visualised using ethidium bromide. The gel was run at 90 Volt (V) for 5 minutes and then at 140 V for 25 minutes. The bands were compared to a 100 base pair (bp) DNA ladder (Biolabs).

Primer name	Fwd./rev.	Product size (bp)	Primer sequence (5' – 3')
R26-tdTomato primers			
ROSA26 WT	Forward	297 bp	AAGGGAGCTGCAGTGGAGTA
ROSA26 WT	Reverse		CCGAAAATCTGTGGGAAGTC
tdTomato	Forward	196 bp	CTGTTCCTGTACGGCATGG
tdTomato	Reverse		GGCATTAAAGCAGCGTATCC
GLAST primers			
GLAST-F8	Forward	WT: 700 bp	GAGGCACTTGGCTAGGCTCTGAGGA
GLAST-R3	WT Reverse		GAGGAGATCCTGACCGATCAGTTGG
GLAST-F8	Forward	Mutant: 400 bp	GAGGCACTTGGCTAGGCTCTGAGGA
CERI	Mutant Reverse		GGTGTACGGTCAGTAAATTGGACAT

Table 2.3. Primer sequences and product size for genotyping. Forward (Fwd). Reverse (Rev). Base pairs (bp).

2.2. Diets

Mice were given either Control diet or HFD. The control diet was purchased from Ssniff Germany with the energy composition of 24% calories from proteins, 7% from fats, and 67% from carbohydrates (#V1535 RM-Haltung, 15 mm pellets).

2.2.1. High Fat Diet

The HFD was prepared following the instructions described previously by Maletinska lab (Maletínská et al. 2015). The diet had energy content of 5.3 kcal/g, with 13% of calories derived from proteins, 60% from fats and 27% from carbohydrates. HFD was made by combining 400 g Sniff base Diet (Ssniff® R/M-H #V1530-000 RM-Haltung, Mehl (ground/powder), Ssniff Spezialdiäten GmbH, Soest, Germany), 340 g of powdered cow-milk-based human baby formula (Sunar Complex 3, Dr Max Pharmacy, Mirakl, a.s., Bratislava, Slovakia), 10 g of Corn

Starch and 250 g of pork lard (Lidl UK, Surbiton, UK). The dry ingredients were first combined in a mixer and the lard was slowly melted in the microwave and gradually poured into the mixture of dry ingrediencies while stirred. The combined liquid and dry ingrediencies were then left to stir on a low stir setting for 15 minutes which was turned up to a high stir setting for another 15 minutes or until it had reached the desired consistency where the resulting dough could be compacted into pellets. Pellets were handmade and stored at -80°C. Enough pellets for one week were thawed in 4°C two days before they were given to the mice. HFD pellets were changed 2-3 times per week.

2.2.2. High fat diet protocols for pharmacological interventions

Short term HFD and LiPrRP (7d): For the short-term HFD and LiPrRP experiments, our collaborators at the Maletínská lab provided isolated brains from control animals (animals on Control diet) or animals subjected to a 7d HFD with or without concurrent injections of LiPrRP (5 mg/kg i.p. daily, n = 5 per group) or LIRA (0.2 mg/kg s.c. daily, n = 5 per group). As a control, LiPrRP vehicle was injected s.c. These animals received two BrdU (150 mg/kg of body weight) i.p. injections 6 hours apart on day 1, followed by a BrdU chase period of 6 days (Figure 2.2A). Brains were cut into 40 μm thick coronal sections using a cryostat and stored in Eppendorf tubes containing 0.1% Sodium Azide (NaN_3) in 1x PBS at 4°C until immunohistochemical staining was performed.

Medium term HFD and LiPrRP (21d): The Maletínská lab provided brains isolated from control animals (animals on Control diet) or animals subjected to a 21d HFD with or without concurrent administration of LiPrRP (5 mg/kg s.c. daily, n = 5 per group) or LIRA (0.2 mg/kg s.c. daily, n = 5 per group). As a control, LiPrRP vehicle was injected s.c. During the first five days, BrdU (10 mg/ml) was given in the drinking water (followed by a 16-day BrdU chase). In the 21d protocols (Figure 2.2B), LiPrRP was also administered to animals on the Control diet. Brains were cut into 40 μm thick coronal sections using cryostat and stored in Eppendorf tubes containing 0.1% NaN_3 in 1x PBS at 4 °C until immunohistochemical staining was carried out.

Long term HFD and LiPrRP (4mo): The Maletínská lab provided isolated brains from control animals and those subjected to 4mo of a HFD with daily LiPrRP injections (5 mg/kg s.c., n = 8 per group) for the last 14 days. As a control, LiPrRP vehicle was injected s.c. BrdU (10 mg/ml) was provided in drinking water during the first 14 days of the final month, followed by a 14-day BrdU chase (Figure 2.2C). These samples were provided by our collaborators at the Maletínská lab. LiPrRP was also given to animals on the Control diet. Brains were cut into 40

μm thick coronal sections using cryostat and stored in Eppendorf tubes containing 0.1% NaN_3 in 1x PBS at 4°C until immunohistochemical staining was carried out.

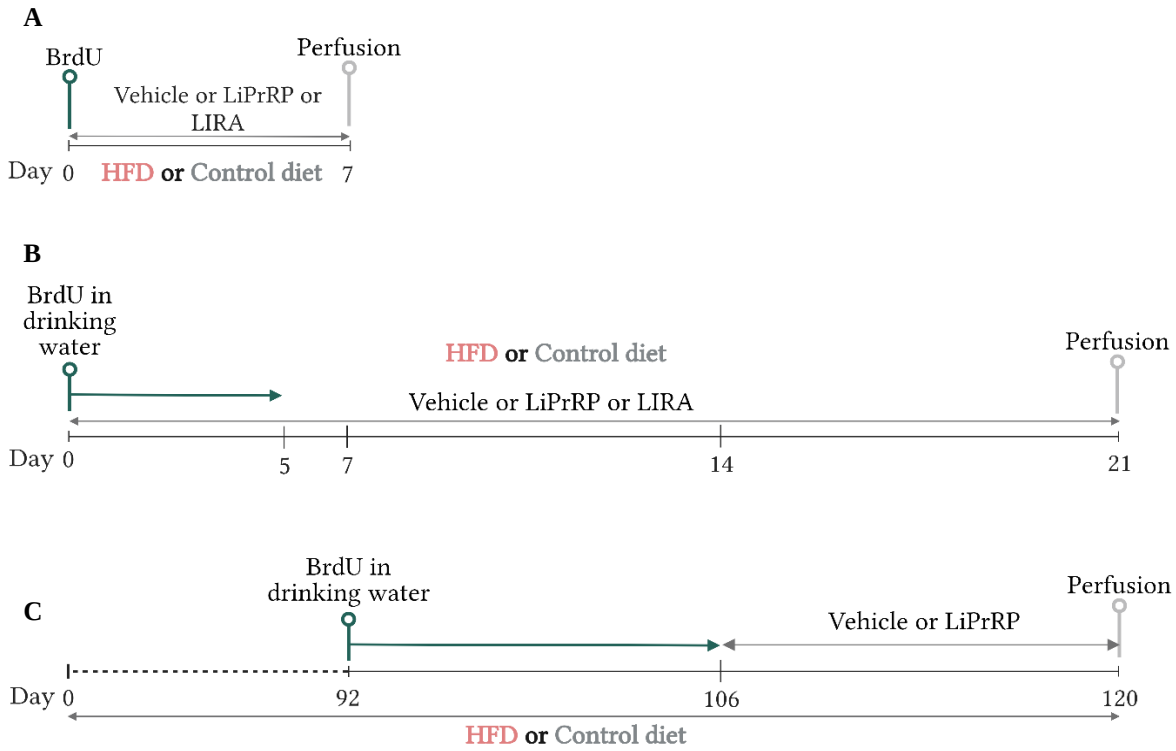

Figure 2.2. Timelines for 7d, 21, and 4mo protocols. Schematic of A) Short term HFD, 7 days of HFD and concurrent LiPrRP with two BrdU injections 6 hours apart on day 1. B) Medium term HFD, 21 days of HFD or Control diet and concurrent LiPrRP, given BrdU in drinking water the first five days. C) Long term HFD, on 4 months HFD or Control diet with or without exposure to LiPrRP (5 mg/kg i.p. daily, n = 8 per group) or LIRA for the last 14 days and BrdU in drinking water was given in the first 14 days of the last month. Figure made in BioRender (Biorender.com).

Two weeks of HFD and LiPrRP: Primary cell cultures for time lapse imaging and neurosphere assays were prepared from male WT C56BL/6j mice on two weeks HFD or Control diet with or without LiPrRP injections (5 mg/kg s.c. daily, n = 3 animals per group; Figure 2.3). The weight of each mouse was recorded at the beginning and end of the experiment as well as every 2 days throughout the protocol duration.

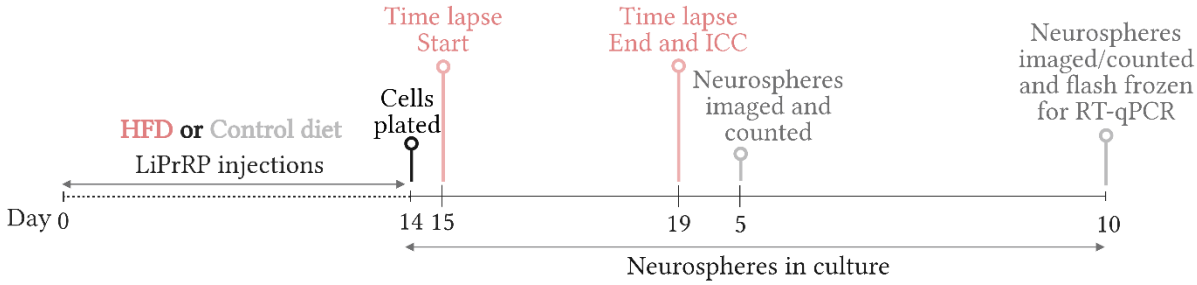

Figure 2.3. Timeline for two week HFD and LiPrRP protocol. Primary cell cultures for time lapse imaging and neurosphere assay were prepared from male WT mice on two weeks HFD or Control diet with or without LiPrRP injections. Figure made in BioRender (Biorender.com).

2.3. Anti-Obesity Drugs

2.3.1. Lipidized Prolactin Releasing Peptide (LiPrRP)

LiPrRP is a human palmitoylated analogue of PrRP that was synthesized at the Institute of Organic Chemistry and Biochemistry, Prague (CAS), as previously described (Prazienkova et al., 2016). Desiccated LiPrRP (M.W. = 4004) was stored at -20°C until reconstituted in the sterile physiological solution (0.9% NaCl, pH = 7.4) as 1 mg/ml concentration (corresponding to approx. 0.25 mM) and aliquoted into protein LoBind tubes (Eppendorf, Stevenage, UK). After LiPrRP was reconstituted, it was kept at -20°C for up to two weeks. A fresh aliquot was thawed each time before administration to animals. Mice received a single s.c. injection of 5 mg LiPrRP/kg of body weight before the onset of the dark cycle.

2.3.2. Liraglutide (LIRA)

Liraglutide (Saxenda, PubChem CID: 16134956, (Cant et al., 2013) was obtained from Pharmacy (Victoza®, Novo Nordisk A/S, Bagsværd, Denmark). Liraglutide works by increasing insulin secretion, it suppresses glucagon secretion, and slows gastric emptying by binding the GLP-1R (Liraglutide, 2020). Liraglutide was administered in physiological solution (40 µg/ml) s.c. daily in 0.2 mg/kg concentration at the Institute of Organic Chemistry and Biochemistry, Prague (CAS).

2.3.3. hPrRP31

Full-length, 31 amino acid long human Prolactin Releasing Peptide (hPrRP31) was used in one time lapse and hiPSC experiment. Purified, desiccated, crystal hPrRP31 (M.W. = 3665.15) was stored at -20°C. Stock solution of 1 mM hPrRP31 in sterile cell culture grade distilled water was added to cell media to the final concentration of 1 μM.

2.4. Running experiments

2.4.1. High fat diet and running protocols

Short HFD and Running (Two weeks): WT C56BL/6j male mice were administered two weeks Control diet or HFD and housed in cages with a vertical running wheel and counter developed and generously provided by Dr. Andrew Want (n = 5 per group). Sedentary animals were held in the same cages with a fixed vertical wheel (Figure 2.4A). Mice were housed in pairs with a clear divider. The divider had holes to allow the mice to smell each other as well as some touch. Mice were given BrdU (10 mg/ml) in drinking water given the first 5 days, with a 9-day BrdU chase. The weight of each mouse was recorded at the beginning and at the end of the experiment due to the configuration of the cages. Brains were cut into 50 μm thick coronal sections using cryostat and stored in Eppendorf tubes containing 0.1% NaN3 in 1x PBS at 4°C until immunohistochemical staining was carried out. This protocol was also used before tissue extraction for time lapse imaging, but without BrdU administration (Figure 2.6).

Long HFD and Running (3mo): Male and female GLAST-CreERT2 x R26-tdTomato mice (n = 5 per group) were administered 3 months (3mo) of Control diet or HFD. Mice were induced by 3 days i.p. tamoxifen injections and placed in the same running cages as described previous (Figure 2.2 B). Mice were given BrdU (10 mg/ml) in drinking water in the first 5 days of the last two weeks with a 9-day BrdU chase (Figure 2.4B). The weight of each mouse was recorded at the beginning and end of the experiments and every two weeks throughout the 3 month protocol. Brains were cut into 50 μm thick coronal sections using cryostat and stored in Eppendorf tubes containing 0.1% NaN3 in 1x PBS at 4°C until immunohistochemical staining was carried out.

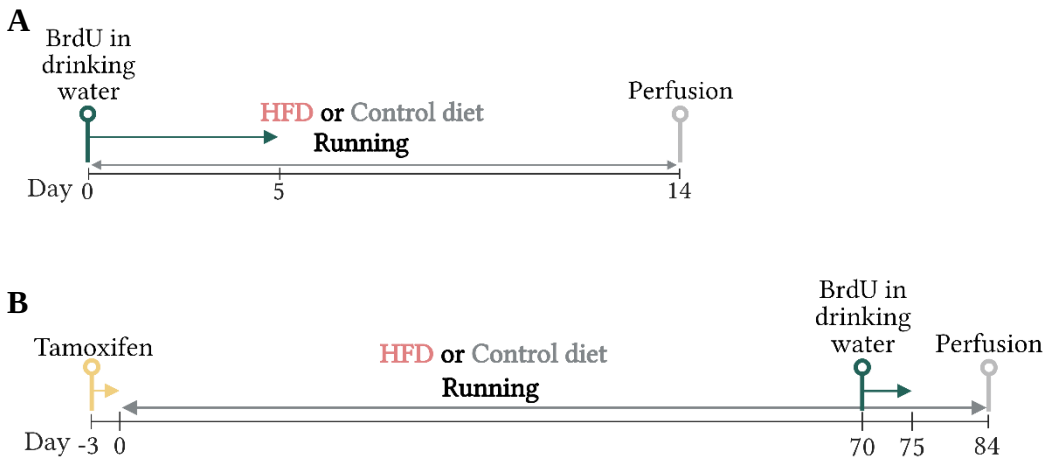

Figure 2.4. High Fat Diet and Running protocols. Schematic of A) Two weeks (14d) HFD and Running. B) 3mo HFD and Running (n = 5 per group). Figure made in BioRender (Biorender.com).

2.4.2. Tamoxifen injections

Tamoxifen powder (M.W. = 371.52) was stored at -20°C. Tamoxifen (ThermoScientific; Cat. No. J63509.03) was diluted in corn oil (Sigma-Aldrich; C8267-500mL; kept sterile at room temperature; 30 mg/ml) and sonicated in a Ultrasonic bath (Grant and administered via i.p. once daily for 3 days in 150 mg/kg body weight.

The modified ER^{T2} receptor is not sensitive to Estrogen but to the chemical analogue Tamoxifen. When Tamoxifen is administered via i.p. to mice, the Cre-ER^{T2} can move from the cytoplasm to the nucleus (Figure 2.1.)

2.4.3. Exercise trackers

Custom tracking equipment was constructed by Dr. Andrew Want to monitor the activity of mice continuously over several days. To reduce isolation stress the cages were constructed to house two mice, separated by a barrier that allowed some social interaction. The barrier was made with small perforations and allowed feeding from a communal food hopper. The divider still allowed the mice to see, smell and interact with each other, while also allowing tracking of running on individual wheels.

Rotations of the wheels were monitored using an infrared sensor (Infrared Obstable Avoidance Sensor Module, 3 wire, Frienda, Frienda-Obstable-431S). The sensor was constructed by Dr. Want from hand cut 3mm Perspex arms secured to a crab clamp (TRIXES Crab Clamp Mount Stand Desk Wall Panel Holder Clip Professional 1/4" and 3/8” Thread), which allowed the

sensor to be mounted outside the cage. The crab clamp allowed for convenient detachment of the sensor for cleaning the cages. The electronic equipment was triggered by the interruption of the infrared beam and the sensors were connected to a Raspberry pi 4B Model B via a breadboard using an electronic circuit designed by Dr. Want. The Raspberry pi was connected to an uninterruptable power supply (Tecnoware UPS ERA PLUS 800 Together On - Uninterruptable power supply). Using a python script, the input from all exercise wheel sensors was tracked simultaneously and the counts of the total number of rotations for each wheel was tracked. At the end of the experiment, all data was collected and processed using RStudio Version 1.2.1335. To account for false positive triggering of the sensors, events with a time interval of 0.275 seconds were excluded. The time interval of the updated results was used to calculate the revolutions per minute (rpm) and kilometres (km) ran.

2.5. Histological analysis

2.5.1. BrdU

Bromodeoxyuridine, BrdU (Sigma-Aldrich, Gillingham, UK) was administrated either by intraperitoneal (i.p.) or in drinking water. For i.p. injections, BrdU (10 mg/ml) was dissolved in the physiological solution (0.9% NaCl, pH = 7.4) and injected as 150 mg/kg of body weight (Petrik et al., 2012). For drinking water, BrdU (1 mg/ml) was dissolved in autoclaved tap water with 1% sucrose (Petrik et al., 2018). BrdU drinking water was protected from light by wrapping the bottles in foil and changed once in the 5 days period.

2.5.2. Perfusion

Animals were euthanized with an intraperitoneal injection of Euthatal. Transcranial perfusion with ice cold 1x phosphate buffered saline (1xPBS; Thermo-Fisher Scientific, 18912014) was followed by ice cold 4% paraformaldehyde (PFA; Sigma-Aldrich, 252549) using a compact pump (World Precision Instruments, Peri-Star Pro). The 1xPBS was used to flush out the blood for 5 minutes (5 ml/minute), followed by 15 minutes of cold 4% PFA (5 ml/minute). The mice were decapitated, and the skull was exposed. Brains were then isolated from the scull by carefully making a straight cut from the brainstem to the rostral part of the brain to uncover the olfactory bulb and the overlapping skull fragments were manually removed carefully by forceps. The brain was then carefully removed without damaging the hypothalamus and post fixed overnight in 4% PFA at room temperature (RT). The brains were the next day transferred into 30% sucrose solution (30% sucrose, 0.1% NaN_3 in 1xPBS) and let to sink and kept in 4°C awaiting cryostat cutting in 4°C. Brains were cut into 40 μm (LiPrRP experiments) or 50 μm (Running experiments) thick coronal sections using cryostat (Observer.Z1 Zeiss LSM780) and

stored in Eppendorf tubes containing 0.1% NaN3 in 1xPBS at 4°C until immunohistochemical staining was carried out. Slide-mounted immunohistochemistry (IHC) was performed.

2.5.3. Immunohistochemistry

The brain sections were mounted and immunohistochemically stained following an established protocol by Dr Petrik (Petrik et al., 2012). Mounted sections were pre-treated with 2.5 N Hydrochloric acid (HCl; Sigma-Aldrich, ACS reagent 37%, 258148-2.5L), prepared fresh from 12 N saturated stock of HCl diluted in 1xPBS, for 30 minutes at room temperature (RT). The sections were neutralised using 0.1 M Na-Borate (Na2B4O7; Sigma-Aldrich, 221732; pH = 8.5) for 10 minutes, pH adjusted to 7.4 by 5-minute incubation of 1xPBS, then blocked with the carrier (3% bovine serum albumin; Sigma-Aldrich, A7030; 0.5% TritonTM X-100; Sigma Aldrich, T9284; in 1x PBS, pH = 7.4) for 30 minutes and incubated overnight at RT with primary antibodies. The primary antibodies used can be found in table 2.4. The next day the slides were washed three times with 1xPBS (5 minutes each), followed by 2 hours of secondary antibody incubation (1:300) at RT (using parafilm to ensure the slides did not dry out). After another three washes with 1xPBS (5 minutes each) the sections were stained with 4′,6-diamidino-2-phenylindole (DAPI; 1:1000; Roche) for 10 minutes. DAPI was used as nuclear stain. After 3 washes with 1xPBS (5 minutes each), the slides were briefly dried and cover-slipped using ProLong Diamond antifade mountant (InvitrogenTM; P36970). The staining was visualised using confocal microscopy (Observer.Z1 Zeiss LSM780).

For Ki67 stained sections Sodium Citrate (10mM tri-sodium citrate; Sigma-Aldrich W302600-1kg-k, pH = 6.0 plus 0.03% Triton X-100) in 70°C (15 minutes) was used instead of HCl as antigen retrieval. The sections were cooled down and pH adjusted to 7.4 by 5-minute incubation of 1xPBS, then blocked with the carrier (1x PBS, 0.5% Triton X-100, 5% normal donkey serum; Sigma-Aldrich, S30-100ML) for 30 minutes and incubated overnight at RT with primary antibodies.

Antibody	Dilution; Supplier
Rat monoclonal anti-BrdU	1:400; MCA6144 BioRad, Watford, UK
Mouse monoclonal anti-NeuN	1:500; MAB377 Thermo
Rabbit polyclonal anti-GFAP	1:500; Z0334 Agilent/Dako, Stockport, UK
Mouse monoclonal anti-HuC/HuD	1:500; A21271 Thermo
Mouse monoclonal anti-Ki67	1:400; CPCA-Ki67-100ul EnCor Biotechnology/2BScientific, Upper Heyford, UK
Rabbit polyclonal anti-GPR10 receptor	1:200; PA5-29809 Thermo Scientific, Paisley, UK
Rabbit polyclonal anti-activated caspase 3(AC3)	1:500; 9661S Cell Signalling, Leiden, The Netherlands
Guinea pig polyclonal anti-Doublecortin (DCX)	1:400; AB2253 Thermo
Rabbit polyclonal anti-NPFF2 receptor	1:200; ab1420 AbCam, Cambridge, UK
Chicken polyclonal anti-MAP2	1:400; a92434 AbCam
Mouse monoclonal anti-beta-III-Tubulin	1:400; ab14545 AbCam
Goat polyclonal anti-Vimentin	1:50; ab1620 Chemicon, Watford, UK
Mouse monoclonal anti-PCNA	1:300; M087901-2 Agilent
Guinea pig polyclonal anti-RAX	1:200; M229 Takara Bio Europe Ab, Goteborg, Sweden
Rabbit anti-NPY	1:600; GR8284305-1 Abcam
Mouse anti A1H5 (POMC)	1:5000 for ICC 1:800 for IHC Developed and generously provided by the lab of Dr Anne White
Goat anti-Sox2	1:300; AF2018 Bio-Techoe
Rabbit polyclonal anti-FOXG1	1:500; AB18259 Abcam
Mouse monoclonal anti-Nkx2.1	1:500; MAB5460 Millipore

Table 2.4. Primary antibody dilutions and distributors.

2.5.4. IHC quantification

Quantification was performed in the Medial Basal Hypothalamus (MBH), including the VMN and DMN, ArcN and ME, as well as the ArcN and ME alone, and the SGZ of the hippocampus was done stereologically (Figure 2.5). Graphs marked with MBH or Parenchyma + ME (4mo group) includes analysis of VMN, DMN, ArcN and ME. If an nuclei was individually analysed the graph was marked accordingly. All images were taken in a sequential scanning mode (z-

stacks) to identify superposed cell nuclei. Z-stack images were obtained in the ZEN Blue software (Zeiss) using 10X, 20X or 40X apochromatic objectives on the Observer.Z1 Zeiss LSM780 confocal microscope. All coronal sections from one well in the series of 12 were stained as described above. The sections containing the hippocampus (around bregma −0.6 to −4.0 mm) and MHB (around bregma −1.2 to −2.3 mm (Paxinos & Franklin, 2004) was analysed as tanycytes are present from bregma −1.3 to −2.5 mm (Pasquettaz et al., 2020). The area of each region mentioned above was measured in the ZEN software in 2–4 brain sections and multiplied by the brain section thickness to obtain the volume. Cell density was quantified as number of cells per mm cubic of tissue.

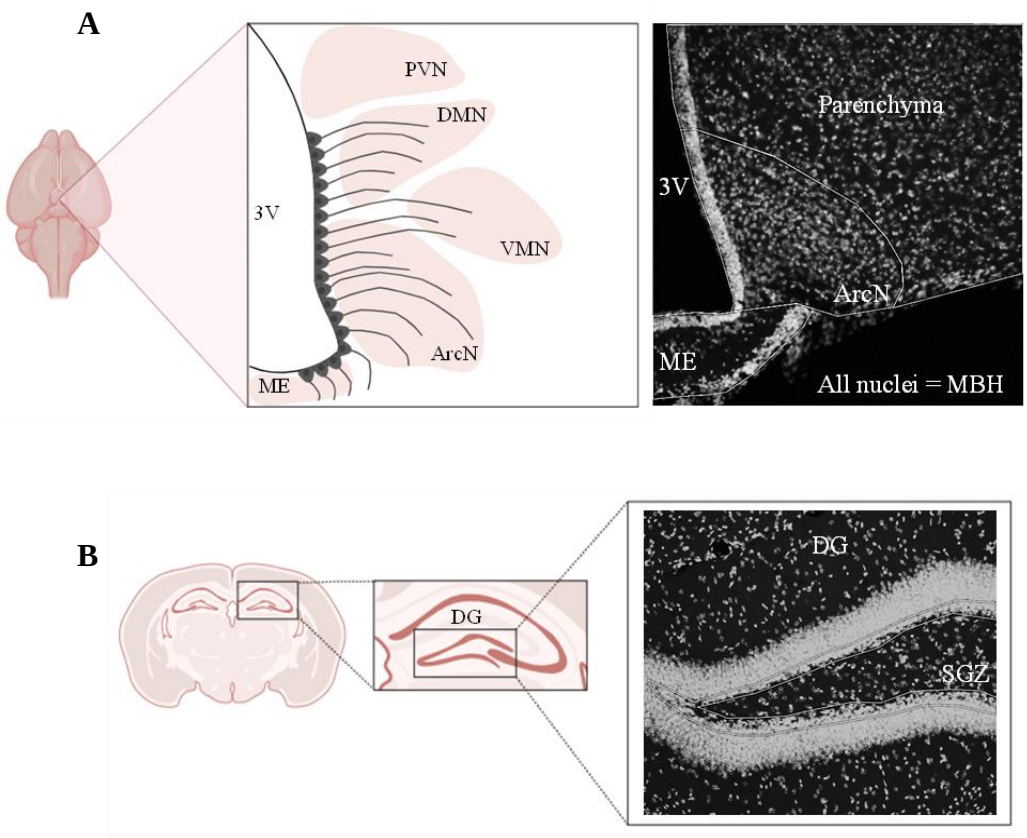

Figure 2.5. Quantification of the Medial Basal Hypothalamus (MBH). A) MBH includes the Parenchyma (VMN and DMN) as well as the ArcN and ME. The ArcN and ME was also analysed individually. B) The Subgranular Zone (SGZ) of Dentate Gyrus (DG) of the hippocampus.

2.6. Cell culture

2.6.1. Tissue generation for cell cultures

Primary cell cultures were prepared from adult male WT C57Bl/6J mice. Mice were given Control diet or HFD for 14 days with or without concurrent administration of LiPrRP daily s.c. injections or vertical running wheels (Figure 2.6B). Tissue from the hypothalamic neurogenic niche was isolated for time lapse imaging and neurosphere assays (Full workflow in Figure 2.7).

Additionally, primary cells from untreated male C57Bl/6J mice were exposed to LiPrRP *in vitro* (1 µM added every day) during the first 3 days of the culture and time lapse imaged for the following 4 days or grown as neurospheres for 10 days (Figure 2.6A).

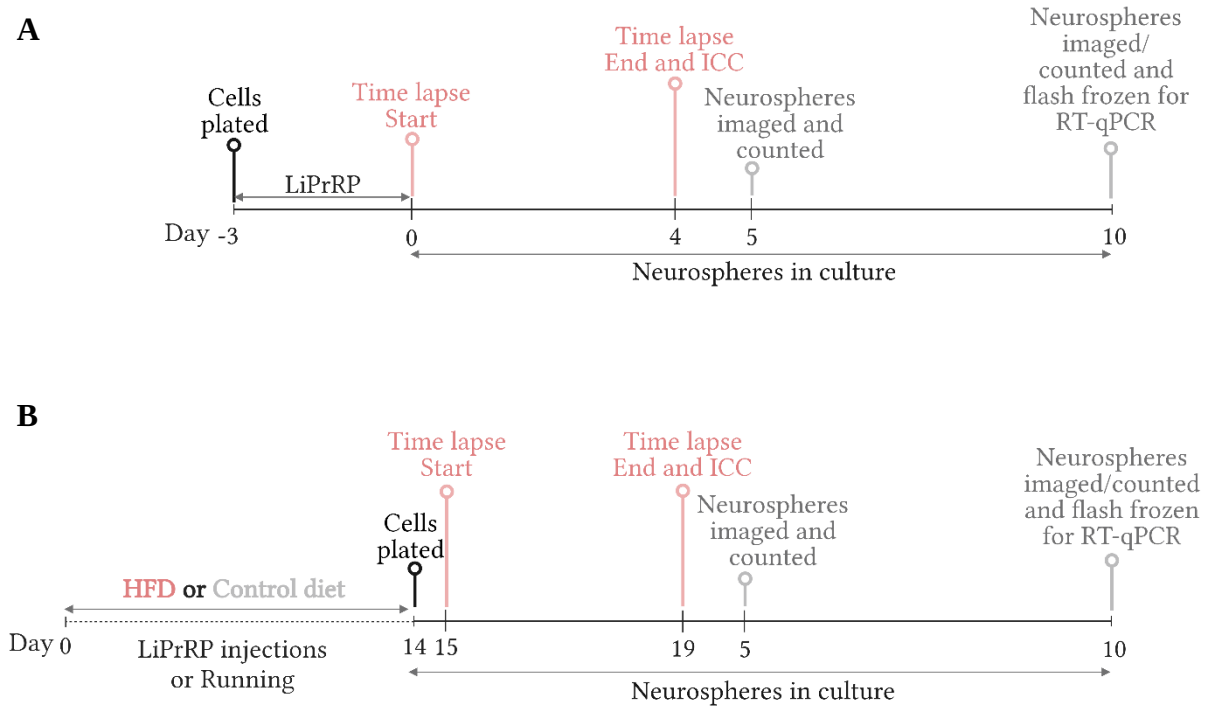

Figure 2.6. Timeline for primary cell cultures used in time lapse and neurosphere assays. A) Primary cells from untreated mice were exposed to LiPrRP in vitro (1 µM added every day) during the first 3 days of the culture and time lapse imaged for the following 4 days or grown as neurospheres for 10 days. B) Mice were given Control diet or HFD for 14 days with or without concurrent administration of LiPrRP daily s.c. injections. After tissue extraction, primary cell cultures were time lapse imaged for the following 4 days or grown as neurospheres for 10 days.

Removal and dissection of the brain:

Adult male mice (6-7 weeks old) were culled by cervical dislocation and decapitated. The surface of the skull was revealed by reflecting the skin. The fur was sprayed with 70% ethanol (EtOH) before cutting the skin on top of the skull open to keep sterile. Additional cuts in the skin were made to expose the sides of the skull just below the ears. The muscles on the back of the skull were removed to expose the spinal cord. The scissor was placed in the canal and small cuts along the mid brain was made. The skull was broken off with forceps, the brain removed and transferred to centrifuge tubes with ice-cold HBSS-HEPES and Penicillin/Streptomycin (final con. 100 units/ml; for all consumables refer to Table 2.5).

Isolation of the hypothalamic 3V:

The brains were washed three times in ice-cold HBSS with 10 mM HEPES and Penicillin/Streptomycin and the MBH and hippocampus were isolated in the same media. First the cerebellum and olfactory bulb were removed and then a horizontal cut was made at the level of the thalamus to separate the cerebral cortex and to level the dorsal aspect. The dorsal aspect was cut in half in the rostro-caudal axis to expose the hippocampus which were isolated using microdissection surgical scissors and forceps. Next to isolate the 3V walls, the ventral aspect was placed facing up, and using microdissection surgical scissors, cuts parallel to the 3V wall were made to isolate the region of interest. Finally, cuts were made in the rostro-caudal axis to separate the segment containing the HVZ corresponding approximately to bregma −1.0 to −2.5 mm.

Dissociation of tissue:

The tissue was collected in 5 ml ice-cold HBSS-HEPES (for all solutions refer to Table 2.5). Once the tissue had settled down the supernatant was removed under sterile hood and 2.5 ml of sterile dissociation media (HBSS, D-Glucose, HEPES 1M, Trypsin, Hyaluronidase) warmed to 37°C was added to the tissue (See table 2.3 for full media details) for digestion of the tissue. Incubation lasted for 15 minutes at 37°C and the tissue was titrated gently with a 1 ml (hippocampus) or 5ml pipette (hypothalamus) to break up the pellet before another 15 minutes of incubation in 37°C. One volume of an ice cold mix of BSA, EBSS and HEPES (solution 3) was used to inactivate the digestion by trypsin. Cells were triturated with a 5ml pipette and passed through a 40 μm filter/strainer into a 50 mL Falcon Tube to remove large pieces of un-digested tissue. The cells were transferred to 15 ml tubes and centrifuged down for 5 minutes at 1300 rpm and the supernatant removed. The cells were resuspended in 1 ml ice cold solution

3 and added slowly on top of another 10 ml ice cold solution 3. The cells were again centrifuged down for 7 minutes at 1500 rpm. The supernatant was again removed and the cells were resuspended in 1 ml Cell Maintenance media (Table 2.5 for full media details) and counted under microscope on a hemacytometer. Cells were then plated in two biological and technical replicates for treatment (hPrRP31/LiPrRP) and control. Cells were plated in DMEM/F12 with EGF/FGF2 (final concentration: 5 ng/ml) to grow as neurospheres or to be attached to PDL-coated bottoms of wells. Plated cells on PDL covered plates (treatment group) were given LiPrRP (1 μM) for 3 consecutive days (starting the day of plating) after which the attached cells were left in a 37°C incubator and continuously imaged (10X objective) (Ortega et al., 2013; Petrik et al., 2018) for 5 days (every 10 minutes). After imaging, cell identity was determined by immunocytochemistry (ICC).

For the next 7 days the neurospheres were incubated at 37°C in DMEM/F12 with EGF/FGF2 (final concentration: 5 ng/mL) boosts ever 3-4 days without LiPrRP boosts. At day 5 and 10 the neurospheres were counted under the microscope. At day 10 the neurospheres were collected by blasting them off gently with the media and transferred to Eppendorf tubes that were centrifuged at 1500 g for 7 minutes. The supernatant were then removed and the neuropsheres were flash frozen on dry ice and placed in -80°C awaiting further analysis by RT-qPCR.

Media	Components	Volume
EGF-Stock with a concentration of 5 µg/ml	EGF (ThermoFisher PHG0311) DMEM:F12 (low Glucose)	100 µg 10 ml
FGF-Stock with a concentration of 5 µg/ml	FGF (Roche PHG0264) DMEM:F12 (low Glucose)	10 µg 1 ml
Dissection medium	1x HBSS (Thermo 24020117) 10 mM HEPES	
Solution 3 (BSA-EBSS-HEPES) 500 ml	BSA (Sigma A2153) HEPES (Life Tech, 1M)	20 g 10 ml in 490 ml EBSS (LifeTech, 1x)
Dissociation Media	Solution 1 Trypsin (Sigma T9201-100MG) Hyaluronidase (Sigma H3884-50MG)	10 ml 7 mg 7 mg Disk filtered to be sterile
Solution1 (HBSS-Glucose) 500 ml	HBSS (Life Tech, 10x) D-Glucose (Stock 45%, Sigma: G8769) HEPES (1M, Gibco: 15630)	50 ml 9.0 ml 7.5 ml in 433.5 ml H_2O
Cell Maintenance Medium	Penicillin/Streptomycin B27 (Thermo 17504044) FGF (Stock 5µg/ml) EGF (Stock 5µg/ml) DMEM:F12/Glutamax (Gibco: 31331)	1:100 (final con. 100 units/ml) 1:50 1:1000 (final con. 5 ng/ml) 1:1000 (final con. 5 ng/ml) Fill up to 50 ml

Table 2.5. Media used for time lapse experiments.

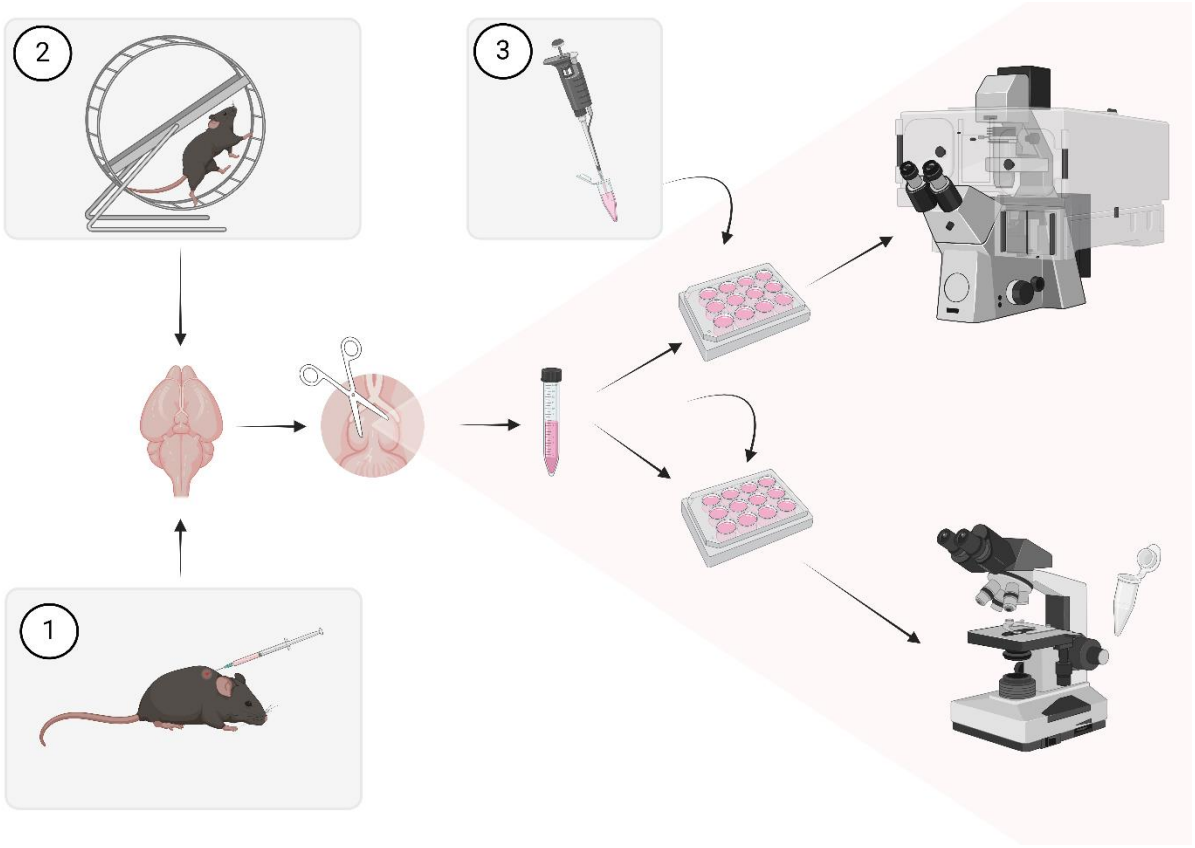

Figure 2.7. Isolation of the hypothalamic 3V. For time lapse experiments and neurosphere assays mice were fed HFD or Control diet and treated 1) *in vivo* with LiPrRP 2) Vertical running wheels 3) or LiPrRP *in vitro* (WT mice on Control diet).

2.6.2. Time lapse imaging

Primary cell cultures, processed as described above, were continuously imaged as described previously (Ortega 2013; Petrik et al. 2018). Four regions of 2x2 tiles were selected in each well using the ZEN Blue software (Zeiss). Imaging was done using an inverted 10X apochromat objective on a Zeiss Axio Observer 7 microscope in an environmental chamber, where the cells were kept in 37°C in 5 % CO_2 and pictures were taken every 10 min for 4 days. The microscope is also equipped with a motorized stage and Zeiss Definitive Focus module. At the end of imaging the cells were fixed and immunocytochemically stained for Vimentin, Sox2 and/or GFAP and Ki67 as described below (Table 2.4). Cellular events from a single seeding stem cell was analysed using Timm's Tracking Tool software as described previously (Hilsenbeck et al., 2016; Petrik et al., 2018). Stem cells were distinguished from rare astrocytes by morphology, where stem cells were identified as marker positive cells with elongated soma and one or two elongated processes compared to astrocytes that had a stellate morphology.

2.6.3. Immunocytochemistry

Firstly, the cells were blocked with carrier media (1x PBS, 0.5% Triton X-100, 2% bovine serum albumin), then the cells were incubated at room temperature (RT) overnight with primary antibodies (Table 2.4), diluted in the carrier media. The next day the slides were washed three times (for the hiPSCs, once for at least 30 minutes) followed by 1.5 hours of secondary antibody incubation (1:300) at RT. After another three washes (for the hiPSCs, once for at least 30 minutes), the cells were stained for DAPI (1:1000; Roche). DAPI was used as nuclear stain. The cells were washed another 3 times and then mounted using the ProLong Diamond antifade mountant. The wells or slides were imaged using a Zeiss Axio Observer 7 microscope for the time lapse imaging or on the confocal microscopy for the hiPSCs (Observer.Z1 Zeiss LSM780).

2.7. Human induced pluripotent stem cells (hiPSCs)

Maintenance and differentiation of the hiPSCs to hypothalamic neurons were performed as previously described with slight modifications (Merkle et al., 2015; Kirwan et al., 2017). To ensure cultures are kept sterile all cells were handled in a Class II biosafety cabinet using standard sterile techniques. The cell lines used were the Kolf-Cl (HPSI0114i-Kolf_2), the 18n6 (CS25iCTR-18n2) and the i900 cell line (generated in Professor Meng Li's lab at Cardiff University). All were from a fibroblasts tissue source from healthy male donors (age 46-75). The passage numbers ranged between 23-28 when received.

2.7.1. Differentiation

6 well plates were coated with 1 ml/well Vitronectin (VTN) (1:100) diluted with DPBS without Calcium and Magnesium and left in 37°C incubator (5% CO2 humidified incubator) for at least one hour. Undifferentiated Kolf, 18n6 and i900 hiPSCs were plated on 6 well VTN coated Nunclon plates (Thermo Scientific™, 140675) to grow to approximately 80% confluence. Undifferentiated hiPSCs were thawed until half frozen and 0.5-1 ml mTesR' (RT) were added to the vial. The cells were transferred to new 15 ml tube and spun down at 1000 rpm for 3 minutes. The media was aspirated from the cell pellet, and a new 1 ml mTesR' was added to the cell pellet and was triturated gently. Another 5 ml media was added and the cells were again titrated carefully, and evenly distributed (1 ml/well) to the plate after aspirating the VTN and adding an additional 1ml of mTesR' to the well (2 ml total/well). The cells were left to settle in the 37°C incubator overnight. The cells were fed with mTesR' (RT) every day until the cells reached 80% confluency when then passaged and replated into 6 well Geltrex (Cat.No. T303; Takara Bio Inc) coated plates at a density of 9.5 x 10^5 cells/well in N2B27 medium (Table 2.9)

for differentiation. To re-plate the cells all media for each well was transferred to a new 15 ml falcon tube and 1 ml/well Accutase was added and the plate was left in the incubator for 5-10 minutes. The cells were gently blasted off completely using the old media and collected into a new falcon tube and spun down for 3 minutes at 1000 rmp. The media was aspirated and cells resuspended in 1 ml mTesR' and Rock Inhibitor (Y-27632, 10 µM). 10 µl was used to count the single cell suspension in a hemacytometer. Correct volume of media and cell suspension was plated into the wells after aspirating the Geltrex. Left over cells were banked as 1 million cells per vile in Cryostor. The cells were left to settle overnight in the incubator and the next day they were fed with N2B27 and first day of small molecules. The small molecules were added as follows:

Small molecules were added freshly with each feeding (Table 2.6) and changed every day for 14 days for directed differentiation into a hypothalamic neuronal cell fate.

Day	Media and small molecules
Day 0	N2B27 + 1.5 µM iwr1 + 100 nM LDN-193189 + 10 µM SB431542
Day 2	N2B27 + 1.5 µM iwr1 + 100 nM LDN-193189 + 10 µM SB431542 + 1 µM SAG + 1 µM Purmorphamine
Day 4	N2B27 + 1 µM iwr1 + 75 nM LDN-193189 + 7.5 µM SB431542 + 1 µM SAG + 1 µM Purmorphamine
Day 6	N2B27 + 0.5 µM iwr1 + 50 nM LDN-193189 + 5 µM SB431542 + 1 µM SAG + 1 µM Purmorphamine
Day 8	N2B27 + 0.25 µM iwr1 + 25 nM LDN-193189 + 2.5 µM SB431542 + 5 µM DAPT
Day 10	N2B27 + 5 µM DAPT
Day 12	N2B27 + 5 µM DAPT
Day 14	dissociation and re-plating in Maturation medium + 5 µM DAPT + Y- 27632

Table 2.6. Differentiation protocol. From Kirwan et al. (2017).

Hypothalamic cultures were frozen down after 14 days differentiation. Some wells were lysed and used for a d14 qPCR checkpoint and some were replated onto PDL and Geltrex coated coverslips for ICC. Cells were dissociated using Accutase as described and banked 6 million cells per vile in Cryostor.

2.7.2. Maturation

The hiPSCs were thawed and replated onto PDL and Geltrex coated 12 well plates and coverslips in 24 well plates (Cat.No. 81156; Ibidi) at a concentration of $1x10^5$ cells per cm^2 (corresponding to density of 500 000 cells/well of a 12 well plate and 80 000 cells/ 13 mm coverslip). The immature neurons were thawed into Geltrex coated t25 flask in N2B27 and Rock Inhibitor to avoid cell death the first day. The cells were let to rest for 4 days with full media changes each day (N2B27 + 5 μM DAPT). On day 4 the cells were dissociated using Accutase as previously described and plated onto the PDL and Geltrex coated 12 well plates and coverslips in 24 well plates as mentioned. Cells were plated into maturation media with 10uM rock inhibitor + 5 μM DAPT and left to settle in the incubator overnight. Full media change was made without Rock Inhibitor and DAPT the following day (day 15) and 75% media changes every other day until day 30. BDNF was added fresh to each feed and the well were split in to control and treatment. hPrRP31 was added into the stock maturation media and then distributed into each well fresh at each feeding. The neurons were matured until day 30 when they were collected for mRNA extraction and later on PCR of target genes or fixed for ICC.

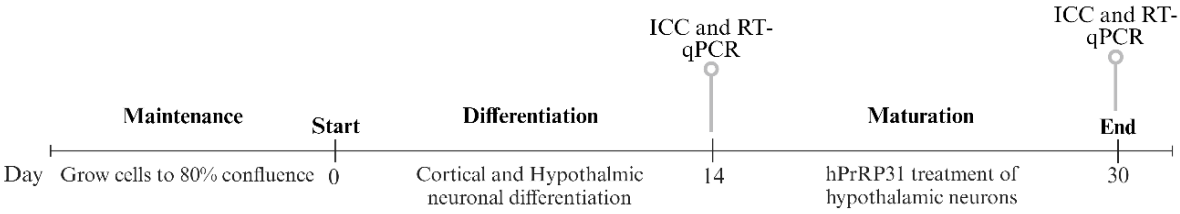

Figure 2.8. Timeline of hiPSC protocol and checkpoints as descried in the text.

2.7.3. Cortical neuronal differentiation and maturation

The cortical neurons were generated concurrently with the hypothalamic neurons and processed as previously described (Figure 2.8), with the modifications as shown in table 2.7.

Day	Media and small molecules
Day 0	N2B27 + 1.5 μM iwr1 + 100 nM LDN-193189 + 10 μM SB431542
Day 2	N2B27 + 1.5 μM iwr1 + 100 nM LDN-193189 + 10 μM SB431542
Day 4	N2B27 + 1 μM iwr1 + 75 nM LDN-193189 + 7.5 μM SB431542
Day 6	N2B27 + 0.5 μM iwr1 + 50 nM LDN-193189 + 5 μM SB431542
Day 8	N2B27 + 0.25 μM iwr1 + 25 nM LDN-193189 + 2.5 μM SB431542
Day 10	N2B27
Day 12	N2B27 + 20 ng/ml FGF2
Day 14	Dissociation and re-plating in Maturation medium + 20 ng/ml FGF2 + Y- 27632

Table 2.7. Differentiation protocol for cortical neurons. From Kirwan et al. (2017).

2.7.4. hiPSC ICC quantification

Quantification was performed from 3 regions of interest per cover slide, resulting in a total of 9 images from each control or treatment group for each cell line (Figure 2.9). All images were taken in a sequential scanning mode (z-stacks) to identify superposed cell nuclei. Z-stack images were obtained in the ZEN Blue software (Zeiss) using 40X apochromatic objectives on the Observer.Z1 Zeiss LSM780 confocal microscope. Cell counts are reported as percentages.

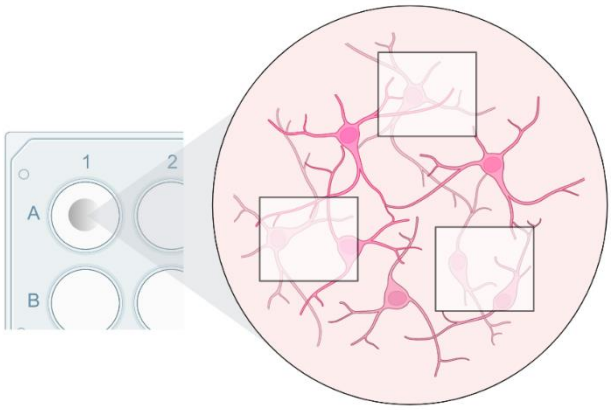

Figure 2.9. ICC quantification of marker positive hiPSC cells. Quantification was performed from 3 regions of interest per cover slide, resulting in a total of 9 images from each control or treatment group for each cell line.

Small molecules	Reconstitution instructions from Kirwan et al. (2017)	Supplier, catalogue number (cat. no.)
BDNF	Reconstitute powder in DPBS with 0.1% BSA (sterile filtered) to 100 µg/ml, aliquot, and store aliquots at -80°C. Use at 1:1000 for a 10 ng/ml final concentration.	Stemcell technologies, cat. no. 78005
DAPT	Reconstitute powder in DMSO to generate a 50 mM stock, aliquot, and store aliquots at -20°C. Use at 1:10000 for a 5 µM final concentration.	Stemcell technologies, Cat. no. 72082
LDN-193189	Reconstitute powder in DMSO according to manufacturer's directions to generate a 1 mM stock, aliquot, and store aliquots at -20°C. Use at 1:10000 for a 100 nM final concentration	Stemgent, cat. no. 04-0074
Purmorphamine	Reconstitute powder in DMSO to generate a 10 mM stock, aliquot, and store aliquots at -80°C. Use at 1:10000 for a 1 µM final concentration.	Stemcell technologies, cat. no. 100-1049
SB431542	Reconstitute powder in DMSO to generate a 10 mM stock, aliquot, and store aliquots at -80°C. Use at 1:1000 for a 10 µM final concentration.	Stemcell technologies, cat. no. 72232
Smoothed agonist (SAG)	Reconstitute powder in DMSO to generate a 10 mM stock, aliquot, and store aliquots at -80°C. Use at 1:10000 for a 1 µM final concentration.	Sigma-Aldrich, 566660-1MG
Y-27632 dihydrochloride Rock inhibitor	Reconstitute powder in sterile distilled water to generate a 10 mM stock, aliquot, and store aliquots at -20°C. Use at 1:1000 for a 10 µM final concentration.	DNSK International, cat. no. DNSK-KI-15-02

Table 2.8. Small molecules and distributors. From Kirwan et al. (2017).

Media	Components, product code and supplier
Maturation Medium (1 L)	1 L N2B27 medium BDNF to a final concentration of 10 ng/ml, added fresh at each feeding, Stemcell technologies, cat. no. 78005
mTeSR1 (0.5 L)	400 ml mTeSR1 medium, Stemcell Technologies, cat. no 05851 100 ml mTeSR1 5x Supplements, Stemcell Technologies, cat. no 05852
N2B27 (1.07 L)	500 ml Neurobasal-A, (LS), Thermo Fisher Scientific, cat. no 10888022 500 ml DMEM/F12 with GlutaMAX, (LS), Thermo Fisher Scientific, cat. no 31331093 10 ml Glutamax, Thermo Fisher Scientific, cat. no 35050038 10 ml Sodium Bicarbonate, Thermo Fisher Scientific, cat. no 25080-094 5 ml MEM Nonessential Amino Acids, Thermo Fisher Scientific, cat. no 11140035 1 ml Ascorbic Acid (200 mM, use 1:1000), Sigma Aldrich, cat. no A4403 10 ml Penicillin-Streptomycin, Thermo Fisher Scientific, cat. no. 15140122 Sterile filter, then add the following supplements: 20 ml B27 supplement (x50), Thermo Fisher Scientific, cat. no 17504044 10 ml N2 supplement (x100), Thermo Fisher Scientific, cat. no 17502048

Table 2.9. Media for hiPS cell cultures. From Kirwan et al. (2017).

Other consumables	Supplier
Geltrex LDEV-Free Reduced Growth Factor Basement Membrane Matrix	Thermo Fisher Scientific, cat. no. A1413202
Phosphate Buffered Saline, calcium and magnesium-free (DPBS), pH range 7.0-7.3	Thermo Fisher Scientific, cat. no. 14190250
Dimethyl Sulfoxide, DMSO	Sigma Aldrich, cat. no. D2650-100 mL
Vitronectin (VTN-N) Recombinant Human Protein, Truncated	Thermo Fisher, cat. no. A14700
Accutase Solution	Sigma, cat. no. A6964
Cryostor	STEMCELL technologies , cat no. CS10
ReLeSR™	STEMCELL technologies, cat. no. 100-0484
Distilled Water	Thermofisher, cat. no. 15230204

Table 2.10. Other media and consumables for hiPS cell cultures. From Kirwan et al. (2017).

2.8. RT-qPCR

2.8.1. RT-qPCR protocol

Total RNA was isolated using the RNeasy Mini plus kit (Qiagen, Manchester, UK) according to manufacturer's manual. The tissue, cells or neurospheres was titrated with 350 µl Buffer RLT Plus and transferred to a gDNA Eliminator spin column. The column was then centrifuged for 30 seconds at 10 000 rpm. 350 µl 70% EtOH was added to the flow through and transferred to an RNeasy spin column. The column was then centrifuged for 15 seconds at 10 000 rpm and flow through discarded. 700 µl RW1 was added to the column that was centrifuged for another 15 seconds (10 000 rpm) and flow through discarded. 500 µl Buffer RPE was then added to the column that was centrifuged for another 15 seconds (10 000 rpm). Another 500 µl Buffer RPE was added to the column and centrifuged for 2 minutes at 10 000 rpm. 30 µl RNase free water

was added on top of the filter in the column and then centrifuged for 1 minute into new Eppendorf tubes that were placed in -80°C until transcribed to cDNA.

To transcribe the isolated RNA into cDNA we used Super Script III polymerase with random primers and RNAse Out (Thermo). The qPCR reaction was performed using Fast SYBR Green dye (Thermo). Technical duplicates was used for each sample and primer pair. First, random primers (1 µl/reaction, 200ng), dNTPs (1 µl/reaction, 10 mM) and RNAse free water (1 µl/reaction or up to 13 µl total including the Total RNA) into one master mix. Three µl of the master mix was added to 10 µl of the thawed RNA and added to RNAse free PCR tubes. The PCR tubes were ran in the PCR cycler for 5 minutes at 65°C (volume 13 µl) the samples were then briefly spun and put on ice for at least 1 minute. A master mix of 4 µl 5x First Strand Buffer/reaction, 1 µl DTT (0.1 M)/reaction, 1 µl RNAse OUT(inhibitor)/ reaction, 1 µl Superscript III/ reaction was made and thoroughly mixed. Seven µl of the master mix was added to the PCR tubes and incubated at 25°C for 5 minutes. The reactions were ran for 5 minutes 25°C, 1h 50°C, 15 minutes 70°C, cooled to 4°C and put in -20°C until qPCR was performed. A Step One Plus Real time PCR system (Life Technologies) was used to determine the relative expression of mRNA transcripts. The cycler was set up for 45 cycles, 95°C for 20 seconds at the holding stage, 95°C for 3 seconds at the first cycling stage (denaturation), and 60°C for 30 seconds at the second cycling stage (annealing and elongation). The sequences of used primers (250 nM for all) were designed by using the Primer-BLAST online tool (NCBI-NIH).

Primer	Forward and reverse reads	Supplier
POMC	Fwd: CTCACCACGGAAAGCAACC Rvs: CTGCTCGTCGCCATTTCC	Sigma-Aldrich (Zimmer et al., 2016)
NPY	Fwd: GCTGCGACACTACATCAACCTC Rvs: CTGTGCTTTCTCTCATCAAGAGG	Sigma-Aldrich
GPR10	Fwd: TTTGGATCCGTTCAGCTCCC Rvs: GGAAGTTCGTCACGTTGTGC	Sigma-Aldrich
NPFFR2	Fwd: TCCTCAGTTGCGAAATTAGGATGT Rvs: CCACTTGAGGCTGGTGAAGA	Sigma-Aldrich
PrRP	Fwd: GCACCCCTGACATCAATCCT Rvs: AGCCATCCTGGGACGACATA	Sigma-Aldrich
NKX2.1	Fwd: ACTCGCTCGCTCATTTGTTG Rvs: GGAGTCGTGTGCTTTGGACT	Sigma-Aldrich
FOXG1	Fwd: CACCTACTCCCTCAACCCCT Rvs: GCTGCTCTGCGAAGTCATTG	Sigma-Aldrich (Neaverson et al., 2023)
GAPDH	Fwd: GCACCGTCAAGGCTGAGAAC Rvs: TGGTGAAGACGCCAGTGGA	Sigma-Aldrich (Chen et al., 2022)

Table 2.11. Primer pairs for hiPSC experiments. If no reference is indicated the primer pair was generated using the Primer-BLAST (NCBI-NIH) function.

The results were analysed using the AccuSEQ software (Life Technologies). The amplification cycle (Ct) values was determined by maximum 2nd derivation method and following the $2^{-\Delta\Delta Ct}$ method (Livak and Schmittgen, 2001) with normalization to the expression levels of GAPDH.

2.9. Statistical analysis

Data were statistically analysed, and graphs generated by using with Microsoft Excel and GraphPad Prism. Numbers of biological and technical replicates are provided in the Figure Legends and in the Methods. The statistical analysis followed a determined workflow. First, data sets were analysed by the Grubb's test (ESD method) to identify statistically significant outliers (alpha = 0.05), which were removed from all statistical analyses. Second, it was determined if the data are normally distributed by D'Agostino & Pearson's omnibus normality test. If the data set is smaller than n = 5, the Kolmogorov–Smirnov normality test was used. If data were not normally distributed or if this could not be reliably determined due to small number of replicates, non-parametric statistical tests were used. Including Mann–Whitney for un-paired experiments, or Kruskal–Wallis test with Dunn's post-hoc test (for group comparison). Parametric tests were instead used if data were normally distributed. For simple comparison of two data groups, the unpaired two-tailed t-test was used. The t-test was also used for selected data groups containing three data sets that were not interdependent. For multiple factor or group comparison, One-way or two-way analysis of variance (ANOVA) was used with the Bonferroni's or Tukey's post-hoc test for the cross-comparison of individual data sets. For non-parametric tests, the data were presented as median ± interquartile range (IQR). For parametric tests, the data were presented as mean ± standard error of mean (SEM). Results were considered significant with $P < 0.05$ (*). In graphs, two asterisks (**) represent values of $P \leq 0.01$, three asterisks (***) for $P \leq 0.001$.

2.9.1. hiPSC ICC statistical analysis

Image analysis and cell quantification of iPSC ICC was performed on Fiji ImageJ. Image processing involved compressing the z-stack using the "Z project" function set to average intensity and adjusting the brightness and contrast levels (min, 60, max, 0). Manual and automated quantification was conducted by May Surrdige-Smith when working in Petrik lab. Automated cell quantification was conducted by using an automated particle analysis macro pipeline. Statistical tests were performed as described above.

2.9.2. RT-qPCR analysis

The results were analysed using the AccuSEQ software (Life Technologies). The amplification cycle (Ct) values were determined by maximum 2^{nd} derivation method and following the $2^{-\Delta\Delta Ct}$ method (Livak and Schmittgen, 2001) with normalisation to the expression levels of GAPDH.

The cycle threshold (Ct) values, which indicate the number of cycles required for the fluorescent signal to exceed a defined threshold, were normalised to the housekeeping gene (GAPDH) to obtain the ΔCt values (ΔCt = Cttest gene – CtGAPDH). The ΔCt values are presented as fold change($2^{-\Delta Ct}$). The relative expression of the gene of interest in the treatment group compared to the control is represented as the ΔΔCt values (ΔΔCt = ΔCttreatment - ΔCtcontrol), calculated using the arithmetic mean average of the ΔCt values for individual cell lines. In qPCR, the Ct value is inversely proportional to the initial quantity of the target nucleic acid in the sample. Thus, a higher Ct value signifies that more PCR cycles were needed to detect the gene of interest, implying lower expression levels of the target gene. Consequently, in graphs displaying fold change, a taller bar indicates diminished gene expression. For graphs depicting ΔΔCt values, a negative value represents increased gene expression, while a positive value indicates reduced gene expression.

Chapter 3: The Effects of a Lipidized Analogue of Prolactin Releasing Peptide on Adult Neurogenesis in the Hypothalamus

Results from this chapter have been published (full figures from the paper are presented in Appendix 1)

Jorgensen, S., Karnošová, A., Mazzaferro, S., Rowley, O., Hsiao-Jou, C C., Robbins, S J., Christofides, S., Merkle, F T., Maletínská, L., & Petrik, D. (2024, January 1). An analogue of the Prolactin Releasing Peptide reduces obesity and promotes adult neurogenesis. EMBO Reports, 25(1). https://doi.org/https://doi.org/10.1038/s44319-023-00016-2

3.1. Short Introduction

Obesity is a chronic serious disease with many co-morbidities (Cope et al., 2018). Unfortunately, due to low long-term adherence, 1 out of 3 individuals return to their original weight within a year (Kushner et al., 2020; Tak & Lee, 2021). Given the multifaceted nature of obesity, alternative treatment options are essential to effectively support patients. To fill this clinical need, research is needed to identify new compounds with anti-obesity potential. One of such compounds is PrRP. A human palmitoylated analogue of PrRP (LiPrRP) was synthesized at the Institute of Organic Chemistry and Biochemistry, Prague (CAS), as previously described (Pražienková et al., 2017). Previous results from Petrik lab suggested that LiPrRP reduces weight in DIO mice and affects adult neurogenesis in the hypothalamus. The only neuroactive medications also approved as anti-obesity treatments in the UK and EU are analogues of the Glucagon-like Peptide-1 Receptor (GLP-1R) (Bray et al., 2016; Collins & Costello, 2022; NICE, 2020), such as Liraglutide (Saxenda) or Semaglutide (Ozempic). However, their primary clinical use is for the treatment of T2DM (Ard et al., 2021; Bailey et al., 2023; Mahase, 2022).

Research has established that the mammalian hypothalamus contains a neurogenic niche, where progenitor cells can proliferate and differentiate into neurons, astrocytes, and oligodendrocytes, integrating into existing neural circuits (Yoo & Blackshaw, 2018; Sharif et al., 2021). Hypothalamic neurogenesis, predominantly studied in the medio-basal region due to its role in regulating feeding and metabolism (Lee et al., 2014; Kokoeva et al., 2005), is a central homeostatic mechanism that governs various physiological processes like sleep,

circadian rhythms, and appetite control (Lee et al., 2014). Metabolic factors, including diet and associated cytokines, can modulate the proliferation of neural precursors and neurogenesis in the hypothalamus. Interestingly, hypothalamic neurogenesis may play a dual role in obesity - contributing to its onset through dysregulation of appetite and metabolism, while also offering a compensatory mechanism in response to over-nutrition and metabolic dysfunction.

In the MBH, neurons that suppress (anorexigenic) or stimulate (orexigenic) appetite sense metabolic and hormonal signals from the periphery to control eating behaviour and appetite (Lechan & Toni, 2013; Timper & Brüning, 2017; Betley et al., 2013; Farooqi, 2022). Anti-obesity compounds exert their effects by targeting neurons in the MBH to reduce the sensation of appetite and the body weight (Tak & Lee, 2021). Appetite-regulating neurons in the MBH are generated from both embryonic development and adult neurogenesis from aNSCs in the HVZ (Petrik et al., 2022). These newly born neurons, along with the aNSCs, play a vital role in regulating energy homeostasis (Gouazé et al., 2013; Kokoeva et al., 2005).

DIO has been demonstrated to reduce adult hypothalamic neurogenesis through reduced survival and increased apoptosis of newborn neurons, or by decreased proliferation of tanycytes (Li et al., 2012; Lee et al., 2014; McNay et al., 2012). Conversely, ablation of adult hypothalamic neurogenesis leads to greater weight gain in HFD-fed animals (Gouazé et al., 2013; Kokoeva et al., 2005), while enhancing hypothalamic adult neurogenesis protects against the adverse effects of HFD, suggesting that newly generated neurons serve an anorexigenic role. Nonetheless, the association between adult hypothalamic neurogenesis and DIO remains incompletely understood, with conflicting findings reported in literature (Lee et al., 2014; Li et al., 2012; McNay et al., 2012).

Given the critical role of adult hypothalamic neurogenesis in energy homeostasis, we hypothesised that anti-obesity compounds may elicit neurogenic effects similar to antidepressants (Eisch & Petrik, 2012; Malberg et al., 2000; Santarelli et al., 2003). To evaluate this hypothesis, we administered LiPrRP and LIRA to mice on a HFD and examined the impact on the cellular and molecular processes of adult hypothalamic neurogenesis.

To determine the neuroprotective effects of LiPrRP and LIRA in the context of DIO, six-week-old male mice were fed HFD for 7 days (7d), 21 days (21d), or 4 months (4mo). The two shorter-duration HFD protocols were expected to trigger HFD-induced neuroinflammation and astrogliosis in the hypothalamus (Sugiyama et al., 2020; Thaler et al., 2012), while the longer protocol would result in the development of DIO (Pražienková et al., 2017). The 4mo protocol

allowed investigating the effects of the anti-obesity compounds in the context of established obesity, while the shorter 7d and 21d protocols enabled examining their effects during neuroinflammation and the developing metabolic syndrome. In the 7d and 21d protocols, LiPrRP and LIRA (21d) were administered concurrently with the HFD. In the 4mo protocol, the LiPrRP was given during the last two weeks. As a control to HFD + LiPrRP, mice were also administered LiPrRP in the context of the Control diet in the 21d and 4mo protocols.

The LiPrRP protocols used in the current study were performed in the Maletínská lab. Their previous research demonstrated that administering the palmitoylated PrRP31 analogue (palm-PrRP31) to freely-fed mice for three consecutive days led to reduced food intake (Maletínská et al., 2015). Additionally, they showed that chronic two week administration of palm-PrRP31 in DIO mice resulted in substantial weight loss and improvements in metabolic parameters that had been elevated due to obesity, such as decreased plasma leptin and insulin levels (Maletínská et al., 2015). In these experiments, mice were treated with LiPrRP or LIRA and exposed to different BrdU pulse and chase protocols as described in Chapter 2. To test the effects of the anti-obesity compounds on the survival of newly generated cells in the MBH, mice exposed to 4mo HFD were administered BrdU for two weeks (on day 92) followed by two week chase. In the 7d and 21d HFD protocols there were 6d and 16d chase periods respectively, to determine the effects of the compounds on newly generated cells in the context of developing metabolic syndrome. Quantification of BrdU labelled cells was done in the MBH (including the DMN, VMN, ArcN and ME, ArcN alone, and the ME alone).

The aim of this chapter was to elucidate the mechanism of action of LiPrRP by determine the effects on cell proliferation, differentiation and survival of adult generated neurons in context of acute HFD and DIO, as well as the impact on stem cell proliferation in the HVZ.

3.1.1. LiPrRP reversed the DIO-induced reduction of newly generated neurons, induced weight loss, and reduced the HFD-induced plasma concentrations of insulin, leptin, and cholesterol

Previous results from Dr Petrik (Figure 3.1) showed that compared to Controls, mice on long-term (4mo) HFD feeding had significantly fewer BrdU labelled neurons in the MBH. Markedly, the reduction of newborn neurons was rescued by LiPrRP in the MBH to the level of Controls. The rescue effect of LiPrRP was observed not only in the MBH but also in the ME alone. This rescue effect was not limited only to new neurons but also to other BrdU labelled cells in the MBH, although DIO did not significantly reduce other BrdU labelled cells in the MBH.

The Maletínská lab showed that exposure to HFD with or without LiPrRP for 7d did not significantly change the body weight (Appendix Figure 1A). In the 21d protocol exposure to HFD or Control diet with or without LiPrRP had a statistical significant effect on body weight of male mice. The Two-Way ANOVA revealed a significant effect, however no significance were found between the groups by the multiple comparison Bonferroni post-hoc test. This indicated that neither HFD or LiPrRP alone could cause the variance found by ANOVA (Appendix Figure 1B). They also showed that LiPrRP administration in the last 2 weeks of 4mo HFD significantly reduced body weight compared to mice on 4mo HFD (Appendix Figure 1C) (Maletínská et al., 2015). In contrast, LiPrRP had no effect on body weight in male mice kept on Control diet (Appendix Figure 1C). In addition, the Maletínská lab showed a reduction of HFD-induced plasma concentration of insulin, leptin and cholesterol which had been significantly elevated in mice on 4mo HFD as expected with the development of obesity (Kennedy et al., 2010).

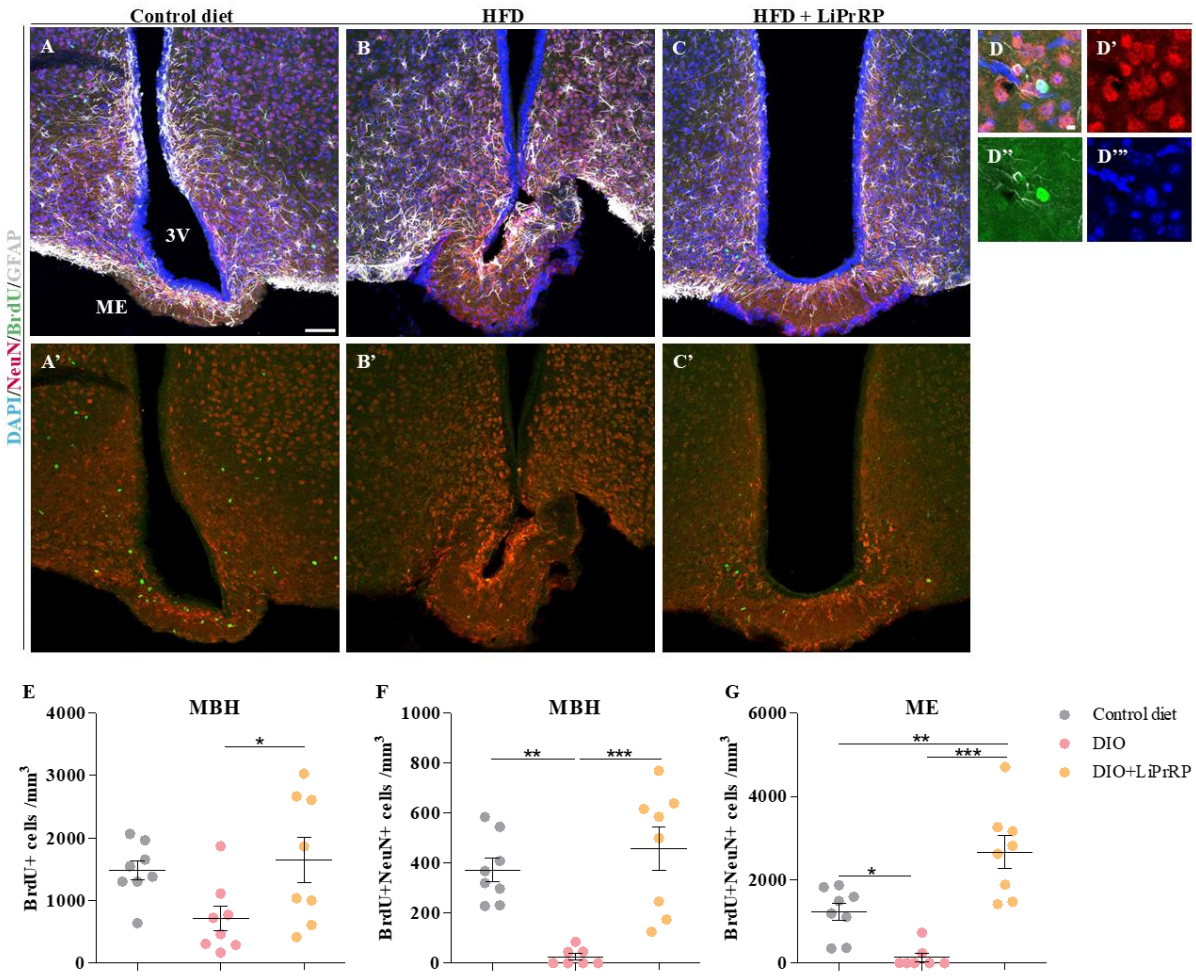

Figure 3.1. LiPrRP rescued newborn neurons in the MBH and ME in obese mice. Mice were exposed to HFD for 4 months. A–C) Representative confocal images of HVZ stained as indicated in Control (A), HFD (B) and HFD + LiPrRP (C) of 4mo HFD group. D-D''') An example of BrdU+ neuron in the MBH parenchyma. E) Quantification of all BrdU+ cells in the MBH. F-G) Quantification of BrdU+ neurons in MBH (F) and ME (G). Data information: Scale bars (s.b.): 50 µm (A–C), 10 µm (D). n = 8 mice per data set for the 4mo group. In all panels, One-way ANOVA with Bonferroni's test (E: $F(2,21) = 3.87$, $p = 0.037$; F: $F(2,20) = 14.21$, $p < 0.0001$; G: $F(2,20) = 21.37$, $p < 0.0001$). Data are presented as mean ± SEM.

3.2. Results

3.2.1. Majority of adult generated neurons in the hypothalamus expressed the PrRP receptor

LiPrRP exerts its effect by binding to the PrRP receptors GPR10 and NPFFR2 (Maletínská et al., 2015). While numerous studies have examined the distribution of GPR10 in the brain, its precise sub-cellular localisation within neurons remains less well characterised. The existing literature primarily focuses on the broader expression patterns of this receptor in brain regions such as the hypothalamus, thalamus, and pituitary gland (Bjursell et al., 2007; Dodd & Luckman, 2013; Pražienková et al., 2019, 2021). As a transmembrane protein, GPCRs like GPR10 span the cell membrane and have portions exposed to both the extracellular and intracellular environments, which is crucial for their role in signal transduction. Dr Karnošová, when working in Petrik lab, identified GPR10 positive puncta co-localized with the cytoskeletal marker Microtubule - associated protein 2 (Map2) and/or Human neuronal protein C and D (HuC/D) surrounding neuronal nuclei, both markers of mature neurons in the MBH (Appendix Figure 1I–K). She also showed that the density of GPR10 was reduced by 21d of HFD exposure which was rescued by LiPrRP administration (Appendix Figure 1L). The data suggests that GPR10 co-localizes with both the cell body and dendrites of neurons, but its precise distribution and density along the neuronal membrane require further study. To further investigate the presence of the receptor in adult born neurons co-immunostaining with BrdU, GPR10 and the cytoskeletal mature neuronal marker Map2 was done in animals on Control diet for 21d. Quantification showed not only that newborn neurons in the MBH express the receptor, but also that over 90% of Map2+BrdU+ cells in the MBH co-localized with GPR10 (Figure 3.2). Thus, the data confirmed that adult-generated hypothalamic neurons expressed the PrRP receptor GPR10. Besides GPR10, Dr Karnošová co-localized neuronal structures with NPFFR2 in the MBH (Appendix Figure 1O and P). NPFFR2 was expressed as previously described in the hypothalamus (Zhang et al., 2021). This suggested that PrRP can act on adult generated neurons in the MBH.

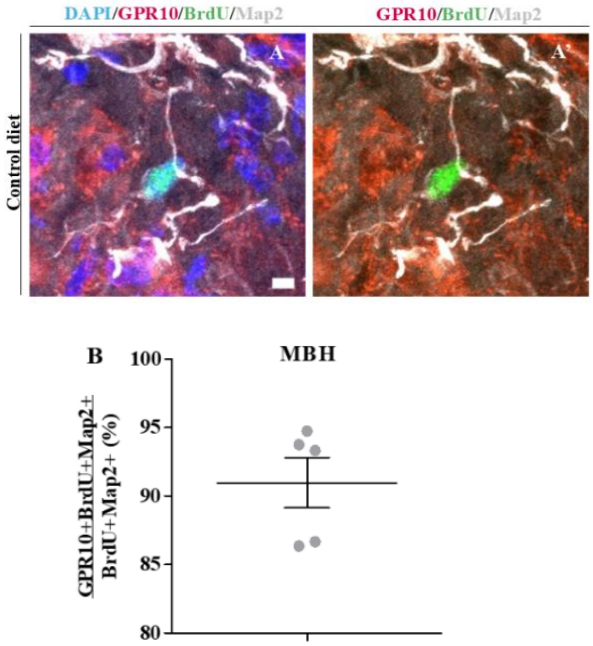

Figure 3.2. Majority of adult generated Map2+ neurons expressed the GPR10 receptor. GPR10 co-localizes with both the cell body and dendrites of neurons. Quantification showed not only that newborn neurons in the MBH express the receptor, but also that over 90% of Map2+BrdU+ cells in the MBH co-localized with GPR10. A-A') A representative image of GPR10+ puncta associated with Map2+ processes around a BrdU+ nucleus in ME. B) Quantification of the proportion of BrdU+Map2+ GPR10+ cells in MBH. Data information: S.b: 10 μm. n = 5 mice for the 21d group on Control diet. Data are presented as mean ± SEM.

3.2.2. LiPrRP treatment restored HFD-induced decrease in new MBH neurons only in the context of DIO

Building on the data by Dr. Petrik as previously described, HFD was administered for shorter periods to investigate the impact of LiPrRP and LIRA during acute HFD. Mice fed HFD for the shorter term of 7d and 21d did not show the same reduction in BrdU-labelled neurons (BrdU+HuC/D+). While 21d of HFD did not change the number of BrdU-labelled cells, or neurons in the MBH, a significant increase of BrdU-labelled neurons (BrdU+HuC/D+) in the ArcN was observed in the HFD group (Figure 3.3I). Interestingly, a significant reduction in all BrdU-labelled cells in mice treated with HFD+LIRA compared to Controls was observed. In addition, treatment with LiPrRP and LIRA reversed the effects of HFD by decreasing the number of BrdU-labelled neurons in the ArcN, however, non-significant. In the 7d protocol, there was no difference between any of the treatment groups in number of BrdU-labelled cells or neurons (Figure 3.3 E-F). Taken together, the data suggested a common mechanism between the anti-obesity compounds that may protect against short and intermediate term HFD by reducing neurogenesis that was elevated by HFD.

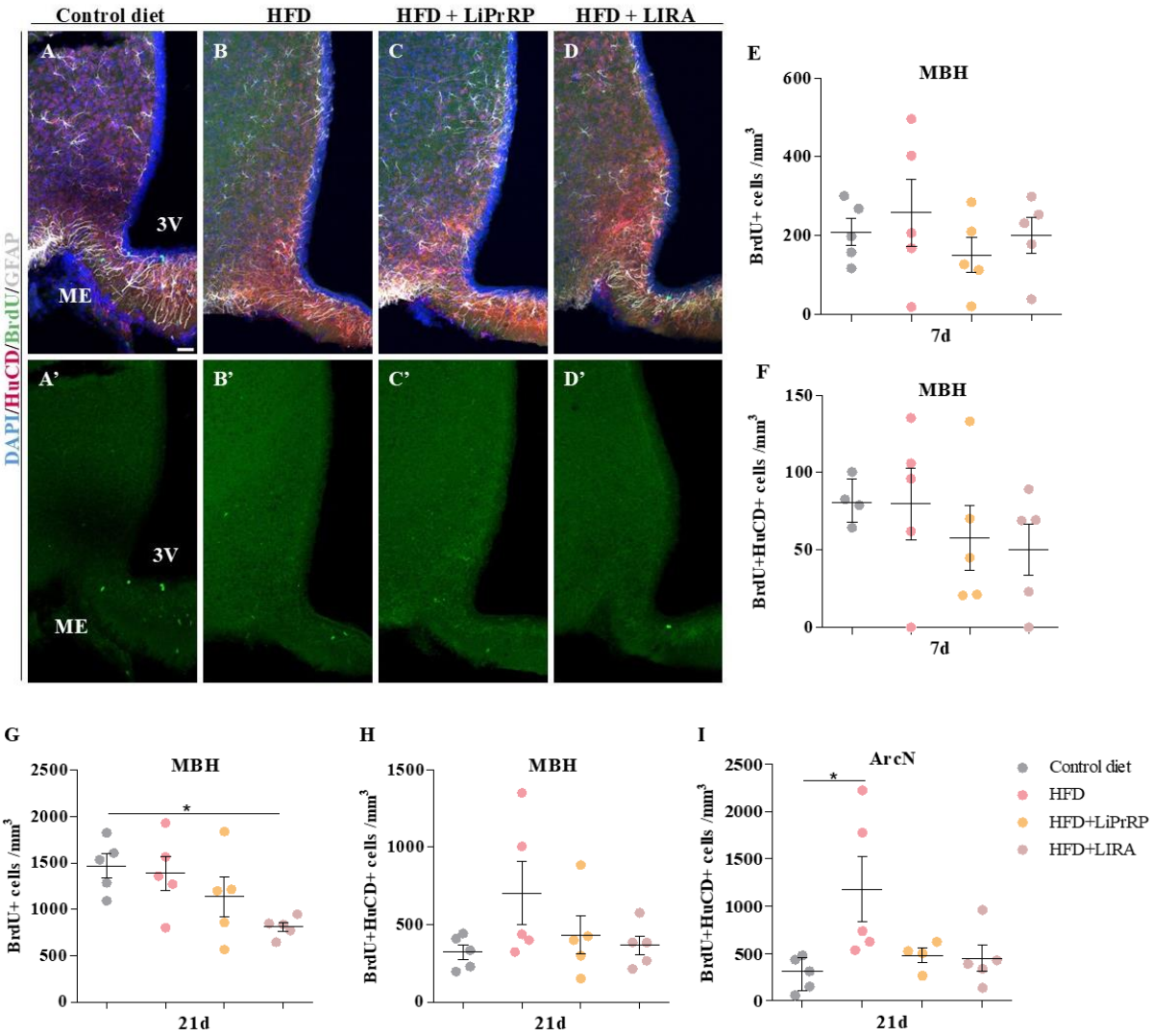

Figure 3.3. 21d HFD increased newly generated neurons in the ArcN. Mice were exposed to HFD for 7d and 21d. A–D) Representative confocal images of HVZ and MBH stained as indicated in Control (A-A'), HFD (B-B'), HFD + LiPrRP (C-C'), HFD + LIRA (D-D') of 21d group. E–F) Quantification of BrdU+ cells (E), BrdU+ neurons (F) in the MBH of 7d groups. G–I) Quantification of BrdU+ cells (G), BrdU+ neurons (H) in the MBH and in the ArcN (I) of 21d group. Data information: S.b.: 20 µm. n = 5 mice per data set for the 7d, 21d groups. In panel I, Kruskal–Wallis test with Dunn's test (H = 9.88, p = 0.02). In panels E, F, G, H, One-Way ANOVA with Tukey's test (G: F(3,19) = 3.58, p = 0.038). Data are presented as median ± IQR (I and F) or mean ± SEM (all other).

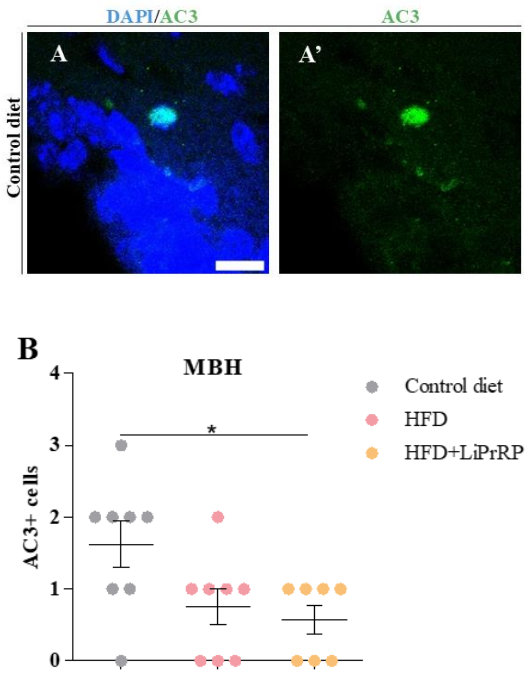

3.2.3. LiPrRP reduced cell death in the MBH

One of the ways LiPrRP can increase number of newborn neurons during DIO is by reducing cell death and thereby promote neuronal survival. To test this, the number of cells positive for the apoptotic marker Activated Caspase 3 (AC3) in the 3V walls and MBH was quantified (Figure 3.4B). DIO mice treated with LiPrRP showed a statistically significant decrease in the number of AC3+ cells compared to Controls but not HFD. Taken together, these findings suggested that LiPrRP reduced cell death in the MBH but not compared to HFD.

Figure 3.4. LiPrRP reduces cell death in the MBH. Cell death was measured by quantifying the number of cells positive for the apoptotic marker AC3 in the MBH. A-A') An example of AC3+ cell near 3V wall. B) Quantification of AC3+ cells in MBH. Data information: S.b.: 10 µm. n = 8 mice per data set for the 4mo group. One-way ANOVA with Bonferroni's test (B: $F(2, 22) = 2.46$, $p = 0.025$). Data are presented as mean ± SEM.

3.2.4. LiPrRP increased neuronal survival even in Control conditions

To address whether LiPrRP exhibits its neuroprotective and neurogenic effects also in physiological conditions, mice on Control diet were administrated the compound. In the context of Control diet, LiPrRP significantly increased the number of BrdU labelled neurons in the MBH (Figure 3.5F) but did not change overall newly generated cells (all BrdU+ cells) in the 4mo protocol. This suggested that the compound promoted neurogenesis in the MBH in old mice even under control conditions. In 21d protocols LiPrRP did not change BrdU labelled neurons or newly generated cells (Figure 3.5C-D).

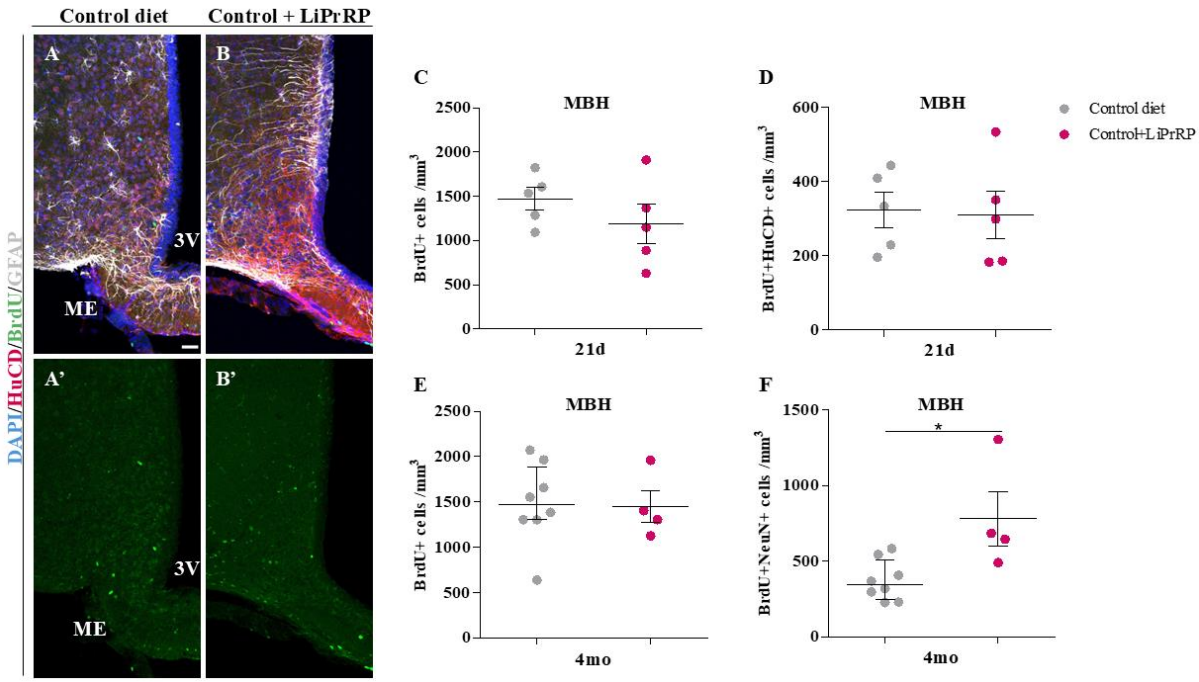

Figure 3.5. LiPrRP promoted neurogenesis in the MBH even under control conditions. A–B) Representative confocal images of HVZ and MBH stained as indicated in Control (A-A'), Control + LiPrRP (B-B') in the 4mo group. C–F) Quantification of BrdU+ cells (C, E) and BrdU+ neurons (D, F) in MBH of Control and Control + LiPrRP treated mice of 21d and 4mo groups. Data information: S.b.: 50 µm. n = 5 mice per data set for the 21d group, n = 4 mice per data set for the 4mo group. In panels C, D, Unpaired T-test, Two-tailed. In panels E, F, Mann Whitney test, Two-tailed (F: p = 0.0162). Data are presented as median ± IQR (E-F) or mean ± SEM (all other).

3.2.5. LiPrRP treatment showed no effect on astrocytes under HFD conditions

Obesity induce an inflammatory response and increases reactivity of glial cells (Thaler et al., 2012; Valdearcos et al., 2017). To investigate the effects of short and long-term HFD and LiPrRP or LIRA administration on astrogliosis and astrogliogenesis, immunohistochemical staining of GFAP and BrdU was performed. Immunostaining for the astrocyte marker GFAP found no significant effects of HFD, LiPrRP, or LIRA on number of new BrdU+ astrocytes in the MBH (Figure 3.6 A-C). Astrogliosis was also investigated by Dr. Petrik as shown in Appendix Figure S1. A significant increase in number of GFAP+ astrocytes in the MBH after 4mo exposure of HFD was observed. However, this increase was not altered by LiPrRP treatment. While treatment with LiPrRP in Control conditions did not affect astrogliosis or astrogliogenesis in 21d but a significant decreased adult born (BrdU+) astrocytes in the 4mo group was found (Figure 3.6D). These data suggested that the effects of LiPrRP is confined to adult generated neurons in the context of HFD, as it has no effect on astrocytes under the same conditions.

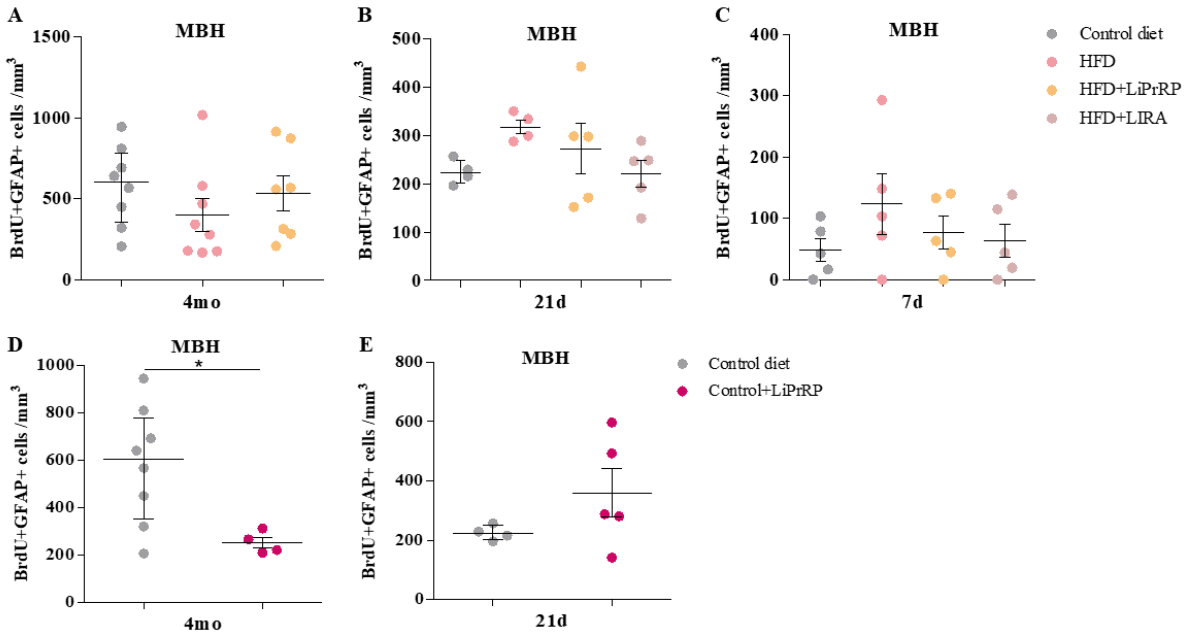

Figure 3.6. LiPrRP did not affect astrogliogenesis when mice are treated with HFD. A–C) Quantification of BrdU+ astrocytes in the MBH of 4mo (A), 21d (B), and 7d (C) HFD groups. D–E) Quantification of BrdU+ astrocytes in the MBH in the 4mo (D) and 21d (D) Control + LiPrRP groups. Data information: S.b.: 50 µm. n = 5 mice per data set for the 7d and 21d groups, n = 8 mice for the HFD 4mo group, n = 4 mice for the Control + LiPrRP 4mo group. In panels A, B, C, One-Way ANOVA. In panels A, B, Bonferroni's test (B: $F(3,19) = 4.3$, $p = 0.021$) or in panel C, Tukey's test. In panels D, E, Mann Whitney test, Two-tailed (D: $p = 0.0485$). Data are presented as median ± IQR (A,B,D,E) or mean ± SEM (C).

3.2.6. Anti-obesity compounds reduced proliferation in the MBH

One of the cellular mechanisms how LiPrRP could influence adult neurogenesis is changing cell proliferation. To examine the effects of LiPrRP on overall cell proliferation in the MBH sections from the three HFD protocols were immunohistochemically stained for the cell proliferation maker Ki67 and cells were quantified in the MBH, and ME (Figure 3.8). 4mo, 21d and 7d HFD had no statistically significant effect on number of Ki67+ cells in the MBH or ME. Which is in accordance with previous studies (Gouazé et al., 2013; Klein et al., 2019). However, LiPrRP reduced cell proliferation compared to Controls when fed HFD for 21d in the MBH, even further than the reduction (non-significant) observed in the HFD group. The same effect was also observed in the group treated with LIRA (Figure 3.8E). In Control conditions LiPrRP also reduced cell proliferation in the MBH and ME, in the 21d group (Figure 3.8E, H). Both obesity compounds therefore exert similar effects on cell proliferation in the MBH in the context of HFD.

The effects of HFD, LiPrRP and LIRA were also investigated in another neurogenic niche, the SGZ of the hippocampus by Dr. Karnošová (Appendix Figure EV2). Dr. Karnošová showed

that LiPrRP treatment significantly reduced Ki67+ and PCNA+ cells in the SGZ (Appendix Figure EV2 E-F), did not rescue HFD-induced reduction of proliferating cells, and in contrast rescued the HFD-induced reduction in DCX+ neurons and neuroblasts in the SGZ in the 21d protocol (Appendix Figure EV2 G-H). In contrast, LIRA rescued the HFD induced decrease in Ki67+ cells in 21d but failed to rescue the same reduction of DCX+ neuroblasts and further reduced DCX+ neurons (Appendix Figure EV2 J-K).

Taken together, while both anti-obesity compounds exert similar effects on cell proliferation in the MBH, they instead exert contrasting effects in the SGZ. Suggesting that their effects are context dependent.

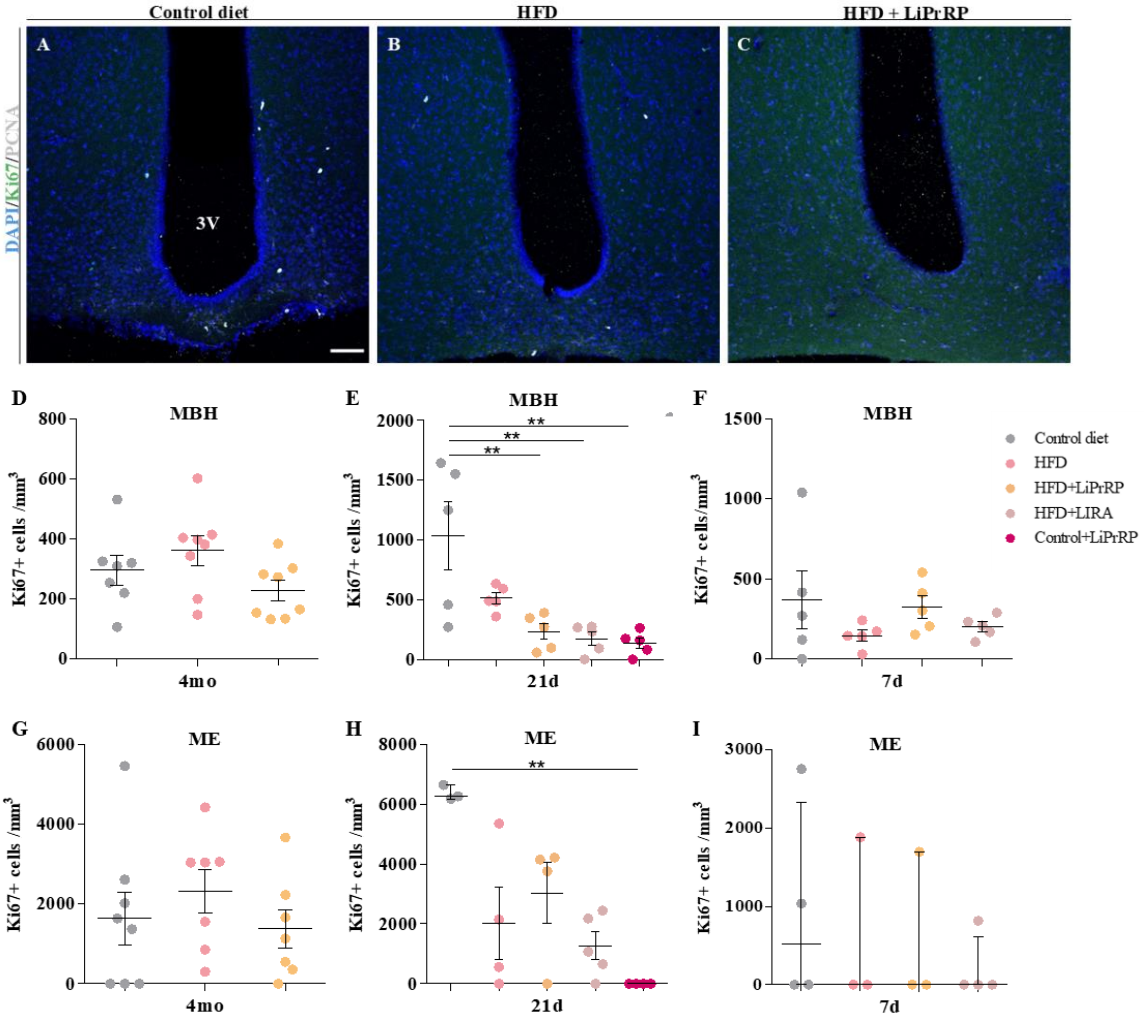

Figure 3.7. LiPrRP and LIRA reduced cell proliferation in the MBH and ME after 21d HFD. A–C) Representative confocal images of the MBH stained as indicated for the 21d group. D–I) Quantification of cells positive for Ki67 in MBH for the 4mo (D), 21d (E) or 7d (F), and in ME for the 4mo (G), 21d (H) and 7d (I) groups. Data information: S.b.: 100 µm, n = 5 mice per data set for the 7d and 21d groups, n = 8 mice per data set for the 4mo group. In panels D, G, One-way ANOVA with Bonferroni's test (E: $F(4,24) = 704725$, $p = 0.0006$). In panels H, I, Kruskal-Wallis test with Dunn's test (H: Control diet vs Control diet + LiPrRP, $p = 0.0172$). Data are presented as mean ± SEM (D-G), median ± IQR (H-I).

3.2.7. LiPrRP treatment did not change Rax+ tanycyte proliferation

Tanycytes are the putative stem cells of the hypothalamic neurogenic niche. Tanycyte specific cell proliferation was investigated by co-staining of Ki67 and the universal marker of tanycytes, the Retina and anterior neural fold homeobox transcription factor, Rax (Miranda-Angulo et al., 2014; Yoo & Blackshaw, 2018). Unfortunately, due to the rare proliferative nature of the Ki67+Rax+ tanycytes it did not allow for reliable quantification. However, volume Rax+ tanycytes was used as a proxy for tanycyte proliferation. Since the volume of the MBH did not change in these animals (results not shown), one could assume that if the volume Rax+ cells increase it is due to an increased proliferation resulting in more cells and increased volume. It was concluded that neither diet nor LiPrRP changes the volume of Rax+ cells in the 3V in animals fed HFD for 4mo. Number of Rax+GFAP+ β-tanycytes and the total number of Rax+ tanycytes were additionally investigated by our lab, which showed that HFD significantly reduced their number which was not rescued by LiPrRP (Appendix Figure 2L-M).This suggested that LiPrRP does not rescue all tanycytes positive by default for Rax.

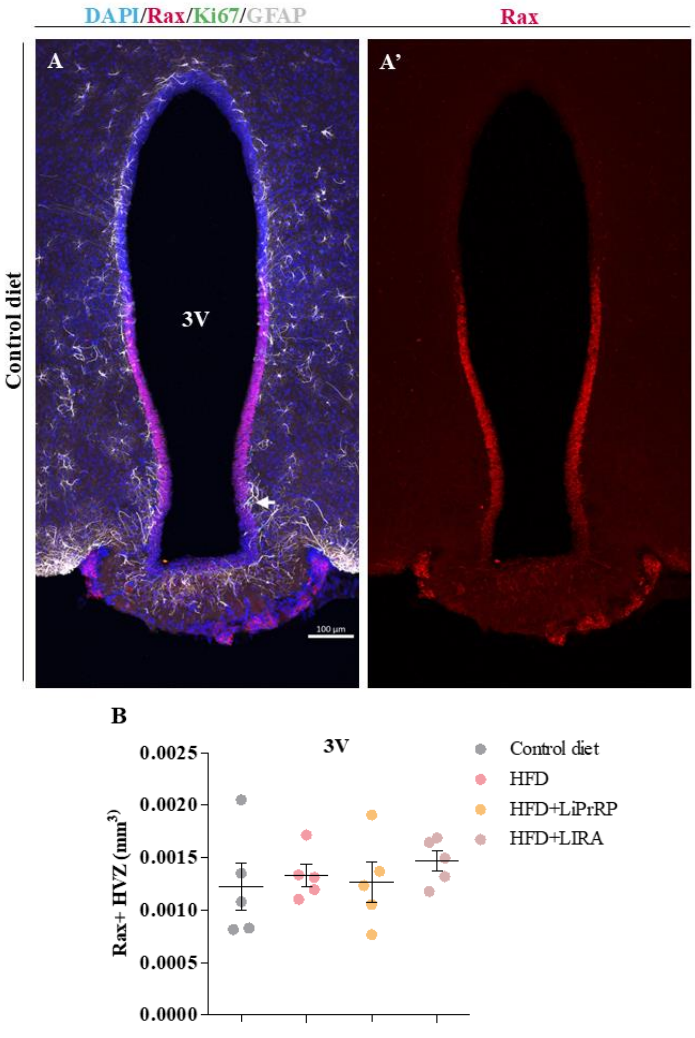

However, results from Sarah Robbins when working in Petrik lab showed that LiPrRP increases the number and proportion of GFAP+ α- and β-tanycytes. The number of β-tanycytes was reduced at 7d and 4mo by the HFD, but this reduction was not rescued by LiPrRP administration. Where the levels of β-tanycytes were increased at all time points, exceeding even the control group levels at 7d (Appendix Figure 2G). This further suggested that LiPrRP can influence tanycyte proliferation.

Figure 3.8. No change observed in volume Rax+ tanycytes in the walls of the 3V. A-A') Representative images of Rax+ tanycytes. B) Volume Rax+ tanycytes in the 3V walls. Data information: S.b.: 100 µm, n = 5 mice per data set for the 21d group. In panel B, One-way ANOVA with Bonferroni's test. Data are presented mean ± SEM.

3.2.8. LiPrRP treatment generated smaller MBH-derived neurospheres and affected cell activation and cell cycle lengths of hypothalamic neural stem cells

One of the mechanisms how LiPrRP could influence adult neurogenesis is changing proliferation and activation of htNSCs. To further understand LiPrRP effect on stem cells, we examined stem cell proliferation in the hypothalamic niche after acute LiPrRP treatment *in vitro*. Primary cell cultures of stem cells from the MBH were treated *in vitro* with LiPrRP as described in Chapter 2 and analysed by time lapse imaging or neurosphere assay in collaboration with Dr Karnošová. Acute, *in vitro* LiPrRP treatment of stem cells from adult mice on normal chow showed no significant difference in number of neurospheres, apoptotic cells per clone or number of cells per clone.

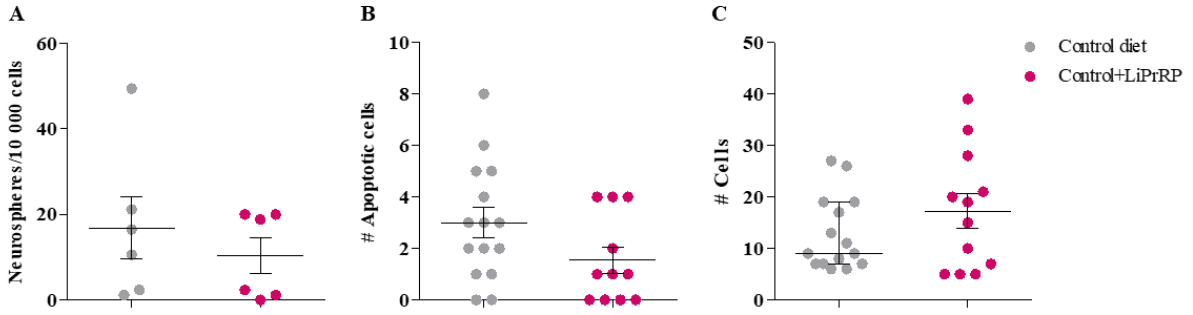

Figure 3.9. *In vitro* LiPrRP treatment of stem cells from adult mice on normal chow showed no significant difference in clone size or apoptotic cell count per clone. A) Neurosphere count per 10 000 plated cells. B) Number of apoptotic cells per clone. C) Number of cells per clone at the end of 4 days of imaging. Data information: n = 3 mice per data set. In panels A, B, Unpaired T-test, Two-tailed. In panel C, Mann Whitney test, Two-tailed. Data are presented as mean ± SEM (A-B), median ± IQR (C).

To further explore the possibility of LiPrRP acting on the htNSCs in the context of DIO, adult mice were fed Control diet or HFD with or without concurrent injections of LiPrRP for 14 days. Primary cell cultures were again prepared and analysed by time lapse imaging and neurosphere assay in collaboration with Oliver Rowley.

Neurospheres from HFD-treated mice showed no difference in diameter after 5 days or 10 days compared to Controls. However, neurospheres from animals exposed to HFD + LiPrRP had smaller diameter at both 5 days and 10 days compared to both Control and HFD. Similarly, neurospheres from animals from the Control + LiPrRP group had a smaller diameter after 5 days in culture compared to Controls. These data are in agreement with the *in vivo* observations, suggesting that LiPrRP reduces the proliferation of htNSCs.

Time lapse imaging analysis was performed to understand the effects of LiPrRP on cell cycle parameters and proliferation *in vitro*. Individual htNSCs were continuously imaged, as described in Chapter 2, to obtain cell division trees for analysis. HFD significantly increased the number of cell divisions per clone (Figure 3.11E). HFD + LiPrRP treatment reduced the number of active clones (defined as clones with at least one cell division during the 4 days widow). Where the generation of observed cell cycle from 1st to 4th has a statistically significant effect on cell cycle length, eventually resulting in shorter cell cycle in HFD + LiPrRP cells. Time lapse imaging also showed that there were fewer clones with at least one apoptotic cell (Figure 3.11I) in both the HFD and HFD + LiPrRP groups (Figure 3.11J). LiPrRP treatment in Control mice did not change the number of cell divisions, but reduced the number of active clones (Figure 3.11H). This suggested that LiPrRP reduced htNSC activation regardless of diet.

Finally, our lab also investigated whether PrRP signalling is cell intrinsic to htNSCs (Appendix figure EV4). Due to LiPrRP being highly adhesive to plasticware, recombinant human PrRP31(hPrRP31) protein was used instead for these experiments. hPrRP31 was added to WT primary htNSCs to determine its effects on cell dynamics and proliferation in contrast to *in vivo* administration as described previously. Exposure to hPrRP31 *in vitro* significantly reduced the number of cell divisions per clone. This suggested that PrRP signalling acted directly on htNSCs to reduce their proliferation. In summary, these results suggested that LiPrRP and hPrRP31 decrease the activation and proliferation of htNSCs *in vitro*.

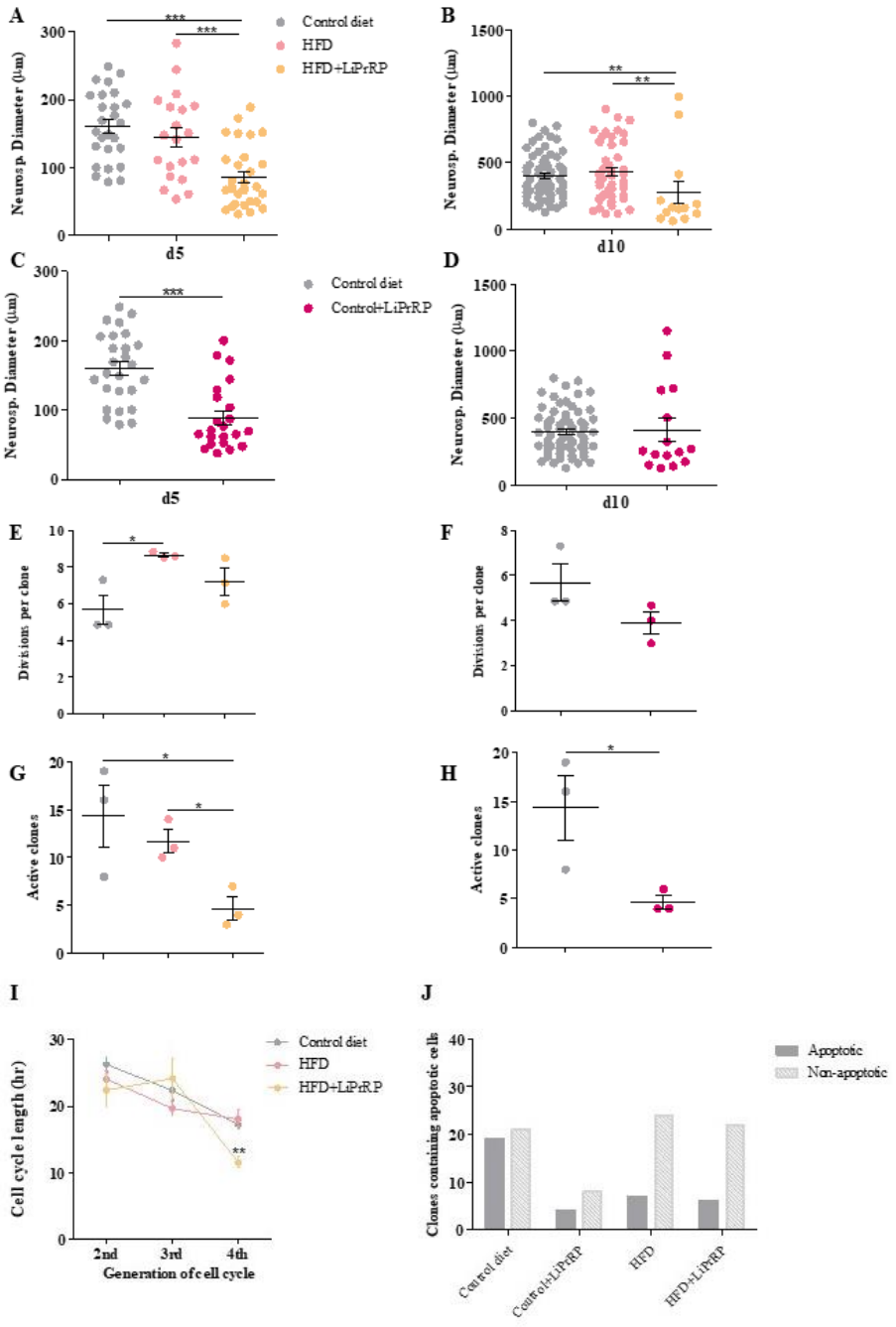

Figure 3.10. LiPrRP reduced cell proliferation of hypothalamic stem cells *in vitro*. A-B) Quantification of diameter of neurospheres 5d (A) and 10d (B) in culture for Control, HFD and HFD + LiPrRP groups. C-D) Quantification of diameter of neurospheres 5d (C) and 10d (D) in culture of Control + LiPrRP group. E) Quantification of the number of cell divisions per division tree for Control, HFD and HFD + LiPrRP (E) and Control + LiPrRP (F). G-H) Time lapse quantification of active (dividing) clones per animal for Control, HFD and HFD + LiPrRP (G) and Control + LiPrRP (H). I) Cell cycle length from the time lapse imaging. J) Proportion of active clones containing at least one apoptotic cell. Data information: In all panels, n = 3 mice for each data set. In panel B, Kruskal–Wallis test with Dunn's test ($H = 10.30$, $p = 0.0058$). In panels C,D,F,G,H, Unpaired T-test, Two-tailed. In other panels, One-way ANOVA with Bonferroni's test (A: $F(2,73) = 15.80$, $p < 0.0001$; E: $F(2,6) = 5.61$, $p = 0.042$). Data are presented as median ± IQR (B) or mean ± SEM (all other panels).

3.3 Short discussion

In this chapter the effects of LiPrRP on neurogenesis, neuronal survival and specification, astrogliogenesis and stem cell proliferation was determined in context of Control diet or DIO using *in vitro* and *in vivo* analysis. The main results detailed here indicated that LiPrRP improved neuronal survival independently of diet in older mice and reduced cell proliferation in the MBH.

3.3.1. LiPrRP increased neuronal survival in older mice in a diet-independent manner

The neurogenic response to HFD is largely attributed to the length of the HFD protocol. The exposure to the HFD was shown to increase or decrease hypothalamic adult neurogenesis depending on the length of HFD treatment and timing of cell birth-dating protocols (Gouazé et al., 2013; Lee et al., 2014; Li et al., 2012; McNay et al., 2012). The short and intermediate HFD protocols used here enabled the examination of effects of LiPrRP on neurogenesis in the context of neuroinflammation and emerging metabolic syndrome (Sugiyama et al., 2020; Thaler et al., 2012), whereas the long protocol provided the context of established obesity (Pražienková et al., 2017).

In vivo analysis of the action of LiPrRP on neurogenesis after HFD administration showed that LiPrRP increased the number of adult generated neurons that was reduced in the context of DIO (at 4mo). The DIO induced reduction in neurons is in agreement with previous literature (Li et al., 2012; McNay et al., 2012). However, this effect was not observed in shorter HFD protocols. While the long-term HFD reduced adult generated neurons, the short and intermediate exposure to HFD did not change the number of newly generated (BrdU+) cells, neurons, or astrocytes in the MBH, and it instead increased the number of new neurons in the ArcN, the primary nutrient and hormone sensing nuclei (Betley et al., 2013), which was reversed by concurrent administration of LiPrRP or LIRA. These findings are also in agreement with previous studies that used short and intermediate HFD protocols (Gouazé et al., 2013; Lee et al., 2014), which can induce reactive gliosis or inflammation but not obesity (Nakandakari et al., 2019; Thaler et al., 2012). While LiPrRP did not alter the number of new cells in the MBH, it was able to reverse the increased production of new neurons in the ArcN observed in the context of the intermediate HFD exposure.

The initial increase in adult generated neurons observed after 21d of HFD may represent a counteractive response aimed at regaining control of the energy circuitry and counterbalancing the effects of the HFD. Indeed, a previous study suggested that acute HFD exposure led to

transient inflammation and hypothalamic injury (Thaler et al., 2012). Additionally, Thaler et al. (2012) indicated that the inflammatory responses are temporarily subsided following the initial increase, implying that neuroprotective mechanisms may initially mitigate the damage (Thaler et al., 2012). Hence, the increased neurogenesis in the intermediate protocol (ArcN) may serve to increase anorexigenic subtypes of neurons to reduce food intake (Gouazé et al., 2013) or replace damaged neurons in this region after inflammatory injury (Thaler et al., 2012) to mitigate HFD induced damage. Indeed, Gouazé et al., (2013) found an increase maturation of newborn cells into POMC expressing neurons in the ArcN in response to 3 weeks HFD feeding. The study revealed that HFD rapidly and transiently increased cell proliferation in the hypothalamus, leading to a surge of newly generated cells within 3 days of HFD exposure before a sharp decline in the number of newly formed cells at 5 days. (Gouazé et al., 2013). Suggesting the fate of POMC neurons is regulated by nutritional conditions. In addition, Thaler et al., (2012) reported that markers of hypothalamic inflammation are elevated within 24 hours of HFD exposure (Thaler et al., 2012). Furthermore, within the first week of HFD consumption, indicators of neuronal injury become apparent in the ArcN and ME, concomitant with reactive gliosis involving the recruitment of both microglia and astrocytes (Thaler et al., 2012). The HFD-fed group exhibited a complex pattern of hypothalamic gene expression, with pro-inflammatory genes like Il6, Tnfa, Socs3, Ikbkb, and Ikbke mRNA showing an "on-off-on" trend. Levels were elevated in the first 3 days of HFD, then declined, and subsequently From days 7-14 and increased again by day 28. These changes in pro-inflammatory gene expression mirrored the initial fluctuations in energy intake, occurring before significant weight gain. This rapid onset of hypothalamic inflammation and reactive gliosis is a hallmark of the neuron injury response observed in rodents consuming a HFD. To directly test if HFD exposure causes injury to ArcN neurons, Thaler et al., (2012) performed immunohistochemistry to detect induction of the chaperone Hsp72, a marker of neuroprotective responses to injury. In rats fed HFD for 7 days, Hsp72 immunostaining, a marker of neuroprotective responses to injury, was increased compared to chow-fed controls. Additionally, hypothalamic Hsp72 mRNA was elevated within 3 days of HFD exposure. The ArcN neurons that showed Hsp72 induction include those containing POMC. The transient nature of this hypothalamic response suggests that neuroprotective mechanisms are activated to mitigate or reverse the injury during the initial stages of HFD feeding (Thaler et al., 2012).However, the specific neuronal subtypes generated following the intermediate HFD protocol in this work were not determined, and the interpretation of the data is currently limited. The finding that LiPrRP reduced the generation of newly generated neurons in the ArcN suggests that LiPrRP counteracts this initial

compensatory response to HFD. It is possible that LiPrRP achieves this by either reducing the proliferation of stem and progenitor cells, or by ameliorating the inflammatory environment associated with short-term HFD exposure, thereby negating the need to generate new neurons to replace those that were lost. Future studies would indeed be advised to investigate the influence of HFD and LiPrRP specifically on distinct neuronal subtypes in this critical hypothalamic region.

The response to HFD observed in the intermediate protocol is not sustained long-term, as evidenced by the reduction in newly generated neurons in DIO mice, as reported in this study and others (McNay et al., 2012). In contrast, LiPrRP increased number of new neurons in the DIO mice. This suggests that LiPrRP may help prolong protective responses in the hypothalamus, possibly by decreasing the activation and proliferation of stem cells and thereby preventing their depletion and thereby prolonging their potential to contribute to and maintain the neural population. Additionally, LiPrRP may increase neuronal survival in the context of DIO.

These data suggested that LiPrRP plays a neuroprotective role, similar to the effects of antidepressants in the hippocampus (D'Sa & Duman, 2002; Banasr et al., 2006; Olianas et al., 2017), or GLP-1 receptor agonists in models of neurodegeneration and type 2 diabetes (Zhao et al., 2021; Maletínská et al., 2019). Indeed, prior studies have shown that DIO can increase cell death in the adult hypothalamus (Moraes et al., 2009; McNay et al., 2012). The results presented here indicate that DIO mice treated with LiPrRP had a statistically significant reduction in the number of AC3+ cells (apoptotic cells), suggesting that LiPrRP increased the survival of cells in the context of DIO. However, the phenotypes of the quantified AC3+ cells were not determined. Therefore, it is unclear whether the reduced number of AC3+ cells indicated a decrease in apoptotic neurons specifically. The neuroprotective effects of LiPrRP is further supported by the fact that LiPrRP did not mitigate gliosis, which could be a contributor to the increased inflammation and cell death observed after HFD intake (Thaler et al., 2012; Seong et al., 2019) and did not affect astrogliogenesis at all time points. This suggested that the pro-survival effects of LiPrRP apply only to adult generated neurons in the context of DIO. This is in agreement with the previous studies that has shown that PrRP and LiPrRP increase neuronal survival in addition to its function in reducing food intake (Lawrence et al., 2000; Lawrence et al., 2002; Pražienková et al., 2019; Maletínská et al., 2019). Since no change in adult-generated neurons was observed in the short and intermediate HFD exposure, one could conclude that the pro-survival effects of LiPrRP are not required in these contexts.

Furthermore, the decreased neuronal survival observed in the long HFD protocol can be compared to the involvement of metabolic dysregulation in the development of neurodegenerative disorders. In the elderly, the combination of obesity, insulin resistance, and metabolic syndrome increases the probability of developing AD and other neurodegenerative diseases (Raffaitin et al., 2009; Razay et al., 2007). The underlying mechanisms driving the development of AD are not fully elucidated. However, one hypothesis posits that AD can be considered a form of "type 3 diabetes mellitus" due to several shared features between AD and T2DM, including insulin resistance, impaired glucose metabolism, and heightened inflammation or oxidative stress (Steen et al., 2005; de la Monte & Wands, 2008; Takeda et al., 2010). Alzheimer's disease is a progressive neurodegenerative disorder characterized by key neuropathological hallmarks, including the extracellular accumulation of amyloid-β into senile plaques and the intraneuronal aggregation of hyperphosphorylated and truncated tau proteins into neurofibrillary tangles. These pathological features are closely associated with neuroinflammation and substantial neuronal loss (Liu et al., 2022). T2DM on the other hand, characterised by hyperglycaemia, insulin resistance, and peripheral inflammation, has been associated with an elevated risk of AD (Profenno et al., 2009). The underlying mechanisms are not fully understood, but may involve the accumulation of misfolded Aβ and hyperphosphorylated Tau proteins in the pancreases and insulin resistance in the brain (Kuehn, 2020; Miklossy et al., 2008). Impairments in brain insulin signalling, reduced glucose utilisation and deficient energy metabolism are early features of AD, suggesting a link between the two conditions. Even without the presence of T2DM, insulin resistance has been associated with accelerated cognitive decline with aging (Messier et al., 2004; Watson & Craft, 2004). Consequently, disruptions in brain insulin signalling and metabolism have been proposed as a potential pathophysiological mechanism underlying this neurodegenerative disorder (de la Monte, 2012; Hölscher & Lin, 2008; Liu et al., 2022; Watson & Craft, 2004).

Overconsumption of HFD leads to obesity and elevated circulating free fatty acids, which can trigger low-grade inflammation that plays a key role in insulin resistance. Studies examining inflammatory pathways in obesity have found that inflammatory events are common in both diabetes and obesity (Lee et al., 2012; Snodgrass et al., 2013). Indeed, a recent study (Liu et al., 2022) found that inflammation associated with obesity and diabetes induced by HFD activates the neuronal C/EBPβ/AEP signalling pathway, which drives the development of AD pathologies and cognitive impairments. The study found that a HFD triggered the onset of diabetes and insulin resistance in neuronal Thy1-C/EBPβ transgenic mice. This was

accompanied by prominent accumulation of amyloid-β and hyperphosphorylated tau aggregation in the brain, leading to cognitive deficits. Remarkably, the anti-inflammatory drug aspirin strongly mitigated the HFD-induced diabetes and Alzheimer's disease pathologies in these transgenic mice. Collectively, these findings demonstrated that inflammation-activated neuronal C/EBPβ/AEP signalling serves as a mechanistic link between diabetes and the pathogenesis of AD (Liu et al., 2022).

Other studies (Karmi et al., 2010; Wilson & Bindert, 1997) have additionally found that fatty acid uptake and accumulation in the brain are associated with metabolic syndrome and AD pathogenesis. Elevated brain uptake and accumulation of fatty acids have been associated with metabolic syndrome, and these changes are reversible through weight loss (Karmi et al., 2010). Additionally, a high-fat, diabetogenic diet has been shown to promote AD pathogenesis, while in contrast, a diet rich in docosahexaenoic acid (such as fish like salmon and tuna) exhibits protective effects against AD (Cole et al., 2010; Liu et al., 2022). Elevated levels of the protein tau have also been observed both in diabetic and AD mice, independent of the peripheral metabolic status indicating a link between these conditions (Takaloa et al., 2014). Free fatty acids can directly stimulate the assembly of amyloid and tau filaments *in vitro* (Wilson & Bindert, 1997). Collectively, these findings suggest that saturated fatty acids can directly influence glial activation in the brain by crossing the BBB. This may represent one potential mechanism by which obesity leads to cognitive dysfunction (Pugazhenthi et al., 2017). The CNS was previously considered immune-privileged, but this view has been challenged due to the bidirectional communication between peripheral and central inflammation (Filippo et al., 2013). Chronic low-grade inflammation, or "inflammaging," is an important factor in insulin resistance and the development of T2DM (Franceschi, 2008; Shoelson et al., 2006). Further research is still required to elucidate the molecular pathways that interconnect diabetes, obesity, and AD (Pugazhenthi et al., 2017).

LiPrRP have been investigated in models of AD where it seems to be a potential tool for the attenuation of neurodegenerative disorders (Špolcová et al., 2015). Further supporting the pro-survival effects in hypothalamic cells after LiPrRP administration observed in this study. The PrRP analogue palm1-PrRP31 and LIRA have both been shown to ameliorate hippocampal insulin signalling, decrease the activity of major tau kinases, and attenuate the pathological hyperphosphorylation of tau in MSG-obese mice, which are a model of obesity and pre-diabetes (Špolcová et al., 2015). In a mouse model of Alzheimer's-like tau pathology (THY-Tau22 mice), treatment with the PrRP analogue palm11-PrRP (LiPrRP) for two months

improved spatial memory and reduced tau hyperphosphorylation at specific sites in the hippocampus. The treatment also increased phosphorylation of Akt, which is important for activating PSD95, which is further important for synaptic stability and proper memory function (Popelova et al., 2018). While the anti-apoptotic and neuroprotective effect of PrRP analogues has been shown by us and others, their mechanism of action is poorly understood. To speculate, the neuroprotective effects of LiPrRP may involve the insulin and leptin signalling pathways, both of which are influenced by the administration of LiPrRP also in this study. Activating receptors for leptin, insulin, PrRP, and GLP-1 can initiate neuroprotective signalling pathways, such as the Insulin Receptor Substrate-1 (IRS-1)/PI3K/Akt pathway, which inhibits apoptosis and increases phosphorylation of glycogen synthase kinase 3β (GSK-3β; Maletínská et al., 2019). In the CNS, insulin plays a crucial role in supporting neuronal synaptic and dendritic plasticity, and cognitive processes such as memory formation (Dineley et al., 2014). PrRP and its lipidized analogue can activate components of the insulin signalling pathway, including increased levels of 3-phosphoinositide-dependent kinase 1 (PDK1) and Akt (Zmeškalová et al., 2020), and enhance the activation of mTORC1, GSK-3β, and the ERK-CREB pathway, similar to insulin (Zmeškalová et al., 2020). The same signalling pathways has been shown to be activated in models of neurodegeneration (Kořínková et al., 2020). These pathways could therefore underlie the neuroprotective effects of PrRP (Zmeškalová et al., 2020), allowing it to exert beneficial impacts on neuropathological processes akin to those of insulin (Chapman et al., 2018). The neuroprotective effects of PrRP may alternatively be mediated through the leptin signalling pathway. Leptin, like insulin, contributes to the activation of the Akt signalling pathway, which is an important anti-apoptotic factor (King et al., 2018; Zmeškalová et al., 2020). Conversely, leptin resistance leads to reduced Akt activation, which has been linked to impaired leptin signalling in AD models (APP/PS1 mice) (King et al., 2018). Additionally, improper leptin signalling can contribute to the development of insulin resistance, which is associated with neurodegenerative disorders (Zmeškalová et al., 2020). Furthermore, leptin modulates the production of PrRP in the hypothalamus, and the anorexigenic effects of PrRP are synergistic with those of leptin (Kořínková et al., 2020). Therefore, the neuroprotective effects of PrRP in the hypothalamus may be partly attributed to its interactions with the leptin signalling pathway through Akt activation.

In a study by Popelova et al. (2018), the researchers found that treatment with the PrRP analogue palm11-PrRP improved spatial memory and reduced tau hyperphosphorylation in a mouse model of Alzheimer's-like tau pathology (THY-Tau22 mice). Interestingly, this study

also showed that long-term administration of the lipidized PrRP analogue did not result in changes to food intake or body weight, even in lean WT littermates of THY-Tau22 mice. This suggests that, outside the context of obesity, the lipidized analogues of PrRP have no influence on body weight. This is consistent with the findings presented here, where LiPrRP increased the survival of newborn neurons in older mice on a Control diet, without causing any weight loss (Popelova et al., 2018). This is similar to the effect of LIRA, which has been previously shown to affect food intake and body weight only in obese animals (Porter et al., 2010) but not in the lean ones (Hansen et al., 2015). Indeed, the pro-survival effects of LiPrRP were observed again in mice fed a Control diet for 4mo, suggesting that LiPrRP exerts its neuroprotective effects in a diet-independent manner in older mice. Moreover, the finding that LiPrRP improved the survival of newborn neurons in Control fed mice indicates that neurogenesis was enhanced as a consequence of LiPrRP-induced activation, rather than solely through the improvement of the brain pathology. Interestingly, in older Control mice, treatment with LiPrRP reduced GFAP-positive astrocytes while increasing NeuN-positive neurons, despite the number of adult-generated cells remaining unchanged. This suggests that under control conditions, LiPrRP promotes neurogenesis without altering overall cellular output in older mice. Taken together, this suggests that LiPrRP can exert neuroprotective effects regardless of the metabolic state, not just in the presence of a dysregulated metabolism. One question that remains unanswered is the impact of LiPrRP on specific neuronal populations involved in feeding regulation, which was further explored by treating hiPSC-derived hypothalamic neurons with PrRP during maturation, as discussed in Chapter 4.

3.3.2. LiPrRP reduced cell proliferation

The pool of proliferating cells in the MBH consists not only of proliferating htNSCs, but also neural and glial precursors as well as invading peripheral macrophages (Valdearcos et al., 2017; Sharif et al., 2021). Further investigation revealed that LiPrRP reduced cell proliferation in the MBH and ME of mice fed either a Control diet or HFD for 21d, compared to Controls. Similarly, LIRA had the same anti-proliferative effect as LiPrRP in the MBH of mice fed HFD for 21d. This indicates that reduced cell proliferation is a shared feature of these anti-obesity compounds. Future studies should quantify the additional proliferating cell types, including macrophages, to further elucidate how the anti-obesity compounds affect the cellular composition in the hypothalamus.

Despite the observed reduction in proliferating cells, proliferating tanycytes were rarely observed *in vivo*. Since it is not technically feasible to image the dynamics of stem cells in the

hypothalamus *in vivo*, we instead observed these characteristics *in vitro*. *In vitro* analysis of htNSCs through neurosphere assays and time-lapse analysis revealed that LiPrRP also reduced cell proliferation when administered for 14 days *in vivo*. The reduction in cell proliferation was accompanied by a decreased number of active clones when mice were treated with HFD and LiPrRP, suggesting that LiPrRP reduces the activation of stem cells. This was further confirmed by immunohistochemical staining for β-tanycytes, and α-tanycytes, performed by Sarah Robbins when she worked in the Petrik lab. Her work showed that LiPrRP increases the number and proportion of GFAP-positive α- and β-tanycytes. The number of β-tanycytes was reduced at 7d and 4mo by the HFD, but this reduction was not only rescued by LiPrRP administration - the levels of β-tanycytes were actually increased at all time points, exceeding even the control group levels at 7d (Appendix Figure 2). The lowered proliferation of stem cells may help preserve the stem cell pool over time. Since stem cells have a limited number of divisions over their lifespan (Petrik et al., 2022), reducing their activation could extend their availability for future tissue regeneration and repair. Together, these findings suggest that LiPrRP increases the number of stem cells by reducing their activation, thereby prolonging their potential to contribute to and maintain the neural population, even during prolonged HFD exposure, as observed. This is further supported by the observed reduction in body weight.

The finding that both LiPrRP and LIRA reduce cell proliferation and increased β-tanycytes in the hypothalamus suggests that this is a critical mechanism for their anti-obesity effects. These intriguing results can be compared to other studies on anti-obesity medications. Similarly to LiPrRP and LIRA, some GLP-1 receptor agonists used to treat T2DM have also been shown to have anti-proliferative effects in cancer studies, although these effects appear to be cancer-type specific (Sánchez-Garrido et al., 2017). Given that obesity is a recognised risk factor for various cancers, as it can create a microenvironment that favours tumour growth, it is plausible that the anti-proliferative effects of LiPrRP and LIRA on hypothalamic cells contribute to their anti-obesity properties. For example, research in rodents has shown that GLP-1 agonists can reduce tumour growth and metastasis in some cancer models, indicating a general anti-proliferative effect of these compounds as part of their mechanism against disease progression (Zhao et al., 2021). LIRA exhibits anti-proliferative and pro-apoptotic effects on gemcitabine-resistant pancreatic cancer cells by inhibiting the PI3K/Akt and NF-κB signalling pathways (Zhao et al., 2020). In fact, NF-κB is a critical transcription factor that regulates a wide range of cellular processes, including inflammation, immune responses, cell proliferation, and apoptosis (Baker et al., 2011). Importantly, it has also been identified as a key mediator of

tumour growth and resistance to chemotherapy resistance (Pramanik et al., 2018). Interestingly, the NF-κB pathway is also dysregulated in htNSCs cells during obesity (Li et al., 2012), where HFD induces inflammation in the hypothalamus, upregulating c-Jun N-terminal kinase (JNK) and NF-κB pathways, leading to increased apoptosis, suppression of neural differentiation of htNSCs and disrupts central insulin and leptin signalling (Zhang et al., 2008). In contrast, the lipidized PrRP analogue, palm11-PrRP31, attenuates diet-induced obesity and reduces JNK/c-JUN phosphorylation in the hypothalamus, suggesting it may modulate these pathways to exert its anti-obesity effects (Holubová et al., 2018). NF-κB is known to be an upstream regulator of the JNK (Nakano, 2004), but research has also shown that JNK can regulate the activity of NF-κB, suggesting a complex interplay (Pan et al., 2013; Yang et al., 2017). The complex interplay between NF-κB and JNK signalling further highlights the importance of these pathways in the regulation of cell proliferation, survival and differentiation in the context of obesity and related disorders. The findings suggest that LiPrRP and LIRA may exert their shared anti-proliferative and tanycyte-protective effects through their influence on the NF-κB signalling pathways in DIO. Nevertheless, given that LiPrRP exhibited neuroprotective effects even in control conditions, this may represent only one of the mechanisms through which LiPrRP influences cell proliferation.

Similar to the protective effects of LiPrRP on the neuronal population in Control conditions, LiPrRP also reduced cell proliferation and activation of stem cells in control conditions, both *in vivo* and *in vitro*. To further investigate whether PrRP signalling is intrinsic to htNSCs, our laboratory conducted additional experiments. Recombinant human PrRP31 protein, which does not adhere to cell culture plasticware, was added to primary WT htNSCs. This allowed us to directly assess the impact of PrRP on the dynamics and proliferation of these stem cells. The findings demonstrated that exposure to hPrRP31 *in vitro* significantly decreased the number of cells per clone and cell divisions (Appendix Figure EV4). These results suggest that PrRP signalling directly acts on htNSCs to suppress their proliferation, indicating that PrRP signalling is cell intrinsic to htNSCs. Further confirming that, the anti-proliferative effects of LiPrRP, similarly to its neuroprotective effects, are not dependent on the pathological conditions of the metabolic syndrome.

Taken together, these results suggest that LiPrRP and PrRP decrease activation and proliferation of htNSCs. Interestingly, mice on a Control diet and treated with the compound did not lose any body weight, in contrast to those treated with LiPrRP and HFD. These findings indicate that LiPrRP protects the neurogenic niche by maintaining the proliferative capacity of

htNSCs under obesity inducing diets, likely through direct signalling on the stem cells themselves, but does not lead to weight loss in healthy, non-obese animals. These findings have important implications for understanding the mechanisms by which LiPrRP mediates its anti-obesity effects and the signalling pathways involved. Future studies should focus on unpacking the intracellular mechanisms by which LiPrRP reduces htNSCs proliferation both in the context of DIO and physiological conditions. Interestingly, the potential applications of this compound may extend beyond just anti-obesity effects, as it could potentially be utilised in the context of neurodegenerative diseases, similar to how LIRA has been shown to have a positive effect on hippocampal neurogenesis (Maletínská et al., 2019). Although our lab did not observe these beneficial effects of LIRA in the hippocampus, as described in Appendix Figure EV2. The data collectively indicates that LiPrRP prolongs the ability of the stem cell population to respond to HFD and also improves the long-term survival of adult-generated neurons. However, it cannot be claimed that LiPrRP reduces body weight in mice solely through neurogenesis.

The cell-intrinsic effects of LiPrRP are indeed intriguing, and the fact that the compound exhibits an effect even in a Control diet suggests that it directly influences hypothalamic cell populations, rather than solely reducing body weight by modulating the surrounding environment. While LiPrRP may assist the normal response to hypothalamic injury to endure even when protective mechanisms become dysregulated, these mechanisms are typically activated as a response. Thus, it is unsurprising that LiPrRP works through the same pathways in both Control and HFD conditions, but with differing physiological outcomes. Obesity is a complex chronic disease, and the influence of LiPrRP on neurogenesis may only be a small part of the mechanism by which it lowers body weight. Future research should therefore investigate whether selective inhibition of neurogenesis in the hypothalamus would attenuate the appetite-suppressing effects of anti-obesity compounds, akin to the evidence that neurogenesis in the hippocampus is necessary for the action of antidepressants (Santarelli et al., 2003).

In conclusion, the main results detailed in this chapter indicated that LiPrRP improved neuronal survival independently of diet in older mice and reduced cell proliferation in the MBH. LiPrRP appears to directly act on hypothalamic neural stem/progenitor cells, suppressing their proliferation and activation, thereby preserving the stem cell pool in adverse conditions such as DIO. However, the underlying mechanisms linking the effects of LiPrRP on neurogenesis and its anti-obesity actions requires further investigation.

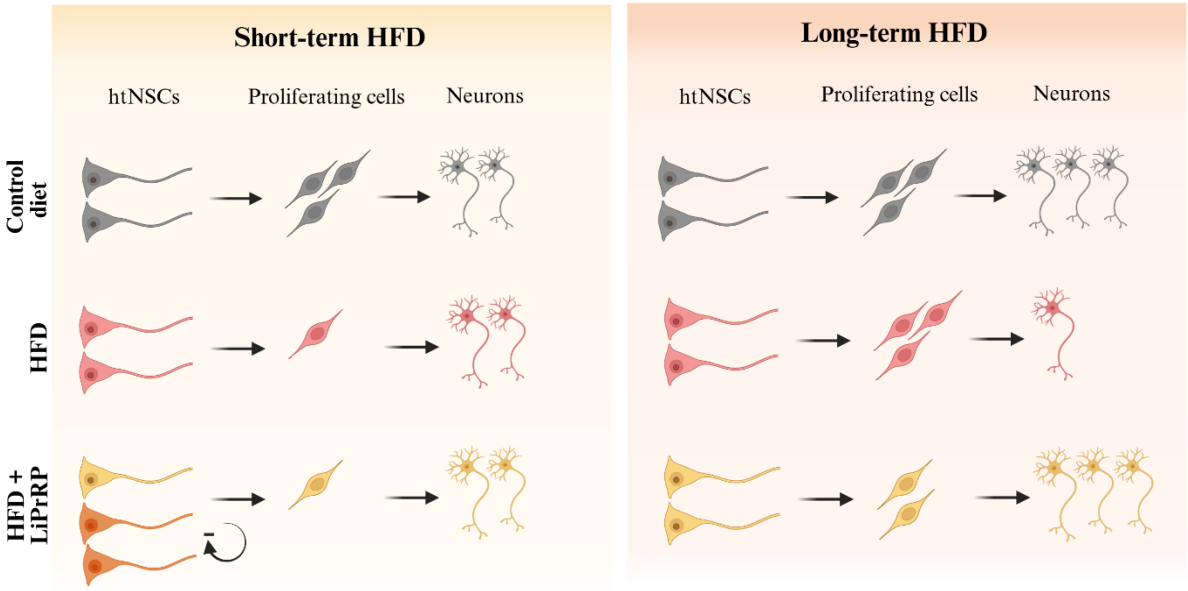

Figure 3.12. Graphical summary of the overall effects of short-term and long-term HFD and LiPrRP administration on adult neurogenesis in the hypothalamus. The summary represents results from the experiments outlined in Chapter 3 and published data outlined in Appendix 1. (Left) LiPrRP decreases proliferation and activation of htNSCs during short and intermediate HFD protocols. (Right) LiPrRP increases survival of new hypothalamic neurons during long-term HFD and obesity. Figure adapted from Jorgensen et al. (2024). Figure made in BioRender (Biorender.com).

Chapter 4: The Effects of a Lipidized Analogue of Prolactin Releasing Peptide on Human Induced Pluripotent Stem cells

4.1. Short Introduction:

The hypothalamus, comprising a mere 0.3 % of the adult human brain, plays a pivotal role in regulating the autonomic nervous system and endocrine function (Rajamani et al., 2018). This small yet vital structure holds significant physiological importance, serving as a central regulator of appetite and energy homeostasis (McNay et al., 2012; Kirwan et al., 2017; Rajamani et al., 2018), making it an ideal target for combatting obesity. Within the MBH lies the ArcN where two distinct populations of anorexigenic and orexigenic neurons reside. The anorexigenic neurons suppress appetite and express POMC, a precursor of the bioactive peptide α-MSH (Millington, 2007; Sonnefeld et al., 2023; Strnadová et al., 2024), which have potent anorectic effects through activation of MC4R in the PVN (Sonnefeld et al., 2023; Merkle et al., 2015; Kirwan et al., 2017). The orexigenic neurons instead promote appetite and secrete NPY. One of the key functions of these neuronal populations is to respond appropriately to hormones and neuropeptides both locally and peripherally (Rajamani et al., 2018). By secreting neuropeptides like NPY and α-MSH (Wang et al., 2015), the hypothalamus coordinates the body's responses to hunger and satiety signals, thereby regulating food intake and energy expenditure (Rajamani et al., 2018). The importance of POMC expressing neurons in the regulation of food intake has been firmly established (Millington, 2007; De Solis et al., 2024). Mutations affecting hypothalamic-specific genes, including POMC, in monogenic obesity syndromes further corroborate the notion that the hypothalamus is a central regulator of obesity in humans (Rajamani et al., 2018). These rare cases in humans where genetic mutations results in POMC deficiency display striking hyperphagia and early onset obesity (Çetinkaya et al., 2018). Given the central role of the hypothalamus in the regulation of appetite and energy homeostasis, it represents an attractive target for anti-obesity pharmacotherapies.

LiPrRP is a novel anti-obesity compound that has shown to reduce food intake (Kuneš et al., 2016) and weight in mice (Maletínská et al., 2015). LiPrRP (palm11-PrRP31) is a lipidized form of the endogenous neuropeptide hPrRP31. PrRP is an anorexigenic neuropeptide and is a ligand of the GPR10 receptor. Importantly, LiPrRP has been shown to have long lasting effects even after treatment cessation with no weight regain after two weeks of stopped treatment

(Holubová et al., 2018). This may indicate a capability to modify the appetite circuitry of the adult brain for long lasting results.

The relative inaccessibility of hypothalamus tissue has hindered the acquisition of live cells from human subjects, which is a significant obstacle for obesity research (Rajamani et al., 2018). However, the utilisation of human induced pluripotent stem cells (hiPSCs) circumvents the challenge of direct collection by enabling the generation of hypothalamic-like neuronal cultures from readily available sources, such as blood or fibroblasts. This approach facilitates the investigation of mechanisms underlying the metabolic dysregulation that affects the CNS. Indeed, hiPSCs have emerged as a powerful tool for regenerative medicine, disease modelling, and drug discovery. These cells have the ability to differentiate into various cell types, making them highly valuable for understanding disease mechanisms and testing novel therapeutic compounds (Singh et al., 2015; Inoue & Yamanaka, 2011). Kirwan et al. (2017) published a protocol to efficiently generate neuropeptidergic hypothalamic neurons from human induced pluripotent stem cells, some of which express POMC (Kirwan et al., 2017). The initial protocol (Merkle et al., 2015) was reported to yield around 0.3% of POMC expressing cells (around 3 POMC-positive cells per 1000 nuclei).

hiPSCs originate from adult somatic cells, including skin or blood cells, that have been genetically reprogrammed to an embryonic stem cell-like state. These hiPSCs can proliferate indefinitely while maintaining the capacity to differentiate into diverse cell types from the three germ layers, through the application of specific small molecules, transcription factors, and growth factors (Takahashi & Yamanaka, 2006; Yamanaka, 2012; Hamazaki et al., 2017; Shi et al., 2016; Karagiannis et al., 2019; Rowe & Daley, 2019). Despite successful differentiation of neuronal progenitors from mouse and human embryonic stem cells (ES) /iPSCs, few studies have managed to pattern these progenitors into diverse hypothalamic neurons. Differentiation methods can be broadly classified as 3D or 2D approaches. While 3D, or self-patterning, approaches have relied on the inherent tendencies of undirected stem cells, 2D, or small molecule induction, approaches have utilised carefully controlled activation of specific pathways (Santos et al., 2021). For example, a study by Wataya et al. (2008) used a 3D culture system with mouse ES to generate hypothalamic progenitor cells by minimising the presence of exogenous signals (Watanabe et al., 2007; Wataya et al., 2008). It involved dissociating ES cells, allowing them to re-aggregate in low-adhesion plates, and culturing the aggregates in a medium containing knockout serum replacement (KSR) with no major exogenous inductive factors. In this condition, the cells spontaneously differentiate into neuronal progenitors with a

forebrain identity (Watanabe et al., 2007). To further refine this approach, the authors replaced the knockout serum replacement with a strictly chemically defined N2 neurobasal medium and B27 supplement, which efficiently directed the cells to express markers of the embryonic rostral hypothalamus, including SIX3 around day 5 of differentiation, and RAX+/NESTIN+/SOX1+ cells around day 7. By day 25, hypothalamic cells expressed NKX2.1, AgRP, and NPY markers when treated with Sonic hedgehog (Shh; Wataya et al., 2008). In contrast, small molecule-based approaches utilise defined combinations of small molecules to guide the differentiation towards a hypothalamic neuron fate (Santos et al., 2021). A protocol for differentiating hPSCs into hypothalamic neurons was published in 2015 by the research group at Harvard University (Merkle et al., 2015). The researchers used inhibitors of the transforming growth factor-beta (TGF-b), Nodal, and Activin signalling pathways, as well as bone morphogenetic protein (BMP) signalling (SMAD inhibitors: LDL-193189 and SB431542), to efficiently promote the generation of neuronal progenitor cells from hPSCs. This involved suppressing Wnt signalling and activating the ventralizing Shh pathway. The differentiation protocol utilised a medium containing KSR initially, before transitioning to the N2 neurobasal medium from day 4 to day 8, consistent with previous methods. Additionally, the Wnt inhibitor XAV939 was included from day 0 to day 8 as well as inhibiting SMAD signalling, and Shh activators SAG and Purmorphamine were introduced on day 2, 48 hours after SMAD inhibition (Merkle et al., 2015). The researchers reported that after 30 days of differentiation, around 93% of the neurons were positive for the early neuronal markers. Merkle et al. (2015) found that actively directing the differentiation towards a hypothalamic fate resulted in a higher proportion of hypothalamic-like cells and lower variability compared to an undirected approach. In a follow-up study (Kirwan et al., 2017), the researchers improved their initial protocol by replacing the KRS serum with N2 medium and introducing Notch inhibition using DAPT during days 8-14 of differentiation, which is the protocol used in the current study (Figure 4.1).

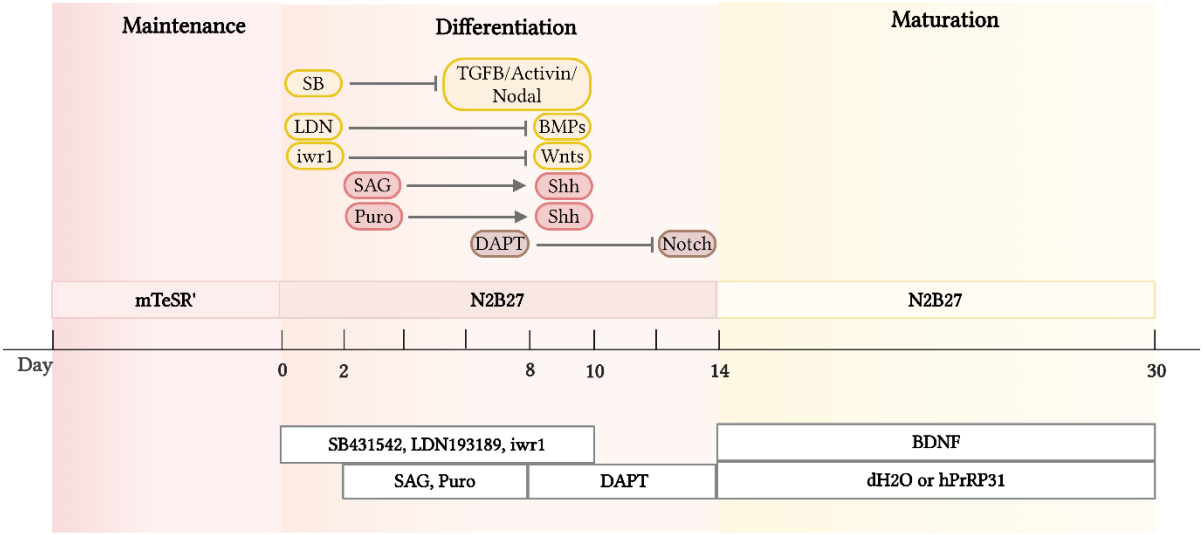

Figure 4.1. hiPSC visual protocol. In this study the protocol published by Kirwan et al. (2017) was used. With one substitution of the Wnt inhibitor XAV939 to iwr1 as indicated in the figure. Treatment with hPrRP31 was introduced during maturation as indicated. Figure made in BioRender (Biorender.com).

The rate of neurogenesis in the hypothalamus have been found to be modulated by environmental interventions (McNay et al., 2012; Jorgensen et al., 2024) However, the research have not yet identified the stages of neurogenesis in the hypothalamic neurogenic niche and if external interventions can drive specific neuronal fate specification. Given that the potential to alter the fate specification of human neurons through external interventions, such as pharmacological interventions, in turn could lead to lasting structural changes with long lasting functional implications within the appetite circuitry of the adult brain highlights the importance of this research. This could offer people who struggle with obesity a treatment option with persisting benefits and efficacy even after treatment cessation.

Thereby, one of the ways LiPrRP may exert their long lasting anti-obesity effects is by modulating the proportion of anorexigenic POMC expressing neurons to the orexigenic NPY expressing neurons. Therefore, these experiments aimed to investigate the effects of the novel anti-obesity compound LiPrRP, on the specification and gene expression profiles of hiPSC-derived hypothalamic neurons. This will provide insights into the mechanisms by which these compounds may modulate energy balance and offer a platform for testing potential therapies targeting the hypothalamic control of feeding behaviour.

Due to the tendency of the LiPrRP compound to adhere to plastic surfaces, the endogenous protein hPrRP31 was used instead. To determine the effects of hPrRP31 on neuronal fate specification *in vitro,* hypothalamic-like neurons were generated from human induced pluripotent stem cells using previously an established protocol (Kirwan et al., 2017) as described in detail in Chapter 2 (Figure 4.1.). Briefly, the hiPSC lines, all from healthy male donors, Kolf-Cl (Kolf), 18n6 and i900 were differentiated into hypothalamic neurons for 14 days. The cells were cryopreserved on d14 and quality checked for expression of Forkhead box protein G1 (*FOXG1*/FOXG1) and NK2 homeobox 1 (*NKX2.1*/NKX2.1). After thawing and re-plating for maturation the immature neurons were matured in the presence or absence of hPrRP31 until d30 when they were fixed and immunocytochemically stained or lysed for RT-qPCR of selected genes. The relative expression of genes and the proportions of neurons expressing key neuropeptides involved in feeding and energy homeostasis, such as POMC, NPY, and the PrRP receptor GPR10, were quantified after treatment with the anti-obesity compound. These experiments were conducted in collaboration with May Surridge-Smith when working in Petrik lab.

4.2. Results:

4.2.1. Preliminary findings indicated a promising increase in the proportion of Map2+ mature neurons that co-expressed POMC after treatment with hPrRP31

Preliminary results using the Kolf cell line, suggested a promising increase in the proportion of Map2+ neurons and POMC+Map2+ neurons out of all Map2+ neurons with hPrRP31 treatment compared to Controls (Figure 4.2A). However, due to the low sample size, the quantifications were conducted with N = 1. Therefore, the experiment was expanded as described above.

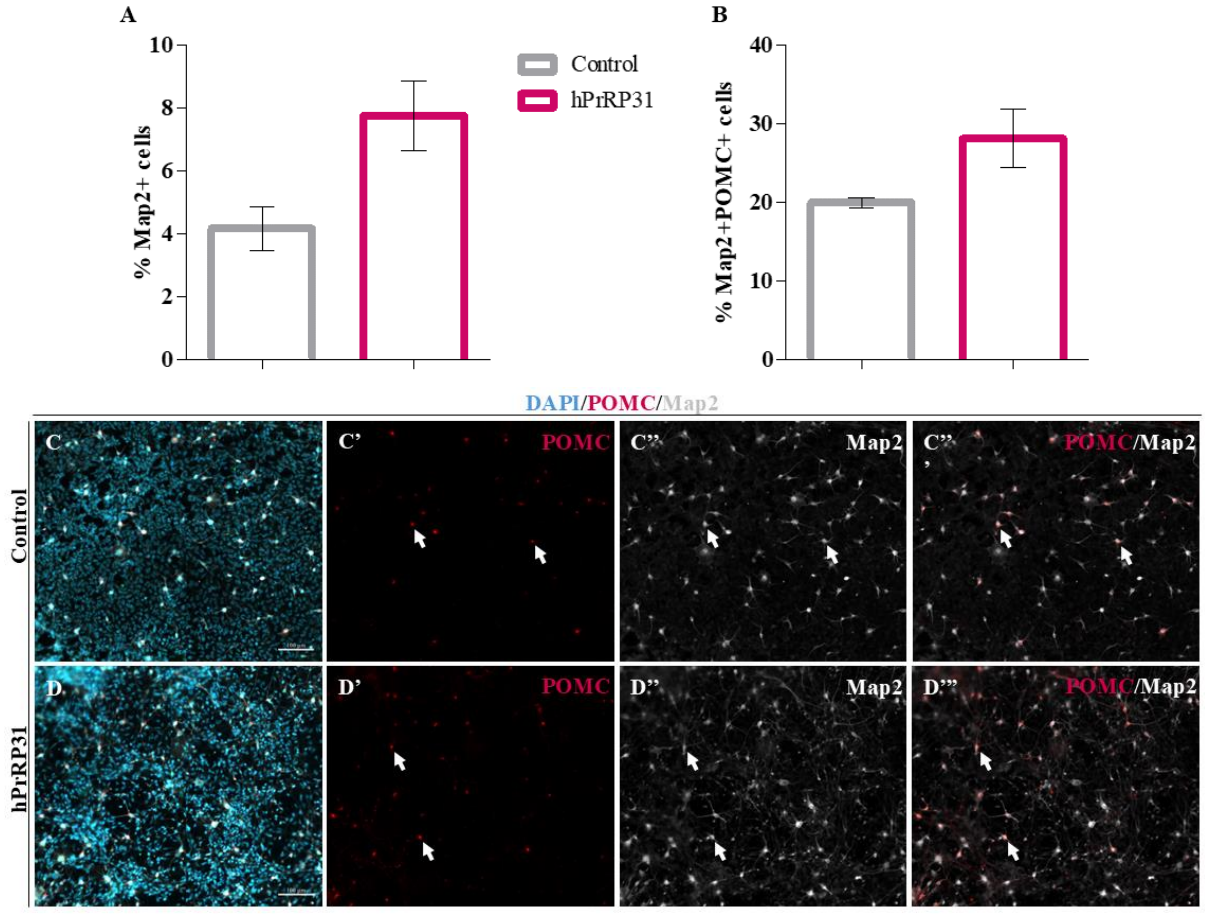

Figure 4.2. Preliminary results showed a promising increase in POMC expressing Map2+ neurons. A) Percent Map2+ neurons out of DAPI+ nuclei generated after 30 days in culture in control and hPrRP31 treated wells. B) Percent Map2+POMC+ cells out of all Map2+ cells (both POMC+ and POMC-) after 30 days in culture in control and hPrRP31 treated wells. C-C''') Representative confocal images of DAPI, POMC, and Map2 in a Control well. D-D''') Representative images of DAPI, POMC and Map2 in a hPrRP31 treated well. Kolf cells were used in this experiment. Data information: S.b.: 100 µm. N = 1 cell line (n = 2 replicate wells). Statistical analysis not possible due to the low number of replicates. Data are presented as median ± IQR (all panels). Confocal scans: 20X.

In the preliminary experiment, human induced pluripotent stem cell derived cortical-like neurons (hiCTNs) were generated as a quality control to the human induced pluripotent stem cell derived hypothalamic-like neurons (hiHTNs). Cell identity was determined by immunocytochemical staining (ICC) of the cortical neuronal markers COUP-TF-interacting protein 2 (CTIP2) and T-box brain 1 (TBR1), as well as the hypothalamic neuronal markers NPY, NKX2.1, POMC and NPY. The ICC of the NPY and NKX2.1 markers showed non-specific staining (Data not shown). The hiHTNs did not express the cortical marker CTIP2, but it was successfully expressed in the hiCTNs. The hiCTNs additionally expressed TBR1, another marker for cortical neuronal differentiation (Kirwan et al., 2017), but did not express the hypothalamic markers for POMC. The quantified hiHTNs were cryopreserved at d14 and thawed for maturation and treatment, in contrast to the hiHTNs shown in Figure 4.3, which were not cryopreserved at day 14 and were not quantified.

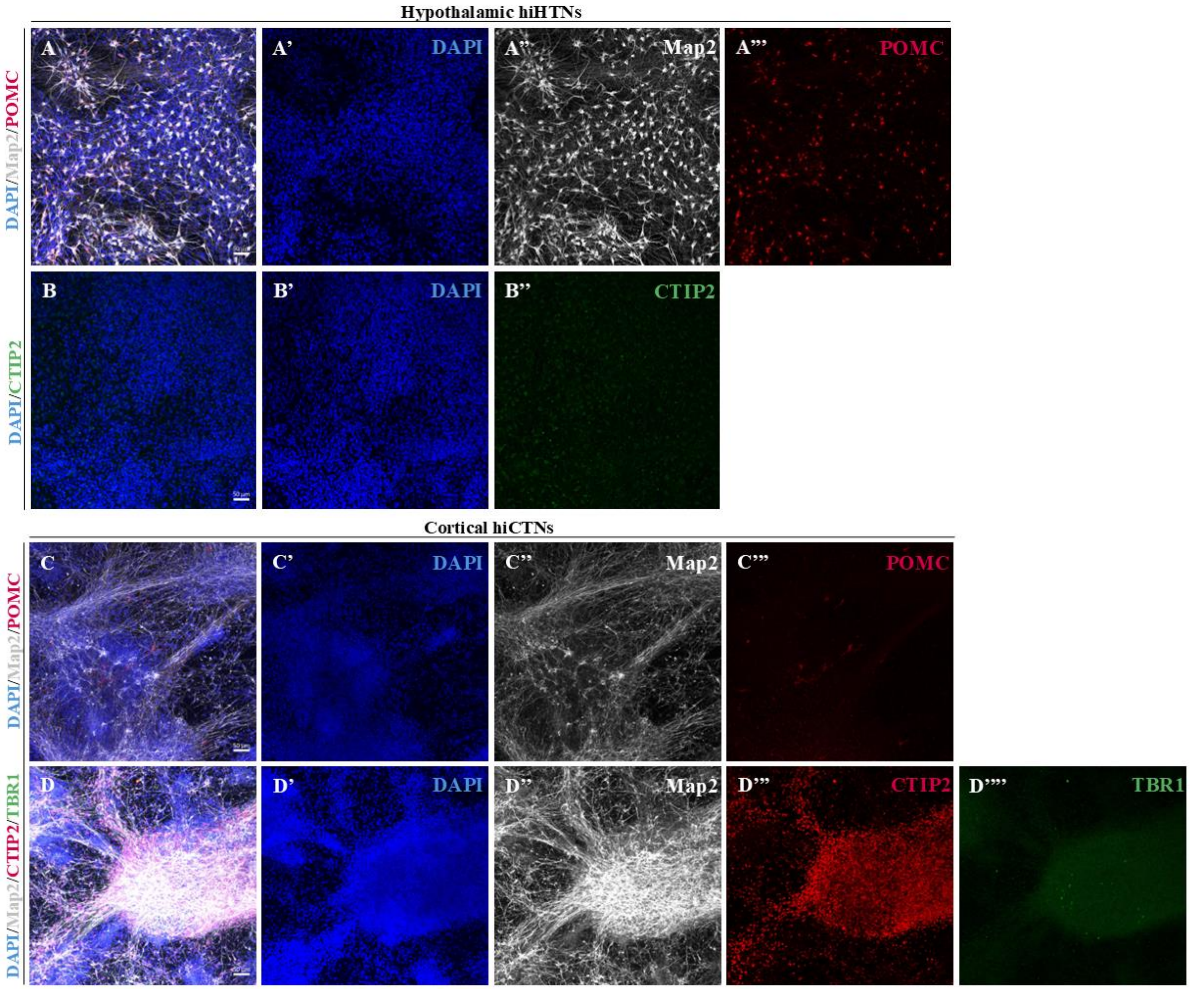

Figure 4.3. Preliminary results showed promising expression of markers specific for hypothalamic differentiation. A-A''') Representative confocal images of DAPI, POMC, and Map2 in hypothalamic neurons at d30 (cells were not cryopreserved at d14 and were treated with hPrRP31). B-B'') Representative images of DAPI, and CITIP2 in hypothalamic neurons at d30 (cells were not cryopreserved at d14 and were treated with hPrRP31). C-C''') Representative images of DAPI, POMC, and Map2 in cortical neurons at d30. D-D''') Representative images of DAPI, Map2, CTIP2, and TBR1 in cortical neurons at d30. Kolf cells were used in this experiment. Qualitative analysis of marker expression only. Data information: S.b.: 50 μm. Confocal scans: 20X.

4.2.3. Treatment with hPrRP31 did not significantly alter the proportion of POMC-expressing hiHTNs

The anti-obesity effects of LiPrRP may be mediated by modulating the balance between anorexigenic POMC-expressing neurons and orexigenic NPY-expressing neurons. To determine if hPrRP31 treatment alter neuronal specification and encourages an anorexigenic fate when administered throughout maturation, ICC analysis of POMC and NPY expression was performed. The preliminary experiments were expanded to include three cell lines as described above and in detail in Chapter 2. The percentage of POMC-expressing Map2+ neurons out of all Map2+ cells were quantified in the Control and treated groups at d30 by May Surridge-Smith. The results showed that treatment with 1 μM hPrRP31 did not significantly alter the proportion of POMC-expressing hiHTNs compared to the Control group as shown in Figure 4.4A. ICC of the orexigenic neuropeptide NPY was deemed unreliable for quantification (Data not shown). Due to the error bars reflecting a wide variability between data points, the cell lines were separated graphically to identify the source of variation. This revealed a big difference in the percent of POMC expressing neurons between the cell lines. Specifically the i900 cell line had a much higher percentage of POMC expressing neurons (ranging 50-60%) in both control and hPrRP31 treated cultures compared to the Kolf (10-20%) and 18n6 cultures (10-20%). This suggested a potential variability in the differentiation efficiency across the hiPSC lines used in the study (Figure 4.4B). All together these data suggests that hPrRP31 did not significantly alter the proportion of POMC-expressing hiHTNs.

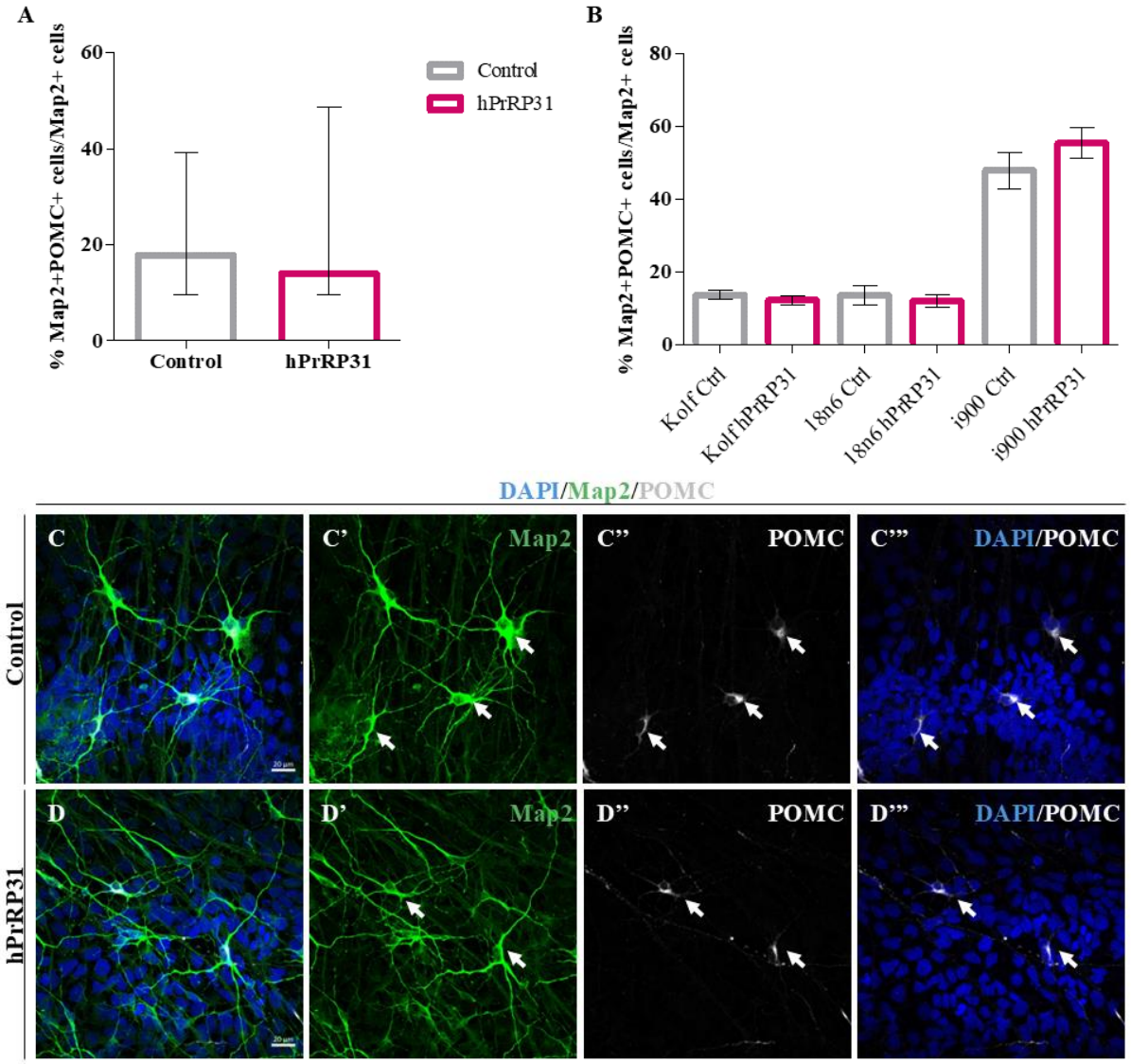

Figure 4.4. Treatment with hPrRP31 did not alter the proportion of hiHTNs expressing POMC. Percentage of POMC positive neurons relative to the total number of Map2 neurons in Control hiHTNs and hiHTNs treated with hPrRP31 show no significant difference between treatment and control. A) Percent Map2+POMC+ cells out of all Map2+ cells (both POMC+ and POMC-) after 30 days in culture in control and hPrRP31 treated wells. B) Percent Map2+POMC+ cells out of all Map2+ cells (both POMC+ and POMC-) after 30 days in culture in control and hPrRP31 treated wells split per cell line. Showing a big difference in Map2+POMC+ cells generated in the i900 cells compared to Kolf and 18n6. C-C''') Representative confocal images of DAPI, POMC, and Map2 in a Control well. D-D''') Representative confocal images of DAPI, POMC, and Map2 in a well treated with hPrRP31. Data information: S.b: 20 µm. N = 3 cell lines (n = 3 replicate wells). In panel A, Mann Whitney test, Two-tailed. In panel B, One-way ANOVA with Bonferroni's test (*** $p < 0.0001$) not shown on graph. Data are presented as median ± IQR (A) or mean ± SEM (B). Confocal scans: 63X.

4.2.4. Treatment with hPrRP31 does not consistently alter the expression of genes encoding POMC, NPY, PrRP or GPR10

The effects of hPrRP31 treatment may be mediated by altering the expression of genes encoding key neuropeptides and receptors involved in energy homeostasis. Thus, RT-qPCR was performed on the matured hypothalamic neurons. The results showed that treatment with 1 μM hPrRP31 did not significantly alter the expression levels of *POMC, NPY, PrRP* or the PrRP receptor *GPR10* compared to control (Figure 4.5A). This suggests that the anti-obesity effects of hPrRP31 may not be mediated through direct modulation of the transcription of these key genes in hypothalamic neurons under the conditions tested. Due to the error bars reflecting a wide variability between data points, the cell lines were separated graphically for individual genes to visualise the source of variation (Figure 4.5B-E). The results showed an independent and inconsistent response to hPrRP31 in each cell line. Specifically, the *POMC* gene expression was reduced in Kolf, whereas it was increased in the 18n6 and i900 cells lines. PrRP expression was reduced in both Kolf and i900 but increased in the 18n6. NPY expression was reduced in all cell lines. *GPR10* expression was reduced in Kolf whereas it was increased in the 18n6 and i900 cell lines. Suggesting that the protocol may need to be optimised further for these specific cell lines. All together, these data suggests that treatment with hPrRP31 did not consistently alter gene expression of key neuropeptides and receptors involved in energy homeostasis.

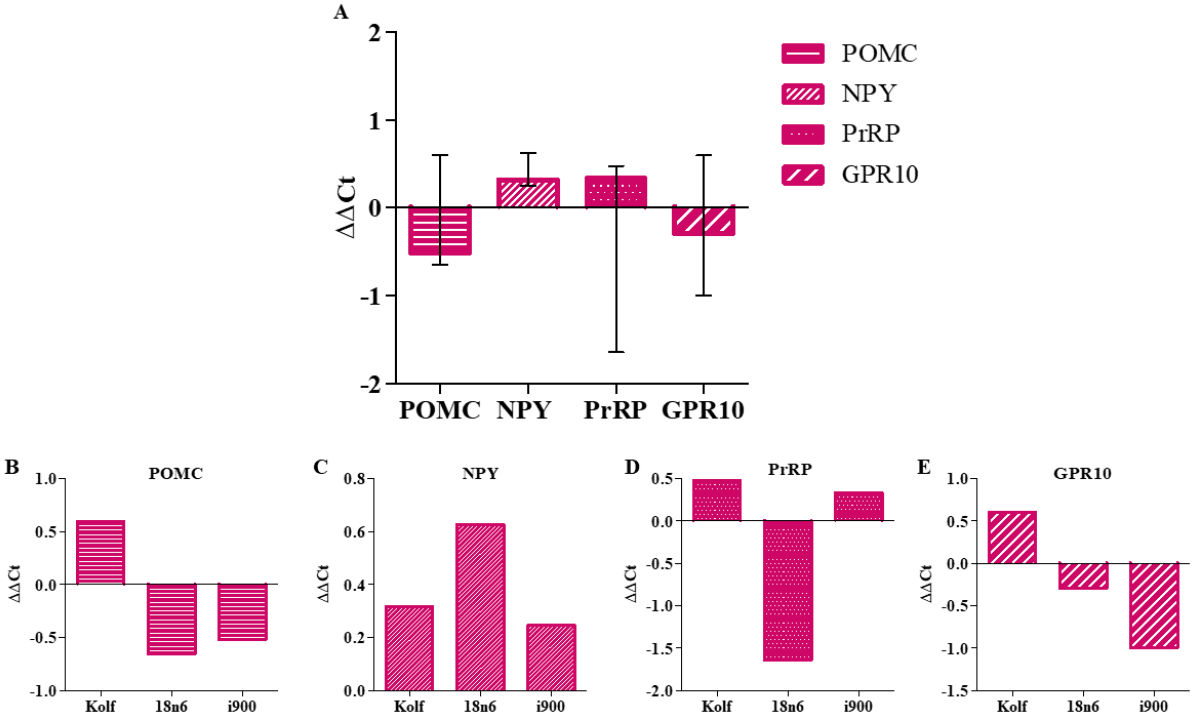

Figure 4.5. Treatment with hPrRP31 did not alter expression of *POMC, NPY, PrRP* or *GPR10*. qPCR found no significant difference between control cells versus cells treated with hPrRP31. A) ΔΔCt values representing gene expression, normalized to the housekeeping gene (*GAPDH*), in cells treated hPrRP31 relative to their control counterparts. B-E) ΔΔCt values of *POMC*, *NPY*, *PrRP*, and *GPR10*, respectively, separated into individual cell lines. Data information: N = 3 cell lines (each with n = 3 replicate wells). In panel A, Kruskal-Wallis test with Dunn's test. Data are presented as median ± IQR.

4.2.5.The gene expression of POMC and GPR10 remained unchanged between d14 and d30

In these experimental parameters, hPrRP31 was administered during maturation. Therefore, it was of interest to further investigate the effects of maturation, both with and without the administration of 1 μM hPrRP31, on the expression of selected genes between d14 and d30. A previous study (Jorgensen et al., 2024) have shown that a LiPrRP can dynamically regulate PrRP signalling. Specifically, LiPrRP has been found to rescue HFD induced decrease in the protein density of the PrRP receptor GPR10 in the MBH. Additionally, LiPrRP has been observed to increase PrRP expression both in the MBH and in MHB-derived neurospheres (Appendix Figure 1 and 3). This LiPrRP-induced increase in PrRP expression may suggest a positive feedback mechanism of the agonist on its own signalling pathway (Jorgensen et al., 2024). Accordingly, the present investigation examined whether the hiHTNs also expressed

the PrRP receptor GPR10.The presence of the PrRP receptor GPR10 at the onset and end of maturation helped establish the responsiveness of the neuronal cells to the presence of hPrRP31, both in the early stages and throughout the maturation process. Furthermore, the expression of POMC was examined before and after maturation, both with and without the presence of hPrRP31, to provide deeper insights into the potential impact of hPrRP31 on the proportion of POMC-expressing cells. No significant difference was observed in the expression of POMC and GPR10 between d14 and d30 in both Control and hPrRP31-treated groups (Figure 4.6). Suggesting that the specification of hiHTNs cannot be changed by hPrRP31 when administered during maturation.

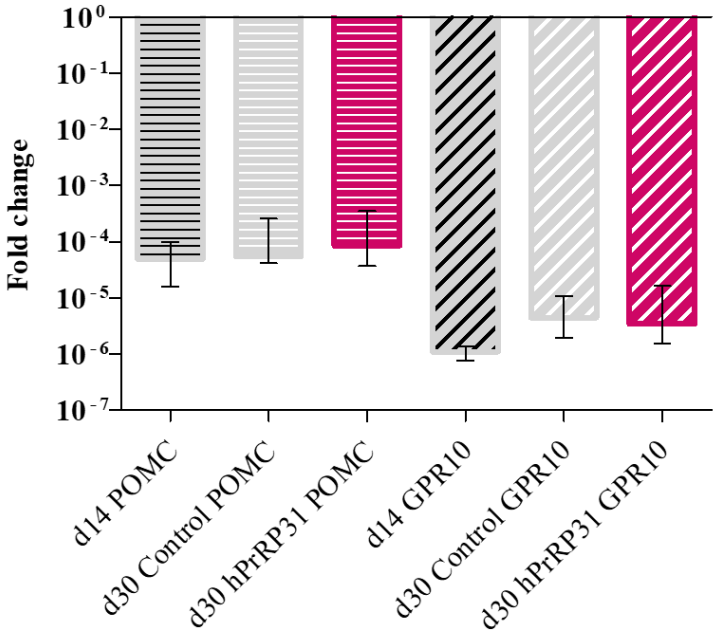

Figure 4.6. Neuronal maturation did not affect gene expression of *POMC* or *GPR10*. Gene expression levels of *POMC* and *GPR10* at d14 post differentiation compared to gene expression levels at d30 post maturation. Either treated with hPrRP31 or their Control counterparts. Gene expression displayed as the fold change representing $2^{-\Delta Ct}$. Data information: N = 3 cell lines (n = 3 replicate wells). Kruskal-Wallis test with Dunn's test. Data are presented as median ± IQR.

4.2.6. hiHTNs showed mixed identity at d14 and d30

To ensure the proper patterning of the hiHTNs, many studies assess the presence of telencephalic and diencephalic markers. Most studies have declared that *FOXG1* is a marker for telencephalic identity, while *NKX2.1* is expressed in the ventral forebrain *in vivo* and is a marker for hypothalamic identity (Kirwan et al., 2017). Determining the expression of these two markers therefore provided insights into the regional identity of the differentiated iPSC-derived neurons. NKX2.1 is essential for the specification and development of POMC neurons in the hypothalamus, as it directly activates the *Pomc* gene expression in the developing hypothalamus. The absence of *NKX2.1* results in a severe reduction or even complete loss of POMC neurons (Orquera et al., 2019). This underscores the importance of assessing *NKX2.1* expression to confirm the hypothalamic identity of the differentiated neurons.

Thus the expression of *FOXG1* and *NKX2.1* was examined by RT-qPCR to confirm that the differentiated hiHTNs had indeed taken on a hypothalamic identity. Contrary to the expected profile described in the hiHTN differentiation and maturation protocol (Kirwan et al., 2017; Merkle et al., 2015), *FOXG1* was expressed significantly more than *NKX2.1* at both time points, irrespective of hPrRP31 treatment (Figure 4.7). Suggesting a stronger telencephalic identity of the hiHTNs. Maturation significantly decreased the expression of both *FOXG1* and *NKX2.1*. However, this was unaffected by hPrRP31 treatment. This indicated that the hiHTNs were differentiated toward a hypothalamic phenotype, although not to the extent that FOXG1 expression was diminished as shown by Merkle et al. (2015).

Qualitative expression analysis by ICC was performed of both markers at d14 and d30 (Figure 4.7A-A'''). Confirming the RT-qPCR data, a high expression of FOXG1 was observed compared to a very low expression of NKX2.1. Surprisingly, many cells showed an overlap between the markers, suggesting that these cells may have adapted a mixed identity and did not successfully differentiate into a phenotype of hypothalamic neurons found in the MBH.

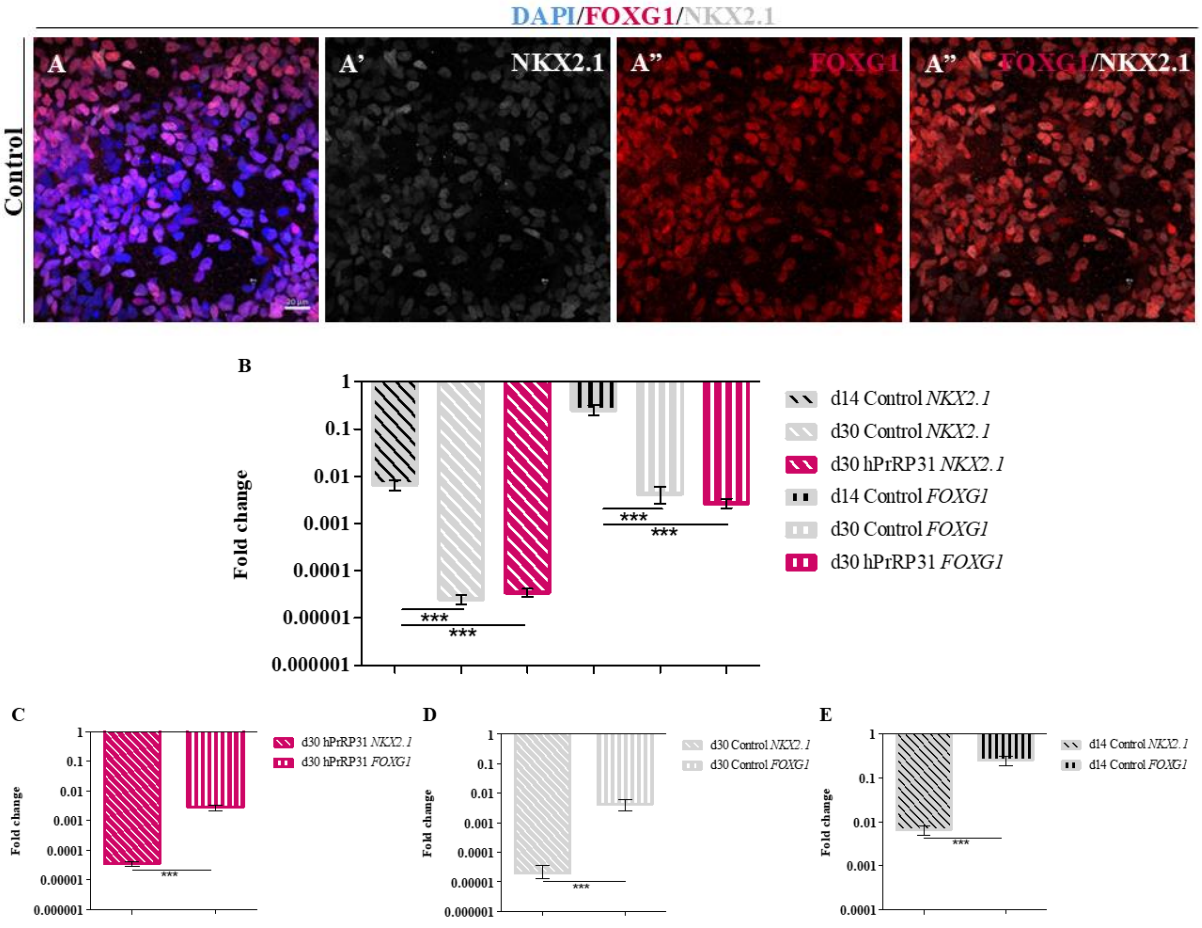

Figure 4.7. hiHTNs co-expressed FOXG1 and NKX2.1. A-A''') Representative confocal image from a i900 d30 Control well. B) Gene expression displayed as the fold change ($2^{-\Delta Ct}$) for *FOXG1* and *NKX2.1* expression for d14 and d30, both Control and hPrRP31. Expression of *FOXG1* and *NKX2.1* increased post-maturation irrespective of treatment with hPrRP31. C) *FOXG1* and *NKX2.1* expression in cells treated with hPrRP31 at d30 (N = 3). D-E) *FOXG1* and *NKX2.1* expression in control cells at d30 (D; N = 3), d14 (E; N = 3). Data information: S.b. = 20 µm. In panels B, Kruskal Wallis test with Dunn's test ($p < 0.0001$). In panels C, E, Unpaired T-test, Two-tailed (B: $p = 0.0005$; E: $p = 0.0009$). In panel D, Mann Whitney test, Two-tailed ($p < 0.0001$). Data are presented as median ± IQR (A, D) or mean ± SEM (all other panels).

4.3. Short discussion:

In this chapter the effects of hPrRP31 on the proportion of POMC expressing hiHTNs when administrated during maturation was determined. The main results detailed here indicated that hPrRP31 did not influence fate specification of hiHTNs to POMC expressing hypothalamic neurons when administered during maturation. Although, the hiHTNs may not have successfully differentiated into a complete hypothalamic identity, which could have obscured the impact of these compounds.

4.3.1. Proportions of POMC expressing hiHTNs was not affected by hPrRP31 treatment

In vivo, LiPrRP has been shown to have long lasting effects even after treatment cessation with no weight regain after stopped treatment (Holubová et al., 2018). This suggests the potential to induce lasting changes within the appetite circuitry of the adult brain, thereby resulting in prolonged anti-obesity effects. The potential to alter fate specification of hypothalamic neurons though pharmacological interventions could be a potential mechanism of action of the long lasting anti-obesity effects seen by LiPrRP.

hPrRP31 did not significantly change the proportion of Map2+POMC+ hiHTNs compared to Controls. Suggesting that hPrRP31 have no influence over fate specification to POMC expressing neurons when administered during maturation. Further investigation is needed to determine if the compounds could impact neuronal specification at earlier stages of differentiation. To do so, it would be advisable to determine if earlier stages of these cells express the hPrRP31 receptor GPR10 and therefore could respond to its administration in culture.

The hPrRP31 effects may be altering other aspects of neuronal function rather than cell specification, including neuronal activation. In fact, results from Jorgensen et al. (2024) showed that PrRP signalling stimulates increase in the intracellular calcium in hiPSC-derived hypothalamic neurons, which suggests a direct responsiveness to PrRP (Appendix Figure 5) (Jorgensen et al., 2024). Furthermore, the detection of gene expression for PrRP and its receptor in the hiHTNs indicates that these neurons can respond to hPrRP31 stimulation. Indeed, *in vivo* studies in rodents have reported a similar reduction in adult born POMC and NPY expressing neurons in response to external stimuli of HFD (Li et al., 2012; Gouazé et al., 2013). This observation is inconsistent with the proposed model which postulates that selective generation of appetite-suppressing (anorexigenic) neurons modulates the neural circuits governing feeding behaviour (Yoo & Blackshaw, 2018). Highlighting the complexity of the interplay and

response of these neurons to external stimuli. Due to unreliable signal, NPY expression was not investigated in these experiments. Further hampering our ability to determine the effects of PrRP on the proportion of cells with anorexigenic compared to orexigenic cell fate. Unravelling the precise mechanism of action of the anorexigenic hPrRP31 and LiPrRP is yet to be elucidated.

As discussed, these findings suggest that the fate specification and cell identity of immature neurons are unaffected by pharmacological intervention. Notably, studies on direct reprogramming have encountered barriers in converting one post-mitotic cell type to another, and evidence indicates that cell identity is determined prior to or in early differentiation, rendering direct reprogramming impossible after this event (Rouaux & Arlotta, 2013; Gascón et al., 2017). The findings indicate that the opportunity to influence the fate of the differentiated hiHTNs had potentially elapsed, as the hiHTNs may had already established their predetermined identity by the time of the interventions. This is further supported by the unchanged gene expression of POMC and GPR10 from d14 to d30, as analysed by RT-qPCR.

Postmitotic neurons generally maintain their identity throughout life, unlike reactive glial cells. Altering neuronal fates is highly complex, as evidenced by the difficulties in direct neuronal reprogramming. This is due to the inherent mechanisms that restrict changes in cell fate as progenitor cells differentiate and commit to specific cellular identities (Niu et al., 2018; Péron et al., 2023; Rouaux & Arlotta, 2013; Gascón et al., 2017). While both fibroblast-to-neuron and neuron-to-neuron direct reprogramming hold promise for regenerative medicine and disease modelling, the latter is technically more challenging due to the inherent stability and complexity of neuronal identity. In contrast, fibroblasts are generally considered more plastic than mature neurons (Schaukowitch et al., 2023; Vierbuchen et al., 2010). A study by Péron et al. (2023) found that the transcription factor Neurog2 can redirect the fate of proliferating aNSCs, shifting them from a GABAergic to a glutamatergic lineage. However, once these cells have differentiated into postmitotic neurons, Neurog2 can no longer induce a lineage switch. This indicates a restricted developmental window during which Neurog2 can alter neuronal identity (Péron et al., 2023). Additionally, there appears to be a critical period of nuclear plasticity that closes as neurons undergo epigenetic changes during maturation (Amamoto & Arlotta, 2014; Gascón et al., 2017). This study suggests that the broader lineage determination of neurons is fixed during direct cell reprogramming, rather than at the level of cell specification. Nonetheless, it provides insights into the inherent rigidity of postmitotic neurons. An earlier study has shown that neuronal identity is relatively plastic during early postmitotic

development, with factors like Fezf2 able to switch neuronal subtypes within the first postnatal week (Rouaux & Arlotta, 2013; Niu et al., 2018) However, this window of plasticity progressively restricts over time, with later-stage postmitotic neurons becoming less amenable to fate reprogramming. This suggests the presence of mechanisms that stabilise neuronal identity as neurons mature (Rouaux & Arlotta, 2013). While the decision to administer hPrRP31 was based on preliminary data of the PrRP receptor GPR10 expression, it is evident that at this late stage of neuronal maturation, the cells are unlikely to be influenced to alter their established cellular identity. Future studies should therefore explore administering hPrRP31 at different time points during differentiation. This would also better replicate the response of stem cells to external cues *in vivo*, and thus represent the neural plasticity observed in adults.

Another general consideration for the lack of observed phenotypic changes in hiHTNs in response to hPrRP31 administration may be inherent limitations of the iPSC-based model system. Although the hiPSC model allows us to investigate the effects of hPrRP31 on hypothalamic neuronal development, these pluripotent cells and succedent neurons have not been exposed to any obesity related epigenetic changes. Instead, they would likely represent the *in vivo* administration in mice on Control diet. An alternative approach could be using iPSC models derived from obese donors, as these have been shown to retain obesity-associated signatures after reprogramming (Rajamani et al., 2018). Thus, the lack of observed phenotypic changes in response to hPrRP31 administration may be attributable to the absence of obesity-associated epigenetic profiles observed *in vivo* in obesity models. Rajamani et al. (2018) utilized lymphoblastoid cells as the as the parent cell type for generating iPSCs from "super obese patients" (BMI $\geq$ 50). Their iPSC differentiation protocol to hypothalamic neurons shares many similarities with the approach used to create the hiHTNs in this experiment. In addition, the use of iPSCs for modelling age-related diseases has significant limitations. The reprogramming process resets the epigenetic age of the original somatic cells, meaning the resulting iPSC-derived neurons may not fully recapitulate the characteristics of mature, adult neurons (Samoylova & Baklaushev, 2020). Utilising direct conversion also known as transdifferentiation techniques may offer a more suitable model for recapitulating the age-related characteristics (Samoylova & Baklaushev, 2020). Although iPSC-based models offer a valuable bridge between animal and human research, they may not fully recapitulate the characteristics of mature, adult neurons, which was the focus of this study's investigation.

4.3.2. The hiHTNs showed an inverse expression of FOXG1 and NKX2.1

The differentiated hiHTNs exhibited an inverse expression pattern of *FOXG1* and *NKX2.1* to the expected expression pattern. This suggested that the cell population contained a mix of telencephalic and hypothalamic identities (Merkle et al., 2015; Kirwan et al., 2017). The co-expression of these markers in some cells further indicated a mixed cell identity, rather than a distinct and homogeneous hypothalamic neuronal population. This discrepancy indicate a deviation from the intended differentiation pathway of these cells and raises doubts to the unresponsiveness to the anti-obesity compounds, as well as their physiological significance. It may additionally explain the huge variations in gene expression profiles and proportions of POMC expressing neurons shown between the cell lines. The discrepancy may be attributed to technical errors in optimisation. From d0 to d9 the (Kirwan et al., 2017) protocol used XAV939 as the tankyrase inhibitor, inhibiting Wnt signalling. In the protocol used here, XAV939 was substituted by iwr1, also a tankyrase inhibitor which work by inhibiting Wnt signalling. Iwr1 was used in relatively low concentrations ranging from 1.5 µM on d1, gradually reduced to 0.25 µM on d9. A recent study evaluated the impact of varying concentrations of iwr1 of *NKX2.1* expression when generating iPSC derived hypothalamic-like neurons (Rajamani et al., 2018). They found that absence and low concentrations of 1 µM generated low proportions of hiHTNs expressing *NKX2.1* at d9 of differentiation while higher concentrations of 10 µM produced the highest number of *NKX2.1* expressing hiHTNs. Interestingly, the higher concentrations of 100 µM of iwr1 again produced low numbers of *NKX2.1*. Indicating that iwr1 concentrations needed to be optimised for this protocol (Rajamani et al., 2018). In addition, XAV939 is a more selective tankyrase inhibitor, directly targeting TNKS1 and TNKS2 involved in Wnt pathway regulation (Huang et al., 2009; Li et al., 2020). While iwr1 is a potent Wnt inhibitor, it might have broader effects on other signalling pathways besides Wnt (Xiao et al., 2021). The regulation of the Wnt pathway signalling is critical for proper hypothalamic patterning. The switch from XAV939 to iwr1 may therefore have influenced successful differentiation. However, Rajamani et al. (2018) and Huang et al. (2021) showed that iwr1 still induces *NKX2.1* hypothalamic specific expression. Interestingly, the study by Huang et al. (2021) also used a higher concentration of 10 µM iwr1. Further confirming that the use of a low concentration of the Wnt signalling inhibitor may have impacted the differentiation here.

Alternatively, the cells might be in an intermediate stage of differentiation. Where co-expression could indicate a transient developmental stage. *NKX2.1* defines the hypothalamic region and is crucial for the development of several hypothalamic neuronal subtypes (Merkle

et al., 2015; Wang et al., 2015). On the other hand, *FOXG1* is primarily known for its role in telencephalon development, but may also transiently expressed in the developing hypothalamus. Indeed, this is in agreement with a recent study by Romanov et al. (2020). Their findings suggest that a substantial proportion, around 47%, of their cells committed to the neuronal lineage in the developing hypothalamus existed in immature states before reaching their final differentiation, as evidenced by the expression of homeobox genes like *Foxg1* and *Nkx2-3* that are believed to determine GABAergic identities (Romanov et al., 2020). In agreement, a recent study by Nasu et al. (2021) also described a Nkx2.1+/Foxg1+ co-expression in a organoid model of the ventral-most telencephalon (MGE/POA; Nasu et al., 2021). Interestingly, the ventral telencephalon includes the preoptic area (POA), which produces both GABAergic and cholinergic neurons (Nasu et al., 2021). In addition, the POA and MBH have a close anatomical relationship (Nasu et al., 2021; Gao & Sun, 2015), where the POA and MBH also function as an integrated system, processing diverse internal and external inputs to coordinate physiological and behavioural responses that maintain homeostasis. All together this suggests the generated hiHTNs may have acquired a transient or mixed identity of POA/MBH GABAergic neurons.

Despite the co-expression of FOXG1 and NKX2.1 was observed in the majority of the generated neurons, a subpopulation of these cells was found to express POMC. Interestingly, there is a subpopulation of ArcN GABAergic-POMC neurons that play a role in regulating body weight (Trotta et al., 2020). Additionally, recent single-cell RNA sequencing studies have revealed that ArcN POMC neurons can be classified into distinct subpopulations based on their transcriptomic profiles (Campbell et al., 2017; Chen et al., 2017; Lam et al., 2017). Specifically, Campbell and colleagues identified three POMC neuron clusters, with two expressing predominantly GABAergic markers (Gad1, Gad2) and the third expressing a glutamatergic marker. Notably, the GABAergic POMC neuron clusters exhibited more pronounced transcriptional changes in response to fasting, suggesting their potential involvement in energy homeostasis regulation (Campbell et al., 2017). Although highly speculative, this suggests that the hiHTNs generated in our cultures may represent a mixed population of GABAergic neurons, co-expressing FOXG1 and NKX2.1 markers, which are found in and around the POA and MBH. Some of these neurons may have matured into GABAergic POMC-expressing neurons, similar to those observed *in vivo* in the MBH.

Interestingly, despite displaying a heterogeneous cell identity with high telencephalic identity, the hiHTNs had a higher expression of POMC expression than expected, where Kirwan et al.

(2017) reported a 0.3% expression of POMC per 1000 nuclei compared to a 15-60% expression per Map2+ neurons. More comparably, when quantified as a proportion of POMC per DAPI, the total yield from all cell lines was around 5 % (Data not shown). The higher proportion of POMC-expressing neurons was beneficial, as it reduced the possibility that any hPrRP31-induced changes in their proportion would be too subtle to be observed. However, this factor may have impacted the RT-qPCR findings. Importantly, even with substantial variability observed between the cell lines, if the anti-obesity compound were to alter the proportion of POMC-positive neurons, this effect should still be detectable regardless of the variability. Future studies seeking to replicate this experiment should consider FACS to isolate cells expressing hypothalamic markers like NKX2.1 or RAX at day 14 and/or d30 (Wang et al., 2015). This approach would reduce the population heterogeneity and permit a more focused analysis of hypothalamic neuronal populations.

Given the challenge of inter- and intra-cell line variability in neuronal differentiation from hiPSC lines, an alternative explanation for the lack of observed difference in POMC proportion is that the protocol used may not have been optimised for the specific cell lines employed. Addressing this issue, to ensure more consistent and homogeneous hypothalamic neuronal populations are generated would enhance the robustness of the differentiation protocol. After similar differentiation efficiency has been obtained, the potential impact of treatment on hypothalamic neuron fate specification could be more reliably assessed. An argument supported by the variability in expression profiles of the selected metabolic genes between the cells lines. While all three cell lines were matured concurrently, potential technical discrepancies cannot be discounted, as the differentiation of the i900 cell line was carried out independently from the Kolf and 18n6 lines. To rule out any such technical inconsistencies, the protocol described must be repeated to increase the sample size and thereby generate more robust results.

Treatment with Shh and inhibitors of SMAD and Notch pathways should cause the hiHTNs to acquire features of ventral hypothalamic neural progenitors, including expression of *NKX2.1* (Wang et al., 2015). Further Notch signalling inhibition can promote differentiation of NKX2.1 expressing cells into ArcN neuronal subtypes like POMC, NPY/AGRP, somatostatin, and TH/dopamine neurons (Orquera et al., 2019). The protocol used reported differentiation into POMC, AGRP, HCRT, CRH, and TRH neuron populations (Kirwan et al., 2017). Future studies should examine a variety of neuronal subtypes and assess NKX2.1 and FOXG1 expression to better characterise the differentiated hypothalamic neurons, particularly at day

30. Analysing markers like RAX and Single-minded 1 (Sim1) could offer a more robust understanding of cell identity. Alternatively, examining the presence of HCRT, CRH, and TRH would further bolster the characterisation, but may require extending the experiment to at least 40 days for sufficient maturation and marker expression (Kirwan et al., 2017). The 30-day time point was chosen as the protocol indicates that hypothalamic neurons begin acquiring functional properties after 30 days in culture without exogenously added primary glia (Kirwan et al., 2017). Additionally, genes like POMC become robustly expressed by day 25. In contrast, genes like HCRT tend to become robustly expressed later, by around day 40 (Kirwan et al., 2017).

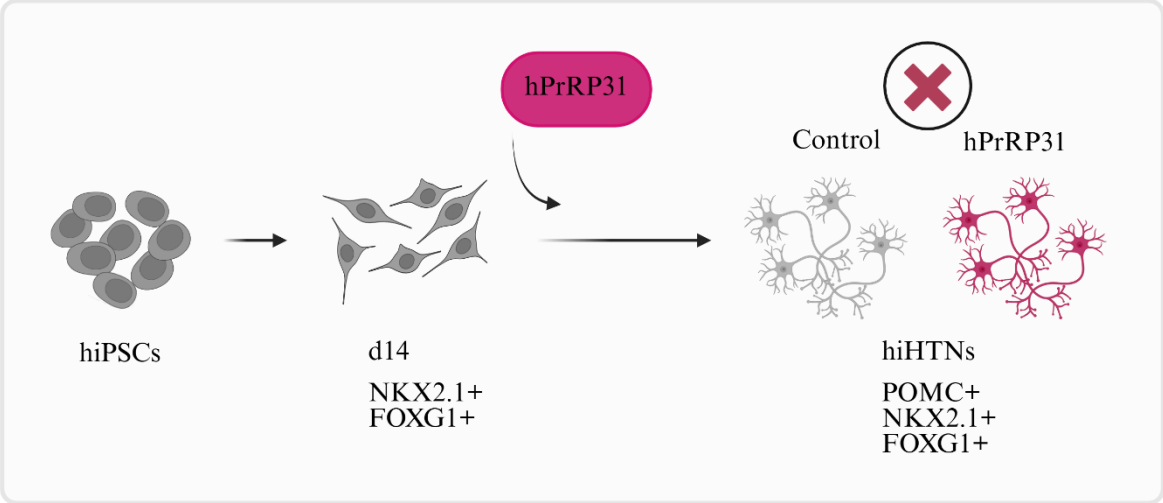

Figure 4.8. Graphical summary of Chapter 4. The main results detailed here indicated that hPrRP31 did not influence fate specification of hiHTNs to POMC expressing hypothalamic neurons when administered during maturation. Additionally, the hiHTNs expressed both NKX2.1 and FOXG1 at d14 and d30. Figure made in BioRender (Biorender.com).

Chapter 5: The Effects of HFD and Voluntary Running on Hypothalamic Adult Neurogenesis

5.1. Short introduction

Adult neurogenesis, the process of generating new neurons, has been observed in various brain regions, with the hippocampus being the most studied site. However, the hypothalamus is now recognized as an important neurogenic niche (Klein et al., 2019). The hypothalamus regulates essential homeostatic processes like sleep, body temperature, and appetite (Lee et al., 2014). Located partially outside the BBB, the hypothalamus can detect fluctuations in circulating metabolites and hormones and regulate behavioural responses accordingly (Yoo & Blackshaw, 2018). This plasticity suggests that even a small addition of new neurons can significantly impact physiology and behaviour. The levels of adult neurogenesis in the hypothalamus are low but highly responsive to changes in hormonal state or diet, highlighting the challenges in this research area (Yoo & Blackshaw, 2018).

Extensive research has demonstrated a positive impact of exercise on adult neurogenesis in the hippocampus (Kempermann et al., 1998). Early studies revealed an increase in the survival of newborn cells and neurons in the DG following voluntary exercise (Praag et al., 1999). Additionally, voluntary exercise was found to restore spatial learning and neurogenesis in aged mice (Praag et al., 2005). The peak of cell proliferation occurs around two weeks of running, after which cell proliferation appears to slow down with prolonged running. In addition HFD administration has been shown to have detrimental effects on adult hippocampal neurogenesis (Lindqvist et al., 2006; Robison et al., 2020), which can be reversed by exercise (Han et al., 2019; Klein et al., 2016).

While the effects of HFD and exercise on hippocampal neurogenesis have been extensively studied, much less is known about the effects of exercise and HFD on adult neurogenesis in the hypothalamus. Diet induced obesity caused by overconsumption of HFD has been shown to reduce hypothalamic adult neurogenesis (hAN) through lower survival and increased apoptosis of newborn neurons or by decreased proliferation of tanycytes (McNay et al., 2012; Li et al., 2012; Lee et al., 2014; Jorgensen et al., 2024). Ablation of hAN has also been shown to lead to higher weight gain in animals fed HFD (Kokoeva et al., 2005; Gouazé et al., 2013), whereas an increase in hAN has been shown to protect against the adverse effects of HFD

(Kokoeva et al., 2005; Pierce & Xu, 2010). However, the relationship between hAN and obesity is insufficiently understood with conflicting findings reported in the literature (McNay et al., 2012; Lee et al., 2014; Li et al., 2012).

Despite currently limited research, there is reason to believe that voluntary exercise may also influence adult neurogenesis in the hypothalamus. Given the plasticity of the hypothalamus and its ability to respond to peripheral changes, exercise could impact adult neurogenesis also in this brain region. Indeed Klein et al. (2019) showed that physical exercise stimulated cell proliferation, but they also showed that HFD increased neurogenesis (Klein et al., 2019) and exercise reduced BrdU-labelled neurons after 12 weeks. Another study by Niwa et al. (2015) showed 5-7 weeks of voluntary running led to beneficial effects in stroke-prone spontaneously hypertensive (SHRSP) rats. Exercise markedly increased both overall cell proliferation (BrdU-labelled cells) and adult neurogenesis in the ArcN and ME of both wild-type and SHRSP rats, compared to Sedentary controls (Niwa et al., 2015). Additionally, Laing et al. (2016) showed that exercise can improve metabolic symptoms caused by HFD after 12 weeks. This was achieved in part by restoring HFD-impaired POMC-expressing neurons in the hypothalamus, which are important for regulating energy balance. As well as restoring HFD damaged cell proliferation of Ki67-positive cells (Laing et al., 2016). In contrast to the current study and others, the study by Borg et al. (2014) is one of the few that investigated the effects of short-term running on adult hypothalamic neurogenesis, utilizing a protocol of forced running. They found that while running induced cell proliferation, very few of the newborn cells adopted a neuronal fate. Additionally, although exercise improved whole-body insulin sensitivity compared to Sedentary mice, the exercise-induced cell proliferation was not required for the enhanced insulin action (Borg et al., 2014). This suggest the improvement in metabolic function induced by exercise may not be directly linked to adult hypothalamic neurogenesis. Indeed, Borg et al. (2014) suggested that exercise could have effects on other non-neuronal cell types in the hypothalamus, rather than stimulating neurogenesis per se, that facilitate improved metabolic function. The existing literature suggests that, similar to the hippocampus, exercise may have a protective and beneficial effect on adult neurogenesis in the hypothalamus. However, the studies mentioned have reported mixed results, with exercise both increasing and decreasing neurogenesis in the hypothalamus. Importantly, the effects of short-term voluntary running on hypothalamic neurogenesis have not been investigated.

This chapter aimed to expand the currently limited knowledge on the effects of exercise and HFD on adult neurogenesis in the hypothalamus. By investigating the impacts of voluntary

running on cell proliferation and neurogenesis, using both short-term and long-term running protocols, with or without co-treatment with HFD. Furthermore, this chapter explored the impacts of running on the stem cell population within this neurogenic region. Notably, this study was the first to utilise lineage tracing of tanycytes in the context of obesity and exercise. Briefly, six-week-old male C57BL/6J mice were exposed to a short-term HFD and running protocol lasting for two weeks. The six-week-old age was selected as it is known that young adult mice typically exhibit a robust neurogenic response to exercise (Praag et al., 2005). This age group is ideal for studying the mechanisms of exercise induced neurogenesis and its effects on learning and memory. As demonstrated by Praag et al. (2005), running increased the number of new cells in young mice, making this age ideal to use hippocampal neurogenesis as a contrasting control to hypothalamic responses. In this protocol, the animals were given BrdU in their drinking water for the first 5 days, with a 9-day chase period. This means that the BrdU-labelled cells analysed in the following results were between 9 and 14 days old. The two week timeline was chosen to replicate the extensive research done on hippocampal neurogenesis. Giving the BrdU in the drinking water was necessary because the stem cells in the hypothalamus divide so rarely, and a single injection would not have been sufficient to label any proliferating cells. The mice were weighed every other day throughout the entire two week period to monitor any weight changes, such as potential weight loss due to BrdU administration or weight gain from the HFD feeding. The long-term HFD and running protocol lasted for 3 months, replicating the previous studies that investigated the effects of exercise on the hypothalamus. This protocol used a combination of lineage tracing and label retention approaches in male and female GLAST-CreER^{T2} x R26-tdTomato mice. The expression of the tdTomato fluorescent protein was induced in the stem cells and their progenies at the beginning of the 3 month protocol. The animals then underwent 2.5 months of voluntary running, followed by a two week replication of the short-term running protocol to enable comparisons. The BrdU labelling protocol was designed to enable a direct comparison between the cells labelled during the two week short-term protocol and the BrdU-retaining cells observed in the final two weeks of the long-term running protocol. This allowed the comparison of cells of the same age (same BrdU labelling protocol) that were exposed to the treatments either in the short-term or the long-term. Analyses were conducted using both serological cell counts and density per volume. Most analyses in this chapter are expressed as density per volume. This decision was made due to the small number of sections containing the MBH that were available for each immunohistochemical staining. It is only possible to stain a sample of two sections per animal for each IHC. Relying on serological quantification and extrapolating the counts by multiplying

them by 12 was observed to be more variable. Quantification as a cell density was therefore considered a more accurate approach. Running distance was measured in both short-term and long term protocols.

5.2. Results:

5.2.1. Short-term Running increased cell proliferation and proliferating DCX+ cells independently of diet in the SGZ

Due to failed preliminary results (data not shown) that showed no increase in cell proliferation in the SGZ after two weeks of voluntary Running with tilted wheels, the cages used in Figure 5.1 B-B' were instead utilised. The cages used in Figure 5.1 B-B' were skilfully crafted and generously provided by Dr Andrew Want. Using these cages, a significant increase in proliferating cells (Ki67+) in the SGZ was successfully observed in Runners on the Control diet, compared to their Sedentary counterparts (Figure 5.1C). This indicated that the two week running protocol and the new cages indeed increased the proliferation of cells in the SGZ, as previously described in the literature. As detailed in Chapter 2, 6-week-old male WT C57Bl6/j mice were exposed to either a HFD or a Control diet, with or without concurrent voluntary Running, for a two week period (Figure 5.1A). The distance run was measured, and as shown in Figure 5.1E. The diet did not significantly impact the distance run over the two week period. Interestingly, the HFD fed mice did not significantly gain weight compared to mice on Control diet at the end of the two weeks, but there was a statistically significant main effect of exercise (Two-way ANOVA, $F(1, 16) = 6.649$, $p < 0.05$) on the weight at d14 (Figure 5.1F). Suggesting that exercise lowered their body weight regardless of diet.

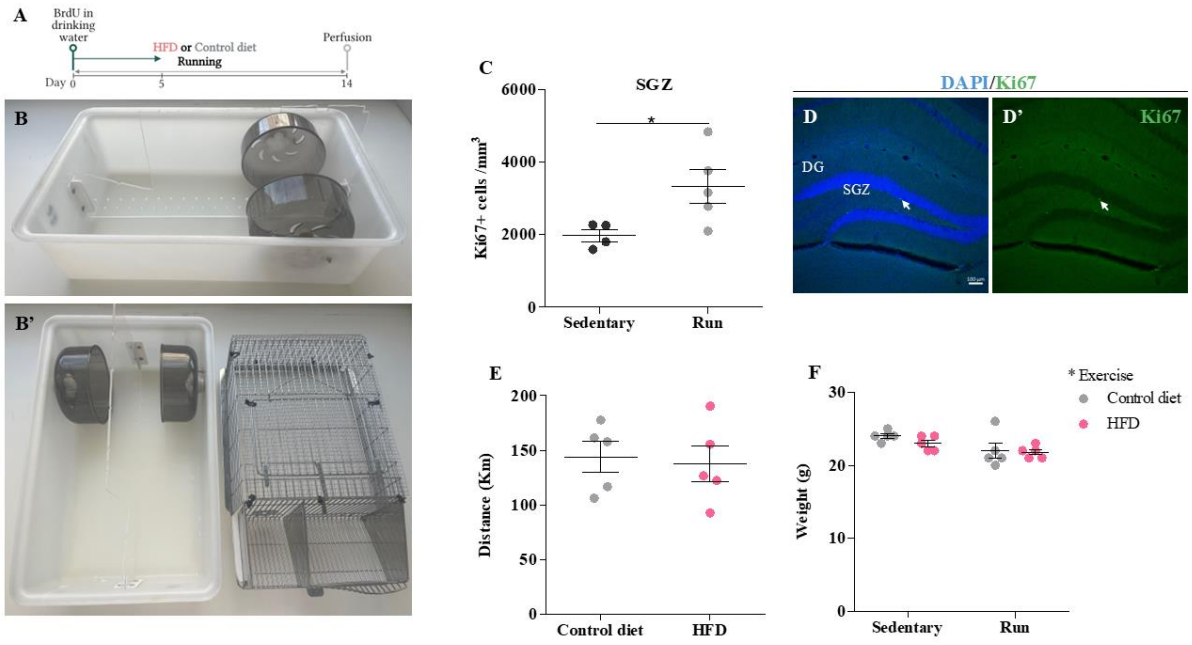

Figure 5.1. Running increased number of Ki67+ cells in the SGZ in mice on Control diet. A) Running and diet timeline. B-B') Representative images of a Sedentary cage. The running cages look the same but the wheel is not locked. C) Quantification of Ki67+ cell density in the SGZ. D-D') Representative confocal images of the SGZ stained as indicated in a Control Runner. E) Distance that the mice ran in Km after two weeks in Runners on Control diet or HFD. F) Weight in g after two weeks in Sedentary and Runners on HFD or Control diet. Data information: S.b.: 100 μm. n = 5 mice per data set for the two week run group. In panels C, E, Unpaired T-test, Two-tailed (C: $p = 0.043$). In panel F, Two-way ANOVA ($F(1, 16) = 6.649$, $p < 0.05$). Data are presented as mean ± SEM.

To further quality control the protocol, absolute counts and density of proliferating cells (Ki67+) in the SGZ were performed. While the animals used were generated by me, these quantifications were carried out by Final Year Project students Joseph Frullo and Caitlin Conway. To replicate the initial analysis (Figure 5.1C), the absolute number of Ki67+ cells in the SGZ of two most rostral brain sections containing the hippocampus were serologically quantified. As only 1/12 of the brain sections were stained and quantified, the cell counts were multiplied by 12 to extrapolate the absolute number of cells per hippocampus. The analysis revealed a statistically significant increase in both the absolute counts and density of Ki67+ cells in Runners compared to Sedentary mice, irrespective of whether they were on the Control diet or the HFD (Figure 5.2B-C). Specifically, there was a statistically significant effect of the diet (Two-way ANOVA, $F(1, 16) = 18.27$, $p = 0.0006$), the exercise ($F(1, 16) = 85.87$, $p < 0.0001$) and their interaction ($F(1, 16) = 7.334$, $p = 0.0155$) on the absolute counts of Ki67+ cells in the SGZ. Bonferroni's Pots-hoc Test found that exercise significantly increased the

absolute counts of Ki67+ cells in the SGZ for both Control diet ($p < 0.001$) and HFD ($p < 0.001$) mice, and that HFD significantly reduced absolute counts of Ki67+ cells in the Runners on HFD compared to the Runners of Control diet ($p < 0.001$; Figure 5.2B). This replicates the initial results and confirms the well-established finding that voluntary exercise increases proliferating cells in the SGZ, as reported extensively in the literature (Praag et al., 1999; Praag et al., 2005). The analysis was also done by expressing the cell counts as cell density per volume. Which also showed a statistically significant effect of the diet (Two-way ANOVA, $F(1, 16) = 47.40$, $p < 0.0001$), the exercise ($F(1, 16) = 78.35$, $p < 0.0001$) and their interaction ($F(1, 16) = 15.38$, $p = 0.0012$) on the density of Ki67+ cells in the SGZ. Where Bonferroni's Pots-hoc Test found that exercise also significantly increased the density of Ki67+ cells in the SGZ for both Control diet ($p < 0.001$) and HFD ($p < 0.01$) mice and that there is a significantly lower density of Ki67+ cells in the Runners on the HFD compared to Runners on the Control diet ($p < 0.001$; Figure 5.2C). Taken together, this suggests that Running increased cell proliferation in the SGZ regardless of the dietary conditions. However, since there is a significant interaction, the effect of exercise on cell proliferation depends on diet. The density of Ki67+ cells in Runners on HFD is significantly lower than in Runners on the Control diet, meaning that while exercise still promotes Ki67+ cell proliferation also under HFD conditions, its effect is weaker compared to the Control diet conditions. This suggests that HFD-induced changes in the brain may limit the full neurogenic benefits of exercise. Although, HFD alone did not reduce proliferation in Sedentary animals which suggested that HFD did not independently impair proliferation in Sedentary animals after two weeks.

Additionally, a significant increase in proliferating neuroblasts (Ki67+DCX+ cells) was observed. There was a statistically significant main effect of the diet (Two-way ANOVA, $F(1, 16) = 31.81$, $p < 0.0001$) and the exercise ($F(1, 16) = 13.40$, $p = 0.0021$) on the density of Ki67+DCX+ cells in the SGZ (Figure 5.2A). This means that regardless of diet, running increased neuroblast density. This is evident from the higher density of neuroblasts in Runners compared to Sedentary mice in both diet groups. But also that regardless of exercise, HFD reduced neuroblast density compared to the Control diet. Since there was no interaction the effects of diet and exercise are additive rather than dependent on each other. This suggests that exercise benefits neurogenesis regardless of diet, but HFD may still impair the overall neurogenic response.

Importantly, the findings presented here align with the established evidence from the literature (Praag et al., 1999; Praag et al., 2005) that Running enhances adult neurogenesis in the hippocampus.

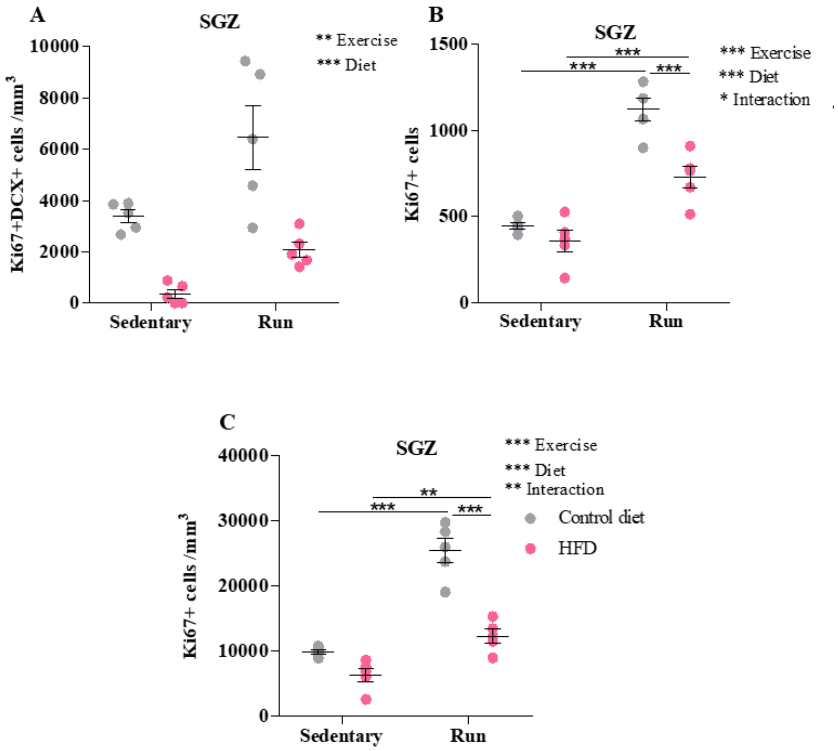

Figure 5.2. Running increased density of proliferating neuroblasts and proliferating Ki67+ cells regardless of diet. A) Quantification of Ki67+DCX+ cell density in the SGZ. B) Quantification of absolute counts of Ki67+ cells in the SGZ. C) Quantification of Ki67+ cell density in the SGZ. Data information: n = 5 mice per data set for the two week run group. In all panels, Two-way ANOVA. In panels B, C, Bonferroni's test. Data represented as mean ± SEM. Asterix (*) over groups represents Post hoc test significance. Main effects shown on the side of the graphs and in Table 5.1.

Parameter	Exercise	Diet	Interaction
Ki67+DCX+ density	**	***	n.s.
Ki67+ counts	***	***	*
Ki67+ density	***	***	**

Table 5.1. Two-Way ANOVA main effects for two week HFD or Control diet with or without concurrent Running. Specifically for Ki67 counts and cell density in the SGZ in addition to proliferating neuroblasts density.

5.2.2. Short exposure to HFD increased the number of Ki67+ cells in the ME but reduced cell proliferation in the 3V

It is established that Running increase cell proliferation in the SGZ (Praag et al., 1999), while HFD has detrimental effects (Lindqvist et al., 2006). To further determine the effects of short-term Running and HFD on the hypothalamus, immunohistochemical staining of the proliferation marker Ki67 was investigated in the entire MBH and the ArcN, ME and 3V alone. No significant difference in density of Ki67+ cells was found in ArcN (Figure 5.3B). However, there was a statistically significant main effect of the diet (Two-way ANOVA, $F(1, 11) = 7.101$, $p = 0.022$) on the density of Ki67+ cells in the ME (Table 5.2). This meant that across all conditions, diet played a role in regulating cell proliferation in the ME. Therefore, HFD increased proliferation in the ME for both Sedentary and Running animals (Table 5.2, Figure 5.3C).

To directly compare the hypothalamic nuclei to the SGZ, the absolute number of Ki67 cells was also counted. Serological analysis showed that there was also a statistically significant effect of the diet (Two-way ANOVA, $F(1, 15) = 8.926$, $p = 0.0092$), on the absolute counts of Ki67+ cells in the 3V (Table 5.2, Figure 5.3D). And there was additionally a statistically significant effect of the diet (Two-way ANOVA, $F(1, 16) = 11.63$, $p = 0.0036$) on the absolute counts of Ki67+ cells in the MBH (Table 5.2, Figure 5.3E). This meant that across all conditions, diet played a role in regulating cell proliferation in the 3V and MBH. Therefore, HFD reduced proliferation in the 3V and MBH for both Sedentary and Running animals (Table 5.2, Figure 5.3D-E). However exercise had no significant effect across the entire MBH and the ArcN, ME and 3V alone.

This also suggested that in contrast to the SGZ, two weeks Running does not increase overall cell proliferation in the MBH or individual nuclei in Control conditions. Interestingly, in the ME of the hypothalamus, treatment with HFD appeared to have a proliferative effect on cells in both Running and Sedentary mice. It is important to note that, in comparison to the SGZ, the hypothalamus hosts a wider range of cell types. As such, immunohistochemical staining for Ki67 does not distinguish the specific cell identities. In contrast to the ME, in the 3V walls, where the stem cells reside, a reduced cell proliferation in response to HFD was observed. This reduction in htNSC proliferation may suggest stem cell exhaustion as a consequence of HFD.

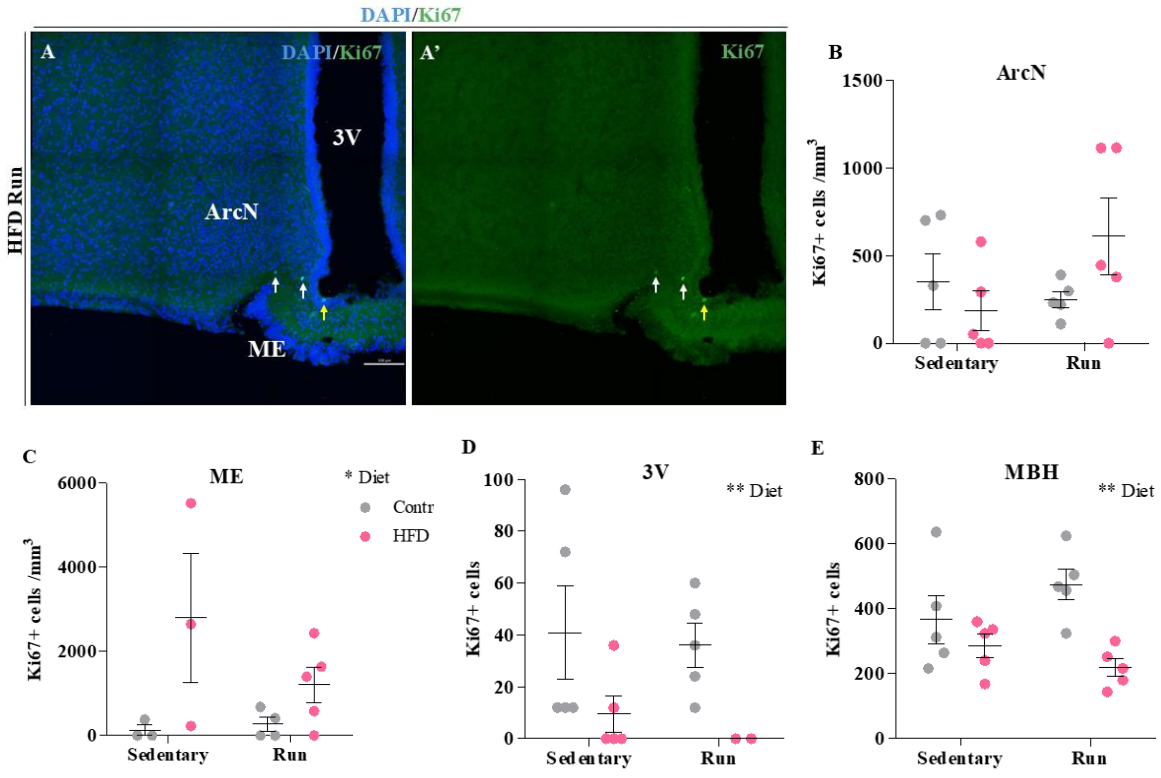

Figure 5.3. Running did not increase the number of Ki67+ cells in the hypothalamus after two weeks. A-A') Representative confocal images of the MBH stained as indicated in a HFD Runner. White arrows represent Ki67+ cells for graph B, C and E. Yellow arrow represent a Ki67+ cell for graph D. B-C) Quantification of Ki67+ cell density in the ArcN (B) and ME (C). D-E) Absolute counts of Ki67+ cells in the 3V (D) and MBH (E). Data information: S.b.: 100 µm. n = 5 mice per data set for the two week run. In all panels, Two-way ANOVA. Data presented as mean ± SEM. Main effects shown on the side of the graphs and in Table 5.2.

Parameter	Exercise	Diet	Interaction
(ME) Ki67+ density	n.s.	*	n.s.
(3V) Ki67+ counts	n.s.	**	n.s.
(MBH) Ki67+ counts	n.s.	**	n.s.

Table 5.2. Two-Way ANOVA main effects for two week HFD or Control diet with or without concurrent Running. Specifically for Ki67 density in the ME and Ki67 absolute counts in the 3V and MBH.

5.2.3. Neither HFD nor Running altered the number of proliferating neuroblasts or astrocytes

To further investigate the identity of the proliferating cells and determine if subtypes of proliferating cells were affected by HFD or Running, immunohistochemical staining co-labelled the immature neuronal marker DCX and the glial marker GFAP with Ki67. No significant difference were found in proliferating DCX+ cells or GFAP+ cells in the hypothalamus or individual nuclei (Figure 5.4). This suggests that two weeks of treatment with HFD and/or Running did not affect the overall proliferation of neurons and astrocytes. Indicating that the increase in proliferating cells in the ME include other cell types not investigated here (Figure 5.3C).

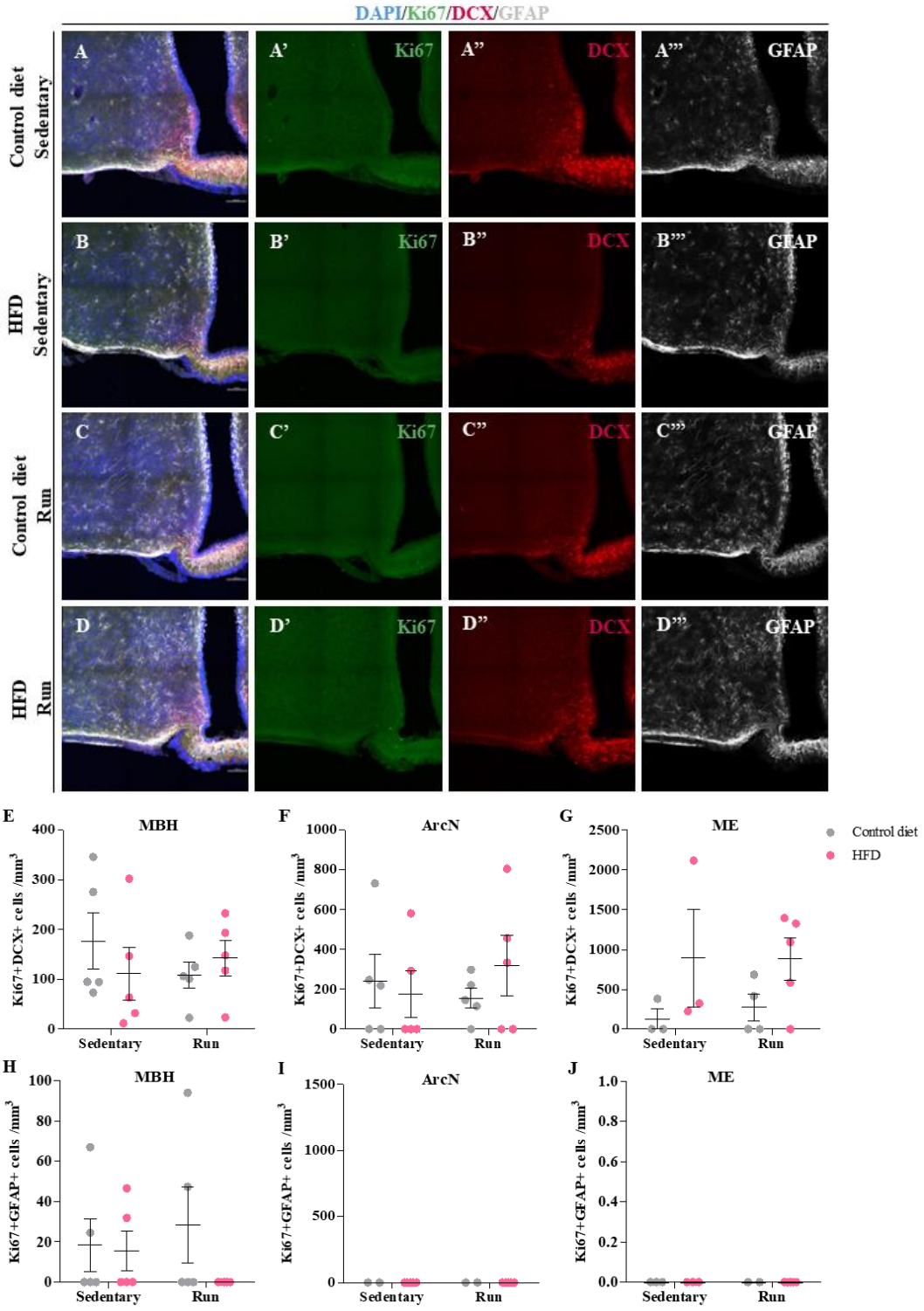

Figure 5.4. Neither running or HFD altered number of proliferating neurons or astrocytes in the hypothalamus. A-D) Representative confocal images of the MBH stained as indicated in Sedentary mice on Control diet (A-A'''), Sedentary mice on HFD (B-B'''), Runners on Control diet (C-C'''), Runners on HFD (D-D'''). E-G) Quantification of Ki67+DCX+ cell density in the MBH (E), ArcN (F) or ME (G). H-J) Quantification of Ki67+GFAP+ cell density in the MBH (H), ArcN (I) or ME (J). Data information: S.b.: 100 µm. n = 5 mice per data set for the two week run. In all panels, Two-way ANOVA with Bonferroni's test. Data presented as mean ± SEM.

5.2.4. Short-term HFD did not alter cell dynamics in vitro in htNSCs isolated from Running mice

Analysis by two-way ANOVA revealed a significant effect of HFD on cell proliferation in the 3V. Due to the low rates of proliferation of tanycytes, it is challenging to study them *in vivo*. Therefore, we opted to investigate them *in vitro* as the next best approach. The most pronounced effects in the Ki67 data appeared to be between the Control Runners and the HFD Runners. To gain a deeper understanding of why this effects was observed, further investigation using time lapse imaging was performed, as detailed in Chapter 2.

No significant differences was found in number of active clones per animal (normalised to nm^2), cell divisions per clone or quiescent cells per animal (normalised to nm^2) in Runners on Control diet or HFD (Figure 5.5). The results suggests that the effects on proliferation observed *in vivo* are such rare events in the HVZ that they cannot be adequately captured *in vitro*. Alternatively, the impact of inflammation may not persist *in vitro*, where the less hostile environment negates the elevated apoptosis seen *in vivo*, thus explaining the lack of an effect.

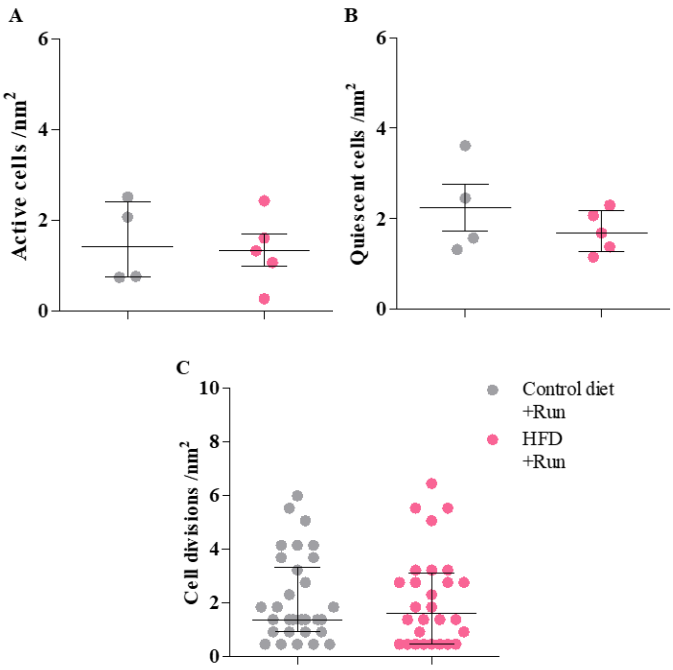

Figure 5.5. HFD does not alter cell dynamics *in vitro* in htNSCs isolated from running mice. A-C) No significant difference observed in number of active clones, quiescent cells per are (nm^2), or cell divisions per area (nm^2) in primary stem cells from the hypothalamus. A-B) Graph showing clones per animal. C) Graph showing individual neurospheres. Data information: n = 5 mice per data set. In all panels, Mann Whitney test, Two tailed. Data are presented as median ± IQR (all panels).

5.2.5. HFD increased the number of newborn cells and neurons and in the ME, which was reversed by Running

To investigate the effects of HFD and Running on newborn neurons and astrocytes in the hypothalamus, adult male mice were given five days of BrdU in drinking water to label proliferating cells and their progeny. Co-staining of BrdU with the neuronal marker DCX and astrocytic marker GFAP allowed for further analysis of the impact of HFD and Running on the identity of newborn cells and how they were affected by treatment (Figure 5.6.1A-D). The whole of MBH was analysed as well as individual nuclei, including the ArcN and ME.

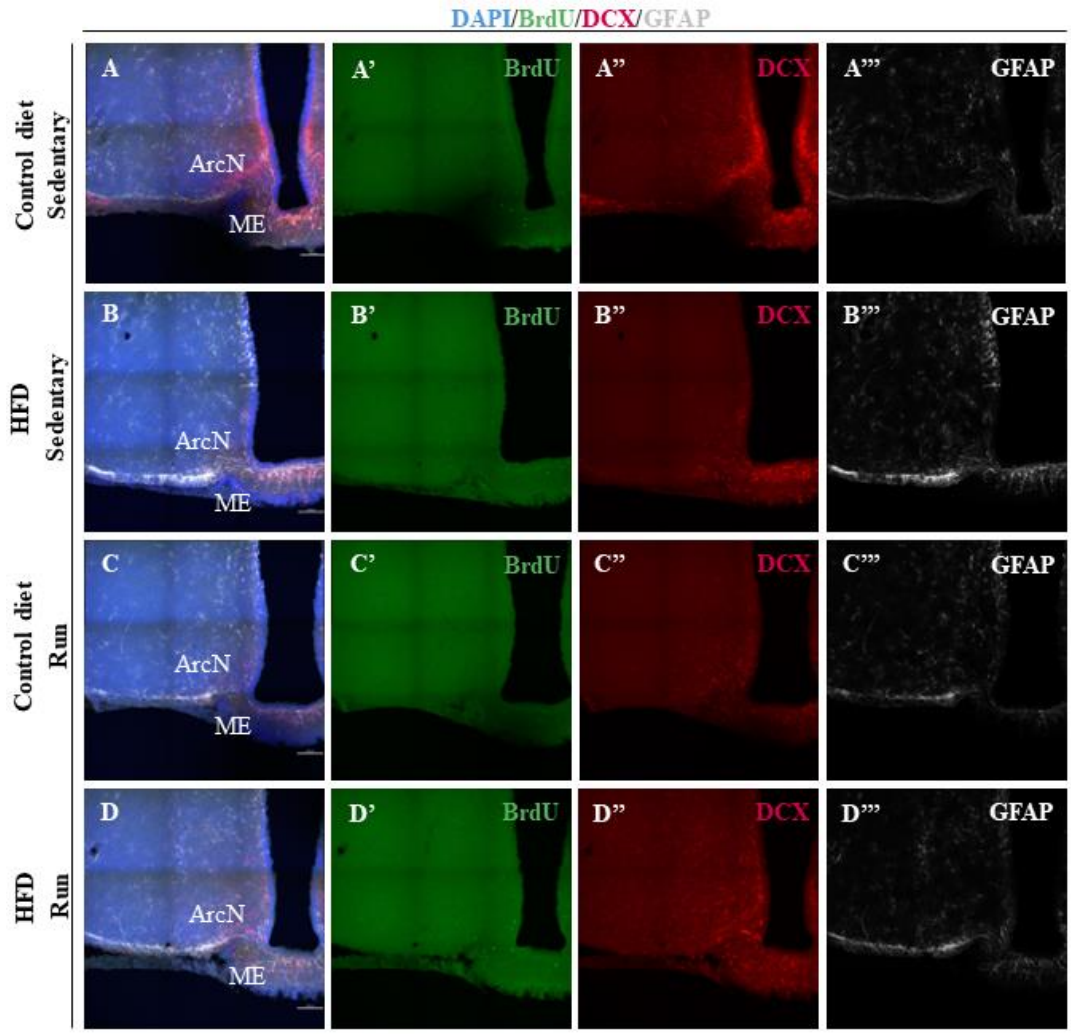

Figure 5.6.1. Co-staining of BrdU with the neuronal marker DCX and astrocyte marker GFAP. A-D) Representative confocal images of the MBH stained as indicated in Sedentary mice on Control diet (A-A'''), Sedentary mice on HFD (B-B'''), Runners on Control diet (C-C'''), Runners on HFD (D-D'''). Data information: S.b.: 100 μm. n = 5 mice per data set for the two week run.

In the ArcN, there was a statistically significant main effect of the diet (Two-way ANOVA, $F(1, 15) = 7.387$, $p = 0.0159$), reducing the density of BrdU+ cells, and BrdU+DCX+ cells (Two-way ANOVA, $F(1, 15) = 6.089$, $p = 0.0261$) in both Sedentary and Running (Figure 5.6.2F and I). The Two way ANOVA therefore shows that both BrdU+ cells and BrdU+DCX+ cells are decreased in HFD-fed animals compared to Control diet animals, regardless of exercise in the ArcN. Since the trend is observed in both Sedentary and Running conditions, it indicates that exercise does not counteract the HFD-induced reduction in neurogenesis in the ArcN. The use of the immature neuronal marker doublecortin, rather than the mature neuronal marker NeuN, in this experiment provided a more comprehensive understanding of the impact on neurogenesis (Klein et al., 2016). DCX is expressed by immature, migrating neuroblasts, while NeuN expression is only detected later in neuronal maturation. Given the shorter, 9-14 day time frame for the BrdU+ neurons to mature, utilising DCX enabled the detection of more cells adopting a neuronal fate, thereby offering better insight into the effects on neurogenesis by examining markers for earlier stages of neuronal development.

Most interestingly, there was a significant increase in newborn cells and newborn neurons in the ME of Sedentary mice fed HFD (Figure 5.6.2G and J). Where there was a statistically significant main effect of the diet (Two-way ANOVA, $F(1, 16) = 7.396$, $p = 0.0193$) and the exercise ($F(1, 16) = 6.767$, $p = 0.0151$) on the density of total BrdU+ cells in the ME (Figure 5.6.2G). Same was observed for newborn neurons (BrdU+DCX+) in the ME. Where there was a statistically significant main effect of the diet (Two-way ANOVA, $F(1, 15) = 11.44$, $p = 0.0041$) and the exercise ($F(1, 15) = 5.191$, $p = 0.0378$) on the density of total BrdU+DCX+ cells in the ME (Figure 5.6.2J). Suggesting that two weeks of HFD increased proliferation of newborn cells and neurons, as indicated by higher BrdU+ and BrdU+DCX+ cell densities. Exercise reduced neurogenesis, including in HFD-fed animals, as shown by the decrease in BrdU+ and BrdU+DCX+ cells. The lack of interaction means that exercise and diet affect neurogenesis independently, without modifying each other's effects. Suggesting that HFD can promote neurogenesis in the ME, but Running may counteract this effect.

In addition, there was a statistically significant main effect of the exercise (Two-way ANOVA, $F(1, 15) = 7.891$, $p = 0.0132$) on the density of BrdU+GFAP+ cells in the ME (Figure 5.6.2M). Suggesting that exercise reduced the density of astrocytes in the ME regardless of diet.

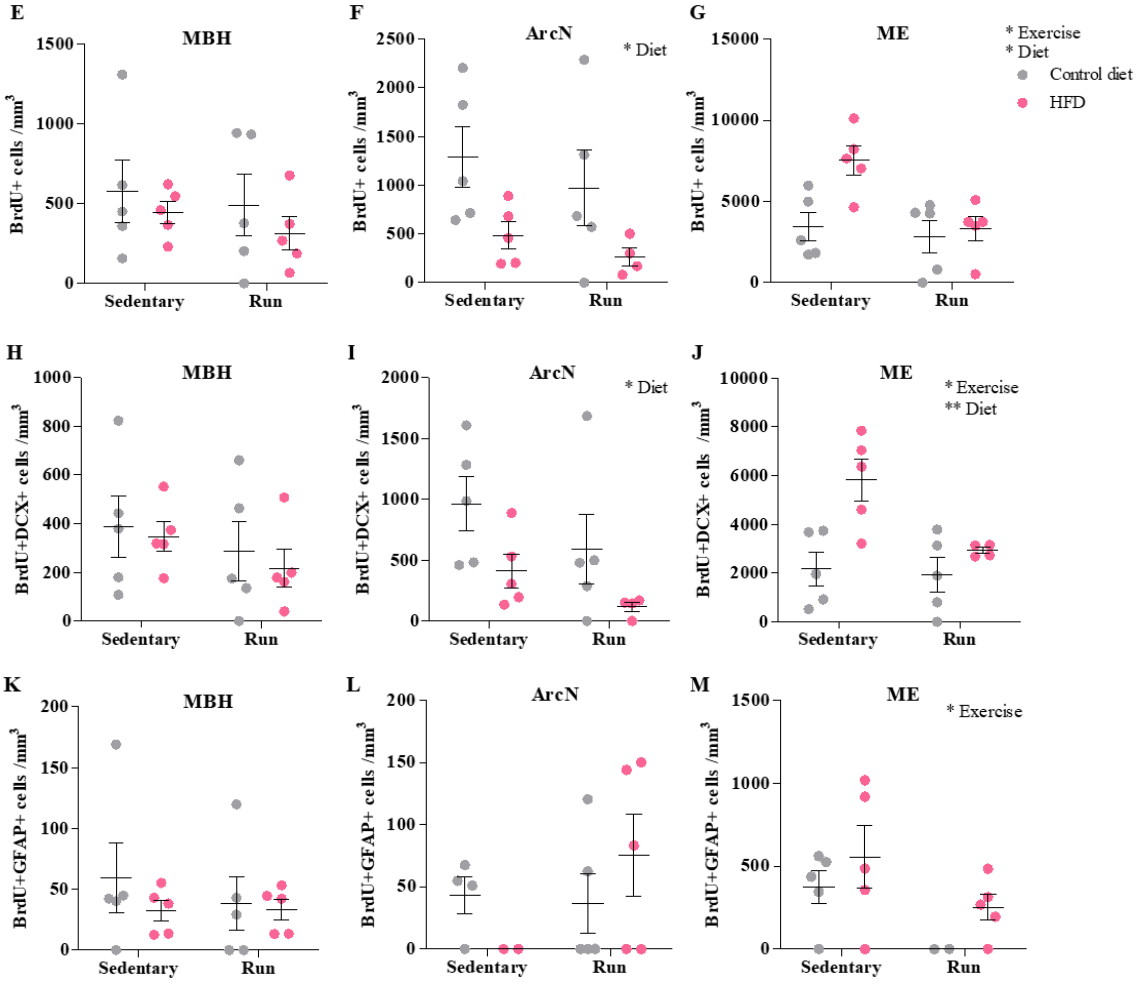

Figure 5.6.2. Running reduced proliferation of newborn neurons in the ME. E-G) Quantification of BrdU+ cell density in the MBH (E), ArcN (F), and ME (G). H-J) Quantification of BrdU+DCX+ cell density in the MBH (H), ArcN (I) and ME (J). K-M) Quantification of BrdU+GFAP+ cell density in the MBH (K), ArcN (L), and ME (M). Data information: S.b.: 100 μm. n = 5 mice per data set for the two week run. In all panels, Two-way ANOVA. Data are presented as mean ± SEM. Main effects shown on the side of the graphs and in Table 5.3.

Parameter	Exercise	Diet	Interaction
(ArcN) BrdU+ density	n.s.	*	n.s.
(ArcN) BrdU+DCX+ density	n.s.	*	n.s.
(ME) BrdU+ density	*	*	n.s.
(ME) BrdU+DCX+ density	*	**	n.s.
(ME) BrdU+GFAP+ density	*	n.s.	n.s.

Table 5.3. Two-Way ANOVA main effects for two week HFD or Control diet with or without concurrent Running on number of newborn cells and influence on cell specification.

5.2.6. Neither HFD or Running changed the density of anorexigenic BrdU+POMC+ neurons

One potential mechanism by which HFD and Running may influence the development of obesity is through their effects on the fate specification of newborn adult neurons. Specifically, by differentially altering the generation of more or less anorexigenic neurons. As these neurons reside in the ME and ArcN of the hypothalamus, the analysis focused on those nuclei. No significant difference was observed in the fate specification of adult-generated hypothalamic neurons into an anorexigenic phenotype, either with HFD or Running (Figure 5.7). This suggests that neither HFD nor Running affects neuronal specification into POMC-expressing neurons in the ArcN and ME after two weeks. This suggests that the effects of HFD and Running may be mediated through alternative mechanisms, such as the activation of anorexigenic neurons, rather than changes in their proportion.

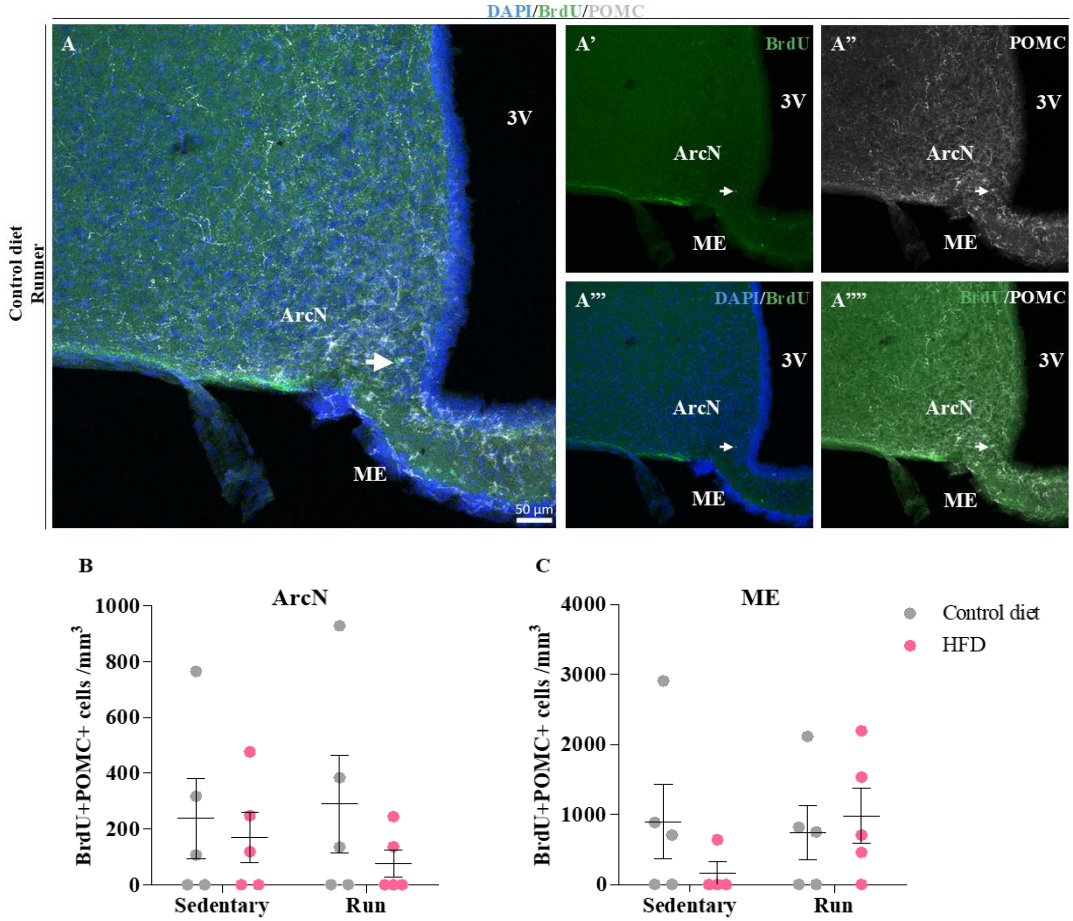

Figure 5.7. Neither HFD nor Running influenced the number of newborn anorexigenic neurons in the hypothalamus. A-A''') Representative confocal images of the MBH stained as indicated in a Runner on Control diet. B-C) Quantification of BrdU+POMC+ cell density in the ArcN (C) and ME (D). Data information: S.b.: 50 µm. n = 5 mice per data set for the two week run. In all panels, Two-way ANOVA. Data presented as mean ± SEM.

5.2.7. Mice on 3 months of HFD significantly gained weight regardless of Running

Obesity is a chronic disease and the effects of long-term HFD on the hypothalamus is still under investigation. Long-term HFD and Running have only been investigated a few times with conflicting results.

In the interest of further investigating the impact of long-term HFD and Running on adult hypothalamic neurogenesis, adult male and female mice were kept in the same cages used in the two week long protocol, but now for 3 months as described in detail in Chapter 2 (Figure 5.8A). A GLAST-CreER^{T2} x R26-tdTomato mouse line was used to lineage trace adult neurogenesis in mice exposed to 3 months of HFD or Control diet with or without concurrent Running. This analysis aimed to gain better insight into the process of cell proliferation and

differentiation of adult-generated hypothalamic cells, and how they respond to external stimuli. By inducing the mice at the start of the experiment, the analysis included continuous neurogenic lineage tracing for 3 months, while the BrdU labelling of cells was identical to the two week protocol. This allowed for a combined analysis of continuous neurogenesis and acute neurogenesis at the end of the 3 month period.

Interestingly, the mice did not show significant weight gain when fed the HFD for 3 months compared to the Control diet (Figure 5.8B). Rather, both Sedentary and Running mice regardless of diet exhibited significant weight gain (Two-way ANOVA, $F(1, 32) = 24.26$, $p < 0.0001$) over time (Figure 5.8D).There was no difference in the distance run by mice on the Control diet and HFD (Figure 5.8C).

These findings suggest that although the HFD did not result in significantly greater weight gain compared to the Control diet, the HFD nonetheless had a measurable impact on the body weight of the mice.

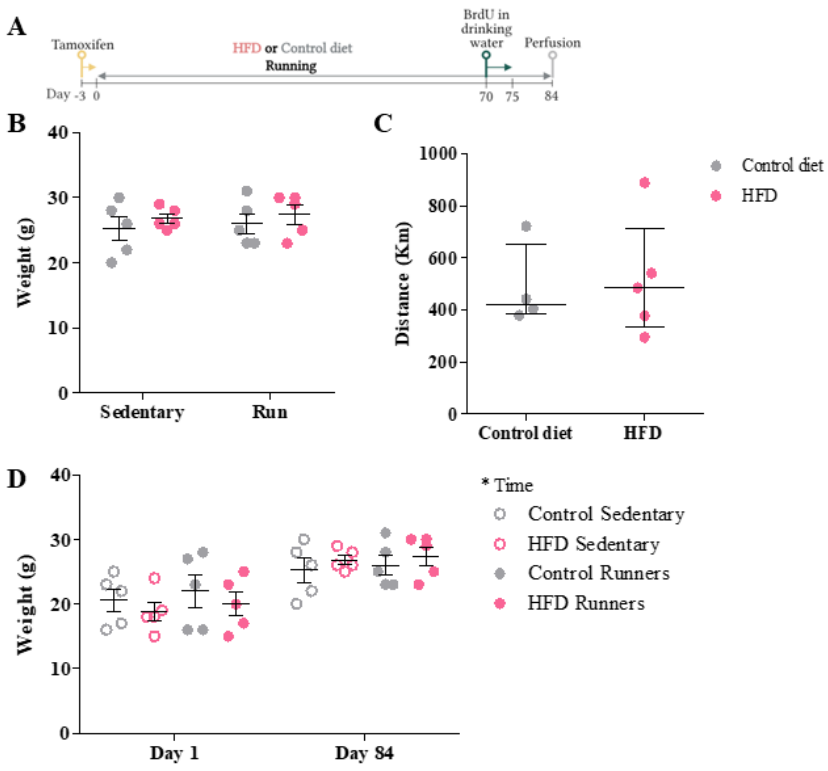

Figure 5.8. Mice on HFD significantly gain weight regardless of running. A) Timeline for 3 month HFD and Running. B) Weight after 3 month HFD and Running. C) Distance that the mice ran in Km after two weeks in Runners on Control or HFD. D) Comparing weight at d1 and d84. Data information: S.b.: 50 µm. n = 5 mice per data set for the 3 months run. In panels, B, D, Two-way ANOVA. In panel C, Unpaired t-test, Two-tailed. Data presented as mean ± SEM (B, C) or median ± IQR (D). Main effects shown on the side of the graph (D).

5.2.8. Long-term HFD reduced the accumulation of new GLAST+ neurons in the hypothalamus, and voluntary Running did not reverse this effect

To investigate the impact of long-term HFD and voluntary Running on adult hypothalamic neurogenesis, inducible in vivo tracking of tdTomato+ aNSCs and their progeny was used. Adult male and female GLAST-CreERT2 x R26-tdTomato mice were equally distributed to one of the four treatment groups and kept in the cages for 3 months. The mice were induced by tamoxifen injections over 3 days before they were placed in the cages. The resulting tdTomato+ cells are therefore a mixture of 3 month old and newborn proliferating GLAST+ (tdTomato+) cells, allowing for analysis of accumulative neurogenesis. GLAST expressing cells in the hypothalamus are aNSCs, and some astrocytes. Astrocytes were therefore excluded from all analysis. The same pulse-chase BrdU labelling protocol used in the short-term HFD and Running study was also applied during the last two weeks of the long-term experiment. This allowed for the investigation of BrdU-labelled newborn cells and neurons in the final two weeks of the protocol, providing a direct comparison between the mice that had been on the short-term HFD and Running regime and those that had become obese and been exposed to prolonged HFD and Running.

Results showed that 3 months of HFD reduced the density of all lineage traced neurons (tdTomato+NeuN+) in the MBH as well as in the ArcN and Parenchyma alone, which was not reversed by Running. Where there was a statistically significant main effect of the diet (Two-way ANOVA, $F(1, 14) = 17.39$, $p = 0.0009$) on lineage traced new neurons (tdTomato+NeuN+) in the MBH, the ArcN (Two-way ANOVA, $F(1, 14) = 17.61$, $p = 0.0009$) and the Parenchyma (Two-way ANOVA, $F(1, 14) = 11$, $p = 0.0051$) alone (Figure 5.9B). The data suggests that HFD reduced tdTomato+NeuN+ cell density in the MBH, ArcN, and Parenchyma, regardless of exercise status. Running did not significantly alter tdTomato+NeuN+ cell density, meaning that Running did not counteract or exacerbate the diet-induced effect. It also indicates that the effect of HFD is consistent across both Sedentary and Running groups, meaning exercise does not modify the diet-induced changes.

In summary, the results suggests that Running failed to reverse the reduction of all lineage-traced neurons in the MBH, ArcN, and Parenchyma caused by the HFD. Additionally, 3 months of Running did not increase accumulative neurogenesis in mice fed the Control diet. These findings imply that the HFD impaired neuronal differentiation from GLAST+ stem cells or reduced long-term survival of the lineage traced mature neurons.

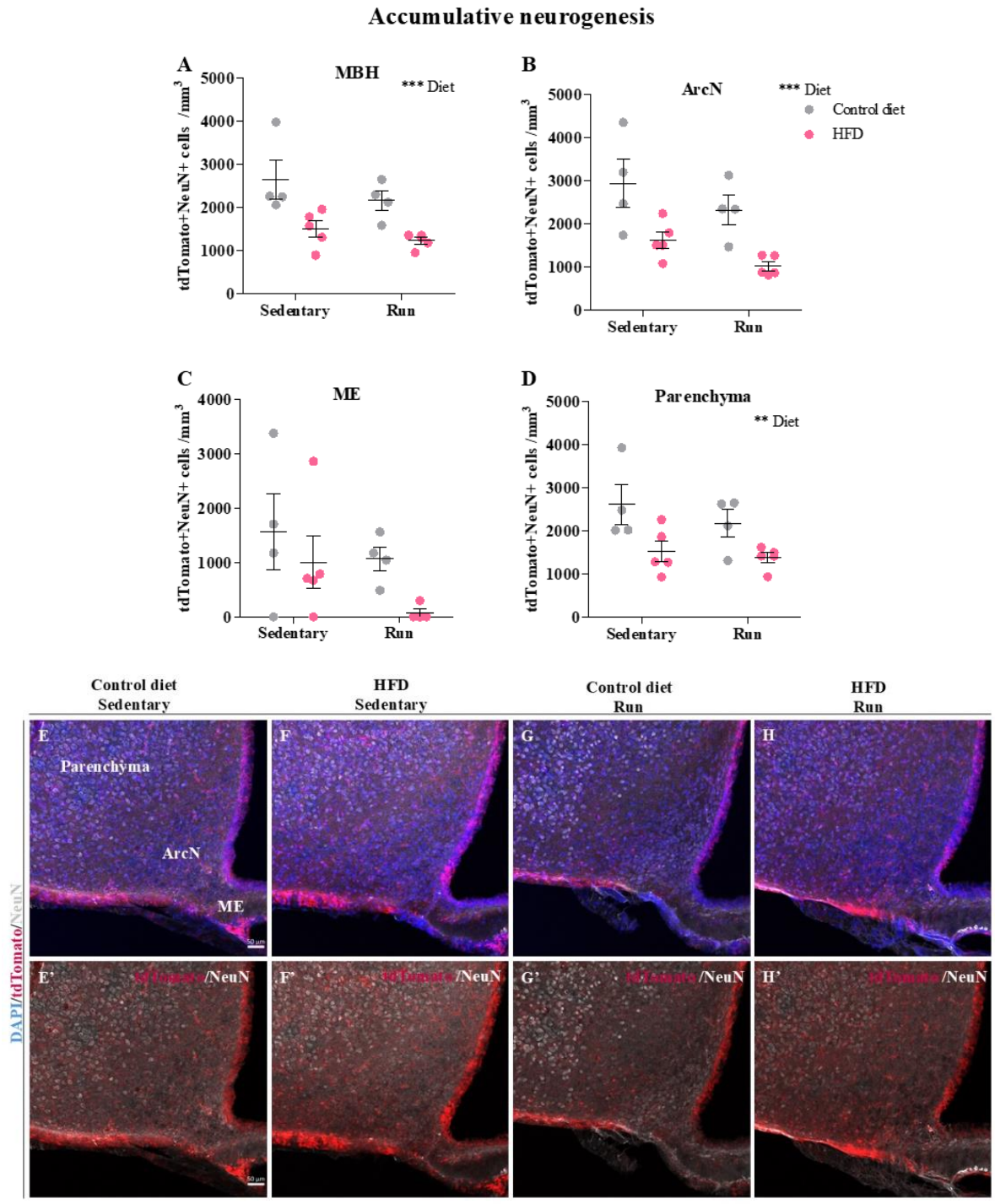

Figure 5.9. Running did not rescue the reduced neurogenesis in mice on long-term HFD. A-D) Quantification of tdTomato+NeuN+ cell density in the MBH (A), ArcN (B), ME (C), Parenchyma (D). E-H) Representative confocal images of the MBH stained as indicated in Sedentary mice on Control diet (E-E'''), Sedentary mice on HFD (F-F'''), Runners on Control diet (G-G'''), Runners on HFD (H-H'''). Data information: S.b.: 50 μm. n = 5 mice per each data set for the 3 month run. In all panels, Two-way ANOVA. Data are presented as mean ± SEM. Main effects shown on the side of the graphs and in Table 5.4.

Parameter	Exercise	Diet	Interaction
(MBH) tdTomato+NeuN+ density	n.s.	***	n.s.
(ArcN) tdTomato+NeuN+ density	n.s.	***	n.s.
(Parenchyma) tdTomato+NeuN+ density	n.s.	**	n.s.

Table 5.4. Two-Way ANOVA main effects for 3 month of HFD or Control diet with or without concurrent Running on lineage traced neurons.

5.2.9. Long-term Running increased the generation of new neurons in mice fed a Control diet, but failed to reverse the reduction of new neurons caused by HFD

Although Running had no significant effect on the accumulative neurogenesis, there was a significant increase in adult born neurons (BrdU+NeuN+) in the last two weeks of the 3 month period in mice fed Control diet (Figure 5.10A). Again, this protocol compares the two-week label-retaining paradigm that was previously used in the short-term HFD and Running study. This allowed for a direct comparison between the effects of short-term and long-term exposure to the dietary and exercise interventions on adult born neurons.

There was a statistically significant effect of the diet (Two-way ANOVA, $F(1, 14) = 24.4$, $p = 0.0002$), the exercise ($F(1, 14) = 4.85$, $p = 0.0449$) and their interaction ($F(1, 14) = 7.774$, $p = 0.0145$) on BrdU+NeuN+ density in the MBH. Bonferroni's Pots-hoc Test found that exercise significantly increased the density of BrdU+NeuN+ cells in the MBH for mice fed Control diet ($p < 0.01$) and a significant difference between Runners on Control diet compared to Runners on HFD ($p < 0.001$; Figure 5.10A; Table 5.5). Running therefore increased adult neurogenesis in Control diet in the last two weeks of the protocol. The data suggests that in contrast to the SGZ, the hypothalamus is responsive to longer Running. However, there was also a significant difference between Runners on Control diet and Runners on HFD, meaning HFD limits the neurogenic benefits of exercise and that the neurogenic response to exercise is diet-dependent. In addition, there was a statistically significant main effect of the diet on BrdU+NeuN+ density

in the ArcN (Two-way ANOVA, F(1, 14) = 7.475, p = 0.0161), ME (Two-way ANOVA, F(1, 15) = 7.108, p = 0.0176), and Parenchyma (Two-way ANOVA, F(1, 15) = 11.96, p = 0.0035; Figure 5.10B-D; Table 5.5). This suggests that HFD reduced the number of adult born neurons in the last two weeks of the 3 month period which was not reversed by Running. Indicating that long-term HFD have detrimental effects on all neuronal populations in the hypothalamus.

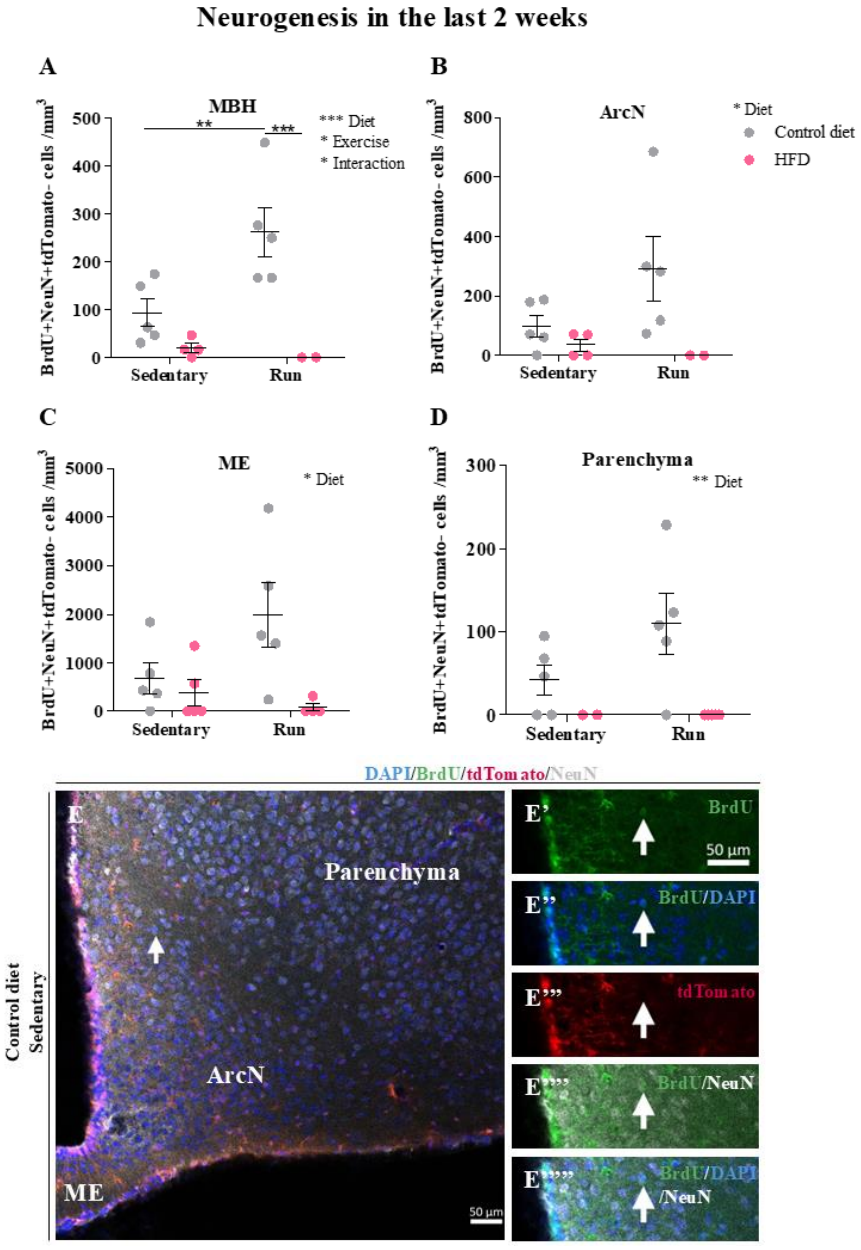

Figure 5.10. Running increased neurogenesis in the hypothalamus in the last two weeks. A-D) Quantification of BrdU+NeuN+ cell density in the MBH, ArcN (B), ME (C), Parenchyma (D). E-E''''') Representative confocal images of DAPI+, BrdU+, NeuN+ and tdTomato-negative cell in the MBH of a Sedentary mice on Control diet. Data information: S.b.: 50 µm. n = 5 mice per data set for 3 month run. In all panels, Two-way ANOVA. In panel A, Bonferroni's test. Data are presented as mean ± SEM. Asterix (*) over groups represents post hoc test significance. Main effects shown on the side of the graphs and in Table 5.5.

Parameter	Exercise	Diet	Interaction
(MBH) BrdU+NeuN+ density	*	***	*
(ArcN) BrdU+NeuN+ density	n.s.	*	n.s.
(ME) BrdU+NeuN+ density	n.s.	*	n.s.
(Parenchyma) BrdU+NeuN+ density	n.s.	**	n.s.

Table 5.5. Two-Way ANOVA main effects for 3 month of HFD or Control diet with or without concurrent Running on BrdU+ neurons.

5.2.10. HFD decreased neurogenesis in the ArcN of Sedentary mice, which is not reversed by Running

The stages of adult neurogenesis have not been fully elucidated in the hypothalamic neurogenic niche. However, it is known that immature neurons express the marker DCX. To investigate the effects of long-term Running and exercise on adult neurogenesis, specifically in immature neurons, immunohistochemical staining of DCX and BrdU was performed and co-analysed by the expression of tdTomato (Figure 5.11). The analysis focused on the ArcN and ME, where DCX is predominantly expressed (Batailler et al., 2014).

Accumulative neurogenesis was further investigated by quantifying tdTomato+ cells co-expressing DCX. In contrast to the mature neurons (tdTomato+NeuN+), that were reduced by HFD, the accumulative neurogenesis of immature neurons (tdTomato+DCX+) showed no significant difference after external stimuli (Figure 5.11E).

Neurogenesis of BrdU-labelled subpopulations in the last two weeks was investigated by co-staining for BrdU and DCX. The newborn cells (BrdU+) that originated from induced stem cells (tdTomato+) that also co expressed DCX in the last two weeks of long-term HFD and Running was analysed to determine the specific response of newborn neurons from cells originating from induced aNSCs. Results of this analysis showed a statistically significant effect of the diet (Two-way ANOVA, $F(1, 13) = 6.234$, $p = 0.0268$), the exercise ($F(1, 13) = 18.34$, $p = 0.0009$) and their interaction ($F(1, 13) = 10.49$, $p = 0.0065$) on the density of

tdTomato+BrdU+DCX+ cells in the ArcN (Figure 5.11D, Table 5.6). Additionally, Bonferroni's Pots-hoc Test found that HFD significantly decreased the density of tdTomato+BrdU+DCX+ cells in the ArcN compared to Sedentary mice on Control Diet ($p < 0.01$). Suggesting that 3 months HFD reduced neurogenesis or neuronal survival in the ArcN, where appetite regulating neurons reside. Interestingly, exercise also significantly decreased the density of tdTomato+BrdU+DCX+ cells in the ArcN compared to Sedentary mice on Control Diet ($p < 0.001$). Suggesting that exercise, in this context, reduced the proliferation, survival or differentiation of these newly generated neurons in the ArcN. The interaction suggests that the effects of exercise on these specific neuronal populations are diet-dependent, and under HFD conditions, exercise does not counteract but may even exacerbate the loss of these neurons. In contrast, BrdU+DCX+ cells that did not originate from induced stem cells (tdTomato-) showed no significant difference in either the ArcN or the ME (Figure 5.11A-B).

These findings suggest that the HFD reduced acute adult neurogenesis from GLAST+ aNSCs, and this was not reversed by Running. However, the HFD did not alter the accumulative neurogenesis of immature neurons in the ArcN or ME. This implies that long-term exposure to the HFD may have enhanced the retention of older neurons, as previously demonstrated (Klein et al., 2019). This could represent a compensatory mechanism to maintain some degree of hypothalamic function despite the reduced neurogenesis.

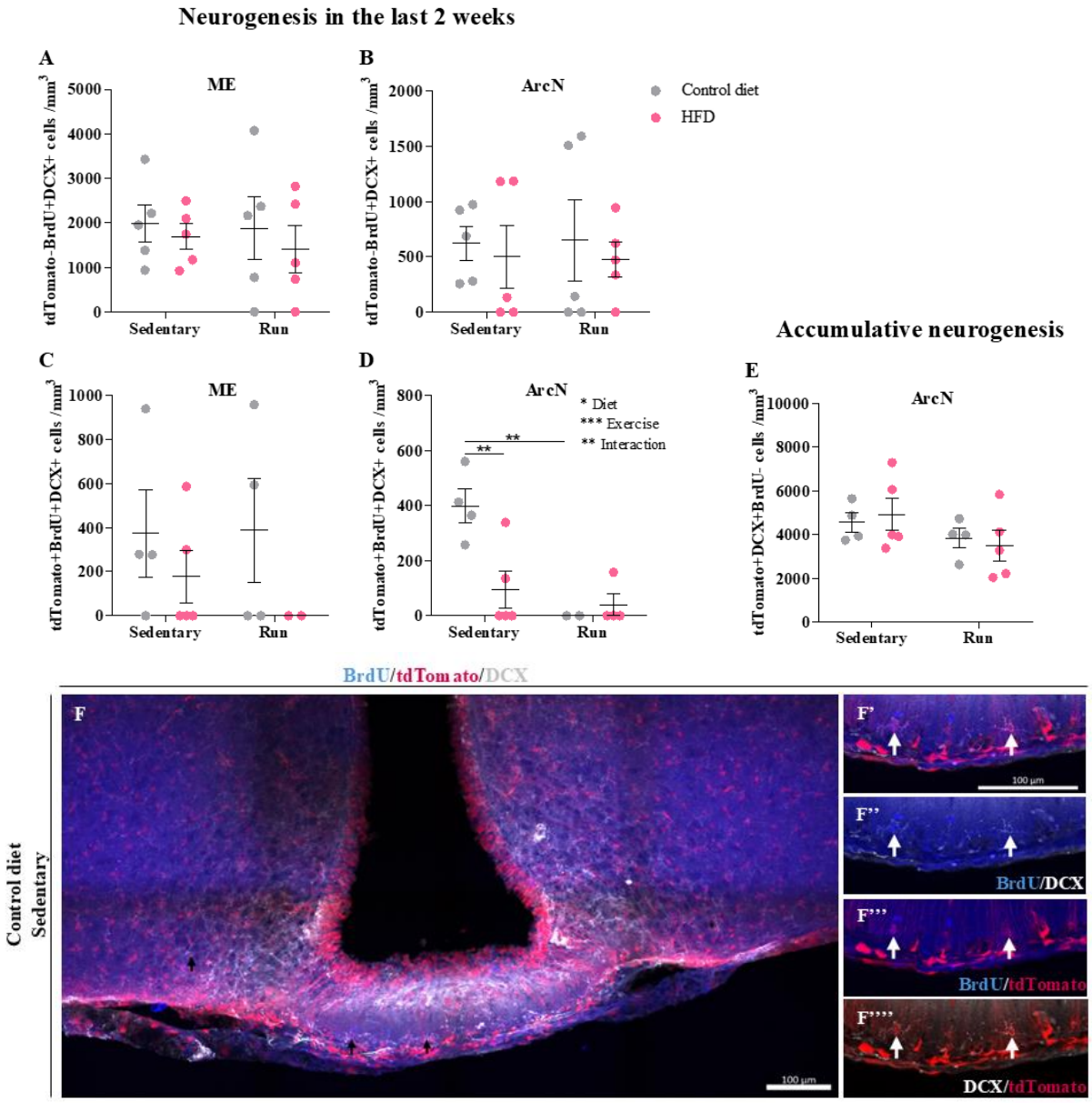

Figure 5.11. Neither long-term Running of HFD alters the rate of neurogenesis in the last two weeks. A-B) Quantification of tdTomato-BrdU+DCX+ cell density in the ME (A) or ArcN (B) in the last two weeks. C-D) Quantification of tdTomato+BrdU+DCX+ cell density in the ME (C) or ArcN (D) in the last two weeks. E) Quantification of tdTomato+DCX+ cell density in the ArcN after 3 months. F-F'''') Representative confocal images of BrdU+DCX+tdTomato-positive cells in the ME of a Sedentary mouse on Control diet. Data information: n = 5 mice per data set for the 3 month run. In all panels, Two-way ANOVA. In panel D, Bonferroni's test. Data are presented as mean ± SEM. Asterix (*) over groups represents post hoc test significance. Main effects shown on the side of the graphs and in Table 5.6.

Parameter	Exercise	Diet	Interaction
(ArcN) tdTomato+BrdU+DCX+ density	***	*	**

Table 5.6. Two-Way ANOVA main effects for 3 month of HFD or Control diet with or without concurrent Running on tdTomato+BrdU+ immature neurons.

5.2.11. Long-term Running increased the density of new cells (BrdU+) in Control conditions

In the short-term protocol, Running had no significant effect on newborn cells in the hypothalamus. Similarly, long-term Running did not have a significant effect on lineage-traced new born (tdTomato+BrdU+) cells (Figure 5.12.1A) in the last two weeks. In contrast to the short-term Running that showed an increase in total BrdU-labelled cells in the ME after HFD which was reversed by Running, no changes can be seen in pool of BrdU-labelled proliferating cells (All BrdU+ cells) in the last two weeks of long-term Running and HFD in the same area. However, HFD significantly reduced the pool of BrdU+ cells (All BrdU+ cells) in the ArcN. Specifically, there was a statistically significant main effect of the diet (Two-way ANOVA, $F(1, 16) = 4.856$, $p = 0.0425$) on the density of BrdU+ cells in the ArcN (Figure 5.12.1F). HFD therefore reduces cell proliferation in the ArcN, regardless of exercise status. Exercise did not significantly alter the number of All BrdU+ cells, meaning Running does not counteract or exacerbate the diet-induced effect.

However, when looking at BrdU-labelled cells that do not originate from tamoxifen-induced cells and do not co-stain for mature neuronal markers, long-term Running significantly increased their density in the Control group (Figure 5.12.2K). Specifically, there was a statistically significant main effect of the diet (Two-way ANOVA, $F(1, 15) = 17.75$, $p = 0.0008$), and the exercise (Two-way ANOVA, $F(1, 15) = 13.13$, $p = 0.0025$) on the density of BrdU+ (tdTomato-negative) cells in the MBH (Table 5.7). This result therefore indicated that HFD reduced cell proliferation in the MBH, regardless of exercise, but Running promotes neurogenesis in the MBH regardless of diet. These results suggested that while exercise generally supported neurogenesis, its benefits may be blunted under HFD conditions in the MBH (Figure 5.12.2K). The findings additionally suggest that the hypothalamus is indeed responsive to long-term Running. However, the specific cellular identity of the newly formed cells remains to be determined.

In addition, diet had a significant main effect (Two-way ANOVA,F(1, 13) = 16.94, p = 0.0012), on the density of BrdU+ cells in the ArcN (Figure 5.12.2M). In the ME, the exercise had a significant main effect (Two-way ANOVA, F(1, 15) = 6.376, p = 0.0233) on the density of BrdU+ cells (Figure 5.12.2L). Running thereby increased the proliferation of an unidentified cell population in the MBH and ArcN under Control diet conditions. Additionally, in the ME, Running increased cell proliferation irrespective of diet of the same undefined population (Table 5.7). The results also suggests that different mechanisms regulates neurogenesis in these regions, with diet influencing the ArcN and exercise influencing the ME. Overall, these findings suggest that the hypothalamus is responsive to long-term Running and that individual hypothalamic nuclei are differentially affected by HFD and exercise.

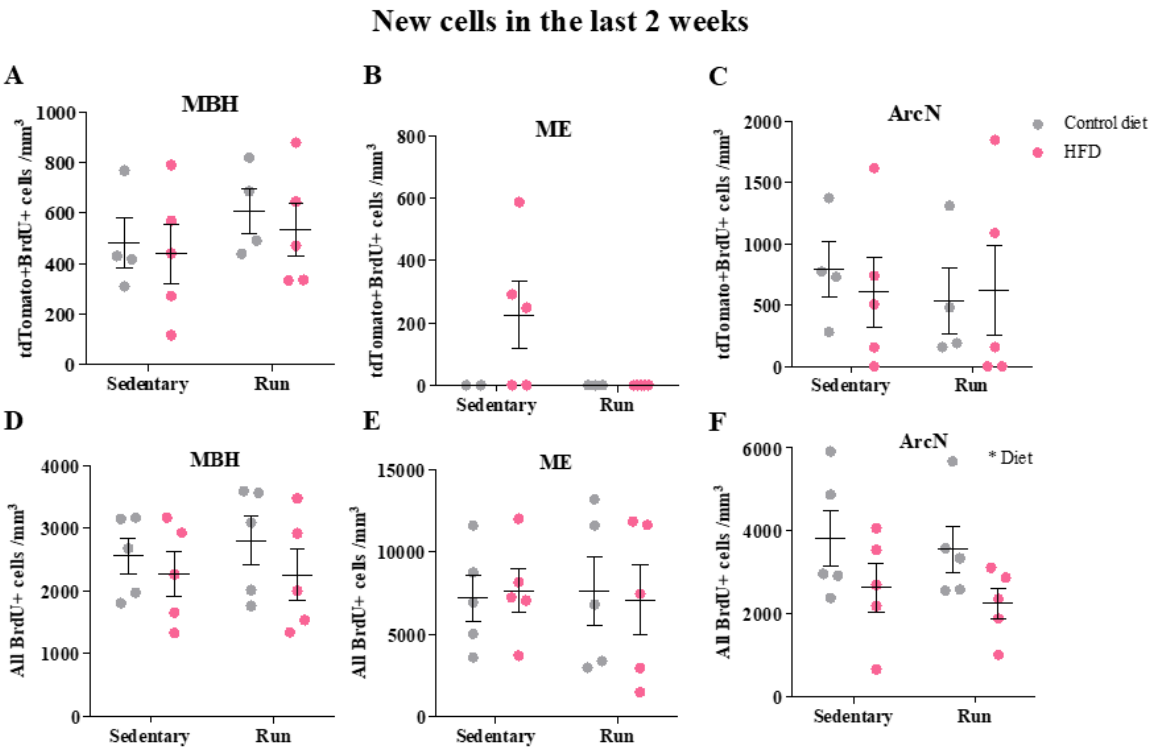

Figure 5.12.1. New cells in the last two weeks of 3 month experiment. A-C) Quantification of tdTomato+BrdU+ cell density in the MBH (A), ME (B), ArcN (C). D-E) Quantification of All BrdU+ cells (density) in the MBH (D), ME (E), and ArcN (F). Data information: n = 5 mice per data set for the 3 month run. In all panels, Two-way ANOVA. Data are presented as mean ± SEM. Main effects shown on the side of the graphs and in Table 5.7.

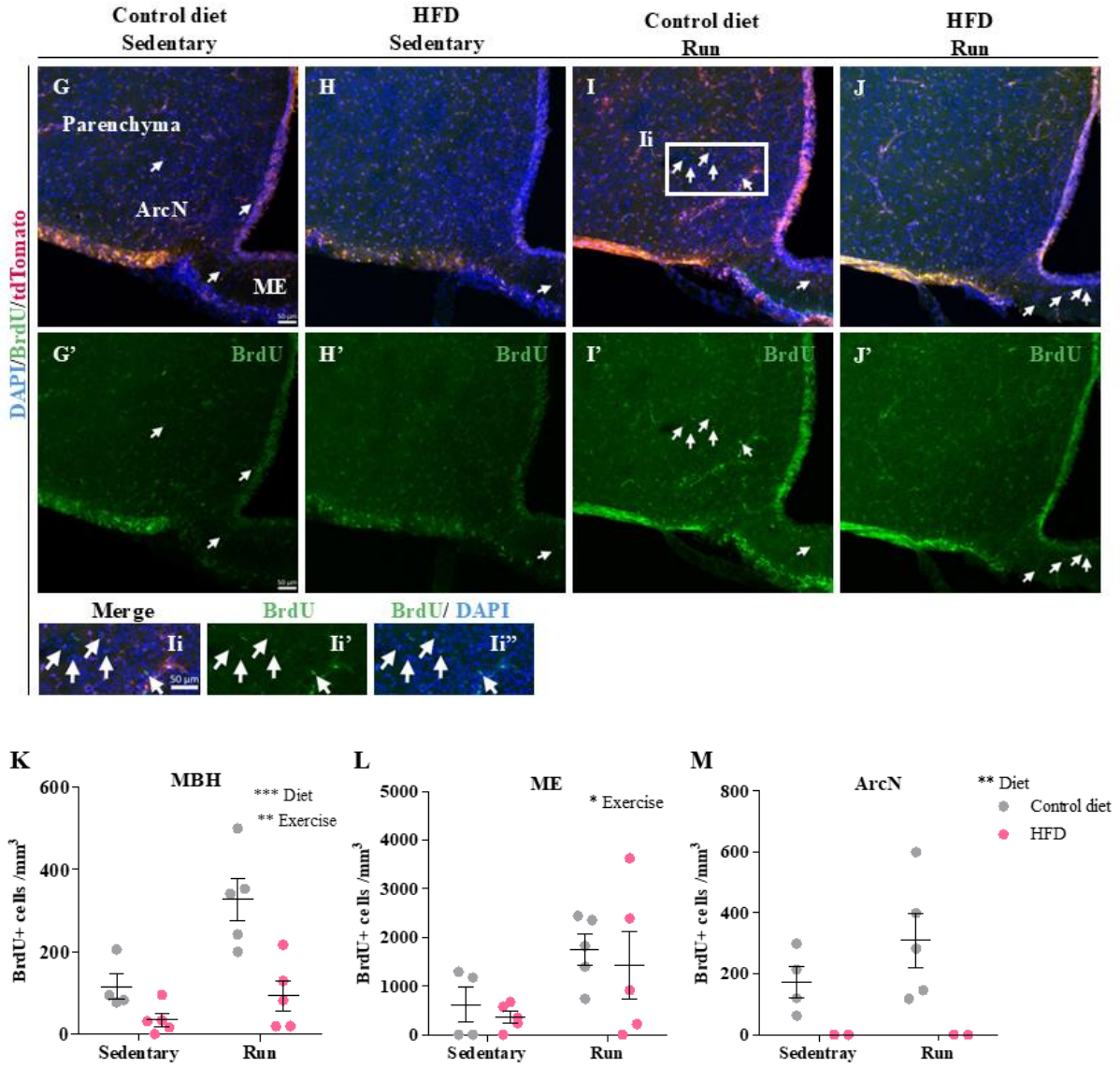

Figure 5.12.2 New cells in the last two weeks of 3 month experiment. G-J) Representative confocal images of the MBH stained as indicated in all treatment groups. G'-J') Representative confocal images of BrdU in the MBH of all treatment groups as indicated. K) Quantification of undefined BrdU+ cells in the MBH (K), ME (L), ArcN (M). Data information: S.b.: 50 µm. n = 5 mice per data set for the 3 month run. In all panels, Two-way ANOVA. Data are presented as mean ± SEM. Main effects shown on the side of the graphs and in Table 5.7.

Parameter	Exercise	Diet	Interaction
(ArcN) All BrdU+ density	n.s.	*	n.s.
(ArcN) BrdU+ density	n.s.	**	n.s.
(ME) BrdU+ density	*	n.s.	n.s.
(MBH) BrdU+ density	**	***	n.s.

Table 5.7. Two-Way ANOVA main effects for 3 month of HFD or Control diet with or without concurrent Running on BrdU+ cells.

5.2.12. Long-term HFD increased cell proliferation in the ArcN of Sedentary mice which was not reduced by Running

In order to compare the effects of HFD and Running in the last two weeks of the long-term running protocol with the short-term running protocol, immunohistochemical staining of Ki67+ proliferating cells and neuroblasts (DCX+) was performed.

The results showed there was a statistically significant main effect of the diet (Two-way ANOVA, $F(1, 16) = 4.881$, $p = 0.0421$) on density of Ki67+ cells in the ArcN (Figure 5.13B). However, similarly to the two week protocol, neither long-term Running or HFD had a significant effect on proliferating neuroblasts (Ki67+DCX+) in the hypothalamus in the last two weeks of the 3 month protocol (Figure 5.13C-D). This data suggests that neither HFD or Running alters accumulative neurogenesis in terms of proliferating immature neurons.

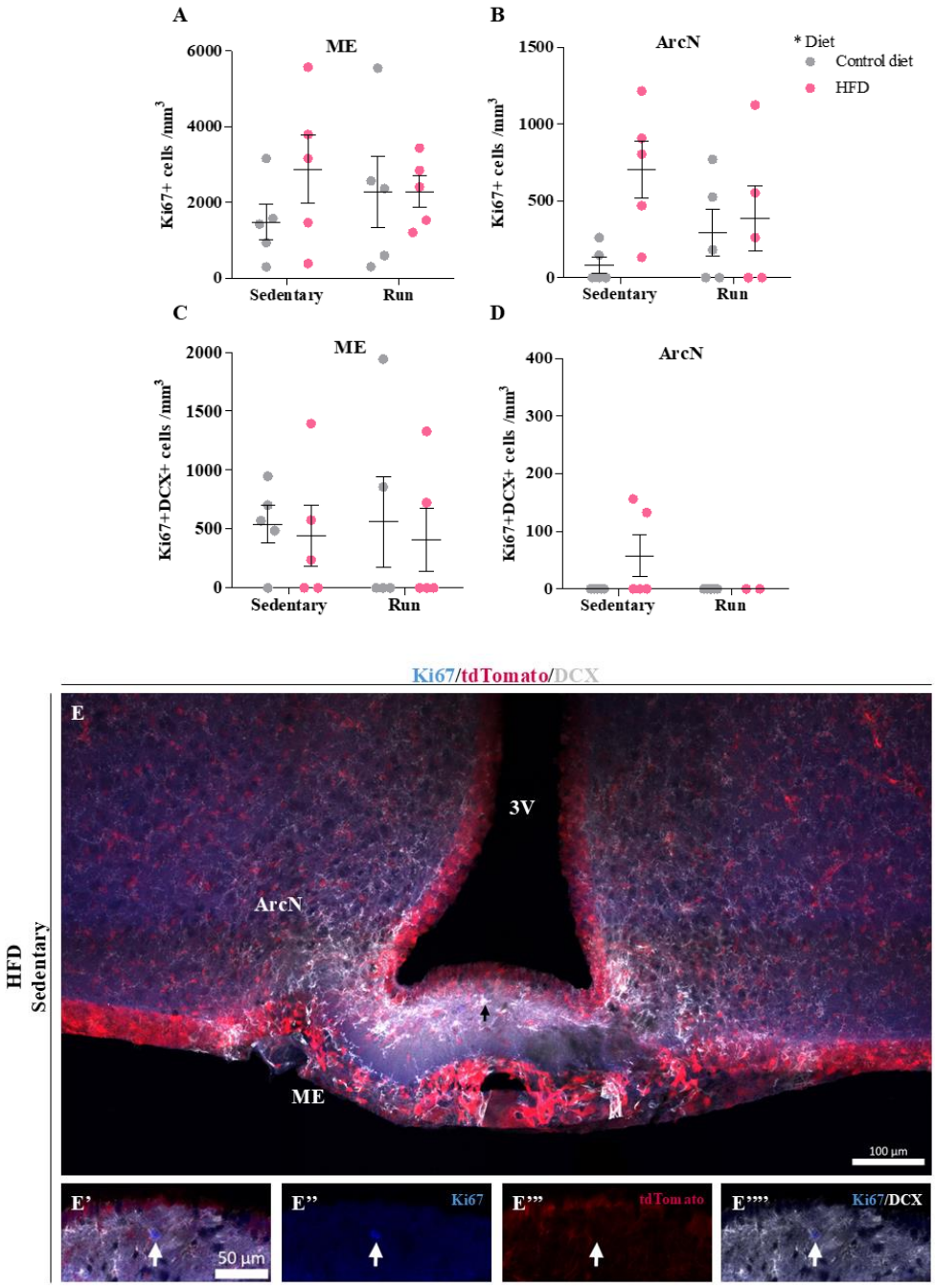

Figure 5.13. Proliferating cells and neuroblasts in the last two weeks of 3 month experiment. A-B) Quantification of Ki67+ cell density in the ME (A) and ArcN (B) at the end of 3 months HFD and Running. C-D) Quantification of Ki67+DCX+ cell density in the ME (C) and ArcN (D) at the end of 3 months HFD and Running. E-E'''') Representative confocal images of a Ki67+DCX+, tdTomato-negative cell in the ME of a Sedentary mouse on HFD. Data information: S.b.: 100 µm and 50 µm. n = 5 mice for each group for each data set. In all panels, Two-way ANOVA. Data are presented as mean ± SEM. Main effects shown on the side of the graphs.

5.3. Short discussion

This chapter aimed to investigate the influence of diet and exercise on adult neurogenesis in short-term and long-term protocols. The results revealed region-specific effects on adult hypothalamic neurogenesis. Under these specific protocol parameters, in tandem housed mice, short-term Running reduced and thereby reversed increased hypothalamic adult neurogenesis that had been elevated by HFD, long-term Running instead increased adult neurogenesis but failed to protect against the detrimental effects of long-term HFD. The lasting detrimental impact of prolonged HFD on hypothalamic neurogenesis underscores the importance of early intervention and the potential limits of exercise as a sole protective measure against the neurogenic consequences of long-term metabolic dysfunction.

5.3.1. High fat diet did not induce obesity

Interestingly, while many studies have shown that a high-calorie diet leads to weight gain and DIO in mice (Buckinx et al., 2021; Lee et al., 2014; Thaler et al., 2012), this study did not observe any weight difference between the HFD and Control groups. Previous studies have demonstrated no significant increase in body weight in short-term HFD protocols. Neither Niwa et al. (2015) nor Gouazé et al. (2013) reported substantial weight gains after two weeks of HFD administration. This indicates that the short-term HFD protocol investigates adult neurogenesis within the context of HFD-induced hypothalamic injury and inflammation, rather than in the setting of obesity.

No significant difference in weight was observed even with long-term feeding. This unexpected result may be explained by the experimental parameters. To ensure individual mouse access to a fixed or free-rotating wheel, the mice were housed separately, but the divider allowed visual, auditory, and olfactory contact between them. Single housing has been shown to induce stress in rodents (Muta et al., 2023; Buckinx et al., 2021), which can also impact their body weight. Although, a study by Buckinx et al. (2021) found no significant differences in body weight, or corticosterone levels of mice on a Control diet after 10 weeks when housed in cages with a partial divider as used in our experiments (Buckinx et al., 2021). However, this study merely suggests that these type of cages does not lead to weight loss in mice on a Control diet, but it is possible that stress could still prevent weight gain in the context of HFD. Conversely, another study (Legendre & Harris, 2006) found that rats fed HFD and also exposed to mild stress stopped gaining weight (Legendre & Harris, 2006).This suggests that while the single housing may not have induced significant stress levels in the mice, it could still have been sufficient to prevent weight gain in the HFD group. Future investigations are advised to measure

corticosterone levels to ascertain whether the mice in this study experienced stress and the extent to which this may have influenced the results. Furthermore, conducting Dual-Energy X-ray Absorptiometry (DEXA) scans could offer important insights into the lipid deposition within various organs, as the accumulation of adipose tissue within vital organs has the potential to conceal weight gain induced by a HFD regimen (Williams et al., 2014). DEXA is a technique that uses two X-ray beams with different energy levels to measure bone mineral density (Khandpur, 2019), but it is also used to assess body composition, including fat mass, lean tissue mass, and bone mass (Fuller et al., 1992).

In the specific protocol parameters used in this study, although the mice did not gain significant weight compared to mice on control diet, the mice on a HFD for 3 months gained significant weight from the beginning to the end of the experiment (both Sedentary and Runners), which was not observed in the Control group. This indicates that although the mice on the HFD did not gain more weight than the Controls, the HFD did have an impact on their body weight. While obesity can be detected by an increase in body weight, it can also be demonstrated by an increase in body fat content, which was not investigated here (Buckinx et al., 2021). Furthermore, we did not assess other metrics such as plasma free fatty acid (FFA) or insulin levels, which could have provided insight into the development of the metabolic syndrome. Importantly, despite the absence of a significant difference in body weight, there were still observable differences in cell quantifications within the MBH.

5.3.2. Short-term Running increased proliferation and the generation of proliferating DCX-positive cells in the SGZ of the hippocampus, independently of diet

Previous research has demonstrated that exercise can enhance adult hippocampal neurogenesis (Praag et al., 1999; Praag et al., 2005; Kronenberg et al., 2006). The results of this study confirmed the established finding that running enhances adult neurogenesis in the hippocampal SGZ. Specifically, an increase in proliferating cells in the SGZ was observed after two weeks of running in the Control diet group. Overall, HFD had a main detrimental effects on cell proliferation and neurogenesis shown by two-way ANOVA. However, Running overrides these detrimental effects of HFD on cell proliferation, which aligns with previous literature (Han et al., 2019; Kim et al., 2016; Klein et al., 2016). Although HFD did not independently reduce proliferation in Sedentary animals, the HFD appears to limit the full neurogenic benefits of exercise after two weeks of administration. The neuroblast data suggests that while exercise promotes neurogenesis regardless of diet, HFD may still limit the overall neurogenic response, indicating that there are changes in the SGZ environment that are detrimental to the neurogenic

process. Most importantly, the successful demonstration of increased cell proliferation in the hippocampus of mice on the Control diet following running provided a reliable positive control for the hypothalamic experiments. This validated the experimental protocols and equipment used, instilling confidence to proceed with the investigation of the hypothalamus.

5.3.3. Short-term HFD reduced cell proliferation in the HVZ, which was not reversed by Running

In contrast to the well-documented increase in cell proliferation in the SGZ induced by short-term Running (Praag et al., 1999; Praag et al., 2005; Praag et al., 1999), two weeks of voluntary Running did not significantly affect cell proliferation in the hypothalamus under Control conditions. This difference may be attributed to the distinct neurogenic niches responding on varied timescales, suggesting the hypothalamus is less responsive to short-term Running compared to the hippocampus. Indeed, previous research by our lab has shown that the hypothalamic neural stem cells have a significantly longer cell cycle than the adult neural stem cells from the SGZ, as observed through *in vitro* time-lapse imaging under proliferating conditions (Jorgensen et al., 2024). In contrast to the results from these experiments, Borg et al. (2014) showed that hypothalamic cell proliferation substantially increased after exercise training, however this study used forced running, thus the data cannot be directly compared to the results here, due to the stress induced response by forced running (Leasure & Jones, 2008). Short-term Running may act primarily through activating existing hypothalamic neurons rather than inducing neurogenesis, particularly under control dietary conditions. This neuronal activation could modulate food intake and appetite regulation without necessitating the generation of new neurons to alter behaviour. Indeed, emerging evidence from studies in mice has revealed that Running possesses a potent ability to modulate the activity of hypothalamic neurons in the ArcN, which are involved in appetite regulation (He et al., 2018; Lieu et al., 2020; Landry et al., 2022; Miletta et al., 2020). Such activation could be determined by immunohistochemical staining for c-fos (an immediate early gene) to determine the changes in neuronal activity after exercise (Landry et al., 2022). The lack of short-term voluntary exercise studies on cell proliferation and neurogenesis in the hypothalamus indicates that further investigation is needed to determine the precise parameters of exercise-induced changes in the hypothalamic neurogenic niche under control dietary conditions. To ascertain the peak of cell proliferation and neurogenesis and how they develop over time, it would be advisable to quantify adult-generated cells at more frequent timepoints.

In contrast, HFD had an overall detrimental effect on cell proliferation in the HVZ after two weeks. This data suggests reduced proliferation of htNSCs *in vivo* by HFD, which was not reversed by short-term Running. This contrasts with the effects of Running observed in the SGZ that has been shown to reverse the effects of HFD, as reported in previous studies (Klein et al., 2016; Han et al., 2019). The observed reduction in htNSCs proliferation could be either due to an increased quiescence of the stem cells to protect them from exhaustion under detrimental conditions, or due to increased apoptosis due to the HFD. To better understand the results, *in vitro* time-lapse imaging analysis of primary htNSCs from Runners was performed. The data revealed that diet had no impact on stem cell activation or quiescence. This would suggest that the decrease in htNSCs was caused by increased apoptosis. However, subsequent analysis of apoptotic cell numbers *in vitr*o found no differences between the HFD and Control diet groups. With this in mind, the data suggests that short HFD depletes the htNSCs, which is also supported by an increase in proliferating cells and neurons, suggesting terminal differentiation (Figure 5.6.2).

Alternatively, the effects observed on the stem cells *in vivo* cannot be fully recapitulated *in vitro.* Previous studies have described an inflammatory response to the HFD, which in turn affects htNSCs, leading to increased apoptosis, and reduced proliferation (Thaler et al., 2012; Li et al., 2012). The impact of inflammation may not be carried over *in vitro* where the environment is less hostile and thus negates the elevated apoptosis observed *in vivo*, which in turn could explain the lack of an effect. The lack of analysis of apoptotic markers *in vivo* means the data remains inconclusive (Li et al., 2012). Alternatively, as shown by (Robins et al., 2013), α-tanycytes display self-renewal potential and have the capacity to generate neurospheres *in vitro* while β-tanycytes have a poor ability to produce neurospheres (Yoo & Blackshaw, 2018). While the effect of HFD on the overall tanycyte population was investigated *in vivo* using Ki67 staining, it is possible that HFD may differentially impact certain tanycyte subpopulations. Indeed, previous research by our lab and others has shown that HFD significantly reduced all Rax labelled tanycyte populations (Jorgensen et al., 2024) (Goodman & Hajihosseini, 2015), however, the same study also described a HFD-induced reduction of β-tanycytes proliferation after 7 days, and a reduction in GFAP+Rax+ β-tanycytes after 21 days of HFD, while the α-tanycytes were not affected in the same time frame (Appendix Figure 2; Jorgensen et al., 2024). This may suggest that the reduction *in vivo* is confined to β-tanycytes and was therefore not observed *in vitro*.

5.3.4. Short-term HFD increased proliferation and proliferating DCX+ cells in the ME, which was reversed by Running

There is ongoing debate in the field about whether hypothalamic adult neurogenesis protects against or exacerbates the detrimental effects of HFD (Li et al., 2012; McNay et al., 2012; Lee et al., 2014; Gouazé et al., 2013). The results here show that two weeks of HFD treatment increased cell proliferation (Ki67+, BrdU+) and proliferation of adult born immature neurons (BrdU+DCX+) in the ME of Sedentary mice, which was reduced by Running. An unexpected yet interesting finding that suggests that Running had a counteractive effect on cell proliferation and neurogenesis in the ME, reducing proliferation to levels observed in Control mice. The ME, located partially outside the BBB, is the first nucleus to respond to increased caloric intake, as shown in female mice by previous studies (Lee et al., 2014; Lee et al., 2012). Indeed, the increase in proliferating cells and neurons in the ME may represent a response to counter HFD-induced hypothalamic injury (Lee et al., 2014; Thaler et al., 2012). The increased neurogenesis may serve to replace damaged neurons in this region. These findings suggest that Running counteracted the need for increased neurogenesis in the ME induced by HFD. Running may have improved the survival of existing neurons, reduced the proliferation and activation of htNSCs, and/or ameliorated the inflammatory environment within the hypothalamus.

Another possibility for the reduction in the number of htNSCs by HFD (described in 5.3.3.) in the HVZ *in vivo* is increased terminal differentiation, leading to depletion of htNSCs and elevated proliferation of progenitor cells and neurons in the ME. The β-tanycytes that reside in the ME, also termed the "proliferative zone", are thought to be more lineage-restricted neurogenic cells with limited proliferative potential (Yoo & Blackshaw, 2018; Robins et al., 2013). Therefore, the increased proliferation observed in the ME may be driven by increased differentiation of the β-tanycytes, potentially explaining the reduction in htNSC numbers in the HVZ. However, even though Running reduced the HFD induced increase of BrdU+ and BrdU+DCX+ cells in the ME, no increase in proliferating htNSCs in the 3V after Running was observed after two weeks. This raises the possibility that Running has no direct impact on the stem cells in the hypothalamus, but may rather affect progenitor cells and neurons while also involve indirect benefits through improved metabolic health. The reduction of proliferating cells and neurons by Running may instead be attributed to an increased quiescence of the progenitor cells that does not need to differentiate to replace lost neurons. Indeed, Yulyaningsih et al. (2017) showed that AgRP expressing neurons in the ME were able to regenerate after excitotoxic destruction, but did not incorporate BrdU. This led the researchers to conclude that

these newly generated neurons were not derived from β-tanycytes, but rather from dedicated quiescent neural precursors that had arisen through direct transdifferentiation of tanycytes (Yulyaningsih et al., 2017; Yoo & Blackshaw, 2018). Suggesting the presence of quiescent progenitor cells in this nuclei. This increases the level of complexity in understanding the responses of this neurogenic niche. The data suggests that external stimuli, such as diet and exercise, may have differential effects on distinct cell populations within the hypothalamus, making the results more difficult to interpret due to the incomplete understanding of the cell stages involved in hypothalamic adult neurogenesis. To best assess this, future research should employ single-cell RNA sequencing to characterize the distinct cell types of tdTomato+ cells after HFD and Running in the hypothalamus. This would help determine which cell populations are more affected by diet and exercise. Additionally, extensive fate-mapping experiments using multiple time points and preferably a Brainbow or confetti reporter line could label neural stem cells and their progeny at different stages of differentiation. This would allow researchers to track the response of these cell populations to dietary and exercise interventions over time.

5.3.5. Neither HFD nor exercise altered density of new anorexigenic neurons in the MBH after two weeks

To expand on the above findings, analysis was done on the number and proportion of newly generated POMC neurons (BrdU+POMC+) generated over the two week period. The data showed no significant effect of either diet or exercise on the density of newborn POMC neurons in the MBH over the two week duration. This suggests that while there are diet and exercise related changes in cell proliferation and neurogenesis in the ME and HVZ, these do not necessarily translate to changes in specific neuronal subtypes such as POMC neurons after two weeks. This suggests that the DCX+ cells generated after two weeks of a HFD exposure are not preferentially neurons that will suppress appetite. Similarly, the decrease in DCX+ cells observed with Running does not preferentially affect the fate of these neurons. In other words, while a HFD increases the number of DCX+ cells, it does not specifically determine what they become. This has been shown by previous studies that reported only a small portion of newly generated neurons differentiate into either subpopulations that play roles in our energy homeostasis (Li et al., 2012; Gouazé et al., 2013). Notably, recent studies have shown that exercise instead can modulate the activity of POMC and NPY neurons in the ArcN. High-intensity interval exercise has been found to activate POMC-expressing neurons in this region, while concurrently inhibiting NPY/AgRP neurons (He et al., 2018). A similar inhibitory effect on NPY/AgRP neurons in the ArcN has also been observed following voluntary exercise in

mice by Miletta et al. (2020) and Hwang et al. (2023). Furthermore, the activity of both POMC and NPY/AgRP neurons in the ArcN during exercise appears to be influenced by nutrient availability and exercise intensity (Hwang et al., 2023). This suggests that while two weeks of Running does not alter the number of newly generated POMC neurons, it may still modulate the functional activity of these neurons leading to physiological changes in appetite and energy homeostasis. Future research could investigate this further by analysing the expression of immediate early genes, such as c-fos, in the BrdU+DCX+ cells located in the MBH.

5.3.6. Long-term Running did not promote accumulation of new mature hypothalamic neurons in Control conditions

To investigate the long-term effects of external stimuli, a 3 month Running protocol was employed. Surprisingly, prolonged Running did not increase accumulative neurogenesis of lineage traced mature neurons in the hypothalamus compared to Sedentary controls. In line with these observations, prior research (Klein et al., 2019) has documented a habituation response to prolonged exercise in mice consuming a “normal” diet. This aligns with findings in the hippocampus demonstrating that exercise-induced cell proliferation peaks after 3-10 days and returns to baseline levels by 32 days of exercise (Kronenberg et al., 2006). A possible explanation is that the hypothalamus has a limited capacity for net neuron addition, alternatively the neurogenic response to exercise in the hypothalamus is restricted to either proportions or activation of subpopulations of neurons, such as orexigenic or anorexigenic populations as described by others (Hwang et al., 2023), without changing the total neuronal population (Klein et al., 2019). In concurrence, previous research (McNay et al., 2012) has demonstrated that the most substantial neuronal turnover within the MBH occurs during the initial 8 weeks of the mouse lifespan. As the mice in the present study were 5-6 months old when culled, they had surpassed the major turnover period, thus suggesting a more limited capacity for hypothalamic neurogenesis in this older cohort. It cannot be excluded that exercise may affect other tanycyte-derived neuronal populations that were not included in the lineage tracing. This is supported by an observed increase in BrdU+ neurons in the MBH that were not generated by tamoxifen-induced htNSCs.

5.3.7. Long-term HFD reduced accumulation of new neurons, which was not reversed by Running

Long-term exposure to a HFD significantly reduced the accumulation of new mature neurons, as evidenced by a decrease in lineage traced mature neurons. Notably, this detrimental effect was not ameliorated by Running. In fact, the HFD seemed to be detrimental to the survival of these cells, regardless of whether the animals were Sedentary or Running. In contrast to the reduction of mature lineage-traced neurons (NeuN+), the density of lineage-traced immature neurons (DCX+) remained unchanged. This suggests that the HFD reduced the survival of lineage traced mature neurons, rather than affecting their generation from the stem cells. In addition, no change in Ki67+ cells was observed in the 3V between Control and HFD Sedentary mice (Data not shown). The detrimental effects observed here, are consistent with previous literature, which has observed a reduction in neurogenesis in the hypothalamus following exposure to long-term HFD (Li et al., 2012; McNay et al., 2012; Jorgensen et al., 2024). To further confirm this data it would be advisable to stain for apoptotic markers such as AC3. The detrimental effects observed are confined to neurons derived from GLAST- labelled stem cells, it can therefore not be excluded that the HFD had no influence on the entire hypothalamic neuronal population but rather affects distinct neuronal populations as also observed by Li et al. (2012).

Although voluntary exercise have previously been shown to restore POMC-expressing neurons in the hypothalamus of obese mice (Laing et al., 2016), suggesting neuroprotective effects, Running failed to reverse the neuronal loss in this study. This may be due to the very long duration of the HFD leading to severe hypothalamic dysfunction that cannot be counteracted by the timeframe of the Running protocol employed. Previous literature suggests that diet-induced hypothalamic dysfunction can be reversed through early interventions to mitigate obesity, these interventions also include caloric restriction, substituting saturated fats with unsaturated fats, or simply replacing a HFD with a regular chow diet (Ignacio-Souza et al., 2014; Tu et al., 2019; Engel & Velloso, 2022). The exact timing of interventions that could facilitate full recovery of hypothalamic function may depend on genetic and environmental factors, particularly dietary composition. However, passing the point-of-no-return may lead to permanent damage of the neural circuits, potentially explaining the refractory nature of prolonged obesity (Engel & Velloso, 2022). This suggests that while exercise is beneficial, it may not completely overcome the adverse effects of HFD in the hypothalamus long-term. The beneficial effects of exercise on neurogenesis may diminish over time, similar to the transient

increase in cell proliferation observed in the hippocampus following exercise as reported in previous studies (Kronenberg et al., 2006). This might be specifically relevant in the context of HFD, as acute neurogenesis appears to still occur under control dietary conditions.

5.3.8. Long-term Running increased cell proliferation and new mature neurons (BrdU+) generated in the last two weeks of the protocol

BrdU was administered to the mice during the final two weeks of the long-term Running protocol, enabling a comparison between the results from the short-term protocol and the effects on the neuronal population after prolonged exposure to the respective treatments. The results showed that long-term Running significantly increased the density of BrdU+ cells and BrdU+NeuN+ neurons generated within the MBH and across all hypothalamic nuclei over the final two weeks under Control dietary conditions. This suggests that prolonged exercise enhanced neurogenesis in mice on a Control diet, in contrast to the shorter protocol where running had no effect. However, the origin of these BrdU-labelled neurons cannot be attributed to GLAST-expressing htNSCs as they did not co-express tdTomato.

The use of GLAST for lineage tracing has some limitations, as it does not label all tanycyte populations within the hypothalamus, and because it also labels a subpopulation of mature parenchymal astrocytes. GLAST has been reported to label α-tanycytes of the HVZ, but not β-tanycytes (Robins et al., 2013). According to (Robins et al., 2013), α-tanycytes are the reserve neural stem cells of the hypothalamus, while β-tanycytes are the active progenitors/neural stem cells. This was demonstrated by their finding that GLAST+ LacZ reporter positive and GLAST+ GFP-expressing α-tanycytes eventually give rise to LacZ and GFP-expressing β1-tanycytes over time. Our experiments found GLAST-expressing tanycytes in the more ventral parts of the third ventricle, where β-tanycytes reside. Following the reasoning by Robins et al. (2013), this suggests that the more ventral GLAST-positive tanycytes originated from α-tanycytes. The results of Robins et al. (2013) indicates that a 3 month period allows for renewal of β-tanycytes, as the greatest number of labelled tanycytes were observed in β-tanycyte regions after 6 weeks. Therefore, the 3 month period in our investigation was sufficient to observe GLAST-labelled β-tanycytes.

According to the study by Robins et al. (2013), LacZ labelled tanycytes were consistently observed in the infundibular recess, an area known to contain β1-tanycytes. Notably, no labelled tanycytes were detected in the most medial parts of the ME (Robins et al., 2013). This suggests that the BrdU-labelled neurons in the ME that did not express the tdTomato lineage

marker in the current investigation may have originated from the GLAST-negative β2-tanycyte populations located in the more medial regions of the ME (Robins et al., 2013; Lee et al., 2012). In accordance with this, while β-tanycytes are known to generate neurons populating the ME and MBH, α-tanycytes primarily give rise to parenchymal astrocytes, along with a minor population of neurons and β-tanycytes, further suggesting that the β-tanycytes are the source of the proliferating neurons in the ME of our study (Lee et al., 2012; Robins et al., 2013).

Furthermore, the GLAST-negative neurons may originate from Fgf10-positive β-tanycytes located in the ME-ventromedial ArcN of the hypothalamus. These tanycytes co-express markers such as Nestin, SOX2, BLBP, and MSI1, but do not express GFAP or GLAST (Prevot et al., 2018). These FGF10+ β-tanycytes have the ability to generate neurons that migrate and populate the ArcN and VMN, although they do not give rise to GFAP-positive neural progenitor cells (Makrygianni & Chrousos, 2023). The ME is a CVO characterised by tanycytes that line the fenestrated capillaries within it (Makrygianni & Chrousos, 2023). These tanycytes act as gatekeepers, regulating the passage of molecules from the bloodstream into the hypothalamus (Makrygianni & Chrousos, 2023). Unlike other hypothalamic regions, the ME lies outside the BBB and is therefore directly exposed to changes in the periphery, which can elicit cellular responses in the hypothalamus, particularly in the β-tanycytes that are localised to the ME (Thaler et al., 2012; Lee et al., 2014). It is therefore possible that the β-tanycytes are more responsive to Running. This is in agreement with the study by Robins et al. (2013) that also found that β2-tanycytes are neither FGF-responsive nor neurospherogenic, in contrast to α-tanycytes. This suggested that tanycyte subsets have distinct functional roles as aNSCs, with α- and β-tanycytes responding differently to various stimuli (Robins et al., 2013). It is therefore plausible that different tanycyte subpopulations may respond distinctively to the stimulus of exercise. Previous research has shown that tanycyte subpopulations exhibit different functions, and this functional distinction between α- and β-tanycytes may explain their differing effects on body weight in response to HFD (Robins et al., 2013; Li et al., 2012; Bolborea & Dale, 2013; Lee et al., 2012).

Furthermore, a study (Campbell et al., 2017) found at least six distinct neuron types in the ArcN-ME, highlighting the need for further investigation to determine the origin of the neurons that appear to respond to long-term exercise. The tanycyte population displays distinct marker expression profiles - α-tanycytes express markers such as Nestin, GLAST, and GFAP, while β-tanycytes express Nestin and Fgf10, though there is some overlap between the populations (Yoo & Blackshaw, 2018). Consequently, lineage tracing using conditional Fgf10 expression

could elucidate whether the β-tanycyte population is more responsive to Running compared to α-tanycytes, and potentially reveal the origin of the BrdU-labelled neurons that lacked the tdTomato lineage marker. A previous study (Lee et al., 2012) using Nestin-CreER^{T2} mice found that lineage traced β2-tanycytes were primarily located in the ME, with some contribution to parenchymal nuclei (DMN, VMN, Arc, and LHN). Importantly, they discovered that the lineage traced ME cells differentiated into neurons of multiple subtypes, including GABAergic, POMC- and NPY-expressing cells, but not glial cells (Lee et al., 2012). Indicating that inducible Nestin-CreER^{T2} mouse lines may additionally be helpful in this investigation.

5.3.9. Long-term HFD reduced the density of new mature neurons and cells (BrdU+) in the MBH in the last two weeks, which cannot be reversed by Running

In contrast to the short-term HFD protocol, the long-term HFD had differential effects on newborn cells and neurons, depending on cell subtype and specific hypothalamic nuclei. There was an overall detrimental effect of HFD on the density of BrdU+NeuN+ neurons and BrdU+ cells that did not originate from GLAST+ stem cells, and this effect was not reversed by Running. As discussed previously, these BrdU-labelled cells and neurons may originate from β-tanycytes that do not express GLAST (Lee et al., 2012: Robins et al., 2013). Furthermore, HFD reduced the proliferation of lineage traced, adult generated neurons in the ArcN, which aligns with previous literature (McNay et al., 2012), and this effect was not either reversed by Running. In contrast, HFD increased the proliferation of lineage traced BrdU+ cells in the ME, as also demonstrated in shorter HFD protocols (Lee et al., 2014), but this increase was reduced by Running.

As discussed for the short-term HFD protocol, the increased proliferation of cells observed in the long-term HFD protocol in the ME may reflect a protective response to HFD-induced hypothalamic injury (Lee et al., 2014). Interestingly, while lineage traced BrdU-labelled cells were increased in the ME, there was no corresponding rise in lineage traced BrdU+DCX+ neurons. This suggests that these additional cells are likely newborn astrocytes, as α-tanycytes are known to primarily give rise to parenchymal astrocytes (Robins et al., 2013), potentially as part of an inflammatory injury response to the HFD.

Furthermore, the reduced number of newborn, lineage traced immature neurons in the ArcN indicates that the detrimental environment caused by long-term HFD may diminish the survival of these newly generated neurons, consequently reducing lineage traced mature neurons in the MBH. Notably, the overall population of lineage traced immature neurons remained

unchanged, this suggests that long-term HFD enhanced the retention of older neurons, as previously shown (Klein et al., 2019). The work by Klein et al. (2019) indicated that HFD simultaneously increased the survival of existing neurons while reducing the generation of new ones. Which could indicate a compensatory mechanism maintain some degree of hypothalamic function in the face of reduced neurogenesis.

In summary, under the given experimental paradigms, short-term Running decreased the elevated adult neurogenesis in the hypothalamus that had been induced by HFD, whereas prolonged exercise increased hypothalamic adult neurogenesis but did not reverse any detrimental effects of long-term HFD.

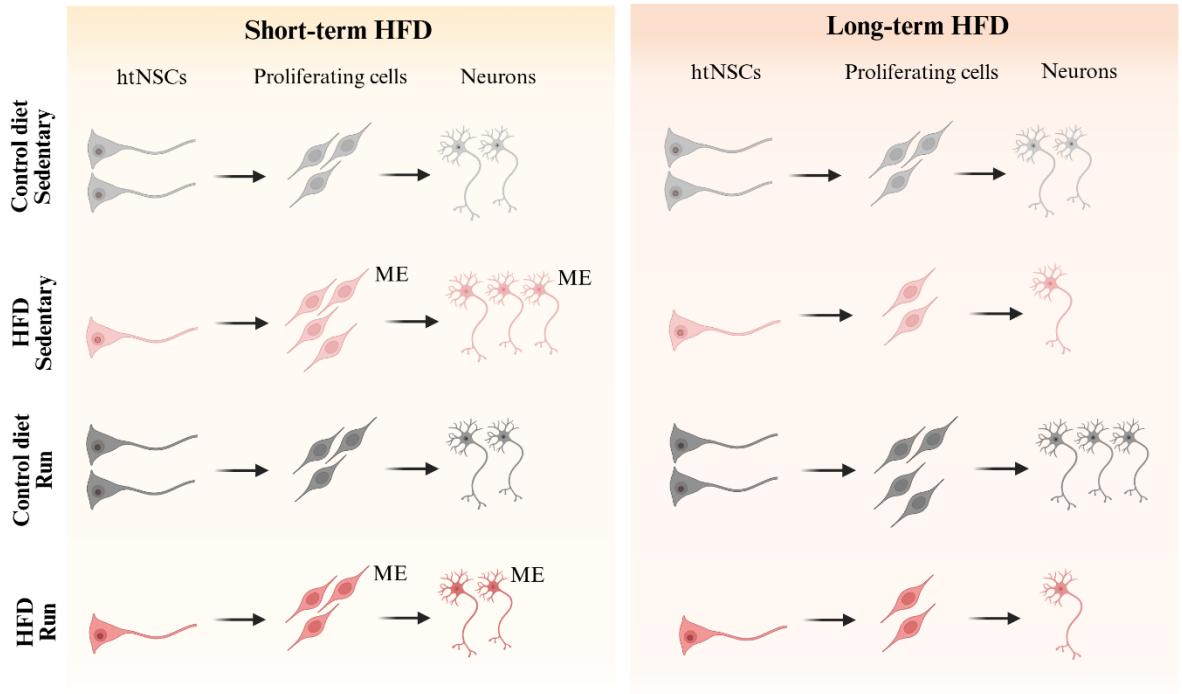

Figure 5.14. Graphical summary of the results in Chapter 5. The results revealed region-specific effects on adult hypothalamic neurogenesis. (Left) Short-term Running reduced and thereby reversed increased hypothalamic adult neurogenesis that had been elevated by HFD. (Right) Long-term Running instead increased adult neurogenesis but failed to protect against the detrimental effects of long-term HFD.

Chapter 6: General Discussion

The widespread consumption of high fat diets has contributed to the obesity crisis. Investigating how targeted interventions can influence the neurobiological mechanisms underlying obesity is crucial for developing future treatments. The hypothalamus contains neural stem and progenitor cells that generate new neurons throughout adulthood (Mackay & Abizaid, 2014; Bouret, 2009; Rojczyk et al., 2014). This neurogenesis is influenced by external factors like diet and exercise, which can enhance the proliferation and differentiation of these neural precursor cells into functional neurons regulating appetite and energy homeostasis (Lee et al., 2002; Rojczyk et al., 2014). Consequently, understanding the complex interactions between HFD, exercise, and pharmacological agents may reveal potential therapeutic avenues for modulating hypothalamic neurogenesis and addressing obesity-related metabolic dysfunctions in adults (Rojczyk et al., 2014). This study aimed to investigate the effects of HFD, exercise, and pharmacological interventions on adult neurogenesis within the hypothalamus. With the overall goal to enhance understanding of the aetiology of obesity and inform the future development of therapeutic pharmacotherapies and exercise regimens.

6.1. Effects of a high fat diet on body weight

Although changes in the neural circuitry of mice fed HFD could be observed, no significant increase in body weight compared to controls in the short-term HFD protocols was observed. With no access to metabolic cages, it is impossible to determine if this is due to a decrease in food intake or rather an increase in percentage body fat compared to controls. However, this phenomenon has been reported before by Gouazé et al. (2013) who observed changes in newborn cells and neurons in the hypothalamic nuclei but did not observe any significant body weight increase after 3 weeks HFD feeding unless co administration of AraC. They reported a decrease in food intake in HFD fed mice during the first week of HFD feeding which was continued throughout week 2-3 (Gouazé et al., 2013), which may also explain the results reported here. In the short and intermediate protocols, we therefore investigate the impact of acute effects of HFD, which has been shown to increase reactive gliosis and inflammation in mice but not obesity (Thaler et al., 2012; Sugiyama et al., 2020).

In the long-term HFD protocols, the Sedentary mice fed HFD for 3 months were single housed with a partial divider and had a fixed running wheel, did not significantly gain weight compared to controls. While the Sedentary group housed mice from the LiPrRP experiments gained

significant body weight after 4 months. A puzzling result which may be due to technical differences between our lab and the Maletínská lab where the 4 month group were treated. While one study by (Buckinx et al., 2021) suggests that single housing with a partial divider should not induce a significant stress response, single housing have been shown to induce considerable stress effects in other studies (Muta et al., 2023; Ieraci et al., 2016). For instance, studies have demonstrated that social isolation stress can induce anxious- and depressive-like behaviours in adult male mice, which correlate with decreased expression of genes related to neuroplasticity in the hippocampus and prefrontal cortex (Ieraci et al., 2016). Conversely, another study (Legendre & Harris, 2006) reported that rats fed HFD and subjected to mild stress did not continue to gain weight (Legendre & Harris, 2006). This suggests that the differences in housing conditions may have influenced weight gain patterns between the 3 month (Figure 5.8) and 4-month protocols (Appendix Figure 1). However, the mice on a HFD for 3 months still gained significant weight from the beginning to the end of the experiment, which was not observed in the Control group. Suggesting that the HFD did have some impact. While obesity is often characterised by an increase in body weight, it can also be manifested through a rise in body fat percentage, an aspect that was not explored in this study (Buckinx et al., 2021).

6.2. Effects of HFD on adult hypothalamic neurogenesis

While the rate of adult neurogenesis in the hypothalamus is low, the addition of new neurons allows the brain to adapt its circuitry in response to environmental challenges (Ortega-Pérez et al., 2007). The results outlined in Chapter 3 and 4 showed that under the specific protocol parameters used, two weeks of HFD increases density of adult born (BrdU+) immature neurons in the ME, at 3 weeks HFD increased adult born mature neurons in the ArcN, and after 4 months HFD had detrimental effects, reducing adult born mature neurons significantly in the entire MBH. Suggesting a transient effect of HFD over time and nucleus specific responses to external stimuli. Where an initial response to the change in caloric intake increases neuronal output in the ME where the most active stem cells and predominantly neurogenic, β-tanycytes reside (Lee et al., 2012). Suggesting that this nucleus is the first to respond to the change in caloric intake, also shown by Lee et al. (2014) and Lee et al. (2012) in female mice. Potentially as a protective response to try to gain control of the energy circuitry and counterbalance the HFD. Indeed, Thaler et al. (2012) have shown that acute HFD lead to transient inflammation and hypothalamic injury. The ME in contrast to other hypothalamic regions, lies outside of the BBB, and is thus directly exposed to circulating toxins and nutrients that can lead to cellular

injury when in oversupply. In addition, Thaler et al. (2012) showed that the inflammatory responses were temporarily subsided after the initial increase, suggesting that neuroprotective mechanisms may initially limit the damage. Hence, the increased neurogenesis in the adult ME may serve to increase anorexigenic subtypes of neurons to reduce food intake (Gouazé et al., 2013) or replace damaged neurons in this region after inflammatory injury (Thaler et al., 2012). Over time these signals lead to an increase in newborn neurons in the ArcN, one of the most critical energy balance sensor among all hypothalamic nuclei (Klein et al., 2019). Because the ArcN have a more limited access to circulating satiety signals and metabolites compared to the ME, it may take longer for this nucleus to respond to the acute effects of HFD (Lee et al., 2014). Another possibility is that the immature neurons generated around the ME as a protective response to HFD migrates to mature in the ArcN to be integrated into the neural network. These neurons would potentially stem from ME-ventromedial ArcN FGF10+ β tanycytes that co-express Nestin, SOX2, Brain lipid binding protein (BLBP) and MSI1 but do not express GFAP or GLAST (Prevot et al., 2018). These tanycytes have the capacity to generate neurons that migrate to populate the ArcN and VMN, but they do not give rise to GFAP+ NPCs (Makrygianni & Chrousos, 2023). In agreement, no increase in newborn GFAP+ cells were observed. In addition, Haan et al. (2013) used a Fgf10-CreER knock-in mice to show that β-tanycytes of adult mice generated a progressive accumulation of tanycyte-derived neurons in the VMH and ArcN over time (Haan et al., 2013; Yoo & Blackshaw, 2018), indicating that β-tanycytes indeed produce neurons that integrate into the ArcN over time. Also, in agreement with Gouazé et al. (2013), who found an increase in anorexigenic POMC expressing neurons in the ArcN in response to 3 weeks HFD feeding. However, an increase in POMC expressing neurons was not confirmed in this study. Suggesting that the increased neuronal proliferation in the ME after short HFD in this study serve to replace damaged neurons.

Prolonged exposure to HFD resulted in a decline in newly generated neurons, suggesting that the rate of neuron replacement observed with short-term HFD exposure may not be sustainable over longer durations. Which is in agreement with previous literature (Li et al., 2012; McNay et al., 2012). Further suggesting that although the initial response to short HFD is protective by replacing damaged neurons, it exhausts the stem cell pool leaving the hypothalamus unable to respond to chronic injury. In agreement with the observed reduction of Ki67+ cells in the 3V in this study after short HFD. The observed reduction in newborn mature neurons in the MBH after 4 months of DIO leaves the hypothalamus unable to respond to long HFD exposure and thereby loses control of the circuit leading to obesity, as shown by an increase in body weight

at 4 months. These results suggests that adult hypothalamic neurogenesis may represent a physiological response attempting to mitigate the detrimental effects of HFD but doing so exacerbates the negative effects of HFD contributing to the development of obesity, similar to the dual role of the immune response in neurodegenerative diseases (Mason & McGavern, 2022). Indeed, Previous studies have also reported bidirectional effects of HFD on adult neurogenesis in the hypothalamus, with both increases and decreases observed (McNay et al., 2012; Li et al., 2012; Lee et al., 2014; Gouazé et al., 2013; Kokoeva et al., 2005).

It is important to closely examine the increased hypothalamic neurogenesis observed following short-term exposure to a HFD. The nature of this response, whether aberrant, pathophysiological, or physiological, requires careful consideration. To determine the underlying significance, one must carefully analyse the contextual implications of this finding. The short-term effects of HFD on hypothalamic neurogenesis are complex and can be interpreted differently depending on the specific timeframe, hypothalamic region studied, and the overall metabolic state of the animal. While the data shown here and other studies show an initial increase in neurogenesis (Gouazé et al., 2013; Lee et al., 2014), it's not consistently viewed as purely physiological or pathophysiological. Instead, it could be considered a physiological response to a potentially pathophysiological insult with the potential to become maladaptive. As discussed, the initial increase in hypothalamic neurogenesis after short-term HFD might be an adaptive response aimed at maintaining energy balance (Gouazé et al., 2013; Recabal et al., 2017). Gouazé et al. (2013) describes a marked transient increase in hypothalamic cell proliferation as early as 2 days after starting HFD, potentially supporting such compensation. The HFD rapidly alters the hypothalamic environment, triggering inflammation and metabolic stress (Lee et al., 2014; Thaler et al., 2012). Therefore, even this initial increase in cell proliferation could already be an indicator of early dysfunction. The increased neurogenesis could be a response to these early changes, reflecting an attempt to repair or compensate for emerging damage. If the HFD persists, the initial increase in neurogenesis is typically followed by a decrease, as shown by us and others, likely due to sustained inflammation and other detrimental effects of the diet (Li et al., 2012; McNay et al., 2012). This decrease in neurogenesis, coupled with developing leptin resistance (Engel & Velloso, 2022), is clearly pathophysiological and contributes to the development of obesity. Therefore, the increased neurogenesis in response to short-term HFD is best described as a physiological response with the potential to become maladaptive. It's a dynamic process, and

whether it remains a compensatory mechanism or transitions into a contributor to pathology depends on the duration and intensity of the dietary insult, along with other individual factors.

The role of the newly generated hypothalamic neurons remains under investigation, and both their function and integration require further examination. The functional characteristics of neurons generated during adulthood likely vary in response to different dietary challenges, and these differences may be dependent on the specific neuronal subtypes that are differentially produced in response to sex-specific and diet-dependent signals. However, some previous studies have addressed the question, where Gouazé et al. (2013) found that short-term HFD increased hypothalamic cell proliferation and the number of newborn anorexigenic POMC neurons in the ArcN in male mice after 15d and 21d of HFD feeding. The authors suggest this may be a compensatory mechanism to regulate energy balance in response to increased caloric intake (Gouazé et al., 2013). This suggests that the increased cell proliferation in response to the HFD is a protective mechanism to limit weight gain (Gouazé et al., 2013). Although no such correlation was observed in our experiment, this may be due to technical differences or could have been revealed by conducting additional measures, such as body composition analysis as described in a previous study (Gouazé et al., 2013), where adiposity was assessed rather than relying solely on total body weight. In addition, the POMC staining in our experiment failed to replicate this result after 2 weeks HFD administration, potentially due to technical differences. Klein et al. (2019) additionally showed that 12 weeks of HFD administration increased the number of newborn neurons expressing POMC in the ArcN. The authors also suggested this might be a counter-regulatory mechanism to prevent excessive weight gain in response to HFD. However, they only analysed female mice. Kokoeva et al. (2005) and Pierce & Xu (2010) showed that newborn neurons in the hypothalamus are functional, as they express orexigenic peptides (AgRP, NPY), and anorexigenic peptide (POMC), and some of them have ability to respond to leptin administration shown by inducing strong phospho-signaling transducer and activator of transcription 3 (pSTAT3) immunoreactivity (Kokoeva et al., 2005; Pierce & Xu, 2010; Rojczyk et al., 2014). Furthermore, (Gouazé et al., 2013) has also shown that administering the anti-mitotic drug AraC, which inhibits global cell division, accelerated the development of obesity in mice consuming a HFD, but not in those on a standard diet (Gouazé et al., 2013). This suggests that the short HFD-induced increase in cell proliferation within the hypothalamus, also seen by our experiment, serves to regulate energy balance and mitigate weight gain when exposed to an obesogenic diet. It's important to note that the studies used global inhibition of cell proliferation

within the hypothalamus. Therefore, they don't necessarily pinpoint the specific role of newborn neurons, as other cell types like glia are also affected by AraC. Also, the long-term effects of blocking cell proliferation in the hypothalamus are complex and may involve multiple physiological systems. Another study (Lee et al., 2014) used focal X-ray irradiation targeted to the ME in mice. They found that this irradiation effectively suppressed cell proliferation in the ME by approximately 85 % while sparing the ArcN. The study concluded that reducing ME neurogenesis led to weight gain in females following irradiation and HFD, suggesting a potential protective role for ME neurogenesis against DIO (Lee et al., 2014). However, definitively demonstrating the functional role of newborn neurons in the hypothalamus remains elusive, despite many studies observing changes in neurogenesis. While previous studies have indicated that dietary factors, including HFD and diet-regulated hormones like leptin, can influence hypothalamic neurogenesis, the specific link between the observed phenotypes and the generated neuronal subtypes remains unclear. The proportion of newly born neurons expressing markers for neuronal subtypes involved in the regulation of feeding and body weight is relatively small, and does not always correlate with the observed behavioural outcomes (Yoo & Blackshaw, 2018). Determining the functional role and identity of adult-born neurons in the future requires a multi-faceted approach. Rigorous research employing a combination of methodologies, such as genetic fate mapping across multiple timepoints and under various dietary manipulations, including HFD, is necessary to elucidate the dynamic nature of neurogenesis and its response to dietary challenges. Integrating fate mapping with targeted ablation techniques and behavioural assessments would facilitate the investigation of the functional role of newly generated cells. Additional research employing a combination of lineage tracing and advanced techniques like single-cell RNA sequencing will be necessary to more thoroughly elucidate the identity of these newly generated neurons and uncover insights into their potential influence on feeding, metabolism, and body weight regulation. Furthermore, the selective manipulation of newborn neurons through optogenetics and chemogenetic in conjunction with behavioural assessments, could provide valuable insights to establish causal relationships. It is important to note that the effects of HFD on hypothalamic neurogenesis can vary depending on factors such as the duration of HFD exposure, the composition of HFD, the sex of the animals, and the specific hypothalamic region being studied (Lee et al., 2014; Recabal et al., 2017).

The observations of increased neurogenesis in the hypothalamus after short-term HFD feeding and decreased neurogenesis after long-term HFD feeding highlight the dynamic and complex

nature of this process. In comparison, HFD generally decreases neurogenesis in the SGZ. This is often attributed to increased inflammation and reduced levels of neurotrophic factors like BDNF (Lindqvist et al., 2006; Park et al., 2010). The hypothalamus and SGZ display contrasting temporal responses to a HFD. The hypothalamus initially exhibits an increase in cell proliferation (Gouazé et al., 2013; Lee et al., 2014), while the SGZ tends to experience a more immediate negative impact (Chiazza et al., 2021). However, both brain regions generally exhibit reduced neurogenesis with prolonged HFD exposure (McNay et al., 2012; Park et al., 2010). The impact of HFD on neurogenesis in the SVZ has been less extensively studied compared to the SGZ and hypothalamus. Nevertheless, some research has indicated a reduction in SVZ neurogenesis under HFD conditions (Li et al., 2012). Specifically, Li et al., (2012) have shown that cultured NSCs isolated from the SVZ and SGZ HFD-fed mice for 4 months exhibited impaired proliferation and neuronal differentiation, although the impairments were less severe in SVZ-derived NSCs compared to hypothalamic NSCs (Li et al., 2012). The reasons for the different initial responses likely relate to the distinct functions of these brain regions. The hypothalamus plays a central role in energy balance, and the initial increase in cell proliferation might represent an attempt to adapt to the sudden influx of dietary fat (Gouazé et al., 2013). The hippocampus, on the other hand, is more involved in learning and memory, and its neurogenic response to HFD might be more directly related to the metabolic stress and inflammation associated with the diet. It's important to consider the methodological differences between studies, including the animal model, diet composition, duration of feeding, and the specific brain regions analysed, when comparing results. Standardisation of experimental protocols and model systems is likely to substantially accelerate future progress in the field.

In a healthy, leptin-sensitive state, hypothalamic neurogenesis plays a role in maintaining energy balance (Recabal et al., 2017). Neurons in the hypothalamus, particularly in the ArcN, are responsive to leptin and other metabolic signals (Kokoeva et al., 2005; Rojczyk et al., 2014). These neurons can differentiate into various neuronal subtypes, including POMC and AgRP neurons, which play critical roles in regulating appetite and energy expenditure. Leptin, acting on these neurons, helps control food intake and maintain a stable body weight (Farr et al., 2015). HFD feeding disrupts this delicate balance. In a recent review (Engel & Velloso, 2022) nicely describe the early events of hypothalamic abnormality after diet induced obesity. Within just 1 day of HFD exposure, alterations are observed in the expression of genes and proteins related to proinflammatory cytokines, microglia, astrocytes, mitochondria, and autophagy, as well as hypothalamic neuropeptides. After 3 days on the HFD, structural abnormalities in

mitochondria and the endoplasmic reticulum are detected, accompanied by impaired leptin and insulin signaling in AgRP and POMC neurons, respectively, and increased microglial number and reactivity. Conversely, an increased number and activation of astrocytes are seen following 7 days of HFD introduction, coinciding with changes in BBB permeability. By 15 days on the HFD, an accumulation of perivascular macrophages and impaired leptin signalling in POMC neurons are observed. The evidence suggests that insulin signalling is impaired in POMC neurons, and leptin signalling is impaired in AgRP neurons, as early as day 3. At day 15, impaired leptin signalling in POMC neurons is observed (Engel & Velloso, 2022). At 2 weeks, we observed an increased density of adult-born neurons in the ME. This was followed by an increase in adult-born neurons in the ArcN at 21 days. However, by 4 months, we detected detrimental effects, with a significant reduction in adult-born mature neurons across the entire MBH. The impairment of leptin and insulin signalling in AgRP and POMC neurons by day 3 precedes the observed increase in neurogenesis at 2 weeks. The disruption of these key metabolic signals could be an early trigger for the neurogenic response. The hypothalamus may be attempting to compensate for the loss of proper leptin and insulin action by generating new neurons. By day 15, there is a continued impairment of leptin signalling, specifically in POMC neurons, along with the accumulation of perivascular macrophages. This suggests that the initial disruption of leptin signalling is not resolved, and an inflammatory response is developing. This sustained disruption and inflammation may contribute to the later decline in neurogenesis. The new neurons generated at 2 and 3 weeks might initially influence the activity of leptin- or insulin-responsive circuits (Rizzoti & Lovell-Badge, 2017). Perhaps the new neurons are intended to help restore proper signalling. However, if the underlying leptin/insulin resistance persists, the impact of these new neurons may be limited. Indeed, Lin et al., (2000) identified three phases in the development of obesity: an initial leptin-sensitive phase (7d), a reduced food intake phase with retained leptin sensitivity (8 weeks), and finally, an increased food intake phase with reduced leptin sensitivity (4 months). Considering the increase in newborn neurons it may serve to replace damaged neurons that can no longer respond to leptin and insulin. The decline in neurogenesis at 4 months occurs in the context of established leptin and insulin resistance. At this point, the hypothalamus may be overwhelmed by the chronic metabolic stress and inflammation, leading to a failure of neurogenesis. It is also possible that the prolonged disruption of leptin and insulin signalling has directly impaired the neurogenic process itself. (McNay et al., 2012) found that leptin deficiency, which is associated with obesity (Roh et al., 2016), also results in loss of hypothalamic stem cells and impaired neurogenesis (McNay et al., 2012). The discussed timeline suggests that leptin and insulin

resistance are early drivers of changes in neurogenesis. The initial increase in neurogenesis may be an attempt to compensate for impaired leptin and insulin signalling, but chronic resistance and inflammation ultimately lead to a decline in neurogenesis and a worsening of metabolic dysfunction. Future research should investigate the early time course of changes in leptin and insulin signalling during the initial stages of HFD exposure in this protocol. Specifically, it would be valuable to examine the temporal dynamics of leptin and insulin resistance in key hypothalamic neuronal populations, such as POMC and AgRP neurons, in the first few days to weeks after the introduction of the HFD. Understanding the precise timing and mechanisms by which leptin and insulin signalling become disrupted could provide important insights into the initial triggers that drive the subsequent neurogenic response and metabolic dysregulation.

Although progress have been made in identifying different tanycyte populations it is still unclear what the intermediate steps of neurogenesis are and how tanycytes repopulates neurons in specific nuclei in the hypothalamus (Goodman et al., 2020). Further investigation using inducible mouse lines such as the GLAST-CreER^{T2} mouse line or even better, a Rax-CreER^{T2} mouse line targeting hypothalamic NSCs, crossed to the 'Confetti' multicolour Cre reporter (Calzolari et al., 2015; Bast et al., 2018) or “Brainbow” (Weissman & Pan, 2015) would deepen our understanding of the intermediate steps in hypothalamic neurogenesis by allowing us to track the lineage and differentiation of neural stem cells and their progeny over time. Rax-CreER^{T2} is more specific to hypothalamic NSCs, providing a more precise labeling of these cells compared to GLAST-CreER^{T2}, which targets a broader population of glial cells, including some NSCs (Mori et al., 2006; Robins et al., 2013). For example, in a study by Calzolari et al., (2015) the researchers used the inducible Confetti mouse model to analyse the progeny of individual aNSCs in the adult subependymal zone of the mouse brain (Calzolari et al., 2015). By administering a low dose of tamoxifen, one could induce Cre activity in a small subset of NSCs (Calzolari et al., 2015). This will induce sparse labelling, which is essential for resolving individual clones and following their developmental trajectory without the confusion of overlapping cell populations. The Brainbow reporter systems express different fluorescent proteins in individual cells within a clone (Calzolari et al., 2015; Hampel et al., 2011; Richier & Salecker, 2014) This would allow to distinguish between the progeny of different NSCs and to follow their migration and differentiation into distinct neuronal subtypes. The tamoxifen-inducible nature of CreER^{T2} allows researchers to control the timing of recombination (Mori et al., 2006). This means one could label NSCs at a specific time point and then follow their

progeny over defined periods, providing a detailed temporal resolution of neurogenic events. By inducing recombination at different ages or timepoints, one could compare the fate of NSCs born at different times. The combination of lineage tracing and temporal control would enable future studies to identify the intermediate steps in hypothalamic neurogenesis. Specifically one could observe the transition of NSCs to progenitor cells, then to neuroblasts, and finally to mature neurons (Zhang et al., 2010). One could analyse the timing of these transitions and the factors influencing them. By observing the spatial distribution of labelled cells, one could gain insights into the interactions between newborn neurons and existing neuronal populations within the hypothalamus (Weissman & Pan, 2015). Using these tools, future research could investigate the effects of different factors, such as diet and exercise, on hypothalamic neurogenesis. As well as track how these interventions influence the proliferation, differentiation, and survival of NSCs and their progeny, ultimately leading to a deeper understanding of how these factors impact hypothalamic function and contribute to conditions like obesity.

The findings collectively suggest that a short-term increase in calorie-dense food consumption, such as during a holiday, can elicit a response from the hypothalamus, the centre of energy homeostasis, in an attempt to replace lost neurons due to hypothalamic injury induced by the HFD intake. However, these protective mechanisms can only withstand such changes for a limited time. Prolonged exposure to a high-calorie diet can have a detrimental impact on the neural circuits involved in energy homeostasis. If a high-calorie intake persists as part of one's daily lifestyle, the disruption of these circuits may contribute to the development of obesity.

6.3. Effects of physiological and pharmacological interventions on the hypothalamic neurogenic niche

Obesity is a chronic disease that is intricately intertwined with various other disorders, including T2DM, depression, and neurodegenerative conditions like AD (Pugazhenthi et al., 2018; Maletínská et al., 2019). The metabolic syndrome, also referred to as insulin resistance syndrome, was first characterised by Barker et al. (1993). Generally, metabolic syndrome encompasses common symptoms involving various vascular risk factors, including obesity, dyslipidaemia, insulin resistance, glucose intolerance, and arterial hypertension (Ricci et al., 2017). The co-occurrence of obesity and insulin resistance with metabolic syndrome also increases the likelihood of developing AD and other neurodegenerative disorders in the elderly (Razay et al., 2007; Raffaitin et al., 2009). Certain food intake-regulating peptides have been proposed as promising candidates for treating obesity and T2DM (Maletínská et al., 2015;

Klaauw, 2018) and may even help alleviate the cognitive deficits associated with neurodegenerative disorders (Giuliani et al., 2017; Hölscher, 2018; Mandal et al., 2018). Additionally, exercise is a cost-effective anti-obesity treatment that offers benefits beyond just weight loss and has been shown to reverse the detrimental effects of high fat diets on adult neurogenesis in the hippocampus (Han et al., 2019; Klein et al., 2016).

Our results showed that running reversed the increased neurogenesis in the ME after short-term HFD by reducing cell proliferation and the production of newborn cells, whereas LiPrRP had little influence on the neuronal populations in acute HFD. Given the neuroprotective nature of LiPrRP, it is not surprising that no neuroprotective effects were observed in the short and intermediate HFD protocols, as there was no reduction in newborn neurons, which would correlate with the onset of neurodegeneration. In agreement, a meta-analysis found a modest association between metabolic syndrome and cognitive decline, with a marginally significant relationship observed in the younger-old age group (Siervo et al., 2014), suggesting that age is an important factor in this correlation. In the 21d protocol, LiPrRP reduced the HFD-induced increase in new neurons in the ArcN, a response also observed with running, suggesting a common protective mechanism against the initial hypothalamic injury. Additionally, HFD + Running decreased overall cell proliferation in the MBH compared to Controls. Interestingly, a similar anti-proliferative effect on Ki67+ cells in the MBH at the 21d HFD time point was seen with both LiPrRP and LIRA. Although this contrasts with findings from other studies showing that GLP-1 agonists and exercise induce cell proliferation and neurogenesis in the hippocampus, this may not be surprising. Exercise and GLP-1 improve the responses to HFD, thereby promoting normal brain function. While the response in the hippocampus is reduced proliferation, the response in the hypothalamus appears to be an initial increase. Therefore, it is logical to assume that LiPrRP and exercise reduce proliferation to maintain normal brain function. This suggests that the effects of exercise and anti-obesity compounds are niche-dependent. In agreement, studies have reported that the GLP-1 agonist LIRA exhibits contrasting effects in different tissues. While it has been shown to promote cell proliferation in the hippocampus, LIRA has also demonstrated anti-proliferative and pro-apoptotic properties in human pancreatic cancer cells that are resistant to gemcitabine and other drugs (Zhao et al., 2020). Furthermore, LIRA has been found to reduce the abnormal proliferation of vascular smooth muscle cells induced by hyperglycaemia (Shi et al., 2015; Zhao et al., 2021), suggesting a regulatory role in controlling aberrant cell growth. The wide distribution of the GLP-1 receptor explains its diverse functions. The fact that the same agonist can elicit different cellular

responses depending on factors like cell specific signalling pathways and cellular context, reflects the complexity of biological systems and the challenges in developing new pharmacotherapies. Interestingly, the GLP-1 agonist LIRA reduces cancer progression and metastasis partly by inhibiting the NF-κB pathway (Zhao et al., 2020). NF-κB is a critical transcription factor that regulates various cellular processes, including inflammation, immunity, cell proliferation, and apoptosis, as well as hippocampal neurogenesis (Bortolotto et al., 2014). While NF-κB activation is important for adult neurogenesis in the hippocampus (Bortolotto et al., 2014), its activation has been associated with impaired aNSCs and the progression of obesity and pre-diabetes in the hypothalamus (Li et al., 2012). Importantly, NF-κB has also been identified as a key mediator of tumour growth and resistance to chemotherapy (Pramanik et al., 2018). This suggests a variety of context-specific roles, similar to those observed for LIRA, as well as for exercise and LiPrRP. The anti-proliferative effects observed with both exercise and anti-obesity compounds may therefore be mediated by their influence on the NF-κB pathways. Indeed, LiPrRP has been previously shown to influence the JNK signalling pathways, which can in turn affect the NF-κB pathways. Exercise induces the expression of interleukin-6 (IL-6) in skeletal muscle as well as in neurons located in the hypothalamus (Laing et al., 2016). The actions of IL-6 might mediate the suppression of IKK-β/NF-κB activation in the hypothalamus, thus helping to maintain normal function (Laing et al., 2016). This suggests a possible molecular mechanism by which exercise, and anti-obesity compounds achieve opposite functions on the hippocampus and the hypothalamus. While running shares some of the anti-proliferative effects of LiPrRP in acute HFD, it did not reduce stem cell proliferation or activation as analysed *in vitro*, which may be why it fails to rescue the DIO induced reduction of tanycyte derived neurons (shown as accumulative neurogenesis in Chapter 5) in contrast to LiPrRP. Indeed, this further suggests that exercise may predominantly have beneficial effects by reducing acute hypothalamic inflammation. One potential explanation is that while LiPrRP was shown to act cell intrinsically and directly on the cell populations in the hypothalamus and therefore may have long lasting effects, it's possible that the initial neuroprotective effects of exercise via inflammation amelioration are not sustained long-term in the face of continued DIO.

As demonstrated by this study and previous research (McNay et al., 2012; Li et al., 2012), DIO has detrimental effects on the hypothalamic neuronal population. Interestingly, LiPrRP administration was able to rescue the DIO induced reduction in newborn mature neurons in

older mice, while 12 weeks of running could not. This suggested differences in mechanisms between the anti-obesity compound and exercise in the context of HFD.

Recent studies have shown that the neuroprotective effects of LiPrRP extend to AD (Špolcová et al., 2015). In obese, pre-diabetic mice, treatment with palm1-PrRP improved insulin signalling and reduced tau phosphorylation in the hippocampus (Špolcová et al., 2015). Similarly, other anti-obesity compounds such as GLP-1 receptor agonists, including LIRA, which was also used in this study, have been shown to have neuroprotective effects in disease models of AD. Highlighting the interplay of obesity and neurodegeneration, but also confirming the neuroprotective qualities of LiPrRP in DIO induced neuronal decline demonstrated in our results. Indeed, in this study, the neuroprotective effects of LiPrRP were observed independently of diet in older mice. Exercise has also been shown to reverse negative impacts of HFD in the hippocampus, an important structure for learning and memory that is also affected in AD (Han et al., 2019; Klein et al., 2016; Rodríguez & Verkhratsky, 2011). While the results in this study were nuanced, the overall finding suggests that exercise cannot counteract the detrimental effects of prolonged HFD in the hypothalamus, a contrasting finding to that of LiPrRP. This further suggests that exercise may predominantly have beneficial effects by reducing acute hypothalamic inflammation.

The findings reported here share both similarities and differences with other studies describing the impacts of GLP-1 receptor agonists and exercise on adult neurogenesis in the hippocampus. Like LiPrRP, GLP-1 agonists can directly and indirectly influence neurogenesis and metabolic health. They can act on GLP-1 receptors found on neurons and neural stem cells in regions like the hippocampus, stimulating neurogenesis and enhancing neuronal survival (Parthsarathy & Hölscher, 2013). Similarly, our lab (Jorgensen et al., 2024) showed GPR10 expression in primary neurospheres and, for the first time, directly in adult generated neurons in the hypothalamus. Studies using techniques like in situ hybridization and RT-PCR have identified the presence of GPR10 expression in several hypothalamic regions (Dodd & Luckman, 2013; Pražienková et al., 2019). However, the specific cell types expressing GPR10 within the hypothalamic regions have not been clearly delineated in the existing literature. While our results indicate that GPR10 is expressed in newborn hypothalamic neurons, the precise neuronal subtypes expressing this receptor remain to be identified. Furthermore, GLP-1 agonists can indirectly promote neurogenesis by reducing inflammation and improving glucose metabolism and insulin sensitivity (Maletínská et al., 2019). Similarly, LiPrRP was found to lower insulin and leptin levels in the blood plasma of mice fed HFD for 4 months (Jorgensen

et al., 2024). Exercise, on the other hand, primarily boosts neurogenesis in the hippocampus by stimulating the release of neurotrophic factors, including BDNF, insulin-like growth factor 1 (IGF-1), and VEGF, thereby promoting neural plasticity and adult hippocampal neurogenesis, anti-inflammatory effects, and induction of angiogenesis (Liu et al., 2019). Interestingly, hypothalamic BDNF action has been linked to the regulation of energy homeostasis (Gray et al., 2006; Hwang et al., 2023). However, the precise mechanism by which exercise regulates BDNF expression in the brain is unclear. While exercise is generally beneficial after brain injury, improving BDNF levels and cognitive function, there can be instances where the effects of exercise are less effective. For example (Griesbach et al., 2004) suggests that exercise too soon after traumatic brain injury might disrupt the molecular response and delay recovery. Perhaps the lack of neuroprotection in the hypothalamus in this study can be attributed to the timing of the exercise regime as these neurotropic factors has also been associated with neuroplasticity of the hypothalamus (Kernie et al., 2000; Hwang et al., 2023). In agreement, HFD reduces BDNF levels due to increased inflammation which has been coupled with impaired hippocampal-dependent learning memory performances (Wallace et al., 2003; Park et al., 2010; Park et al., 2015; Sobesky et al., 2016). Furthermore, GLP-1 agonists increase neurogenesis though increased BDNF singling (Gümüşlü et al., 2016; Reich & Hölscher, 2022). Further suggesting an importance of restoring BDNF signalling to elicit neuroprotective effects. Unfortunately, increased stress levels due to social isolation may also indirectly alter BDNF expression. Both HFD (Lindqvist et al., 2006) and social isolation stress (Dong et al., 2008) increases corticosterone levels in the brain which in turn induce inflammation and consequently reduce BDNF signalling (Park et al., 2015; Sobesky et al., 2016; Ho-yin Lee & Yau, 2020). Due to the partial divider and social isolation, the exercise may only be able to reverse some of the effects of both HFD induced inflammation and high corticosterone expression that consequently reduce BDNF levels.

Indeed, the lack of significant weight change in the HFD fed mice suggests that the 3 month HFD model may represent a state of chronic inflammation rather than fully developed obesity. Future studies examining a similar experimental setup should further investigate the inflammatory state of the tissue. This could be achieved by measuring the mRNA levels of pro-inflammatory genes to quantify the inflammatory response at the transcriptional level (Thaler et al., 2012) or by staining for markers of microglial activation. Such an approach would provide a more comprehensive understanding of the inflammatory milieu within the tissue. This further implies that excessive inflammation could potentially hamper the neuroprotective

effectiveness of exercise in our study. In agreement, in neurodegenerative diseases like AD, chronic neuroinflammation is a significant contributor to disease progression (Nunomura et al., 2006). While exercise shows promise in these conditions, the effectiveness might be hampered by the already heightened inflammatory state, especially in later stages. A handful of studies, using AD models, show no effects of exercise on cognition (Xu et al., 2013). Svensson et al. (2020) reported running exercise may not only lack protective effects on the development of the AD phenotype in 5xFAD mice, which show an aggressive disease progression, but may also accelerate and aggravate it. Indeed, (Cerqueira et al., 2020) also showed that intense long exercise can lead, in general, to higher levels of inflammatory mediators, thus might increase the risk of injury and chronic inflammation. In contrast, moderate exercise or vigorous exercise with appropriate resting periods can achieve maximum benefit (Cerqueira et al., 2020). Highlighting the complexity of exercise studies, as discrepancies in housing conditions, exercise initiation, duration, and exercise modality needs to be resolved. Furthermore, the lack of neuroprotective effects of exercise in our study may also explain the absence of weight loss after 3 months of HFD and Running, while LiPrRP showed both neuroprotective effects and weight loss after 4 months HFD. However, the absence of weight loss may also be attributed to the social isolation-induced stress. Future studies should aim to refine the current protocol to significantly induce DIO, enabling a more robust comparison to LiPrRP administration. To fully elucidate the absence of neuroprotective response in our protocol future studies should aim to determining the peaks and habitual effect of neurogenesis to exercise in the hypothalamus and troubleshoot the HFD protocol and housing conditions to induce DIO.

In the healthy brain, both LiPrRP and physical exercise enhanced the production of new neurons in aged mice without changing the overall cell population. This suggests that LiPrRP can exert neuroprotective effects regardless of the metabolic state, not solely in the presence of a dysregulated metabolism. Consistent with the distinct mechanisms of LiPrRP and exercise in HFD conditions, LiPrRP in Controls reduced cell proliferation and stem cell activation *in vitro,* whereas exercise had no impact on stem cell proliferation in the same assay. This further confirms that while LiPrRP acts intrinsically on htNSCs, the effects of exercise primarily influence and promote a favourable hypothalamic environment. The effects of exercise on the hypothalamus appear to be similar to those observed in the hippocampus. In the healthy hippocampus, cell proliferation shows a transient peak around 3-10 days followed by a plateau around 32 days, but continued physical activity maintains a stimulating effect on adult neurogenesis (Kronenberg et al., 2006). The existence of this transient peak may explain the

lack of accumulative stimulation in Controls also in the hypothalamus. They also found that prolonged physical activity sustains a stimulatory effect on adult hippocampal neurogenesis, but the quality of this effect changes over time. While sustained exercise preserves precursor cell division at levels comparable to a younger age, this enhanced potential does not translate into a prolonged boost in net neurogenesis or total granule cell numbers. Our results showed that 3 months of running increased acute hypothalamic neurogenesis, but without altering accumulative neurogenesis, suggesting that prolonged running stimulates a subset of hypothalamic stem cells to generate new neurons without necessarily changing the net neuronal addition, akin to the effects in the hippocampus. Similarly, Klein et al. (2019) also reported a habituation response of proliferating cells to prolonged exercise in the MBH of mice on a normal diet (Klein et al., 2019). The effects of exercise on the hypothalamus appear more complex in literature, where the outcomes may differ depending on whether the analysis examines the overall neuronal population, specific neuronal subtypes, or distinct nuclei (Laing et al., 2016; Niwa et al., 2015; Klein et al., 2019; Landry et al., 2022; Borg et al., 2014).

Considering the impacts of LiPrRP on adult neurogenesis, we were interested in exploring whether anti-obesity agents demonstrate similar neurogenic potential, as observed with many antidepressant compounds (Eisch and Petrik, 2012; Malberg et al., 2000). LIRA and Semaglutide, two GLP-1 receptor agonists, have demonstrated the ability to induce weight loss within the first 5 weeks of administration in both animal and human studies (Ard et al., 2021). Clinical trials have shown that these medications can result in significant weight reductions relatively soon after initiation (Tak & Lee, 2021). Although initial weight loss can be significant, the rate of loss typically decelerates as the body adapts (Ryan et al., 2024). This plateau effect is characteristic of most weight loss interventions (Ryan et al., 2024). Studies have also found that most individuals regain weight after discontinuing anti-obesity medications like LIRA and Semaglutide, suggesting the need for sustained treatment to maintain the weight loss benefits (Holst, 2024). Randomised trials have shown that participants who stopped taking the active compounds and switched to placebo quickly reverted to their initial weight (Holst, 2024). Thus, the existing evidence indicates that the weight loss effects of LIRA and Semaglutide are largely contingent on continued administration of these therapies. Interestingly, both LIRA and LiPrRP reduced Ki67+ cells in the 21d protocol and increased beta tanycytes in the 3V in the 7d and the 21d protocol (Appendix Figure EV1) (Jorgensen et al., 2024). A key distinction is however that LiPrRP has been shown to sustain weight loss without regaining weight after treatment cessation (Holubová et al., 2018). The reasons for

these differences remain unclear, and our data do not provide an explanation based on differences in neurogenic responses. Further research is needed to determine whether the distinct effects observed between LiPrRP and LIRA can be attributed to sustained modifications in the neural circuitry that are not evident with LIRA administration. Future investigations should determine if selectively inhibiting adult neurogenesis in the hypothalamus would attenuate the anorexigenic properties of the anti-obesity compounds, akin to the causative evidence demonstrating the requirement of hippocampal neurogenesis for the therapeutic efficacy of antidepressants (Santarelli et al., 2003).

The data suggest that a brief period of increased caloric intake, such as during a holiday, may elicit a compensatory response in the hypothalamic regulation of energy homeostasis to mitigate any potential injury. This neurogenic response could potentially be prevented by engaging in regular exercise during such a period. However, if the high caloric intake persists, exercise alone may not be sufficient to maintain this protective effect. While the anti-obesity drug LiPrRP may not be effective for short-term weight loss during a holiday, it could aid in restoring normal energy homeostasis and inducing long-term weight loss for individuals struggling to maintain a healthy lifestyle. It is important to note that these conclusions are based on the data presented in this study, and it cannot be claimed that the anorexigenic actions of LiPrRP nor exercise are conveyed through neurogenesis.

6.4. Limitations and Future directions

The finding that LiPrRP can influence neurogenesis to mediate its anti-obesity effect is indeed intriguing. However, further studies are needed to determine whether LiPrRP, similar to antidepressants (Santarelli et al., 2003; D'Sa & Duman, 2002), acts through neurogenesis. To gain insights, studies should investigate the effects of ablating hypothalamic neurogenesis concurrently with LiPrRP administration.

While some studies have indicated a decline in tanycyte proliferation after 3-4 weeks of age in mice, the current investigation detected newly generated BrdU-labelled and GLAST lineage-traced cells even in 4-5 month old animals. This contrasts with reports that β-tanycytes exhibit a marked reduction in BrdU incorporation between postnatal days 7 and 45 (Haan et al., 2013). Haan et al. (2013) further showed that no BrdU labelling could be detected in either β1 or β2 tanycyte subtypes by 12 months of age, even under cumulative labelling paradigms (Haan et al., 2013). On the other hand, the study by (Robins et al., 2013) revealed that while Fgf10+ tanycytes (β-tanycytes) cycled at least once every 9-15 days, the α tanycytes had much slower cycling rates. Investigations utilising LacZ-reporter GLAST-CreER^{T2} mice further revealed that the numbers of α2-tanycytes increased significantly after a 6 week chase period, and these elevated levels were maintained even at 9 months of age (Robins et al., 2013). In the same study, analysis of GFP-reporter GLAST-CreER^{T2} mice showed a comparable trend. The extent and density of reporter-positive tanycytes significantly increased at 9 months compared to 5 days across all three tanycytic zones. Notably, no difference was observed in the total number of ventricular zone cells during this period, suggesting that they must have been replaced over time (Robins et al., 2013). Along similar lines, a study (McNay et al., 2012) found that a substantial portion of the BrdU-retaining post-mitotic neurons in the ArcN were lost during embryonic development but were subsequently replaced over the first three postnatal months (McNay et al., 2012). This indicates a substantial cell turnover and suggests that tanycytes likely maintain their neurogenic capacity well beyond the initial 3-4 weeks, consistent with our own findings.

Although transgenic lines expressing inducible Cre recombinase provide powerful and effective tools for lineage analysis, no studies have previously combined BrdU labelling with Cre-based lineage tracing to directly demonstrate that adult-generated hypothalamic neurons originate from proliferating progenitor cells (Haan et al., 2013; Robins et al., 2013). Here, for the first time, GLAST+ stem cells in the hypothalamus were lineage traced and BrdU labelled. However, GLAST+ tanycytes represent only a portion of the tanycytes in the hypothalamus,

where GLAST has been reported to label α-tanycytes of the HVZ, but not β-tanycytes (Robins et al., 2013) and it also labels a subpopulation of mature parenchymal astrocytes. While lineage tracing of the GLAST+ tanycyte population provides valuable insights, it may not offer a complete picture of the adult hypothalamic neurogenesis responses to external stimuli, as β-tanycytes and astrogliogenesis were not traced in this analysis.

It is essential that the behavioural and environmental factors that produce the highest levels of neurogenesis in adult mice be identified. Determining the ideal conditions for studying adult hypothalamic neurogenesis will enable the utilisation of a wide range of transgenic models and molecular tools to investigate the underlying mechanisms of hypothalamic neurogenesis in DIO and the impact of interventions. Further investigation employing inducible mouse models, such as the already existing GLAST-CreER^{T2} or Nestin-CreER^{T2} to target aNSCs and the Confetti multicolour Cre reporter (DeCarolis et al., 2013; Calzolari et al., 2015; Bast et al., 2018) or Brainbow, could provide insights into the step-by-step process of adult neurogenesis in the hypothalamus and elucidate how tanycytes generate specific neuronal progeny in response to stimuli over time. Additionally, generating a Rax-CreER^{T2} mouse line to allow inducible *in vivo* tracking of hypothalamus specific aNSCs and their progeny, in combination with the Brainbow reporter, would significantly enhance the investigation.

The role of hypothalamic neurogenesis in food intake and energy homeostasis remains under investigation. While the relationship is complex, some studies suggest that inhibiting cell proliferation in the hypothalamus using AraC can increase weight gain or prevent weight loss (Gouazé et al., 2013; Kokoeva et al., 2005). In contrast, using computer-guided focal irradiation to inhibit neurogenesis in the ME has led to reduced HFD induced weight gain in female mice, but not in males (Lee et al., 2014). These results indicate that adult-generated neurons in the ME may contribute to weight gain in females, and that the neural circuitry regulating body weight differs between genders (Lee et al., 2014). However, the overall effects of increased or decreased hypothalamic neurogenesis on food intake and energy balance are not straightforward, and likely depend on various experimental factors and potential compensatory mechanisms. While the relationship between hypothalamic neurogenesis and food intake regulation is complex, it has been suggested that neurogenesis may serve as a counter-regulatory mechanism to maintain energy balance in response to environmental or physiological challenges. If this is the case, then hypothalamic neurogenesis itself may not be the direct cause of reduced or increased food intake, but rather the specific neuronal subpopulations generated. The environmental factors that these progenitor cells are exposed to

within the hypothalamic niche may determine the phenotype of the newly generated neurons and their subsequent influence on feeding behaviour.

It is worth mentioning that although the plasticity of adult neurogenesis has been well-established in laboratory strains of house mice and brown rats, Häuser et al. (2009) have shown that voluntary running and environmental changes, which effectively enhance adult hippocampal neurogenesis in these laboratory rodents, do not influence adult hippocampal neurogenesis in wild long-tailed wood mice (Häuser et al., 2009). While adult hippocampal neurogenesis has been reported to positively correlate with hippocampus-dependent learning tasks, especially spatial learning (Drapeau et al., 2003; Kempermann et al., 1998; Praag et al., 1999; Praag et al., 2005; Kronenberg et al., 2006; Praag et al., 1999), the complete elimination of adult hippocampal neurogenesis has also been shown to have minimal or no effects on a wide range of behavioural measures in mice (Meshi et al., 2006). Importantly, the study by Häuser et al. (2009) demonstrated that in wild wood mice, voluntary running had no impact on cell proliferation, neurogenesis, or apoptosis in the hippocampus. This indicates that adult hippocampal neurogenesis in these wild rodents is resistant to changes in the environment, as evidenced by the lack of differences between animals sacrificed immediately after trapping and those housed in the laboratory (Häuser et al., 2009). These findings highlight the importance of studying adult neurogenesis in wild animal populations to gain a more comprehensive understanding of its true functional significance for human medicine. While voluntary exercise may only increase neurogenesis in sedentary laboratory mice, it could potentially be compared to the more sedentary lifestyle adopted by modern society in recent times. These models therefore remain relevant for research on this topic, as they provide valuable insights despite the limitations.

It is also worth mentioning that the understanding of hypothalamic neurogenesis in humans remains extremely limited compared to rodents, due to methodological challenges. Researchers must rely on postmortem analyses, which are hindered by issues like the preservation of neuronal markers (Sharif et al., 2021). Evidence for adult neurogenesis in the human hypothalamus primarily comes from the detection of DCX (Batailler et al., 2014), a marker of immature neurons, but this may not accurately reflect the true morphology of these cells in the living brain. Factors like postmortem delay and duration of DCX expression in humans are not well understood, limiting the ability to reliably estimate the birth date and age of DCX-positive cells (Boekhoorn et al., 2006). Furthermore, the maturation of adult-generated neurons in humans may occur over a more protracted period compared to rodents (Kohler et al., 2011;

Kempermann et al., 2018), as mentioned in the general introduction. Overall, the limited knowledge of hypothalamic neurogenesis in humans highlights the need for further research and developments of translational models to fully understand human hypothalamic neurogenesis and its potential functions and implications for human health and disease.

6.5. Conclusion and Outlook

Obesity is a multifaceted disorder underlying persistent health issues, yet our understanding of the neurobiological mechanisms governing feeding behaviour and energy balance remains incomplete. This body of research has significantly advanced our comprehension of the relationship between a high-fat diet, physical and pharmacological interventions, and adult neurogenesis in the hypothalamus - a crucial brain region for regulating energy homeostasis.

Our findings indicated that HFD initially stimulated a neurogenic response, but over time diminished the survival and production of adult-born neurons. In contrast, treatment with LiPrRP was found to act directly and intrinsically on the cell populations within the hypothalamus, potentially extending the ability of the stem cell population to respond to the HFD, as well as enhancing the long-term survival of adult-generated neurons. Meanwhile, exercise appeared to primarily have beneficial effects by alleviating acute hypothalamic inflammation, although these effects were not maintained long-term in the context of persistent DIO.

This study has laid the groundwork for further exciting investigations into the role of hypothalamic neurogenesis in pathological regulation of our energy balance, an imperative area for future study with promising implications for the development of novel therapeutic strategies targeting obesity and associated metabolic disorders.

References

Adams, J M., Pei, H., Sandoval, D A., Seeley, R J., Chang, R B., Liberles, S D., & Olson, D P. (2018, May 18). Liraglutide Modulates Appetite and Body Weight Through Glucagon-Like Peptide 1 Receptor–Expressing Glutamatergic Neurons. American Diabetes Association, 67(8), 1538-1548. https://doi.org/10.2337/db17-1385

Alford, S., Patel, D., Perakakis, N., & Mantzoros, C S. (2018, February 1). Obesity as a risk factor for Alzheimer's disease: weighing the evidence. Obesity Reviews. https://doi.org/10.1111/obr.12629

Allen, D M., Praag, H V., Ray, J., Weaver, Z., Winrow, C J., Carter, T A., Braquet, R., Harrington, E., Ried, T., Brown, K D., Gage, F H., & Barlow, C. (2001, January 1). Ataxia telangiectasia mutated is essential during adult neurogenesis. Genes & Development . https://doi.org/www.genesdev.org/cgi/doi/10.1101/gad.869001

Altman, J., & Das, G D. (1965, January 1). Autoradiographic and Histoloaical Evidence of Postnatal Hippocampal Neurogenesis in Rats. The Journal of Comparative Neurology. https://doi.org/ https://doi.org/10.1002/cne.901240303

Amamoto, R., & Arlotta, P. (2014, January 31). Development-Inspired Reprogramming of the Mammalian Central Nervous System. American Association for the Advancement of Science, 343(6170). https://doi.org/10.1126/science.1239882

Anstey, K J., Cherbuin, N., Budge, M., & Young, J. (2011, January 1). Body mass index in midlife and late-life as a risk factor for dementia: a meta-analysis of prospective studies. Obesity Reviews. https://doi.org/10.1111/j.1467-789X.2010.00825.x

Ard, J. D., Fitch, A., Fruh, S., & Herman, L. (2021). Weight Loss and Maintenance Related to the Mechanism of Action of Glucagon-Like Peptide 1 Receptor Agonists [Review of Weight Loss and Maintenance Related to the Mechanism of Action of Glucagon-Like Peptide 1 Receptor Agonists]. Advances in Therapy, 38(6). https://doi.org/10.1007/s12325-021-01710-0

Ayloo, S., & Gu, C. (2019, August 1). Transcytosis at the Blood-Brain Barrier. Current Opinion In Neurobiology. https://doi.org/10.1016/j.conb.2018.12.014

Baek, S. (2016, January 1). Role of exercise on the brain. Journal of Exercise Rehabilitation. https://doi.org/10.12965/jer.1632808.404

Bailey, C J., Flatt, P R., & Conlon, J M. (2023, March 1). An update on peptide-based therapies for type 2 diabetes and obesity. Peptides, 161, 170939-170939. https://doi.org/10.1016/j.peptides.2023.170939

Baker, R G., Hayden, M S., & Ghosh, S. (2011, January 1). NF-kB, Inflammation, and Metabolic Disease. Cell Metabolism . https://doi.org/10.1016/j.cmet.2010.12.008

Balland, E., Dam, J., Langlet, F., Caron, E., Steculorum, S., Messina, A., Rasika, S., Falluel-Morel, A., Anouar, Y., Dehouck, B., Trinquet, E., Jockers, R., Bouret, S G., Prévot, V., & . (2014, February 4). Hypothalamic tanycytes are an ERK-gated conduit for leptin into the brain. Cell Metabolism . https://doi.org/doi:10.1016/j.cmet.2013.12.015.

Balthasar, N., Dalgaard, L T., Lee, C E., Yu, J., Funahashi, H., Williams, T., Ferreira, M., Tang, V., McGovern, R A., Kenny, C D., Christiansen, L M., Edelstein, E., Choi, B., Boss, O., Aschkenasi, C., Zhang, C., Mountjoy, K., Kishi, T., Elmquist, J K., & Lowell, B B. (2005, November 4). Divergence of Melanocortin Pathways in the Control of Food Intake and Energy Expenditure. Cell. https://doi.org/10.1016/j.cell.2005.08.035

Banasr, M., Soumier, A., Héry, M., Mocaër, E., & Daszuta, A. (2006, June 1). Agomelatine, a New Antidepressant, Induces Regional Changes in Hippocampal Neurogenesis. Biological Psychiatry, 59(11), 1087-1096. https://doi.org/10.1016/j.biopsych.2005.11.025

Barker, D J., Hales, C N., Fall, C., Osmond, C., Phipps, K R., & Clark, P M. (1993, January 1). Type 2 (non-insulin-dependent) diabetes mellitus, hypertension and hyperlipidaemia (syndrome X): relation to reduced fetal growth. Diabetologia, 36(1), 62-67. https://doi.org/10.1007/bf00399095

Bast, L., Calzolari, F., Strasser, M., Hasenauer, J., Theis, F J., Ninkovic, J., & Marr, C. (2018, December 1). Increasing Neural Stem Cell Division Asymmetry and Quiescence Are Predicted to Contribute to the Age-Related Decline in Neurogenesis. Cell Press, 25(12), 3231-3240.e8. https://doi.org/10.1016/j.celrep.2018.11.088

Batailler, M., Droguerre, M., Baroncini, M., Fontaine, C., Prevot, V., & Migaud, M. (2014, January 1). DCX-Expressing Cells in the Vicinity of the Hypothalamic Neurogenic Niche: A Comparative Study Between Mouse, Sheep, and Human Tissues. The Journal of Comparative Neurology. https://doi.org/ https://doi.org/10.1002/cne.23514

Bayer, S A. (1982, June 1). Changes in the total number of dentate granule cells in juvenile and adult rats: A correlated volumetric and 3H-thymidine autoradiographic study. Experimental brain research, 46(3), 315-323. https://doi.org/10.1007/bf00238626

Benarroch, E E. (2011, September 20). Circumventricular organs: Receptive and homeostatic functions and clinical implications. Neurology. https://doi.org/10.1212/WNL.0b013e31822f04a0

Betley, J N., Cao, Z., Meshnick, S R., & Sternson, S M. (2013, December 1). Parallel, Redundant Circuit Organization for Homeostatic Control of Feeding Behavior. Cell Press, 155(6), 1337-1350. https://doi.org/10.1016/j.cell.2013.11.002

Biessels, G J., Staekenborg, S S., Brunner, E J., Brayne, C., & Scheltens, P. (2006, January 1). Risk of dementia in diabetes mellitus: a systematic review. The Lancet. Neurology, 5(1), 64-74. https://doi.org/10.1016/s1474-4422(05)70284-2

Bjursell, M., Lenners, M., Goransson, M., Elmgren, A., & Bohlooly-Y, M. (2007, September 18). GPR10 deficiency in mice results in altered energy expenditure and obesity. Biochemical and Biophysical Research Communications. https://doi.org/10.1016/j.bbrc.2007.09.016

Blüher, M., & Mantzoros, C S. (2015, January 1). From leptin to other adipokines in health and disease: Facts and expectations at the beginning of the 21st century. Metabolism, 64(1), 131-145. https://doi.org/10.1016/j.metabol.2014.10.016

Boekhoorn, K., Joëls, M., & Lucassen, P J. (2006, July 4). Increased proliferation reflects glial and vascular-associated changes, but not neurogenesis in the presenile Alzheimer hippocampus. Neurobiology of Disease, 24(1), 1-14. https://doi.org/10.1016/j.nbd.2006.04.017

Bolborea, M., & Dale, N. (2013, February 1). Hypothalamic tanycytes: potential roles in the control of feeding and energy balance. Trends in Neurosciences, 36(2), 91-100. https://doi.org/10.1016/j.tins.2012.12.008

Boldrini, M., Fulmore, C A., Tartt, A N., Simeon, L R., Pavlova, I., Poposka, V., Rosoklija, G B., Stankov, A., Arango, V., Dwork, A J., Hen, R., & Mann, J J. (2018, January 1). Human Hippocampal Neurogenesis Persists throughout Aging. Cell Stem Cell. https://doi.org/10.1016/j.stem.2018.03.015

Borg, M. L., Lemus, M. B., Reichenbach, A., Selathurai, A., Oldfield, B. J., Andrews, Z. B., & Watt, M. J. (2014). Hypothalamic Neurogenesis Is Not Required for the Improved Insulin Sensitivity Following Exercise Training. Diabetes, 63(11), 3647. https://doi.org/10.2337/db13-1762

Borght, K V D., Ferrari, F., Klauke, K., Román, V., Havekes, R., Sgoifo, A., Zee, E A V D., & Meerlo, P. (2006, February 1). Hippocampal cell proliferation across the day: Increase by running wheel activity, but no effect of sleep and wakefulness. Behavioural Brain Research, 167(1), 36-41. https://doi.org/10.1016/j.bbr.2005.08.012

Bortolotto, V., Cuccurazzu, B., Canonico, P L., & Grilli, M. (2014, February 12). NF-κB Mediated Regulation of Adult Hippocampal Neurogenesis: Relevance to Mood Disorders and Antidepressant Activity. BioMed Research International. https://doi.org/10.1155/2014/612798

Bouret, S G. (2009, November 27). Development of Hypothalamic Neural Networks Controlling Appetite. Karger Publishers, 84-93. https://doi.org/10.1159/000264396

Boyle, R. G., Downham, R., Ganguly, T., Humphries, J. E., Smith, J. D., & Travers, S. (2004). Structure-activity studies on prolactin-releasing peptide (PrRP). Analogues of PrRP-(19-31)-peptide. In Journal of Peptide Science (Vol. 11, Issue 3, p. 161). Wiley. https://doi.org/10.1002/psc.612

Bray, G A., Frühbeck, G., Ryan, D H., & Wilding, J P H. (2016, January 1). Management of obesity. Lancet. https://doi.org/10.1016/S0140-6736(16)00271-3

Buckinx, A., Schuerbeek, A V., Bossuyt, J., Allaoui, W., Herrewegen, Y V D., Smolders, I., & Bundel, D D. (2021, October 28). Exploring Refinement Strategies for Single Housing of Male C57BL/6JRj Mice: Effect of Cage Divider on Stress-Related Behavior and Hypothalamic-Pituitary-Adrenal-Axis Activity. Frontiers in Behavioral Neuroscience. https://doi.org/10.3389/fnbeh.2021.743959

Buckman, L B., Hasty, A H., Flaherty, D K., Buckman, C T., Thompson, M M., Matlock, B K., Weller, K., & Ellacott, K L. (2013, July 4). Obesity induced by a high-fat diet is associated with increased immune cell entry into the central nervous system. Brain, Behavior, and Immunity. https://doi.org/https://doi.org/10.1016/j.bbi.2013.06.007

Calzolari, F., Michel, J., Baumgart, E V., Theis, F J., Götz, M., & Ninkovic, J. (2015, March 2). Fast clonal expansion and limited neural stem cell self-renewal in the adult subependymal zone. Nature Neuroscience, 18(4), 490-492. https://doi.org/10.1038/nn.3963

Cameron, H A., & McKay, R. (2001, June 8). Adult neurogenesis produces a large pool of new granule cells in the dentate gyrus. Wiley, 435(4), 406-417. https://doi.org/10.1002/cne.1040

Campbell, J N., Macosko, E Z., Fenselau, H., Pers, T H., Lyubetskaya, A., Tenen, D., Goldman, M., Verstegen, A M., Resch, J M., McCarroll, S A., Rosen, E D., Lowell, B B., & Tsai, L. (2017, January 1). A Molecular Census of Arcuate Hypothalamus and Median Eminence Cell Types. Nature Neuroscience . https://doi.org/ doi:10.1038/nn.4495

Cant, J., Sloth, B., Jensen, C B., Flint, A., Blaak, E E., & Saris, W H M. (2013, September 3). Effects of the once-daily GLP-1 analog liraglutide on gastric emptying, glycemic parameters, appetite and energy metabolism in obese, non-diabetic adults. Springer Nature, 38(6), 784-793. https://doi.org/10.1038/ijo.2013.162

Casado, M. E., Collado-Pérez, R., Frago, L. M., & Barrios, V. (2023). Recent Advances in the Knowledge of the Mechanisms of Leptin Physiology and Actions in Neurological and Metabolic Pathologies [Review of Recent Advances in the Knowledge of the Mechanisms of Leptin Physiology and Actions in Neurological and Metabolic Pathologies]. International Journal of Molecular Sciences, 24(2), 1422. Multidisciplinary Digital Publishing Institute. https://doi.org/10.3390/ijms24021422

Cerqueira, É., Marinho, D A., Neiva, H P., & Lourenço, O. (2020, January 9). Inflammatory Effects of High and Moderate Intensity Exercise—A Systematic Review. Frontiers in Physiology. https://doi.org/10.3389/fphys.2019.01550

Çetinkaya, S., Güran2, T., Kurnaz, E., Keskin, M., Sağsak, E., Erdeve, S S., Suntharalingham, J P., Buonocore, F., Achermann, J C., & Aycan, Z. (2018, March 1). A Patient with Proopiomelanocortin Deficiency: An Increasingly Important Diagnosis to Make. Journal of clinical research in pediatric endocrinology. https://doi.org/10.4274/jcrpe.4638

Ceylan, H İ., Silva, A F., Ramírez-Campillo, R., & Murawska-Ciałowicz, E. (2024, May 6). Exploring the Effect of Acute and Regular Physical Exercise on Circulating Brain-Derived Neurotrophic Factor Levels in Individuals with Obesity: A Comprehensive Systematic Review and Meta-Analysis. Multidisciplinary Digital Publishing Institute, 13(5), 323-323. https://doi.org/10.3390/biology13050323

Chaker, Z., George, C., Petrovska, M., Caron, J., Lacube, P., Caillé, I., & Holzenberger, M. (2016, May 1). Hypothalamic neurogenesis persists in the aging brain and is controlled by energy-sensing IGF-I pathway. Neurobiology of aging, 41, 64-72. https://doi.org/10.1016/j.neurobiolaging.2016.02.008

Chambers, A P., Sorrell, J., Haller, A., Roelofs, K., Hutch, C R., Kim, K., Gutierrez-Aguilar, R., Li, B., Drucker, D J., D'Alessio, D A., Seeley, R J., & Sandoval, D A. (2017, January 1). The role of pancreatic preproglucagon in glucose homeostasis in mice. Cell Metabolism . https://doi.org/10.1016/j.cmet.2017.02.008

Chapman, C D., Schiöth, H B., Grillo, C A., & Benedict, C. (2018, July 1). Intranasal insulin in Alzheimer's disease: Food for thought. Neuropharmacology. https://doi.org/10.1016/j.neuropharm.2017.11.037

Chen, R., Wu, X., Jiang, L., & Zhang, Y. (2017, March 1). Single-Cell RNA-Seq Reveals Hypothalamic Cell Diversity. Cell Press, 18(13), 3227-3241. https://doi.org/10.1016/j.celrep.2017.03.004

Chen, X., Peng, M., Cai, Y., Zhou, C., Liu, L. (2022). Human iPSC-derived neural stem cells with ALDH5A1 mutation as a model of succinic semialdehyde dehydrogenase deficiency. BMC Neuroscience. https://doi.org/10.1186/s12868-022-00755-3

Chen, Y., Essner, R., Kosar, S., Miller, O H., Lin, Y., Mesgarzadeh, S., & Knight, Z A. (2019, April 29). Sustained NPY signaling enables AgRP neurons to drive feeding. eLife Sciences Publications Ltd, 8. https://doi.org/10.7554/elife.46348

Chiazza, F., Bondi, H., Masante, I., Ugazio, F., Bortolotto, V., Canonico, P. L., & Grilli, M. (2021). Short high fat diet triggers reversible and region specific effects in DCX+ hippocampal immature neurons of adolescent male mice. Scientific Reports, 11(1). https://doi.org/10.1038/s41598-021-01059-y

Clark, P., Brzezinska, W J., Puchalski, E K., Krone, D A., & Rhodes, J S. (2009, January 8). Functional analysis of neurovascular adaptations to exercise in the dentate gyrus of young adult mice associated with cognitive gain. Wiley, 19(10), 937-950. https://doi.org/10.1002/hipo.20543

Cole, G. M., Ma, Q., & Frautschy, S. A. (2010). Dietary fatty acids and the aging brain. Nutrition Reviews, 68. https://doi.org/10.1111/j.1753-4887.2010.00345.x

Collins, L., & Costello, R A. (2022, January 1). Glucagon-Like Peptide-1 Receptor Agonists. StatPearls Publishing

Conibear, E., & Davis, N. G. (2010). Palmitoylation and depalmitoylation dynamics at a glance. 123(23), 4007.

Cope, E C., LaMarca, E A., Monari, P K., Olson, L B., Rodríguez, S., Zych, A D., Katchur, N J., & Gould, E. (2018, September 10). Microglia Play an Active Role in Obesity-Associated Cognitive Decline. Society for Neuroscience, 38(41), 8889-8904. https://doi.org/10.1523/jneurosci.0789-18.2018

Cork, S. C., Richards, J. E., Holt, M. K., Gribble, F. M., Reimann, F., & Trapp, S. (2015). Distribution and characterisation of Glucagon-like peptide-1 receptor expressing cells in the mouse brain. Molecular Metabolism, 4(10), 718. https://doi.org/10.1016/j.molmet.2015.07.008

Couillard-Despres, S., Winner, B., Schaubeck, S., Aigner, R., Vroemen, M., Weidner, N., Bogdahn, U., Winkler, J., Kuhn, H., & Aigner, L. (2005, January 1). Doublecortin expression levels in adult brain reflect neurogenesis. The European Journal of Neuroscience. https://doi.org/10.1111/j.1460-9568.2004.03813.x

Cummings, J L., Osse, A M L., & Kinney, J W. (2023, September 20). Alzheimer's Disease: Novel Targets and Investigational Drugs for Disease Modification. Adis, Springer Healthcare, 83(15), 1387-1408. https://doi.org/10.1007/s40265-023-01938-w

Davanzo, G G., Castro, G., Monteiro, L D B., Castelucci, B G., Jaccomo, V H., Silva, F C D., Marques, A M., Francelin, C., Campos, B B D., Aguiar, C F D., Joazeiro, P P., Consonni, S R., Farias, A D S., & Moraes-Vieira, P M. (2023, January 1). Obesity increases blood-brain barrier permeability and aggravates the mouse model of multiple sclerosis. Multiple Sclerosis and Related Disorders. https://doi.org/https://doi.org/10.1016/j.msard.2023.104605

De la Monte, S. M. (2012). Brain Insulin Resistance and Deficiency as Therapeutic Targets in Alzheimer's Disease.

DeCarolis, N A., Mechanic, M., Petrik, D., Carlton, A., Ables, J L., Malhotra, S., Bachoo, R., Götz, M., Lagace, D C., & Eisch, A J. (2013, January 1). In vivo contribution of nestin- and GLAST-lineage cells to adult hippocampal neurogenesis. Hippocampus. https://doi.org/10.1002/hipo.22130

Deem, J D., Faber, C L., & Morton, G J. (2021, September 13). AgRP neurons: Regulators of feeding, energy expenditure, and behavior. Wiley, 289(8), 2362-2381. https://doi.org/10.1111/febs.16176

Dennis, C., Suh, L S., Rodriguez, M., Kril, J J., & Sutherland, G T. (2016, August 28). Human adult neurogenesis across the ages: An immunohistochemical study. Wiley, 42(7), 621-638. https://doi.org/10.1111/nan.12337

Dicken, M. S., Tooker, R. E., & Hentges, S. T. (2012). Cellular/Molecular Regulation of GABA and Glutamate Release from Proopiomelanocortin Neuron Terminals in Intact Hypothalamic Networks. https://doi.org/10.1523/JNEUROSCI.6032-11.2012

Dineley, K T., Jahrling, J B., & Denner, L. (2014, January 1). Insulin Resistance in Alzheimer's Disease. International Journal of Molecular Sciences. https://doi.org/10.3390/ijms22189987

Dodd, G. T., & Luckman, S. M. (2013). Physiological Roles of GPR10 and PrRP Signaling. Frontiers in Endocrinology, 4. https://doi.org/10.3389/fendo.2013.00020

Dong, H., Yuede, C M., Yoo, H., Martin, M V., Deal, C., Mace, A G., & Csernansky, J G. (2008, January 1). Corticosterone and related receptor expression are associated with increased β-amyloid plaques in isolated Tg2576 mice. Neuroscience. https://doi.org/10.1016/j.neuroscience.2008.05.017

Drapeau, E., Mayo, W., Aurousseau, C., Moal, M L., Piazza, P., & Abrous, D N. (2003, November 12). Spatial memory performances of aged rats in the water maze predict levels of hippocampal neurogenesis. National Academy of Sciences, 100(24), 14385-14390. https://doi.org/10.1073/pnas.2334169100

Drucker, D J., Habener, J F., & Holst, J J. (2017, November 30). Discovery, characterization, and clinical development of the glucagon-like peptides. American Society for Clinical Investigation, 127(12), 4217-4227. https://doi.org/10.1172/jci97233

D'Sa, C., & Duman, R S. (2002, June 1). Antidepressants and neuroplasticity. Wiley, 4(3), 183-194. https://doi.org/10.1034/j.1399-5618.2002.01203.x

Duan, X., Kang, E., Liu, C Y., Ming, G., & Song, H. (2008, February 1). Development of neural stem cell in the adult brain. Current Opinion In Neurobiology, 18(1), 108-115. https://doi.org/10.1016/j.conb.2008.04.001

Eisch, A J., & Petřík, D. (2012, October 5). Depression and Hippocampal Neurogenesis: A Road to Remission?. American Association for the Advancement of Science, 338(6103), 72-75. https://doi.org/10.1126/science.1222941

Ellacott, K L J., Lawrence, C B., Pritchard, L E., & Luckman, S M. (2003, November 1). Repeated administration of the anorectic factor prolactin-releasing peptide leads to tolerance to its effects on energy homeostasis. American Physiological Society, 285(5), R1005-R1010. https://doi.org/10.1152/ajpregu.00237.2003

Ellacott, K L J., Lawrence, C B., Rothwell, N J., & Luckman, S M. (2002, February 1). PRL-Releasing Peptide Interacts with Leptin to Reduce Food Intake and Body Weight. Oxford University Press, 143(2), 368-374. https://doi.org/10.1210/endo.143.2.8608

Engel, D F., & Velloso, L A. (2022, January 1). The timeline of neuronal and glial alterations in experimental obesity. Neuropharmacology. https://doi.org/https://doi.org/10.1016/j.neuropharm.2022.108983

Engström, L., Pereira, M M A., Solís, A J D., Fenselau, H., & Brüning, J C. (2020, January 23). NPY mediates the rapid feeding and glucose metabolism regulatory functions of AgRP neurons. Nature Portfolio, 11(1). https://doi.org/10.1038/s41467-020-14291-3

Eriksson, P S., Perfilieva, E., Björk-Eriksson, T., Alborn, A., Nordborg, C., Peterson, D A., & Gage, F H. (1998, November 1). Neurogenesis in the adult human hippocampus. Nature Portfolio, 4(11), 1313-1317. https://doi.org/10.1038/3305

Farooqi, I S. (2022, February 5). Monogenic Obesity Syndromes Provide Insights Into the Hypothalamic Regulation of Appetite and Associated Behaviors. Biological Psychiatry, 91(10), 856-859. https://doi.org/10.1016/j.biopsych.2022.01.018

Farr, O. M., Tsoukas, M. A., & Mantzoros, C. S. (2015). Leptin and the brain: Influences on brain development, cognitive functioning and psychiatric disorders. In Metabolism (Vol. 64, Issue 1, p. 114). Metabolism. https://doi.org/10.1016/j.metabol.2014.07.004

FDA Approves First Treatment to Reduce Risk of Serious Heart Problems Specifcally in Adults with Obesity or Overweight. (2024, March 8). https://www.fda.gov/news-events/press-announcements/fda-approves-first-treatment-reduce-risk-serious-heart-problems-specifically-adults-obesity-or

Felice, F G D., & Ferreira, S T. (2014, January 1). Inflammation, Defective Insulin Signaling, and Mitochondrial Dysfunction as Common Molecular Denominators Connecting Type 2 Diabetes to Alzheimer Disease. Diabetes. https://doi.org/10.2337/db13-1954

Filippo, M. D., Chiasserini, D., Gardoni, F., Viviani, B., Tozzi, A., Giampà, C., Costa, C., Tantucci, M., Zianni, E., Boraso, M., Siliquini, S., Iure, A. de, Ghiglieri, V., Colcelli, E., Baker, D., Sarchielli, P., Fusco, F. R., Luca, M. D., & Calabresi, P. (2013). Effects of central and peripheral inflammation on hippocampal synaptic plasticity. Neurobiology of Disease, 52, 229. https://doi.org/10.1016/j.nbd.2012.12.009

Fortin, S M., Lipsky, R K., Lhamo, R., Chen, J., Kim, E K., Borner, T., Schmidt, H D., & Hayes, M R. (2020, March 4). GABA neurons in the nucleus tractus solitarius express GLP-1 receptors and mediate anorectic effects of liraglutide in rats. American Association for the Advancement of Science, 12(533). https://doi.org/10.1126/scitranslmed.aay8071

Franceschi, C. (2008). Inflammaging as a Major Characteristic of Old People: Can It Be Prevented or Cured? Nutrition Reviews, 65. https://doi.org/10.1111/j.1753-4887.2007.tb00358.x

Frielingsdorf, H., Schwarz, K. P., Brundin, P., & Mohapel, P. (2004). No evidence for new dopaminergic neurons in the adult mammalian substantia nigra. Proceedings of the National Academy of Sciences, 101(27), 10177. https://doi.org/10.1073/pnas.0401229101

Fuller, N. J., Laskey, M. A., & Elia, M. (1992). Assessment of the composition of major body regions by dual-energy X-ray absorptiometry (DEXA), with special reference to limb muscle mass. Clinical Physiology, 12(3), 253. https://doi.org/10.1111/j.1475-097x.1992.tb00831.x

Gabery, S., Salinas, C G., Paulsen, S J., Ahnfelt-Rønne, J., Alanentalo, T., Baquero, A F., Buckley, S T., Farkas, E., Fekete, C., Frederiksen, K S., Hogendor, W F J., Helm, H C C., Jeppesen, J F., John, L M., Pyke, C., Nøhr, J., Lu, T T., Polex-Wolf, J., Prevot, V., . . . Knudsen, L B. (2020, March 26). Semaglutide lowers body weight in rodents via distributed neural pathways. JCI Insight . https://doi.org/https://doi.org/10.1172/jci.insight.13342

Gage, F H. (2002, February 1). Neurogenesis in the Adult Brain. Society for Neuroscience, 22(3), 612-613. https://doi.org/10.1523/jneurosci.22-03-00612.2002

Galán, L., Gómez-Pinedo, U., Guerrero, A., García-Verdugo, J. M., & Matías-Guiu, J. (2017). Amyotrophic lateral sclerosis modifies progenitor neural proliferation in adult classic neurogenic brain niches. BMC Neurology, 17(1). https://doi.org/10.1186/s12883-017-0956-5

Gao, Y., & Sun, T. (2015, July 30). Molecular regulation of hypothalamic development and physiological functions. Molecular Neurobiology, 53(7), 4275-4285. https://doi.org/10.1007/s12035-015-9367-z

Garfield, A S., Li, C., Madara, J C., Shah, B P., Webber, E., Steger, J S., Campbell, J N., Gavrilova, O., Lee, C E., Olson, D P., Elmquist, J K., Tannous, B A., Krashes, M J., Lowell, B B., & . (2015, April 27). A neural basis for melanocortin-4 receptor-regulated appetite. Nature Neuroscience . https://doi.org/10.1038/nn.4011

Gascón, S., Masserdotti, G., Russo, G L., & Götz, M. (2017, July 1). Direct Neuronal Reprogramming: Achievements, Hurdles, and New Roads to Success. Cell Stem Cell, 21(1), 18-34. https://doi.org/10.1016/j.stem.2017.06.011

Gault, V. A., Kerr, B. D., Harriott, P., & Flatt, P. R. (2011). Administration of an acylated GLP-1 and GIP preparation provides added beneficial glucose-lowering and insulinotropic actions over single incretins in mice with Type 2 diabetes and obesity. Clinical Science, 121(3), 107. https://doi.org/10.1042/cs20110006

Giuliani, D., Ottani, A., Neri, L., Zaffe, D., Grieco, P., Jochem, J., Cavallini, G M., Catania, A., & Guarini, S. (2017, January 1). Multiple beneficial effects of melanocortin MC4 receptor agonists in experimental neurodegenerative disorders: Therapeutic perspectives. Progress in Neurobiology. https://doi.org/https://doi.org/10.1016/j.pneurobio.2016.11.004

Goodman, T., & Hajihosseini, M K. (2015, October 29). Hypothalamic tanycytes—masters and servants of metabolic, neuroendocrine, and neurogenic functions. Frontiers Media, 9. https://doi.org/10.3389/fnins.2015.00387

Goodman, T., Nayar, S G., Clare, S., Mikolajczak, M., Rice, R., Mansour, S., Bellusci, S., & Hajihosseini, M K. (2020, July 1). Fibroblast growth factor 10 is a negative regulator of postnatal neurogenesis in the mouse hypothalamus. Development (Cambridge, England). https://doi.org/10.1242/dev.180950

Gouazé, A., Brenachot, X., Rigault, C., Krezymon, A., Rauch, C., Emmanuelle, N., Lemoine, A., Gascuel, J., Bauer, S., Luc, P., & Benani, A. (2013, August 13). Cerebral Cell Renewal in Adult Mice Controls the Onset of Obesity. Plos One. https://doi.org/doi:10.1371/journal.pone.0072029

Gould, E., Reeves, A J., Fallah, M., Tanapat, P., Gross, C G., & Fuchs, E. (1999, April 27). Hippocampal neurogenesis in adult Old World primates. National Academy of Sciences, 96(9), 5263-5267. https://doi.org/10.1073/pnas.96.9.5263

Gould, E., Vail, N. K., Wagers, M., & Gross, C. G. (2001). Adult-generated hippocampal and neocortical neurons in macaques have a transient existence. Proceedings of the National Academy of Sciences, 98(19), 10910. https://doi.org/10.1073/pnas.181354698

Gray, J., Yeo, G S., Cox, J J., Morton, J., Adlam, A R., Keogh, J M., Yanovski, J A., Gharbawy, A E., Han, J C., Tung, Y L., Hodges, J R., Raymond, F L., O'Rahilly, S., & Farooqi, I S. (2006, January 1). Hyperphagia, Severe Obesity, Impaired Cognitive Function, and Hyperactivity Associated With Functional Loss of One Copy of the Brain-Derived Neurotrophic Factor (BDNF) Gene. Diabetes

Griesbach, G S., Hovda, D A., Molteni, R., Wallace, A., & Gómez-Pinilla, F. (2004, January 1). Voluntary exercise following traumatic brain injury: brain-derived neurotrophic factor upregulation and recovery of function. Neuroscience, 125(1), 129-139. https://doi.org/10.1016/j.neuroscience.2004.01.030

Guan, X., & Fierke, C. A. (2011). Understanding protein palmitoylation: Biological significance and enzymology. 54(12), 1888.

Gudzune, K. A., & Kushner, R. F. (2024). Medications for Obesity A Review.

Gümüşlü, E., Mutlu, O., Çelikyurt, İ K., Ulak, G., Akar, F., Erden, F., & Ertan, M. (2016, March 21). Exenatide enhances cognitive performance and upregulates neurotrophic factor gene expression levels in diabetic mice. Wiley, 30(4), 376-384. https://doi.org/10.1111/fcp.12192

Gupta, B., Errington, A C., Jimenez-Pascual, A., Eftychidis, V., Brabletz, S., Stemmler, M P., Brabletz, T., Petrik, D., & Siebzehnrubl, F A. (2021, January 1). The transcription factor ZEB1 regulates stem cell self-renewal and cell fate in the adult hippocampus. Cell Reports. https://doi.org/10.1016/j.celrep.2021.109588

Gustafson, D. (2012, June 8). Adiposity and Cognitive Decline: Underlying Mechanisms. IOS Press, 30(s2), S97-S112. https://doi.org/10.3233/jad-2012-120487

Haan, N., Goodman, T., Najdi-Samiei, A., Stratford, C M., Rice, R., Agha, E E., Bellusci, S., & Hajihosseini, M K. (2013, April 3). Fgf10-Expressing Tanycytes Add New Neurons to the Appetite/Energy-Balance Regulating Centers of the Postnatal and Adult Hypothalamus. Society for Neuroscience, 33(14), 6170-6180. https://doi.org/10.1523/jneurosci.2437-12.2013

Hamazaki, T., Rouby, N E., Fredette, N C., Santostefano, K E., & Terada, N. (2017, February 5). Concise Review: Induced Pluripotent Stem Cell Research in the Era of Precision Medicine. Oxford University Press, 35(3), 545-550. https://doi.org/10.1002/stem.2570

Hampel, S., Chung, P., McKellar, C., Hall, D., Looger, L. L., & Simpson, J. (2011). Drosophila Brainbow: a recombinase-based fluorescence labeling technique to subdivide neural expression patterns. Nature Methods, 8(3), 253. https://doi.org/10.1038/nmeth.1566

Han, T K., Leem, Y., & Kim, H. (2019, March 1). Treadmill exercise restores high fat diet-induced disturbance of hippocampal neurogenesis through β2-adrenergic receptor-dependent induction of thioredoxin-1 and brain-derived neurotrophic factor. Brain Research, 1707, 154-163. https://doi.org/10.1016/j.brainres.2018.11.035

Hansen, H H., Fabricius, K., Barkholt, P., Niehoff, M L., Morley, J E., Jelsing, J., Pyke, C., Knudsen, L B., Farr, S A., & Vrang, N. (2015, January 1). The GLP-1 Receptor Agonist Liraglutide Improves Memory Function and Increases Hippocampal CA1 Neuronal Numbers in a Senescence-Accelerated Mouse Model of Alzheimer's Disease. Journal of Alzheimer's Disease . https://doi.org/10.3233/JAD-143090

Häuser, T., Klaus, F., Lipp, H., & Amrein, I. (2009, May 6). No effect of running and laboratory housing on adult hippocampal neurogenesis in wild caught long-tailed wood mouse. BioMed Central, 10(1). https://doi.org/10.1186/1471-2202-10-43

He, Z., Gao, Y., Alhadeff, A L., Castorena, C M., Huang, Y., Lieu, L., Afrin, S., Sun, J., Betley, J N., Guo, H., & Williams, K W. (2018, September 12). Cellular and synaptic reorganization of arcuate NPY/AgRP and POMC neurons after exercise. Molecular Metabolism. https://doi.org/https://doi.org/10.1016/j.molmet.2018.08.011

He, Z., Gao, Y., Lieu, L., Afrin, S., Cao, J., Michael, N. J., Dong, Y., Sun, J., Guo, H., & Williams, K. W. (2019). Direct and indirect effects of liraglutide on hypothalamic POMC and NPY/AgRP neurons - Implications for energy balance and glucose control. Molecular metabolism, 28, 120–134. https://doi.org/10.1016/j.molmet.2019.07.008

Hicks, A., Kobrinsky, S., Zhou, S., Yang, J., & Prager-Khoutorsky, M. (2021, September 6). Anatomical Organization of the Rat Subfornical Organ. Frontiers, 15. https://doi.org/https://doi.org/10.3389/fncel.2021.691711

Hilsenbeck, O., Schwarzfischer, M., Skylaki, S., Schauberger, B., Hoppe, P S., Loeffler, D., Kokkaliaris, K D., Hastreiter, S., Skylaki, E., Filipczyk, A., Strasser, M., Buggenthin, F., Feigelman, J S., Krumsiek, J., Berg, A J J V D., Endele, M., Etzrodt, M., Marr, C., Theis, F J., & Schroeder, T. (2016, January 1). Software tools for single-cell tracking and quantification of cellular and molecular properties. Nature Biotechnology. https://www.nature.com/articles/nbt.3626

Hinuma, S., Habata, Y., Fujii, R., Kawamata, Y., Hosoya, M., Fukusumi, S., Kitada, C., Masuo, Y., Asano, T., Matsumoto, H., Sekiguchi, M., Kurokawa, T., Nishimura, O., Onda, H., & Fujino, M. (1998). A prolactin-releasing peptide in the brain. Nature, 393(6682), 272. https://doi.org/10.1038/30515

Hölscher, C. (2018, January 1). Novel dual GLP-1/GIP receptor agonists show neuroprotective effects in Alzheimer's and Parkinson's disease models. Neuropharmacology. https://doi.org/https://doi.org/10.1016/j.neuropharm.2018.01.040

Hölscher, C., & Lin, L. (2008). New roles for insulin-like hormones in neuronal signalling and protection: New hopes for novel treatments of Alzheimer’s disease? Neurobiology of Aging, 31(9), 1495. https://doi.org/10.1016/j.neurobiolaging.2008.08.023

Holst, J. J. (2024). GLP-1 physiology in obesity and development of incretin-based drugs for chronic weight management [Review of GLP-1 physiology in obesity and development of incretin-based drugs for chronic weight management]. Nature Metabolism. https://doi.org/10.1038/s42255-024-01113-9

Holt, M K., Richards, J E., Cook, D R., Brierley, D I., Williams, D., Reimann, F., Gribble, F M., & Trapp, S. (2019, October 2). Preproglucagon Neurons in the Nucleus of the Solitary Tract Are the Main Source of Brain GLP-1, Mediate Stress-Induced Hypophagia, and Limit Unusually Large Intakes of Food. American Diabetes Association, 68(1), 21-33. https://doi.org/10.2337/db18-0729

Holubová, M., Hrubá, L., Neprašová, B., Majerčíková, Z., Lacinová, Z., Kuneš, J., Maletínská, L., & Železná, B. (2018, February 1). Prolactin-releasing peptide improved leptin hypothalamic signaling in obese mice. Journal of Molecular Endocrinology, 60(2), 85-94. https://doi.org/10.1530/jme-17-0171

Huang, S A., Mishina, Y M., Liu, S., Cheung, A., Stegmeier, F., Michaud, G A., Charlat, O., Wiellette, E., Zhang, Y., Wiessner, S., Hild, M., Shi, X., Wilson, C J., Mickanin, C., Myer, V., Fazal, A., Tomlinson, R., Serluca, F., Shao, W., . . . Cong, F. (2009, January 1). Tankyrase inhibition stabilizes axin and antagonizes Wnt signalling . Nature. https://doi.org/10.1038/nature08356

Huang, W., Wong, S Z H., Pather, S R., Nguyen, P T., Zhang, F., Zhang, D Y., Zhang, Z., Lu, L., Fang, W., Chen, L., Fernandes, A., Su, Y., Song, H., & Ming, G. (2021, January 1). Generation of Hypothalamic Arcuate Organoids from Human Induced Pluripotent Stem Cells. Cell Stem Cell. https://doi.org/ 10.1016/j.stem.2021.04.006

Hwang, E., Portillo, B., Grose, K., Fujikawa, T., & Williams, K W. (2023, July 1). Exercise-induced hypothalamic neuroplasticity: Implications for energy and glucose metabolism. Molecular Metabolism, 73, 101745-101745. https://doi.org/10.1016/j.molmet.2023.101745

Ieraci, A., Mallei, A., & Popoli, M. (2016, January 1). Social Isolation Stress Induces Anxious-Depressive-Like Behavior and Alterations of Neuroplasticity-Related Genes in Adult Male Mice. Hindawi Publishing Corporation, 2016, 1-13. https://doi.org/10.1155/2016/6212983

Ignacio-Souza, L M., Bombassaro, B., Pascoal, L B., Portovedo, M A., Razolli, D S., Coope, A., Victorio, S C., Moura, R F D., Nascimento, L F., Arruda, A P., Anhe, G F., Milanski, M., & Velloso, L A. (2014, August 1). Defective Regulation of the Ubiquitin/Proteasome System in the Hypothalamus of Obese Male Mice. Endocrinology. https://doi.org/https://doi.org/10.1210/en.2014-1090

Imayoshi, I., Sakamoto, M., Ohtsuka, T., Takao, K., Miyakawa, T., Yamaguchi, M., Mori, K., Ikeda, T., Itohara, S., & Kageyama, R. (2008, January 1). Roles of continuous neurogenesis in the structural and functional integrity of the adult forebrain. Nature Neuroscience . https://doi.org/10.1038/nn.2185

Imbernon, M., Saponaro, C., Helms, H C C., Duquenne, M., Fernandois, D., Deligia, E., Denis, R G., Herrera, D., Chao, M., Rasika, S., Staels, B., Pattou, F., Pfrieger, F W., Brodin, B., Luquet, S., Bonner, C., & Prevot, V. (2022, July 5). Tanycytes Control Hypothalamic Liraglutide Uptake and its Anti- Obesity Actions. Cell Metabolism . https://doi.org/10.1016/j.cmet.2022.06.0

Inoue, H., & Yamanaka, S. (2011, March 23). The Use of Induced Pluripotent Stem Cells in Drug Development. Wiley, 89(5), 655-661. https://doi.org/10.1038/clpt.2011.38

Jacobsen, L. V., Flint, A., Olsen, A., & Ingwersen, S. H. (2015). Liraglutide in Type 2 Diabetes Mellitus: Clinical Pharmacokinetics and Pharmacodynamics. Clinical Pharmacokinetics, 55(6), 657. https://doi.org/10.1007/s40262-015-0343-6

Jin, X., Qiu, T., Li, L., Yu, R., Chen, X., Li, C., Proud, C G., & Jiang, T. (2023, June 1). Pathophysiology of obesity and its associated diseases. Acta Pharmaceutica Sinica B, 13(6), 2403-2424. https://doi.org/10.1016/j.apsb.2023.01.012

Jones, G. L., Wittmann, G., Yokosawa, E. B., Yu, H., Mercer, A. J., Lechan, R. M., & Low, M. J. (2019). Selective Restoration of Pomc Expression in Glutamatergic POMC Neurons: Evidence for a Dynamic Hypothalamic Neurotransmitter Network. https://doi.org/https://doi.org/10.1523/ENEURO.0400-18.2019

Jorgensen, S., Karnošová, A., Mazzaferro, S., Rowley, O., Hsiao-Jou, C C., Robbins, S J., Christofides, S., Merkle, F T., Maletínská, L., & Petrik, D. (2024, January 1). An analogue of the Prolactin Releasing Peptide reduces obesity and promotes adult neurogenesis. EMBO Reports, 25(1). https://doi.org/https://doi.org/10.1038/s44319-023-00016-2

Jurkowski, M. P., Bettio, L. E. B., Woo, E. K., Patten, A., Yau, S.-Y., & Gil-Mohapel, J. (2020). Beyond the Hippocampus and the SVZ: Adult Neurogenesis Throughout the Brain [Review of Beyond the

Hippocampus and the SVZ: Adult Neurogenesis Throughout the Brain]. Frontiers in Cellular Neuroscience, 14. Frontiers Media. https://doi.org/10.3389/fncel.2020.576444

Kanoski, S. E., Rupprecht, L. E., Fortin, S. M., Jonghe, B. C. D., & Hayes, M. R. (2011). The role of nausea in food intake and body weight suppression by peripheral GLP-1 receptor agonists, exendin-4 and liraglutide. Neuropharmacology, 62, 1916. https://doi.org/10.1016/j.neuropharm.2011.12.022

Kaplan, M., & Hinds, J W. (1977, September 9). Neurogenesis in the Adult Rat: Electron Microscopic Analysis of Light Radioautographs. American Association for the Advancement of Science, 197(4308), 1092-1094. https://doi.org/10.1126/science.887941

Karagiannis, P., Takahashi, K., Saito, M., Yoshida, Y., Okita, K., Watanabe, A., Inoue, H., Yamashita, J K J K., Todani, M., Nakagawa, M., Osawa, M., Yashiro, Y., Yamanaka, S., & Osafune, K. (2019, January 1). Induced Pluripotent Stem Cells And Their Use In Human Models Of Disease And Development. Physiological Reviews. https://doi.org/10.1152/physrev.00039.2017

Karmi, A., Iozzo, P., Viljanen, A., Hirvonen, J., Fielding, B. A., Virtanen, K. A., Oikonen, V., Kemppainen, J., Viljanen, T., Guiducci, L., Haaparanta-Solin, M., Någren, K., Solin, O., & Nuutila, P. (2010). Increased Brain Fatty Acid Uptake in Metabolic Syndrome. Diabetes, 59(9), 2171. https://doi.org/10.2337/db09-0138

Kempermann, G., Gage, F H., Aigner, L., Song, H., Curtis, M A., Thuret, S., Kuhn, H G., Jessberger, S., Frankland, P W., Cameron, H A., Gould, E., Hen, R., Abrous, D N., Toni, N., Schinder, A F., Zhao, X., Lucassen, P J., & Frisén, J. (2018, July 5). Human Adult Neurogenesis: Evidence and Remaining Questions. Cell Stem Cell. https://doi.org/https://doi.org/10.1016/j.stem.2018.04.004

Kempermann, G., Kuhn, H G., & Gage, F H. (1998, May 1). Experience-Induced Neurogenesis in the Senescent Dentate Gyrus. Society for Neuroscience, 18(9), 3206-3212. https://doi.org/10.1523/jneurosci.18-09-03206.1998

Kennedy, A J., Ellacott, K L J., King, V L., & Hasty, A H. (2010, January 1). Mouse models of the metabolic syndrome. Disease models & mechanisms. https://doi.org/ 10.1242/dmm.003467

Kernie, S G., Liebl, D J., & Parada, L F. (2000, March 15). BDNF regulates eating behavior and locomotor activity in mice. Springer Nature, 19(6), 1290-1300. https://doi.org/10.1093/emboj/19.6.1290

Khandpur, R. S. (2019). Bone Density Measurement: Dual Energy X -ray Technique. In Compendium of Biomedical Instrumentation (p. 295). https://doi.org/10.1002/9781119288190.ch55

Kim, T., Choi, H., & Chung, Y. (2016, June 30). Treadmill exercise alleviates impairment of cognitive function by enhancing hippocampal neuroplasticity in the high-fat diet-induced obese mice. Journal of Exercise Rehabilitation, 12(3), 156-162. https://doi.org/10.12965/jer.1632644.322

King, A E., Brain, A M., Hanson, K., Dittmann, J., Vickers, J C., & Fernandez-Martos, C. (2018, March 15). Disruption of leptin signalling in a mouse model of Alzheimer's disease. Metabolic Brain Disease, 33(4), 1097-1110. https://doi.org/10.1007/s11011-018-0203-9

Kirwan, P., Jura, M., & Merkle, F T. (2017, October 1). Generation and Characterization of Functional Human Hypothalamic Neurons. Wiley, 81(1). https://doi.org/10.1002/cpns.40

Kjems, L L., Holst, J J., Vølund, A., & Madsbad, S. (2003, February 1). The Influence of GLP-1 on Glucose-Stimulated Insulin Secretion Effects on b-Cell Sensitivity in Type 2 and Nondiabetic Subjects. Diabetes. https://doi.org/https://doi.org/10.2337/diabetes.52.2.380

Klaauw, A A V D. (2018, January 1). Neuropeptides in Obesity and Metabolic Disease. American Association for Clinical Chemistry, 64(1), 173-182. https://doi.org/10.1373/clinchem.2017.281568

Klein, C., Jonas, W., Iggena, D., Empl, L., Rivalan, M., Wiedmer, P., Spranger, J., Hellweg, R., Winter, Y., & Steiner, B. (2016, March 1). Exercise prevents high-fat diet-induced impairment of flexible memory expression in the water maze and modulates adult hippocampal neurogenesis in mice

Klein, C., Jonas, W., Wiedmer, P., Schreyer, S., Akyüz, L., Spranger, J., Hellweg, R., & Steiner, B. (2019, January 1). High-fat Diet and Physical Exercise Differentially Modulate Adult Neurogenesis in the Mouse Hypothalamus. Neuroscience. https://doi.org/ 10.1016/j.neuroscience.2018.12.037

Knudsen, L. B., Nielsen, P. F., Huusfeldt, P. O., Johansen, N. L., Madsen, K., Pedersen, F. Z., Thøgersen, H., Wilken, M., & Agersø, H. (2000). Potent Derivatives of Glucagon-like Peptide-1 with Pharmacokinetic Properties Suitable for Once Daily Administration. Journal of Medicinal Chemistry, 43(9), 1664. https://doi.org/10.1021/jm9909645

Kohler, S., Williams, N I., Stanton, G B., Cameron, J L., & Greenough, W T. (2011, June 6). Maturation time of new granule cells in the dentate gyrus of adult macaque monkeys exceeds six months. National Academy of Sciences, 108(25), 10326-10331. https://doi.org/10.1073/pnas.1017099108

Koketsu, D., Mikami, A., Miyamoto, Y., & Hisatsune, T. (2003). Nonrenewal of Neurons in the Cerebral Neocortex of Adult Macaque Monkeys. Journal of Neuroscience, 23(3), 937. https://doi.org/10.1523/jneurosci.23-03-00937.2003

Kokoeva, M. V., Yin, H., & Flier, J. S. (2005). Neurogenesis in the Hypothalamus of Adult Mice: Potential Role in Energy Balance. Science, 310(5748), 679. https://doi.org/10.1126/science.1115360

Kokoeva, M. V., Yin, H., & Flier, J. S. (2007). Evidence for constitutive neural cell proliferation in the adult murine hypothalamus. The Journal of Comparative Neurology, 505(2), 209. https://doi.org/10.1002/cne.21492

Korf, H., & Moller, M. (2021, January 1). Chapter 15 Arcuate nucleus, median eminence, and hypophysial pars tuberalis. Handbook of Clinical Neurology

Kořínková, L., Holubová, M., Nepraśová, B., & Hru, L. (2020, January 1). Synergistic effect of leptin and lipidized PrRP on metabolic pathways in ob/ob mice. https://doi.org/ 10.1530/JME-19-0188

Kornack, D R., & Rakić, P. (1999, May 11). Continuation of neurogenesis in the hippocampus of the adult macaque monkey. National Academy of Sciences, 96(10), 5768-5773. https://doi.org/10.1073/pnas.96.10.5768

Kronenberg, G., Bick-Sander, A., Bunk, E C., Wolf, C., Ehninger, D., & Kempermann, G. (2006, October 1). Physical exercise prevents age-related decline in precursor cell activity in the mouse dentate gyrus. Neurobiology of aging, 27(10), 1505-1513. https://doi.org/10.1016/j.neurobiolaging.2005.09.016

Kuehn, B. M. (2020). Medical News & Perspectives In Alzheimer Research, Glucose Metabolism Moves to Center Stage. https://doi.org/10.1001/jama.2019.20939

Kuhn, H G., Dickinson-Anson, H., & Gage, F H. (1996, March 15). Neurogenesis in the dentate gyrus of the adult rat: age-related decrease of neuronal progenitor proliferation. Society for Neuroscience, 16(6), 2027-2033. https://doi.org/10.1523/jneurosci.16-06-02027.1996

Kuhn, H G., Toda, T., & Gage, F H. (2018, October 31). Adult Hippocampal Neurogenesis: A Coming-of-Age Story. Society for Neuroscience, 38(49), 10401-10410. https://doi.org/10.1523/jneurosci.2144-18.2018

Kuneš, J., Pražienková, V., Popelová, A., Mikulášková, B., Zemenová, J., & Maletínská, L. (2016, August 1). Prolactin-releasing peptide: a new tool for obesity treatment. Bioscientifica, 230(2), R51-R58. https://doi.org/10.1530/joe-16-0046

Kushner, R F., Calanna, S., Davies, M., Dicker, D., Garvey, W T., Goldman, B., Lingvay, I., Thomsen, M., Wadden, T A., Wharton, S., Wilding, J P H., & Rubino, D. (2020, January 1). Semaglutide 2.4 mg for the Treatment of Obesity: Key Elements of the STEP Trials 1 to 5. Obesity. https://doi.org/10.1002/oby.22794.

Laing, B T., Do, K., Matsubara, T., Wert, D., Avery, M J., Langdon, E M., Zheng, D., & Hu, H. (2016, May 1). Voluntary exercise improves hypothalamic and metabolic function in obese mice. Bioscientifica, 229(2), 109-122. https://doi.org/10.1530/joe-15-0510

Lam, B Y., Cimino, I., Polex-Wolf, J., Kohnke, S N., Rimmington, D., Iyemere, V., Heeley, N., Cossetti, C., Schult, R., Saraiva, L R., Logan, D W., Blouet, C., O'Rahilly, S., Coll, A P., & Yeo, G S. (2017, January 1). Heterogeneity of hypothalamic pro-opiomelanocortin-expressing neurons revealed by single-cell RNA sequencing. Molecular Metabolism. https://doi.org/ 10.1016/j.molmet.2017.02.007

Landry, T., Shookster, D., Chaves, A., Free, K., Nguyen, T., & Hu, H. (2022, March 1). Exercise increases NPY/AgRP and TH neuron activity in the hypothalamus of female mice. Bioscientifica, 252(3), 167-177. https://doi.org/10.1530/joe-21-0250

Langlet, F. (2014, October 16). Tanycytes: A Gateway to the Metabolic Hypothalamus. Wiley, 26(11), 753-760. https://doi.org/10.1111/jne.12191

Lawrence, C B., Celsi, F., Brennand, J., & Luckman, S M. (2000, July 1). Alternative role for prolactin-releasing peptide in the regulation of food intake. Nature Portfolio, 3(7), 645-646. https://doi.org/10.1038/76597

Lawrence, C B., Ellacott, K L J., & Luckman, S M. (2002, February 1). PRL-Releasing Peptide Reduces Food Intake and May Mediate Satiety Signaling. Oxford University Press, 143(2), 360-367. https://doi.org/10.1210/endo.143.2.8609

Leasure, J L., & Jones, M. (2008, October 1). Forced and voluntary exercise differentially affect brain and behavior. Neuroscience, 156(3), 456-465. https://doi.org/10.1016/j.neuroscience.2008.07.041

Lechan, R M., & Toni, R. (2013, February 22). Functional Anatomy of the Hypothalamus and Pituitary. Endotext. https://pubmed.ncbi.nlm.nih.gov/25905349/

Lee, D A., & Blackshaw, S. (2012, July 31). Functional implications of hypothalamic neurogenesis in the adult mammalian brain. Wiley, 30(8), 615-621. https://doi.org/10.1016/j.ijdevneu.2012.07.003

Lee, D A., Bedont, J L., Pak, T., Wang, H., Song, J., Miranda-Angulo, A., Takiar, V., Charubhumi, V., Balordi, F., Takebayashi, H., Aja, S., Ford, E., Fishell, G., & Blackshaw, S. (2012, November 1). Tanycytes of the Hypothalamic Median Eminence Form a Diet Responsive Neurogenic Niche. Nature Neuroscience . https://doi.org/10.1038/nn.3079

Lee, D A., Yoo, S., Pak, T., Salvatierra, J., Velarde, E., Aja, S., & Blackshaw, S. (2014, June 13). Dietary and sex-specific factors regulate hypothalamic neurogenesis in young adult mice. Frontiers in Neuroscience. https://doi.org/10.3389/fnins.2014.00157

Lee, H., Kim, J.-J., Kim, H. J., Shong, M., Ku, B. J., & Jo, E. (2012). Upregulated NLRP3 Inflammasome Activation in Patients With Type 2 Diabetes. Diabetes, 62(1), 194. https://doi.org/10.2337/db12-0420

Lee, J., Seroogy, K B., & Mattson, M P. (2002, January 21). Dietary restriction enhances neurotrophin expression and neurogenesis in the hippocampus of adult mice. Wiley, 80(3), 539-547. https://doi.org/10.1046/j.0022-3042.2001.00747.x

Lee, T H., & Yau, S. (2020, December 28). From Obesity to Hippocampal Neurodegeneration: Pathogenesis and Non-Pharmacological Interventions. International Journal of Molecular Sciences. https://doi.org/https://dx.doi.org/10.3390/ ijms22010201

Legendre, A., & Harris, R B S. (2006, November 1). Exaggerated response to mild stress in rats fed high-fat diet. American Physiological Society, 291(5), R1288-1294. https://doi.org/10.1152/ajpregu.00234.2006

Leuner, B., Kozorovitskiy, Y., Gross, C G., & Gould, E. (2007, October 23). Diminished adult neurogenesis in the marmoset brain precedes old age. National Academy of Sciences, 104(43), 17169-17173. https://doi.org/10.1073/pnas.0708228104

Li, B., Liang, J., Lu, F., Zeng, G., Zhang, J., Ma, Y., Liu, P., Wang, Q., Zhou, Q., & Chen, L. (2020, April 6). Discovery of Novel Inhibitor for WNT/β-Catenin Pathway by Tankyrase 1/2 Structure-Based Virtual Screening. Multidisciplinary Digital Publishing Institute, 25(7), 1680-1680. https://doi.org/10.3390/molecules25071680

Li, J., Tang, Y., & Cai, D. (2012, October 1). IKKβ/NF-κB Disrupts Adult Hypothalamic Neural Stem Cells to Mediate Neurodegenerative Mechanism of Dietary Obesity and Pre-Diabetes. Nature Cell Biology. https://doi.org/10.1038/ncb2562

Lie, D. C., Dziewczapolski, G., Willhoite, A. R., Kaspar, B. K., Shults, C. W., & Gage, F. H. (2002). The Adult Substantia Nigra Contains Progenitor Cells with Neurogenic Potential. Journal of Neuroscience, 22(15), 6639. https://doi.org/10.1523/jneurosci.22-15-06639.2002

Lieu, L., Chau, D., Afrin, S., Dong, Y., Alhadeff, A L., Betley, J N., & Williams, K W. (2020, October 1). Effects of metabolic state on the regulation of melanocortin circuits. Physiology and Behavior. https://doi.org/10.1016/j.physbeh.2020.113039

Lin, S., Thomas, T. C., Storlien, L., & Huang, X. (2000). Development of high fat diet-induced obesity and leptin resistance in C57Bl/6J mice. International Journal of Obesity, 24(5), 639. https://doi.org/10.1038/sj.ijo.0801209

Lindqvist, A., Mohapel, P., Bouter, B., Frielingsdorf, H., Pizzoc, D., Brundin, P., & Erlanson-Albertsson, C. (2006, January 1). High-fat diet impairs hippocampal neurogenesis in male rats. European Journal of Neurology. https://doi.org/10.1111/j.1468-1331.2006.01500.x

Lionetti, L., Mollica, M., Lombardi, A., Cavaliere, G., Gifuni, G., & Barletta, A. (2009, January 1). From chronic overnutrition to insulin resistance: The role of fat-storing capacity and inflammation. Nutrition, Metabolism, and Dardiovascular Diseases. https://doi.org/10.1016/j.numecd.2008.10.010

Liraglutide. (2020, January 1). https://bnf.nice.org.uk/drugs/liraglutide/

Liu, P., Wang, Z.-H., Kang, S. S., Liu, X., Xia, Y., Chan, C.-B., & Ye, K. (2022). High-fat diet-induced diabetes couples to Alzheimer's disease through inflammation-activated C/EBPβ/AEP pathway. Molecular Psychiatry, 27(8), 3396. https://doi.org/10.1038/s41380-022-01600-z

Liu, Y., Yan, T., Chu, J M., Chen, Y., Dunnett, S., Ho, Y., Wong, G T., & Chang, R C. (2019, January 1). The beneficial effects of physical exercise in the brain and related pathophysiological mechanisms in neurodegenerative diseases. Laboratory investigation; a journal of technical methods and pathology. https://doi.org/ 10.1038/s41374-019-0232-y

Lledo, P., Alonso, M., & Grubb, M S. (2006, March 1). Adult neurogenesis and functional plasticity in neuronal circuits. Nature Reviews Neuroscience . https://www.nature.com/articles/nrn1867

Loprinzi, P D., Ponce, P., Zou, L., & Li, H. (2019, June 20). The Counteracting Effects of Exercise on High-Fat Diet-Induced Memory Impairment: A Systematic Review. Brain Sciences. https://doi.org/https://doi.org/10.3390/brainsci9060145

Luppino, F S., Wit, L M D., Bouvy, P F., Stijnen, T., Cuijpers, P., Penninx, B W J H., & Zitman, F G. (2010, January 1). Overweight, Obesity, and Depression: A Systematic Review and Meta-analysis of Longitudinal Studies. Archives of General Psychiatry. https://doi.org/10.1001/archgenpsychiatry.2010.2

Mackay, H A., & Abizaid, A. (2014, December 1). Embryonic development of the hypothalamic feeding circuitry: Transcriptional, nutritional, and hormonal influences. Molecular Metabolism, 3(9), 813-822. https://doi.org/10.1016/j.molmet.2014.09.004

Madisen, L., Zwingman, T A., Sunkin, S M., Oh, S W., Zariwala, H A., Gu, H., Ng, L L., Palmiter, R D., Hawrylycz, M J., Jones, A R., Lein, E S., & Zeng, H. (2010, January 1). A robust and high-throughput Cre reporting and characterization system for the whole mouse brain. Nature Neuroscience . https://www.nature.com/articles/nn.2467

Mahase, E. (2022, February 8). NICE recommends weight loss drug semaglutide for obese adults. , o340-o340. https://doi.org/10.1136/bmj.o340

Makrygianni, E A., & Chrousos, G P. (2022, September 22). Extracellular Vesicles and the Stress System. Karger Publishers, 113(2), 120-167. https://doi.org/10.1159/000527182

Makrygianni, E A., & Chrousos, G P. (2023, July 11). Neural Progenitor Cells and the Hypothalamus. Multidisciplinary Digital Publishing Institute, 12(14), 1822-1822. https://doi.org/10.3390/cells12141822

Malberg, J E., Eisch, A J., Nestler, E J., & Duman, R S. (2000, December 15). Chronic Antidepressant Treatment Increases Neurogenesis in Adult Rat Hippocampus. Society for Neuroscience, 20(24), 9104-9110. https://doi.org/10.1523/jneurosci.20-24-09104.2000

Maletínská, L., Nagelová, V., Tichá, A., Zemenová, J., Pirník, Z., Holubová, M., Špolcová, A., Mikulášková, B., Blechová, M., Sýkora, D., Lacinová, Z., Haluzík, M., Železná, B., & Kuneš, J. (2015, April 14). Novel lipidized analogs of prolactin-releasing peptide have prolonged half-lives and exert anti-obesity effects after peripheral administration. International Journal of Obesity. https://doi.org/https://doi.org/10.1038/ijo.2015.28

Maletínská, L., Popelová, A., Železná, B., Bencze, M., & Kuneš, J. (2019, February 1). The impact of anorexigenic peptides in experimental models of Alzheimer's disease pathology. The Journal of Endocrinology. https://doi.org/10.1530/JOE-18-0532

Maletínská, L., Spolcová, A., Maixnerová, J., Blechová, M., & Zelezná, B. (2011, January 1). Biological properties of prolactin-releasing peptide analogs with a modified aromatic ring of a C-terminal phenylalanine amide. Peptides. https://doi.org/https://doi.org/10.1016/j.peptides.2011.08.011

Mandal, A., Prabhavalkar, K S., & Bhatt, L K. (2018, February 14). Gastrointestinal hormones in regulation of memory. Peptides. https://doi.org/https://doi.org/10.1016/j.peptides.2018.02.003

Mason, H D., & McGavern, D B. (2022, October 1). How the immune system shapes neurodegenerative diseases. Peptides, 45(10), 733-748. https://doi.org/10.1016/j.tins.2022.08.001

Mathews, K J., Allen, K M., Boerrigter, D., Ball, H J., Weickert, C S., & Double, K L. (2017, August 1). Evidence for reduced neurogenesis in the aging human hippocampus despite stable stem cell markers. Wiley, 16(5), 1195-1199. https://doi.org/10.1111/acel.12641

McNay, D., Briançon, N., Kokoeva, M V., Maratos–Flier, E., & Flier, J S. (2012, January 3). Remodeling of the arcuate nucleus energy-balance circuit is inhibited in obese mice. Journal of Clinical Investigation, 122(1), 142-152. https://doi.org/10.1172/jci43134

Mercer, A. J., Hentges, S. T., Meshul, C. K., & Low, M. J. (2013). Unraveling the Central Proopiomelanocortin Neural Circuits. Frontiers in Neuroscience, 7. https://doi.org/10.3389/fnins.2013.00019

Merkle, F. T., Maroof, A., Wataya, T., Sasai, Y., Studer, L., Eggan, K., & Schier, A. F. (2015). Generation of neuropeptidergic hypothalamic neurons from human pluripotent stem cells. Development, 142(4), 633. https://doi.org/10.1242/dev.117978

Meshi, D., Drew, M R., Saxe, M., Ansorge, M S., David, D J., Santarelli, L., Malapani, C., Moore, H., & Hen, R. (2006, April 30). Hippocampal neurogenesis is not required for behavioral effects of environmental enrichment. Nature Portfolio, 9(6), 729-731. https://doi.org/10.1038/nn1696

Messier, C., Awad, N., & Gagnon, M. (2004). The relationships between atherosclerosis, heart disease, type 2 diabetes and dementia. Neurological Research, 26(5), 567. https://doi.org/10.1179/016164104225016263

Migaud, M., Batailler, M., Segura, S., Duittoz, A., Franceschini, I., & Pillon, D. (2010, December 1). Emerging new sites for adult neurogenesis in the mammalian brain: a comparative study between the hypothalamus and the classical neurogenic zones. Wiley, 32(12), 2042-2052. https://doi.org/10.1111/j.1460-9568.2010.07521.x

Miklossy, J., Qing, H., Radenović, A., Kis, A., Vileno, B., Forró, L., Miller, L. M., Martins, R. N., Waeber, G., Mooser, V., Bosman, F. T., Khalili, K., Darbinian, N., & McGeer, P. L. (2008). Beta amyloid and hyperphosphorylated tau deposits in the pancreas in type 2 diabetes. Neurobiology of Aging, 31(9), 1503. https://doi.org/10.1016/j.neurobiolaging.2008.08.019

Mikulaskova, B., Zemenová, J., Pirnik, Z., Prazienkova, V., Bednarova, L., Zelezna, B., Maletinska, L., & Kunes, J. (2016, January 1). Effect of palmitoylated prolactin-releasing peptide on food intake and neural activation after different routes of peripheral administration in rats. Peptides. https://doi.org/10.1016/j.peptides.2015.11.005

Miletta, M C., Iyilikci, O., Shanabrough, M., Šestan-Peša, M., Cammisa, A., Zeiss, C J., Dietrich, M O., & Horváth, T L. (2020, October 26). AgRP neurons control compulsive exercise and survival in an activity-based anorexia model. Nature Portfolio, 2(11), 1204-1211. https://doi.org/10.1038/s42255-020-00300-8

Millington, G W M. (2007, January 1). The role of proopiomelanocortin (POMC) neurones in feeding behaviour. BioMed Central, 4(1), 18-18. https://doi.org/10.1186/1743-7075-4-18

Miranda-Angulo, A L., Byerly, M S., Mesa, J., Wang, H., & Blackshaw, S. (2014, March 1). Rax regulates hypothalamic tanycyte differentiation and barrier function in mice. The Journal of Comparative Neurology. https://doi.org/10.1002/cne.23451

Monte, S M D L. (2012, January 1). Brain Insulin Resistance and Deficiency as Therapeutic Targets in Alzheimer's Disease. Current Alzheimer Research. https://doi.org/10.2174/156720512799015037

Monte, S M D L., & Wands, J R. (2008, November 1). Alzheimer's Disease Is Type 3 Diabetes—Evidence Reviewed. Journal of Diabetes Science and Technology. https://doi.org/10.1177/193229680800200619

Moraes, J C., Coope, A., Morari, J., Cintra, D E., Roma, E A., Pauli, J R., Romanatto, T., Carvalheira, J B., Oliveira, A L R., Saad, M J., & Velloso, L A. (2009, January 2). High-Fat Diet Induces Apoptosis of Hypothalamic Neurons. Plos One. https://doi.org/10.1371/journal.pone.0005045

Mori, T., Tanaka, K., Buffo, A., Wurst, W., Kühn, R., & Götz, M. (2006, May 1). Inducible gene deletion in astroglia and radial glia—A valuable tool for functional and lineage analysis. Wiley, 54(1), 21-34. https://doi.org/10.1002/glia.20350

Morita, S., & Miyata, S. (2012, May 16). Different vascular permeability between the sensory and secretory circumventricular organs of adult mouse brain. Cell and Tissue Research, 349(2), 589-603. https://doi.org/10.1007/s00441-012-1421-9

Muta, O., Odaka, M., Fujii, Y., Fushimi, T., Sato, H., & Osakabe, N. (2023, May 1). Difference in endocrine and behavior between short-term single- and paired-housing mice in metabolic cage. Neuroscience Letters, 806, 137246-137246. https://doi.org/10.1016/j.neulet.2023.137246

Myšková, A., Sýkora, D., Kuneš, J., & Maletínská, L. (2023). Lipidization as a tool toward peptide therapeutics. Drug Delivery, 30(1). https://doi.org/10.1080/10717544.2023.2284685

Nakandakari, S C B R., Muñoz, V R., Kuga, G K., Gaspar, R C., Sant'Ana, M R., Pavan, I C B., Silva, L G S D., Morelli, A P., Simabuco, F M., Silva, A S R D., Moura, L P D., Ropelle, E R., Cintra, D E., & Pauli, J R. (2019, January 1). Short-term high-fat diet modulates several inflammatory, ER stress, and apoptosis markers in the hippocampus of young mice. Brain, behavior, and immunity. https://doi.org/10.1016/j.bbi.2019.02.016

Nakano, H. (2004, January 1). Signaling crosstalk between NF-kB and JNK. Trends in Immunology. https://doi.org/10.1016/j.it.2004.05.007

Nasu, M., Esumi, S., Hatakeyama, J., Tamamaki, N., & Shimamura, K. (2021, April 16). Two-Phase Lineage Specification of Telencephalon Progenitors Generated From Mouse Embryonic Stem Cells. Frontiers in Cell and Developmental Biology . https://doi.org/https://doi.org/10.3389/fcell.2021.632381

Neaverson, A., Andersson, M. H. L., Arshad, O. A., Foulser, L., Goodwin-Trotman, M., Hunter, A., Newman, B., Patel, M., Roth, C., Thwaites, T., Kilpinen, H., Hurles, M. E., Day, A., & Gerety, S. S. (2023). Differentiation of human induced pluripotent stem cells into cortical neural stem cells. Frontiers in cell and developmental biology, 10, 1023340. https://doi.org/10.3389/fcell.2022.1023340

Neto, A., Fernandes, A., & Barateiro, A. (2023, November 9). The complex relationship between obesity and neurodegenerative diseases: an updated review. Frontiers Media, 17. https://doi.org/10.3389/fncel.2023.1294420

NICE. (2020, December 9). Liraglutide for managing overweight and obesity. https://www.nice.org.uk/guidance/TA664

Niu, W., Zhang, T., Wang, L L., Zou, Y., & Zhang, C. (2018, November 1). Phenotypic Reprogramming of Striatal Neurons into Dopaminergic Neuron-like Cells in the Adult Mouse Brain. Stem Cell Reports, 11(5), 1156-1170. https://doi.org/10.1016/j.stemcr.2018.09.004

Niwa, A., Nishibori, M., Hamasaki, S., Kobori, T., Liu, K., Wake, H., Mori, S., Yoshino, T., & Takahashi, H. (2015, January 30). Voluntary exercise induces neurogenesis in the hypothalamus and ependymal lining of the third ventricle. Brain structure & function, 221(3), 1653-1666. https://doi.org/10.1007/s00429-015-0995-x

Nottebohm, F., & Arnold, A P. (1976, October 8). Sexual Dimorphism in Vocal Control Areas of the Songbird Brain. American Association for the Advancement of Science, 194(4261), 211-213. https://doi.org/10.1126/science.959852

Nunomura, A., Castellani, R J., Zhu, X., Moreira, P I., Perry, G., & Smith, M A. (2006, July 1). Involvement of Oxidative Stress in Alzheimer Disease. Oxford University Press, 65(7), 631-641. https://doi.org/10.1097/01.jnen.0000228136.58062.bf

O'Brien, P D., Hinder, L M., Callaghan, B C., & Feldman, E L. (2017, June 1). Neurological consequences of obesity. The Lancet. Neurology, 16(6), 465-477. https://doi.org/10.1016/s1474-4422(17)30084-4

Okamoto, A., Fujii, R., Yoshimura, R., & Miyata, S. (2022, January 13). Transcytosis of tanycytes in the circumventricular organs of adult mouse brain. Neuroscience letters. https://doi.org/https://doi.org/10.1016/j.neulet.2022.136633

Olianas, M C., Dedoni, S., Ingianni, A., & Onali, P. (2017, January 1). LPA1-mediated antidepressant actions in neurons. Journal of Neurochemistry. https://doi.org/10.1111/jnc.14150

Orquera, D. P., Tavella, M. B., de Souza, F. S. J., Nasif, S., Low, M. J., & Rubinstein, M. (2019). The Homeodomain Transcription Factor NKX2.1 Is Essential for the Early Specification of Melanocortin Neuron Identity and Activates Pomc Expression in the Developing Hypothalamus.

Ortega, F., Berninger, B., & Costa, M R. (2013, January 1). Primary Culture and Live Imaging of Adult Neural Stem Cells and Their Progeny. Imaging and Tracking Stem Cells. https://doi.org/10.1007/7651_2013_22

Ortega-Pérez, I., Murray, K., & Lledo, P. (2007, June 29). The how and why of adult neurogenesis. Journal of Molecular Histology, 38(6), 555-562. https://doi.org/10.1007/s10735-007-9114-5

Owji, S., & Shoja, M M. (2019, August 19). The History of Discovery of Adult Neurogenesis. Wiley, 33(1), 41-55. https://doi.org/10.1002/ca.23447

Özcan, U., Cao, Q., Yilmaz, E., Lee, A., Iwakoshi, N N., Özdelen, E., Tuncman, G., Görgün, C., Glimcher, L H., & Hotamisligil, G S. (2004, January 1). Endoplasmic Reticulum Stress Links Obesity, Insulin Action, and Type 2 Diabetes. Science. https://doi.org/10.1126/science.1103160

Palmer, T D., Schwartz, P H., Taupin, P., Kaspar, B., Stein, S A., & Gage, F H. (2001, January 1). Cell culture. Progenitor cells from human brain after death. Nature. https://doi.org/10.1038/35075141

Pan, Y., Zhang, X., Wang, Y., Cai, L., Ren, L., Tang, L., Wang, J., Zhao, Y., Wang, Y., Liu, Q., Li, X., & Liang, G. (2013, November 18). Targeting JNK by a New Curcumin Analog to Inhibit NF-kB-

Mediated Expression of Cell Adhesion Molecules Attenuates Renal Macrophage Infiltration and Injury in Diabetic Mice. Plos One. https://doi.org/https://doi.org/10.1371/journal.pone.0079084

Park, H R., Park, M., Choi, J., Park, K., Chung, H Y., & Lee, J. (2010, October 1). A high-fat diet impairs neurogenesis: Involvement of lipid peroxidation and brain-derived neurotrophic factor. Neuroscience Letters, 482(3), 235-239. https://doi.org/10.1016/j.neulet.2010.07.046

Park, H., Lee, S., Jung, J W., Kim, B C., Ryu, J H., & Kim, D H. (2015, January 7). Glucocorticoid- and long-term stress-induced aberrant synaptic plasticity are mediated by activation of the glucocorticoid receptor. Springer Nature, 38(6), 1204-1212. https://doi.org/10.1007/s12272-015-0548-0

Parthsarathy, V., & Hölscher, C. (2013, March 11). Chronic Treatment with the GLP1 Analogue Liraglutide Increases Cell Proliferation and Differentiation into Neurons in an AD Mouse Model. Public Library of Science, 8(3), e58784-e58784. https://doi.org/10.1371/journal.pone.0058784

Pasquettaz, R., Kolotuev, I., Rohrbach, A., Gouelle, C., Pellerin, L., & Langlet, F. (2020, June 9). Peculiar protrusions along tanycyte processes face diverse neural and nonneural cell types in the hypothalamic parenchyma. Wiley, 529(3), 553-575. https://doi.org/10.1002/cne.24965

Patel, D., & Stanford, F C. (2018, February 1). Safety and tolerability of new-generation anti-obesity medications: a narrative review. Taylor & Francis, 130(2), 173-182. https://doi.org/10.1080/00325481.2018.1435129

Paxinos, G., & Franklin, K B. (2004, January 1). Paxinos and Franklin’s The Mouse Brain in Stereotaxic Coordinates, Fifth Edition. Elsevier Academic

Pencea, V., Bingaman, K D., Wiegand, S J., & Luskin, M B. (2001, September 1). Infusion of Brain-Derived Neurotrophic Factor into the Lateral Ventricle of the Adult Rat Leads to New Neurons in the Parenchyma of the Striatum, Septum, Thalamus, and Hypothalamus. Journal of Neuroscience, 21(17), 6706-6717. https://doi.org/10.1523/jneurosci.21-17-06706.2001

Pérez-González, R., Antequera, D., Vargas, T., Spuch, C., Bolós, M., & Carro, E. (2011, April 22). Leptin Induces Proliferation of Neuronal Progenitors and Neuroprotection in a Mouse Model of Alzheimer\'s Disease. Journal of Alzheimer's Disease

Pérez-Martín, M., Cifuentes, M., Grondona, J M., López-Ávalos, M D., Gómez-Pinedo, U., García-Verdugo, J M., & Fernández-Llebrez, P. (2010, March 9). IGF-I stimulates neurogenesis in the hypothalamus of adult rats. The European Journal of Neuroscience. https://doi.org/10.1111/j.1460-9568.2010.07220.x

Pergola, G D., & Silvestris, F. (2013, January 1). Obesity as a Major Risk Factor for Cancer. Hindawi Publishing Corporation, 2013, 1-11. https://doi.org/10.1155/2013/291546

Péron, S., Miyakosh, L M., Bril, M S., Manzano-Franco, D., Serrano-López, J., Fan, W., Marichal, N., Ghanem, A., Conzelmann, K., Karow, M., Ortega, F., Gascón, S., & Berninger, B. (2023, December 12). Programming of neural progenitors of the adult subependymal zone towards a glutamatergic neuron lineage by neurogenin 2. Stem Cell Reports, 18. https://doi.org/https://doi.org/10.1016/j.stemcr.2023.10.01

Petrik, D., Jiang, Y., Birnbaum, S G., Powell, C M., Kim, M., Hsieh, J., & Eisch, A J. (2012, August 1). Functional and mechanistic exploration of an adult neurogenesis-promoting small molecule. The FASEB Journal. https://doi.org/10.1096/fj.11-201426: 10.1096/fj.11-201426

Petrik, D., Jörgensen, S., Eftychidis, V., & Siebzehnrübl, F A. (2022, February 18). Singular Adult Neural Stem Cells Do Not Exist. Multidisciplinary Digital Publishing Institute, 11(4), 722-722. https://doi.org/10.3390/cells11040722

Petrik, D., Myoga, M H., Grade, S., Gerkau, N J., Pusch, M., Rose, C R., Grothe, B., & Götz, M. (2018, May 17). Epithelial Sodium Channel Regulates Adult Neural Stem Cell Proliferation in a Flow-Dependent Manner. Cell Stem Cell, 22(6), 865-878.e8. https://doi.org/10.1016/j.stem.2018.04.016

Peyot, M., Gray, J P., Lamontagne, J., Smith, P J S., Holz, G G., Madiraju, S R M., Prentki, M., & Heart, E. (2009, July 13). Glucagon-Like Peptide-1 Induced Signaling and Insulin Secretion Do Not Drive Fuel and Energy Metabolism in Primary Rodent Pancreatic b-Cells. Plos One

Pierce, A A., & Xu, A W. (2010, January 13). De Novo Neurogenesis in Adult Hypothalamus as a Compensatory Mechanism to Regulate Energy Balance. The Journal of neuroscience : the official journal of the Society for Neuroscience. https://doi.org/10.1523/JNEUROSCI.2479-09.2010

Pirník, Z., Kolesárová, M., Železná, B., & Maletínská, L. (2018). Repeated peripheral administration of lipidized prolactin-releasing peptide analog induces c-fos and FosB expression in neurons of dorsomedial hypothalamic nucleus in male C57 mice. Neurochemistry International, 116, 77. https://doi.org/10.1016/j.neuint.2018.03.013

Pirník, Z., Železná, B., Kiss, A., & Maletínská, L. (2015). Peripheral administration of palmitoylated prolactin-releasing peptide induces Fos expression in hypothalamic neurons involved in energy homeostasis in NMRI male mice. Brain Research, 1625, 151. https://doi.org/10.1016/j.brainres.2015.08.042

Popelova, A., Prazienkov, V., Neprasova, B., Kasperova, B J., Hruba, L., Holubova, M., Zemenova, J., Blum, D., Zelezna, B., Galas, M., Kunes, J., & Maletinska, L. (2018, January 1). Novel Lipidized Analog of Prolactin-Releasing Peptide Improves Memory Impairment and Attenuates Hyperphosphorylation of Tau Protein in a Mouse Model of Tauopathy. Journal of Alzheimer's Disease . https://doi.org/10.3233/JAD-171041

Porter, D W., Kerr, B D., Flatt, P R., Hölscher, C., & Gault, V A. (2010, June 24). Four weeks administration of Liraglutide improves memory and learning as well as glycaemic control in mice with high fat dietary-induced obesity and insulin resistance. Wiley, 12(10), 891-899. https://doi.org/10.1111/j.1463-1326.2010.01259.x

Praag, H V. (2008, February 20). Neurogenesis and Exercise: Past and Future Directions. Neuromolecular Medicine, 10(2), 128-140. https://doi.org/10.1007/s12017-008-8028-z

Praag, H V., Christie, B R., Sejnowski, T J., & Gage, F H. (1999, November 9). Running enhances neurogenesis, learning, and long-term potentiation in mice. National Academy of Sciences, 96(23), 13427-13431. https://doi.org/10.1073/pnas.96.23.13427

Praag, H V., Kempermann, G., & Gage, F H. (1999, March 1). Running increases cell proliferation and neurogenesis in the adult mouse dentate gyrus. Nature Portfolio, 2(3), 266-270. https://doi.org/10.1038/6368

Praag, H V., Shubert, T E., Zhao, C., & Gage, F H. (2005, September 21). Exercise Enhances Learning and Hippocampal Neurogenesis in Aged Mice. Society for Neuroscience, 25(38), 8680-8685. https://doi.org/10.1523/jneurosci.1731-05.2005

Pramanik, K C., Makena, M R., Bhowmick, K., & Pandey, M K. (2018, December 5). Advancement of NF-κB Signaling Pathway: A Novel Target in Pancreatic Cancer. Multidisciplinary Digital Publishing Institute, 19(12), 3890-3890. https://doi.org/10.3390/ijms19123890

Pražienková, V., Funda , J., Pirník, Z., Karnošová, A., Hrubá , L., Kořínková, L., Neprašová, B., Janovská, P., Benzce, M., Kadlecov, M., Blaho, J., Kopecký, J., Železná, B., Kuneš, J., Bardova, K., & Maletínská, L. (2021). GPR10 gene deletion in mice increases basal neuronal activity, disturbs insulin sensitivity and alters lipid homeostasis . Gene. https://doi.org/10.1016/j.gene.2021.145427

Pražienková, V., Funda, J., Pirník, Z., Karnošová, A., Hrubá, L., Kořínková, L., Neprašová, B., Janovská, P., Benzce, M., Kadlecov, M., Blaho, J., Kopecký, J., Železná, B., Kuneš, J., Bardova, K., & Maletínská, L. (2021, January 5). GPR10 gene deletion in mice increases basal neuronal activity, disturbs insulin sensitivity and alters lipid homeostasis . Gene. https://doi.org/https://doi.org/10.1016/j.gene.2021.145427

Pražienková, V., Holubová, M., Pelantová, H., Bugáňová, M., Pirník, Z., Mikulášková, B., Popelová, A., Blechová, M., Haluzík, M., Železná, B., Kuzma, M., Kuneš, J., & Maletínská, L. (2017, January 1). Impact of novel palmitoylated prolactin-releasing peptide analogs on metabolic changes in mice with diet-induced obesity. Plos One. https://doi.org/10.1371/journal.pone.0183449

Prazienkova, V., Ticha, A., Blechova, M., Spolcova, A., Zelenza, B., & Malentinska, L. (2016, January 1). Pharmacological Characterization Of Lipidized Analogs Of Prolactin-Releasing Peptide With A Modified C-Terminal Aromatic Ring. Journal Of Physiology And Pharmacology. https://www.jpp.krakow.pl/journal/archive/02_16/pdf/121_02_16_article.pdf

Pražienková., Popelová., Kuneš, J., & Maletínská. (2019, October 24). Prolactin-Releasing Peptide: Physiological and Pharmacological Properties. Multidisciplinary Digital Publishing Institute, 20(21), 5297-5297. https://doi.org/10.3390/ijms20215297

Prevot, V., Dehouck, B., Sharif, A., Ciofi, P., Giacobini, P., & Clasadonte, J. (2018, January 17). The Versatile Tanycyte: A Hypothalamic Integrator of Reproduction and Energy Metabolism. Endocrine Reviews. https://doi.org/10.1210/er.2017-00235

Profenno, L. A., Porsteinsson, A. P., & Faraone, S. V. (2009). Meta-Analysis of Alzheimer's Disease Risk with Obesity, Diabetes, and Related Disorders. https://doi.org/10.1016/j.biopsych.2009.02.013

Pugazhenthi, S., Qin, L., & Reddy, P H. (2018, May 1). Common Neurodegenerative Pathways in Obesity, Diabetes, and Alzheimer's Disease. Molecular basis of disease. https://doi.org/10.1016/j.bbadis.2016.04.017

Raffaitin, C., Gin, H., Empana, J., Helmer, C., Berr, C., Tzourio, C., Portet, F., Dartigues, J., Alpérovitch, A., & Barberger-Gateau, P. (2009, January 1). Metabolic syndrome and risk for incident Alzheimer's disease or vascular dementia: the Three-City Study. Diabetes care. https://doi.org/10.2337/dc08-0272

Rajamani, U., Gross, A R., Hjelm, B E., Sequeira, A., Vawter, M P., Tang, J., Gangalapudi, V., Wang, Y., Andres, A M., Gottlieb, R A., & Sareen, D. (2018, May 3). Super-Obese Patient-Derived iPSC Hypothalamic Neurons Exhibit Obesogenic Signatures and Hormone Responses. Cell Stem Cell. https://doi.org/10.1016/j.stem.2018.03.009

Razay, G., Vreugdenhil, A., & Wilcock, G. (2007, January 1). The Metabolic Syndrome and Alzheimer Disease. International Journal of Molecular Sciences. https://doi.org/10.3390/ijms24054354

Recabal, A., Caprile, T., & García, M. de los Á. (2017). Hypothalamic Neurogenesis as an Adaptive Metabolic Mechanism [Review of Hypothalamic Neurogenesis as an Adaptive Metabolic Mechanism]. Frontiers in Neuroscience, 11. Frontiers Media. https://doi.org/10.3389/fnins.2017.00190

Reich, N., & Hölscher, C. (2022, September 1). The neuroprotective effects of glucagon-like peptide 1 in Alzheimer's and Parkinson's disease: An in-depth review. Frontiers Media, 16. https://doi.org/10.3389/fnins.2022.970925

Ricci, G., Pirillo, I., Tomassoni, D., Sirignano, A., & Grappasonni, I. (2017, January 2). Metabolic syndrome, hypertension, and nervous system injury: Epidemiological correlates. Informa, 39(1), 8-16. https://doi.org/10.1080/10641963.2016.1210629

Richards, P., Parker, H. E., Adriaenssens, A. E., Hodgson, J. M., Cork, S. C., Trapp, S., Gribble, F. M., & Reimann, F. (2014). Identification and characterisation of glucagon-like peptide-1 receptor expressing cells using a new transgenic mouse model. https://doi.org/ 10.2337/db13-1440

Richier, B., & Salecker, I. (2014). Versatile genetic paintbrushes: Brainbow technologies. Wiley Interdisciplinary Reviews Developmental Biology, 4(2), 161. https://doi.org/10.1002/wdev.166

Rizzoti, K., & Lovell-Badge, R. (2017, April 1). Pivotal role of median eminence tanycytes for hypothalamic function and neurogenesis. Molecular and Cellular Endocrinology, 445, 7-13. https://doi.org/10.1016/j.mce.2016.08.020

Robins, S., Stewart, I., McNay, D., Taylor, V., Giachino, C., Goetz, M., Ninkovic, J., Briancon, N., Maratos-Flier, E., Flier, J., Kokoeva, M., & Placzek, M. (2013, June 27). a-Tanycytes of the adult hypothalamic thirdventricle include distinct populations of FGF-responsive neural progenitors. Nature Communications. https://doi.org/10.1038/ncomms3049

Robison, L S., Albert, N M., Camargo, L A., Anderson, B M., Salinero, A E., Riccio, D A., Abi-Ghanem, C., Gannon, O J., & Zuloaga, K L. (2020, January 1). High-Fat Diet-Induced Obesity Causes Sex- Specific

Deficits in Adult Hippocampal Neurogenesis in Mice. eNeuro. https://doi.org/ 10.1523/ENEURO.0391-19.2019

Rodriguez, E., Blázquez, J L., Pastor, F., Peláez, B., Peña, P L., Peruzzo, B., & Amat, P. (2005, January 1). Hypothalamic Tanycytes: A Key Component of Brain–Endocrine Interaction. International Review of Cytology, 247, 89-164. https://doi.org/10.1016/s0074-7696(05)47003-5

Rodríguez, J J., & Verkhratsky, A. (2011, January 1). Neurogenesis in Alzheimer's disease. Journal of Anatomy. https://doi.org/ 10.1111/j.1469-7580.2011.01343.x

Roh, E., Song, D. K., & Kim, M.-S. (2016). Emerging role of the brain in the homeostatic regulation of energy and glucose metabolism [Review of Emerging role of the brain in the homeostatic regulation of energy and glucose metabolism]. Experimental & Molecular Medicine, 48(3). Springer Nature. https://doi.org/10.1038/emm.2016.4

Rojczyk, E., Pałasz, A., & Wiaderkiewicz, R. (2014, April 18). Hypothalamic Subependymal Niche: A Novel Site of the Adult Neurogenesis. Cellular and Molecular Neurobiology, 34(5), 631-642. https://doi.org/10.1007/s10571-014-0058-5

Roland, B., Sutton, S. W., Wilson, S. J., Luo, L., Pyati, J., Huvar, R., Erlander, M. G., & Lovenberg, T. W. (1999). Anatomical Distribution of Prolactin-Releasing Peptide and Its Receptor Suggests Additional Functions in the Central Nervous System and Periphery. Endocrinology, 140(12), 5736. https://doi.org/10.1210/endo.140.12.7211

Romanov, R A., Tretiakov, E O., Kastriti, M E., Zupancic, M., Häring, M., Korchynska, S., Popadin, K., Benevento, M., Rebernik, P., Lallemend, F., Nishimori, K., Clotman, F., Andrews, W D., Parnavela, J G., Farlik, M., Bock, C., Adameyko, I., Hökfelt, T., Keimpema, E., & Harkany, T. (2020, January 1). Molecular design of hypothalamus development . Nature. https://doi.org/ 10.1038/s41586-020-2266-0

Rouaux, C., & Arlotta, P. (2013, February 1). Direct lineage reprogramming of postmitotic callosal neurons into corticofugal neurons in vivo. Nature Cell Biology. https://doi.org/10.1038/ncb2660

Rowe, R G., & Daley, G Q. (2019, February 8). Induced pluripotent stem cells in disease modelling and drug discovery. Nature Portfolio, 20(7), 377-388. https://doi.org/10.1038/s41576-019-0100-z

Ryan, D. H., Lingvay, I., Deanfield, J., Kahn, S. E., Barros, E., Burguera, B., Colhoun, H. M., Cercato, C., Dicker, D., Horn, D. B., Hovingh, G. K., Jeppesen, O. K., Kokkinos, A., Lincoff, A. M., Meyhöfer, S. M., Oral, T. K., Plutzky, J., Beek, A. P. van, Wilding, J., & Kushner, R. F. (2024). Long-term weight loss effects of semaglutide in obesity without diabetes in the SELECT trial. Nature Medicine, 30(7), 2049. https://doi.org/10.1038/s41591-024-02996-7

Sahay, A., Scobie, K N., Hill, A S., O'Carroll, C., Kheirbek, M A., Burghardt, N S., Fenton, A A., Dranovsky, A., & Hen, R. (2011, April 1). Increasing adult hippocampal neurogenesis is sufficient to improve pattern separation. Nature Portfolio, 472(7344), 466-470. https://doi.org/10.1038/nature09817

Samoylova, E., & Baklaushev, V P. (2020, September 1). Cell Reprogramming Preserving Epigenetic Age: Advantages and Limitations. Pleiades Publishing, 85(9), 1035-1047. https://doi.org/10.1134/s0006297920090047

Sánchez-Garrido, M A., Brandt, S J., Clemmensen, C., Müller, T D., DiMarchi, R D., & Tschöp, M H. (2017, July 21). GLP-1/glucagon receptor co-agonism for treatment of obesity. Diabetologia, 60(10), 1851-1861. https://doi.org/10.1007/s00125-017-4354-8

Santarelli, L., Saxe, M., Gross, C., Surget, A., Battaglia, F., Dulawa, S., Weisstaub, N., Lee, J., Duman, R., Arancio, O., Belzung, C., & Hen, R. (2003, January 1). Requirement of hippocampal neurogenesis for the behavioral effects of antidepressants. Science. https://doi.org/10.1126/science.1083328

Santos, R D S., Gross, A R., & Sareen, D. (2021, January 1). Hypothalamus and neuroendocrine diseases: The use of human-induced pluripotent stem cells for disease modeling. Handbook of Clinical Neurology. https://doi.org/10.1016/B978-0-12-820683-6.00025-7

Saunders, K H., Kumar, R B., Igel, L I., & Aronne, L J. (2016, May 15). Pharmacologic Approaches to Weight Management: Recent Gains and Shortfalls in Combating Obesity. Current Atherosclerosis Reports, 18(7). https://doi.org/10.1007/s11883-016-0589-y

Schaukowitch, K., Janas, J. A., & Wernig, M. (2023). Insights and applications of direct neuronal reprogramming [Review of Insights and applications of direct neuronal reprogramming]. Current Opinion in Genetics & Development, 83, 102128. Elsevier BV. https://doi.org/10.1016/j.gde.2023.102128

Schwartz, M W., Woods, S C., Porte, D., Seeley, R J., & Baskin, D G. (2000, April 1). Central nervous system control of food intake. Nature Portfolio, 404(6778), 661-671. https://doi.org/10.1038/35007534

Seal, L., Small, C J., Dhillo, W S., Stanley, S A., Abbott, C R., Ghatei, M A., & Bloom, S R. (2001, October 1). PRL-Releasing Peptide Inhibits Food Intake in Male Rats via the Dorsomedial Hypothalamic Nucleus and not the Paraventricular Hypothalamic Nucleus. Oxford University Press, 142(10), 4236-4243. https://doi.org/10.1210/endo.142.10.8419

Secher, A., Jelsing, J., Baquero, A F., Hecksher-Sørensen, J., Cowley, M A., Dalbøge, L S., Hansen, G., Grove, K L., Pyke, C., Raun, K., Schäffer, L., Tang-Christensen, M., Verma, S., Witgen, B M., Vrang, N., & Knudsen, L B. (2014, July 31). The arcuate nucleus mediates GLP-1 receptor agonist liraglutide-dependent weight loss. The Journal of Clinical Investigation . https://doi.org/10.1172/JCI75276.

Seong, J., Kang, J Y., Sun, J S., & Kim, K W. (2019, March 5). Hypothalamic inflammation and obesity: a mechanistic review. Archives of Pharmacalogical Research. https://doi.org/10.1007/s12272-019-01138-9

Sharif, A., Fitzsimons, C P., & Lucassen, P J. (2021, January 1). Neurogenesis in the adult hypothalamus: A distinct form of structural plasticity involved in metabolic and circadian regulation, with potential relevance for human pathophysiology. Handbook of Clinical Neurology. https://doi.org/10.1016/B978-0-12-819975-6.00006-6

Shi, L., Ji, Y., Jiang, X., Zhou, L., Xu, Y., Li, Y., Jiang, W., Meng, P., & Liu, X. (2015, February 7). Liraglutide attenuates high glucose-induced abnormal cell migration, proliferation, and apoptosis of vascular smooth muscle cells by activating the GLP-1 receptor, and inhibiting ERK1/2 and PI3K/Akt signaling pathways. BioMed Central, 14(1). https://doi.org/10.1186/s12933-015-0177-4

Shi, Y., Inoue, H., Wu, J C., & Yamanaka, S. (2016, December 16). Induced pluripotent stem cell technology: a decade of progress. Nature Portfolio, 16(2), 115-130. https://doi.org/10.1038/nrd.2016.245

Shoelson, S. E., Lee, J., & Goldfine, A. B. (2006). Inflammation and insulin resistance. Journal of Clinical Investigation, 116(7), 1793. https://doi.org/10.1172/jci29069

Siervo, M., Harrison, S L., Jagger, C., Robinson, L., & Stephan, B C M. (2014, June 4). Metabolic Syndrome and Longitudinal Changes in Cognitive Function: A Systematic Review and Meta-Analysis. IOS Press, 41(1), 151-161. https://doi.org/10.3233/jad-132279

Singh, I., Wang, L., Xia, B., Liu, J., Tahiri, A., Ouaamari, A E., Wheeler, M B., & Pang, Z P. (2022, October 29). Activation of arcuate nucleus glucagon-like peptide-1 receptor-expressing neurons suppresses food intake. BioMed Central, 12(1). https://doi.org/10.1186/s13578-022-00914-3

Singh, V K., Kalsan, M., Kumar, N., Saini, A., & Chandra, R. (2015, February 2). Induced pluripotent stem cells: applications in regenerative medicine, disease modeling, and drug discovery. Frontiers Media, 3. https://doi.org/10.3389/fcell.2015.00002

Sisley, S., Gutiérrez-Aguilar, R., Scott, M M., D'Alessio, D A., Sandoval, D A., & Seeley, R J. (2014, April 24). Neuronal GLP1R mediates liraglutide's anorectic but not glucose-lowering effect. Journal of Clinical Investigation, 124(6), 2456-2463. https://doi.org/10.1172/jci72434

Snodgrass, R. G., Huang, S., Choi, I.-W., Rutledge, J. C., & Hwang, D. H. (2013). Inflammasome-Mediated Secretion of IL-1b in Human Monocytes through TLR2 Activation; Modulation by Dietary Fatty Acids.

Snyder, J. S., Choe, J. S., Clifford, M. A., Jeurling, S. I., Hurley, P., Brown, A., Kamhi, J. F., & Cameron, H. A. (2009). Adult-Born Hippocampal Neurons Are More Numerous, Faster Maturing, and More Involved in Behavior in Rats than in Mice. Journal of Neuroscience, 29(46), 14484. https://doi.org/10.1523/jneurosci.1768-09.2009

Sobesky, J L., D'Angelo, H., Weber, M., Anderson, N D., Frank, M G., Watkins, L R., Maier, S F., & Barrientos, R M. (2016, July 1). Glucocorticoids Mediate Short-Term High-Fat Diet Induction of Neuroinflammatory Priming, the NLRP3 Inflammasome, and the Danger Signal HMGB1. Society for Neuroscience, 3(4), ENEURO.0113-16.2016. https://doi.org/10.1523/eneuro.0113-16.2016

Sohn, J., Elmquist, J K., & Williams, K W. (2013, September 1). Neuronal circuits that regulate feeding behavior and metabolism. Trends in Neurosciences, 36(9), 504-512. https://doi.org/10.1016/j.tins.2013.05.003

Solis, A J D., Río-Martín, A D., Radermacher, J., Chen, W., Steuernagel, L., Bauder, C A., Eggersmann, F R., Morgan, D A., Cremer, A., Sué, M., Germer, M., Kukat, C., Vollmar, S., Backes, H., Rahmouni, K.,

Kloppenburg, P., & Brüning, J C. (2024, February 20). Reciprocal activity of AgRP and POMC neurons governs coordinated control of feeding and metabolism. Nature Metabolism. https://doi.org/https://doi.org/10.1038/s42255-024-00987-z

Sonnefeld, L., Rohmann, N., Geisler, C., & Laudes, M. (2023, March 2). Is human obesity an inflammatory disease of the hypothalamus?. Oxford University Press, 188(3), R37-R45. https://doi.org/10.1093/ejendo/lvad030

Sorrells, S F., Paredes, M F., Cebrian-Silla, A., Sandoval, K., Qi, D., Kelley, K W., James, D., Mayer, S., Chang, J., Auguste, K I., Chang, E F., Gutierrez, A J., Kriegstein, A R., Mathern, G W., Oldham, M C., Huang, E J., Garcia-Verdugo, J M., Yang, Z., Alvarez-Buylla, A., & . (2018, March 7). Human hippocampal neurogenesis drops sharply in children to undetectable levels in adults. Nature. https://www.nature.com/articles/nature25975

Soudahome, A. G., Catan, A., Giraud, P., Kouao, S. A., Guérin-Dubourg, A., Debussche, X., Moullec, N. L., Bourdon, E., Bravo, S. B., Paradela-Dobarro, B., Álvarez, E., Meilhac, O., Rondeau, P., & Couprie, J. (2018). Glycation of human serum albumin impairs binding to the glucagon-like peptide-1 analogue liraglutide. Journal of Biological Chemistry, 293(13), 4778. https://doi.org/10.1074/jbc.m117.815274

Špolcová, A., Mikulášková, B., Holubová, M., Nagelová, V., Pirnik, Z., Zemenová, J., Haluzík, M., Železná, B., Galas, M., & Maletínská, L. (2015, January 1). Anorexigenic lipopeptides ameliorate central insulin signaling and attenuate tau phosphorylation in hippocampi of mice with monosodium glutamate-induced obesity. Journal of Alzheimer's disease. https://doi.org/10.3233/JAD-143150

Steen, E., Terry, B M., Rivera, E J., Cannon, J L., Neely, T R., Tavares, R., Xu, X J., Wands, J R., & Monte, S M D L. (2005, February 1). Impaired insulin and insulin-like growth factor expression and signaling mechanisms in Alzheimer's disease-is this type 3 diabetes?. Journal of Alzheimer's Disease. https://doi.org/10.3233/jad-2005-7107

Strnadová, V., Pacesová, A., Charvát, V., Smotková, Z., Zelezná, B., Kune, J., & Maletínská, L. (2024, April 24). Anorexigenic neuropeptides as anti-obesity and neuroprotective agents: exploring the neuroprotective effects of anorexigenic neuropeptides. Portland Press. https://doi.org/10.1042/BSR20231385

Strnadová, V., Pacesová, A., Charvát, V., Smotková, Z., Zelezná, B., Kune, J., & Maletínská, L. (2024, April 24). Anorexigenic neuropeptides as anti-obesity and neuroprotective agents: exploring the neuroprotective effects of anorexigenic neuropeptides. Portland Press. https://doi.org/https://doi.org/10.1042/BSR20231385

Sugiyama, M., Banno, R., Yaginuma, H., Taki, K., Mizoguchi, A., Tsunekawa, T., Onoue, T., Takagi, H., Ito, Y., Iwama, S., Goto, M., Suga, H., Komine, O., Yamanaka, K., & Arima, H. (2020, January 1). Hypothalamic glial cells isolated by MACS reveal that microglia and astrocytes induce hypothalamic inflammation via different processes under high-fat diet conditions. Neurochemistry International. https://doi.org/10.1016/j.neuint.2020.104733

Svensson, M., Andersson, E., Manouchehrian, O., Yang, Y., & Deierborg, T. (2020, January 28). Voluntary running does not reduce neuroinflammation or improve non-cognitive behavior in the 5xFAD mouse model of Alzheimer's disease. Nature Portfolio, 10(1). https://doi.org/10.1038/s41598-020-58309-8

Tak, Y J., & Lee, S Y. (2021, January 6). Long-Term Efficacy and Safety of Anti-Obesity Treatment: Where Do We Stand?. Current Obesity Reports, 10(1), 14-30. https://doi.org/10.1007/s13679-020-00422-w

Takahashi, K., & Yamanaka, S. (2006, August 25). Induction of Pluripotent Stem Cells from Mouse Embryonic and Adult Fibroblast Cultures by Defined Factors. Cell. https://doi.org/10.1016/j.cell.2006.07.024

Takaloa, M., Haapasaloa, A., Martiskainen, H., Kurkinen, K. M. A., Koivisto, H., Miettinen, P., Khandelwal, V. K. M., Kemppainen, S., Kaminska, D., Mäkinen, P., Leinonen, V., Pihlajamäki, J., Soininen, H., Laakso, M., Tanila, H., & Hiltunen, M. (2014). High-fat diet increases tau expression in the brain of T2DM and AD mice independently of peripheral metabolic status☆. https://doi.org/https://doi.org/10.1016/j.jnutbio.2014.02.003

Takayanagi, Y., Matsumoto, H., Nakata, M., Mera, T., Fukusumi, S., Hinuma, S., Ueta, Y., Yada, T., Leng, G., & Onaka, T. (2008, December 1). Endogenous prolactin-releasing peptide regulates food intake in rodents. American Society for Clinical Investigation, 118(12), 4014-4024. https://doi.org/10.1172/jci34682

Takeda, S., Sato, N., Uchio-Yamada, K., Sawada, K., Kunieda, T., Takeuchi, D., Kurinami, H., Shinohara, M., Rakugi, H., & Morishita, R. (2010, January 1). Diabetes-accelerated memory dysfunction via cerebrovascular inflammation and Aβ deposition in an Alzheimer mouse model with diabetes. Proceedings of the National Academy of Sciences of the United States of America. https://doi.org/10.1073/pnas.1000645107

Thaler, J. P., Yi, C.-X., Schur, E. A., Guyene, S. J., Hwang, B. H., Dietrich, M. O., Zhao, X., Sarruf, D. A., Izgur, V., Maravilla, K. R., Nguyen, H. T., Fischer, J. D., Matsen, M. E., Wisse, B. E., Morton, G. J., Horvath, T. L., Baskin, D. G., Tschöp, M. H., & Schwartz, M. W. (2012b). Obesity is associated with hypothalamic injury in rodents and humans. https://doi.org/10.1172/JCI59660

Timper, K., & Brüning, J C. (2017, June 1). Hypothalamic circuits regulating appetite and energy homeostasis: pathways to obesity. The Company of Biologists, 10(6), 679-689. https://doi.org/10.1242/dmm.026609

Tornehave, D., Kristensen, P. L., Rømer, J., Knudsen, L. B., & Heller, R. S. (2008). Expression of the GLP-1 Receptor in Mouse, Rat, and Human Pancreas. Journal of Histochemistry & Cytochemistry, 56(9), 841. https://doi.org/10.1369/jhc.2008.951319

Tronieri, J S., Wurst, C M., Pearl, R., & Allison, K C. (2017, April 24). Sex Differences in Obesity and Mental Health. Current Psychiatry Reports, 19(6). https://doi.org/10.1007/s11920-017-0784-8

Trotta, M., Bello, E P., Alsina, R., Tavella, M B., Ferrán, J L., Rubinstein, M., & Bumaschny, V F. (2020, July 1). Hypothalamic Pomc expression restricted to GABAergic neurons suppresses Npy overexpression and restores food intake in obese mice. Molecular Metabolism, 37, 100985-100985. https://doi.org/10.1016/j.molmet.2020.100985

Tu, T H., Kim, H., Yang, S., Kim, J K., & Kim, J G. (2019, April 2). Linoleic acid rescues microglia inflammation triggered by saturated fatty acid. Biochemical and Biophysical Research Communications. https://doi.org/https://doi.org/10.1016/j.bbrc.2019.03.047

Urbán, Z., Maglóczky, Z., & Freund, T. F. (2002). Calretinin-containing interneurons innervate both principal cells and interneurons in the CA1 region of the human hippocampus. 53, 205.

Valdearcos, M., Douglass, J D., Robblee, M M., Dorfman, M D., Stifler, D R., Bennett, M L., Gerritse, I., Fasnacht, R., Barres, B A., Thaler, J P., & Koliwad, S K. (2017, January 1). Microglial Inflammatory Signaling Orchestrates the Hypothalamic Immune Response to Dietary Excess and Mediates Obesity Susceptibility. Cell Metabolism . https://doi.org/10.1016/j.cmet.2017.05.015

Varela, L., & Horváth, T L. (2012, November 13). Leptin and insulin pathways in POMC and AgRP neurons that modulate energy balance and glucose homeostasis. Springer Nature, 13(12), 1079-1086. https://doi.org/10.1038/embor.2012.174

Vierbuchen, T., Ostermeier, A., Pang, Z. P., Kokubu, Y., Südhof, T. C., & Wernig, M. (2010). Direct conversion of fibroblasts to functional neurons by defined factors. Nature, 463(7284), 1035. https://doi.org/10.1038/nature08797

Wallace, A., Molteni, R., Ying, Z., & Gómez-Pinilla, F. (2003, June 1). A saturated-fat diet aggravates the outcome of traumatic brain injury on hippocampal plasticity and cognitive function by reducing brain-derived neurotrophic factor. Neuroscience, 119(2), 365-375. https://doi.org/10.1016/s0306-4522(03)00154-4

Wang, L., Meece, K., William, D J., Lo, K A., Zimmer, M., Heinrich, G., Carli, J M., Leduc, C A., Sun, L., Zeltser, L M., Freeby, M., Goland, R., Tsang, S H., Wardlaw, S L., Egli, D., & Leibe, R L. (2015, January 1). Differentiation of hypothalamic-like neurons from human pluripotent stem cells. The Journal of Clinical Investigation, 125(2). https://doi.org/10.1172/JCI79220

Watanabe, K., Ueno, M., Kamiya, D., Nishiyama, A., Matsumura, M., Wataya, T., Takahashi, J B., Nishikawa, S., Nishikawa, S., Muguruma, K., & Sasai, Y. (2007, January 1). A ROCK inhibitor permits survival of dissociated human embryonic stem cells. Nature Biotechnology. https://doi.org/doi:10.1038/nbt13

Wataya, T., Ando, S., Muguruma, K., Ikeda, H., Watanabe, K., Eiraku, M., Kawada, M., Takahashi, J., Hashimoto, N., & Sasa, Y. (2008, January 1). Minimization of exogenous signals in ES cell cultureinduces rostral hypothalamic differentiation. PNAS. https://www.pnas.org/doi/epdf/10.1073/pnas.0803078105

Watson, G. S., & Craft, S. (2004). Modulation of memory by insulin and glucose: neuropsychological observations in Alzheimer's disease. https://doi.org/10.1016/j.ejphar.2004.02.048

Weissman, T. A., & Pan, Y. A. (2015). Brainbow: New Resources and Emerging Biological Applications for Multicolor Genetic Labeling and Analysis. Genetics, 199(2), 293. https://doi.org/10.1534/genetics.114.172510

Williams, L M., Campbell, F M., Drew, J E., Koch, C., Hoggard, N., Rees, W D., Kamolrat, T., Ngo, H T., Steffensen, I., Gray, S R., & Tups, A. (2014, August 29). The development of diet-induced obesity and glucose intolerance in C57BL/6 mice on a high-fat diet consists of distinct phases. Plos One. https://doi.org/10.1371/journal.pone.0106159

Wilson, D. M., & Bindert, L. I. (1997). Free Fatty Acids Stimulate the Polymerization of Tau and Amyloid f Peptides.

Wittmann, G., Hrabovszky, E., & Lechan, R. M. (2013). Distinct glutamatergic and GABAergic subsets of hypothalamic pro-opiomelanocortin neurons revealed by in situ hybridization in male rats and mice. The Journal of Comparative Neurology, 521(14), 3287. https://doi.org/10.1002/cne.23350

Xiao, Y., Amaral, T F., Ross, P J., Soto, D A., Diffenderfer, K E., Pankonin, A R., Jeensuk, S., Tríbulo, P., & Hansen, P J. (2021, April 23). Importance of WNT-dependent signaling for derivation and maintenance of primed pluripotent bovine embryonic stem cells. Biology of Reproduction. https://doi.org/10.1093/biolre/ioab075

Xu, Y., Tamamaki, N., Noda, T., Kimura, K., Itokazu, Y., Matsumoto, N., Dezawa, M., & Idé, C. (2005, February 12). Neurogenesis in the ependymal layer of the adult rat 3rd ventricle. Experimental Neurology, 192(2), 251-264. https://doi.org/10.1016/j.expneurol.2004.12.021

Xu, Z., Zhang, L., Wang, Q., Marshall, C., Xiao, N., Gao, J., Wu, T., Ding, J., Hu, G., & Xiao, M. (2013, May 1). Aerobic Exercise Combined with Antioxidative Treatment does not Counteract Moderate- or Mid-Stage Alzheimer-Like Pathophysiology of APP/PS1 Mice. CNS Neuroscience & Therapeutics. https://doi.org/10.1111/cns.12139

Yamanaka, S. (2012, June 1). Induced Pluripotent Stem Cells: Past, Present, and Future. Cell Stem Cell, 10(6), 678-684. https://doi.org/10.1016/j.stem.2012.05.005

Yang, S., Qiang, L., Sample, A., Shah, P., & He, Y. (2017, February 24). NF-KB Signaling Activation Induced by Chloroquine Requires Autophagosome, p62 Protein, and c-Jun N-terminal Kinase (JNK) Signaling and Promotes Tumor Cell Resistance. The Journal of Biological Chemistry. https://doi.org/10.1074/jbc.M116.756536

Yoo, S., & Blackshaw, S. (2018, November 1). Regulation and function of neurogenesis in the adult mammalian hypothalamus. Progress in Neurobiology, 170, 53-66. https://doi.org/10.1016/j.pneurobio.2018.04.001

Yoo, S., Kim, J., Lyu, P., Hoang, T., Ma, A., Trinh, V., Dai, W., Jiang, L., Leavey, P J., Duncan, L H., Won, J., Park, S., Qian, J., Brown, S P., & Blackshaw, S. (2021, May 28). Control of neurogenic competence in mammalian hypothalamic tanycytes. American Association for the Advancement of Science, 7(22). https://doi.org/10.1126/sciadv.abg3777

Yulyaningsih, E., Rudenko, I A., Valdearcos, M., Dahlén, E., Vagena, E., Chan, A., Alvarez-Buylla, A., Vaisse, C., Koliwad, S K., & Xu, A W. (2017, June 13). Acute Lesioning and Rapid Repair of Hypothalamic Neurons outside the Blood-Brain Barrier. Cell Reports. https://doi.org/doi: 10.1016/j.celrep.2017.05.060.

Zhang, G., Li, J., Purkayastha, S., Tang, Y., Zhang, H., Yin, Y., Li, B., Liu, G., & Cai, D. (2013, May 9). Hypothalamic Programming of Systemic Aging Involving IKKβ/NF-κB and GnRH. Nature. https://doi.org/10.1038/nature12143

Zhang, J., Giesert, F., Kloos, K., Weisenhorn, D. M. V., Aigner, L., Wurst, W., & Couillard-Després, S. (2010). A powerful transgenic tool for fate mapping and functional analysis of newly generated neurons. BMC Neuroscience, 11(1). https://doi.org/10.1186/1471-2202-11-158

Zhang, L., Koller, J., Ip, C K., Gopalasingam, G., Bajaj, N., Lee, N J., Enriquez, R F., & Herzog, H. (2021, October 25). Lack of neuropeptide FF signalling in mice leads to reduced repetitive behavior, altered drinking behavior, and fuel type selection. Wiley, 35(11). https://doi.org/10.1096/fj.202100703r

Zhang, X., Zhang, G., Zhang, H., Karin, M., Bai, H., & Cai, D. (2008, October 3). Hypothalamic IKKβ/NF-κB and ER Stress Link Overnutrition to Energy Imbalance and Obesity. Cell. https://doi.org/10.1016/j.cell.2008.07.043

Zhang, Y., Kim, M S., Jia, B., Yan, J., Zuniga-Hertz, J P., Li, Y., & Cai, D. (2017, July 26). Hypothalamic stem cells control ageing speed partly through exosomal miRNAs. Nature Portfolio, 548(7665), 52-57. https://doi.org/10.1038/nature23282

Zhao, H., Jiang, X., Hu, L., Yang, L., Deng, L., Wang, Y P., & Ren, Z. (2020, February 1). Activation of GLP-1 receptor enhances the chemosensitivity of pancreatic cancer cells. Bioscientifica, 64(2), 103-113. https://doi.org/10.1530/jme-19-0186

Zhao, M., Momma, S., Delfani, K., Carlén, M., Cassidy, R. M., Johansson, C. B., Brismar, H., Shupliakov, O., Frisén, J., & Janson, A. M. (2003). Evidence for neurogenesis in the adult mammalian substantia nigra. Proceedings of the National Academy of Sciences, 100(13), 7925. https://doi.org/10.1073/pnas.1131955100

Zhao, X., Wang, M., Wen, Z., Lu, Z., Cui, L., Fu, C., Xue, H., Liu, Y., & Zhang, Y. (2021, August 23). GLP-1 Receptor Agonists: Beyond Their Pancreatic Effects. Frontiers in Endocrinology. https://doi.org/ https://doi.org/10.3389/fendo.2021.721135

Zheng, C., Zhou, X., & Wang, J. (2016, January 1). The dual roles of cytokines in Alzheimer's disease: update on interleukins, TNF-α, TGF-β and IFN-γ. Translational Neurodegeneration. https://doi.org/10.1186/s40035-016-0054-4

Zimmer, B., Piao, J., Ramnarine, K., Tomishima, M. J., Tabar, V., & Studer, L. (2016). Derivation of Diverse Hormone-Releasing Pituitary Cells from Human Pluripotent Stem Cells. Stem cell reports, 6(6), 858–872. https://doi.org/10.1016/j.stemcr.2016.05.005

Zmeškalová, A., Popelová, A., Exnerová, A., Železná, B., Kuneš, J., & Maletínská, L. (2020, September 1). Cellular Signaling and Anti-Apoptotic Effects of Prolactin-Releasing Peptide and Its Analog on SH-SY5Y Cells. International Journal of Molecular Sciences. https://doi.org/10.3390/ijms21176343

Appendix

Appendix 1

An analogue of the Prolactin Releasing Peptide reduces obesity and promotes adult neurogenesis

These figures have been published:

Jorgensen, S., Karnošová, A., Mazzaferro, S., Rowley, O., Hsiao-Jou, C C., Robbins, S J., Christofides, S., Merkle, F T., Maletínská, L., & Petrik, D. (2024, January 1). An analogue of the Prolactin Releasing Peptide reduces obesity and promotes adult neurogenesis. EMBO Reports, 25(1). https://doi.org/https://doi.org/10.1038/s44319-023-00016-2

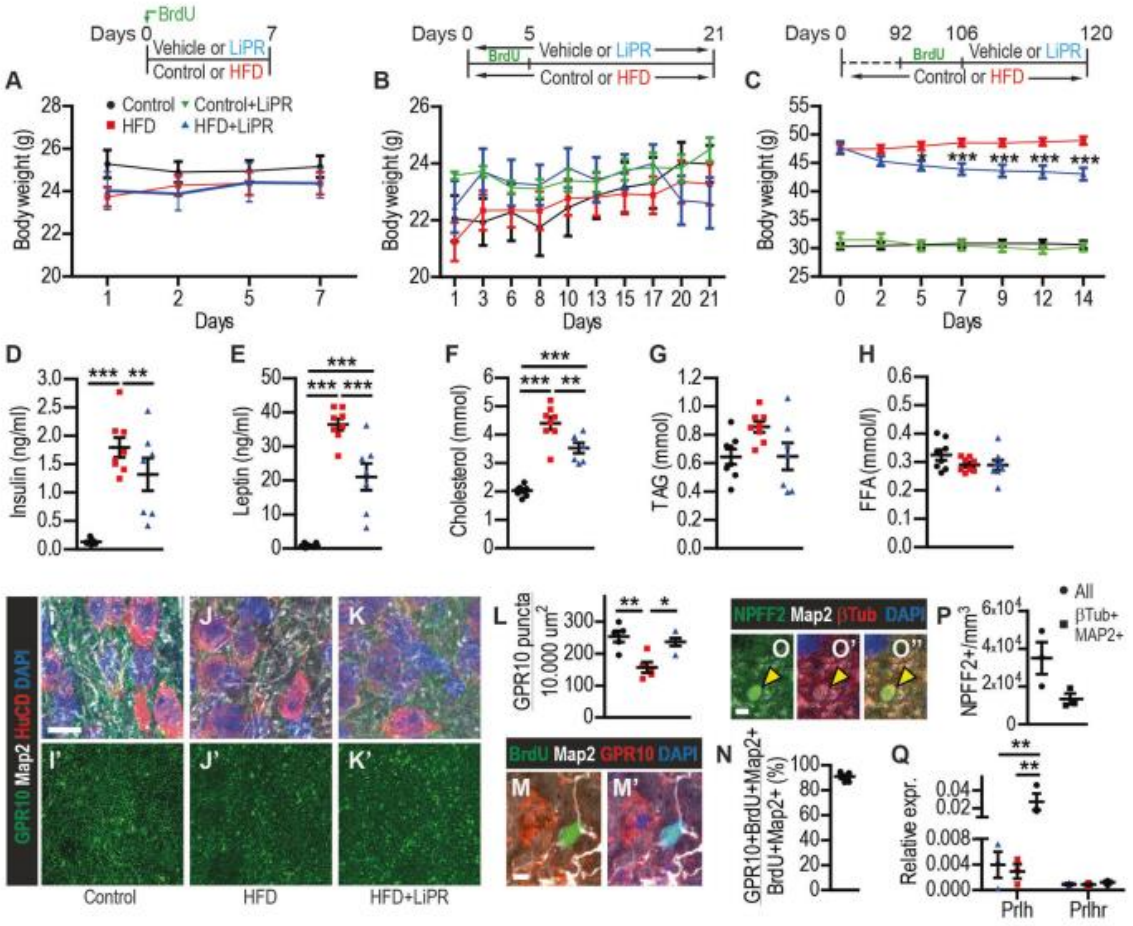

Figure 1. Effects of LiPR on body weight, plasma metabolites and expression of PrRP and its receptors.

(**A–C**) Mouse body weigh over time for the 7d (**A**), 21d (**B**) and 4mo (**C**) HFD protocols, which are summarized in the schematics above panels. (**D–H**) Plasma concentration of selected hormones and metabolites from 4mo HFD group. (**I–K**) Representative confocal microphotographs of MBH stained as indicated for GPR10 and neuronal markers from 21d HFD group in Control (**I**), HFD (**J**) and HFD + LiPR (**K**) mice. (**L**) Quantification of GPR10+ puncta in MBH of 21d group. (**M**) A representative image of GPR10+ puncta associated with Map2+ processes around a BrdU+ nucleus in ME. (**N**) Quantification of the proportion of BrdU+Map2 + GPR10+ cells in MBH. (**O**) A representative confocal image of a NPFF2 punctum (marked by arrowhead) in MBH stained as indicated from a control animal of 21d HFD group. (**P**) Quantification of NPFF2 puncta in MBH of 21d group. (**Q**) Relative mRNA fold change of Prlh and Prlhr compared to Gapdh in cDNA from MBH from mice 2 weeks on Control diet, HFD or HFD +LiPR. Data information: Scale bars (s.b.): 10 µm (**I–K**), 5 µm (M), 2 µm (**O**). $n = 5$ mice per data set in panels **A**,**B**,**L**,**N**. $n = 8$ mice per data set in panels **C**,**D**, **E–H**. $n = 3$ mice per data group in panels **P–Q**. In panels **A–C**, Repeated measure two-way ANOVA ((**B**): treatment $F(3, 160) = 4.351$, $p < 0.0056$; **C**: treatment $F(3, 150) = 130.7$, $p < 0.0001$, duration of treatment $F(6, 150) = 10.42$, $p < 0.0001$, interaction $F(18, 150) = 20.70$, $p < 0.0001$). In panels **D–H**,**L**,**P**, One-way ANOVA. In panel **Q**, Two-way ANOVA ($F(2, 12) = 5.95$, $p = 0.016$). $^*p < 0.05$, $^{**}p < 0.01$, $^{***}p < 0.001$ (Bonferroni's test). Data are presented as mean ± SEM. Source data are available online for this figure.

Appendix Figure 1. Effects of LiPrRP on body weight, plasma, metabolites and expression of PrRP and its receptors

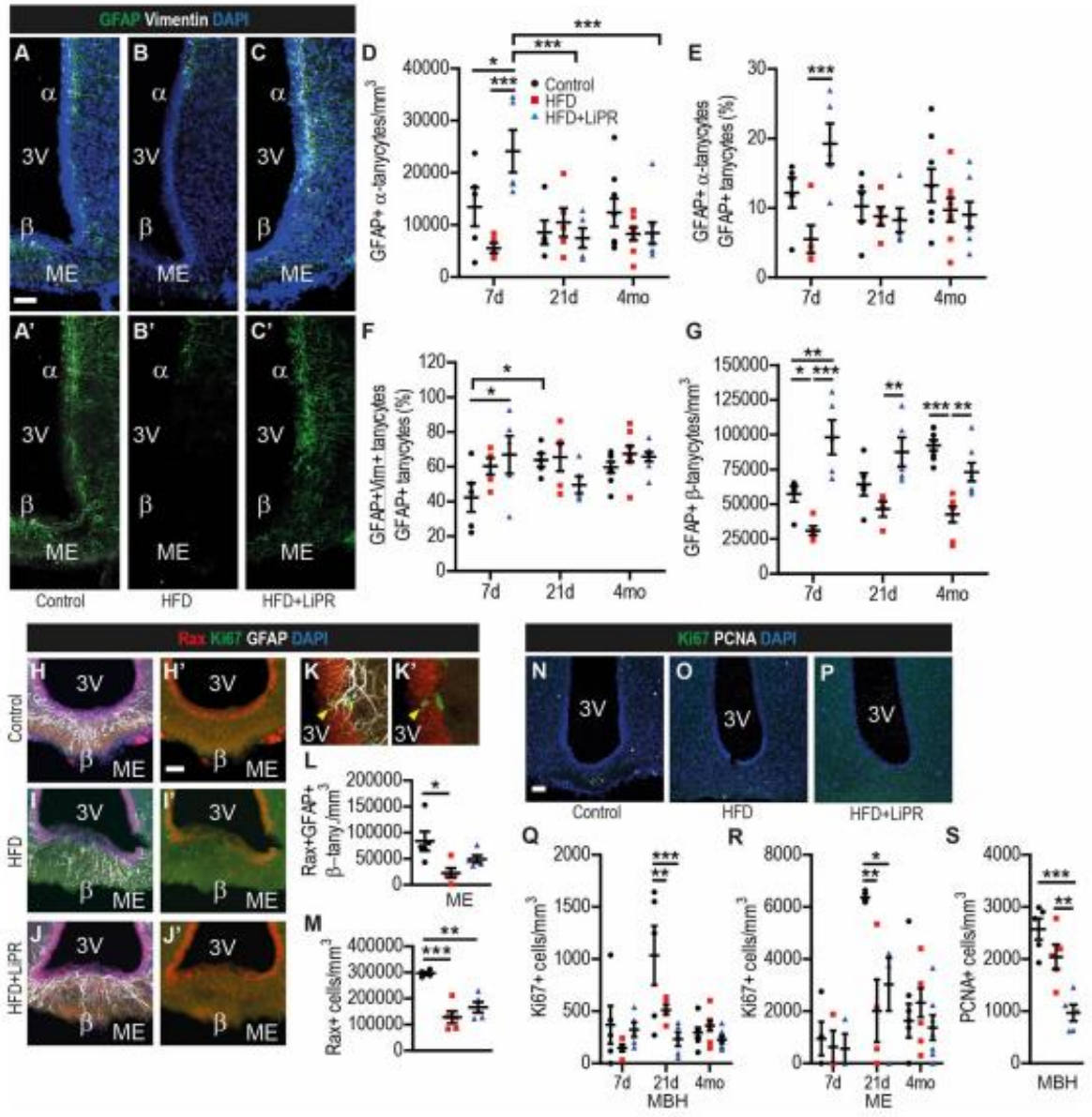

Figure 2. Effects of LiPR on tanycytes and proliferating cells in the MBH.

(**A–C**) Representative confocal images of HVZ with 3rd Ventricle (3V) and Medial Eminence (ME) stained as indicated in Control (**A**), HFD (**B**) and HFD + LiPR (**C**) of 7d HFD group. (**D**) Quantification of GFAP+ α-tanycytes per volume of MBH. (**E**) Proportional analysis of GFAP+ α-tanycytes in MBH. (**F**) Proportional analysis of GFAP+Vimentin+ tanycytes in MBH. (**G**) Quantification of GFAP+ β-tanycytes per volume of ME. (**H–J**) Representative images of MBH stained as indicated (21d group). (**K**) Representative image of Rax+Ki67+GFAP+ tanycyte (yellow arrowhead). (**L**) Quantification of Rax+GFAP+ β-tanycytes per volume of ME (21d group). (**M**) Quantification of Rax+ cells per volume of the HVZ (21d group). (**N–P**) Representative images of the MBH stained as indicated (21d group). (**Q–S**) Quantification of cells positive for Ki67 in MBH (**Q**) or in ME for 21d (**R**) and for PCNA (**S**). Data information: Scale bars: 10 μm (**K**), 50 μm (all other). In all panels but panel **S**, $n = 5$ mice per data set for 7d and 21d groups, $n = 8$ mice per data set for 4mo group. In panel **S**, $n = 3$–8 mice per data set. In panels **D–G**, Two-way ANOVA (**D**: treatment $F(2,45) = 3.28$, $p = 0.047$, duration of treatment $F(2,45) = 3.76$, $p = 0.031$, interaction $F(4,45) = 5.29$, $p = 0.0014$; **E**: treatment $F(2, 44) = 3.58$, $p = 0.036$, interaction $F(4, 44) = 3.88$, $p < 0.009$; **F**: interaction $F(4,45) = 2.61$, $p = 0.048$; **G**: treatment $F(2, 42) = 31.3$, $p < 0.0001$, interaction $F(4, 42) = 5.79$, $p = 0.0008$; **Q**: treatment $F(2,44) = 6.59$, $p < 0.0031$, duration $F(2,44) = 7.78$, $p = 0.0013$, interaction $F(4, 44) = 4.63$, $p = 0.0033$; **R**: treatment $F(2,34) = 2.94$, $p < 0.066$, duration $F(2,34) = 10.43$, $p = 0.0003$, interaction $F(4, 34) = 3.07$, $p = 0.029$). In other panels (**L,M,S**), One-way ANOVA (**L**: $F(2,14) = 6.04$), $p = 0.015$; **M**: $F(2,13) = 18.81$, $p = 0.0003$; **S**: $F(2,14) = 16.66$, $p = 0.0003$). $^*p < 0.05$, $^{**}p < 0.01$, $^{***}p < 0.001$ (Bonferroni's test). Data are presented as mean ± SEM. Source data are available online for this figure.

Appendix Figure 2. Effects of LiPrRP on tanycytes and proliferating cells in the MBH.

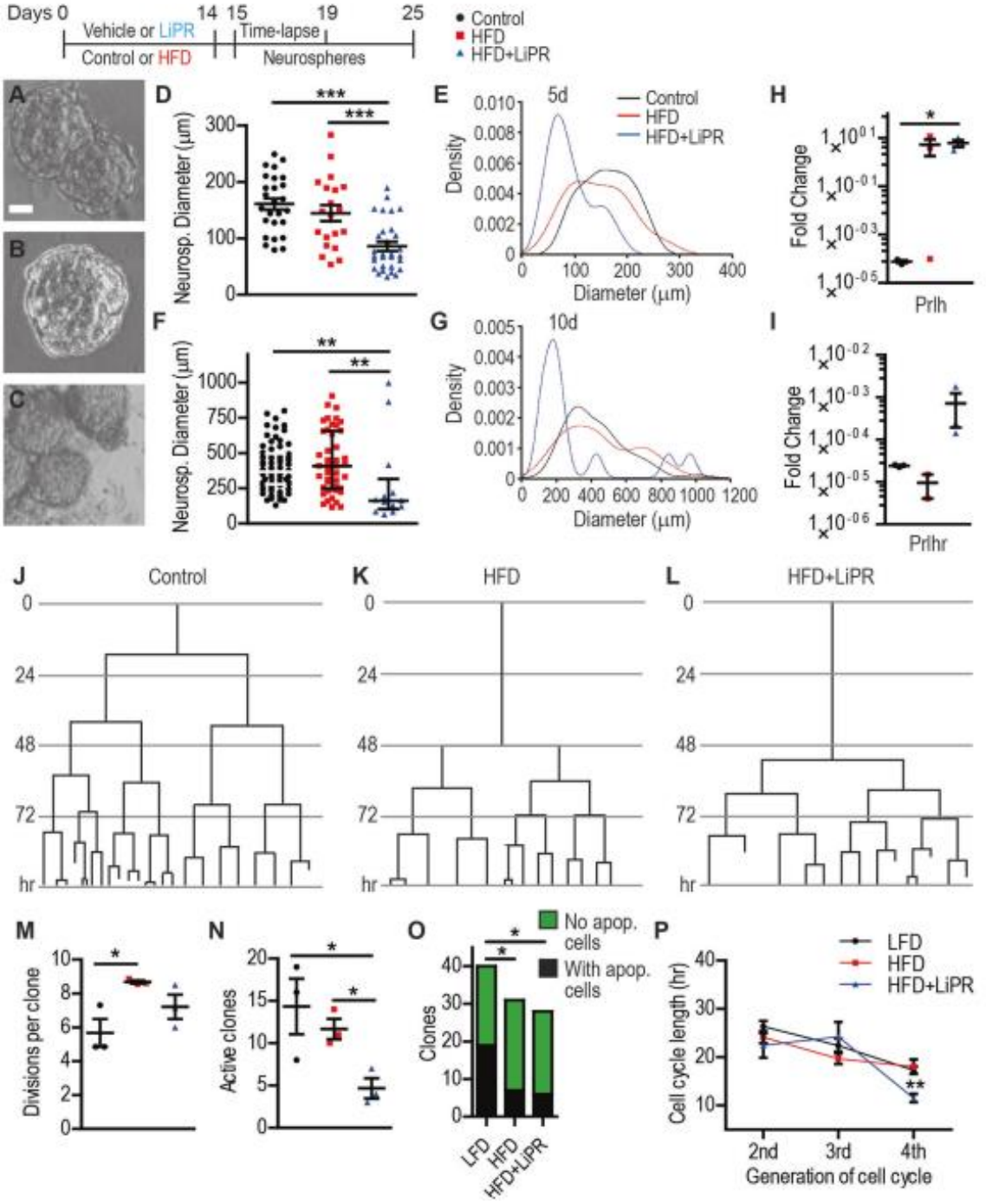

Figure 3. LiPR reduces cell activation and proliferation of htNSCs in vitro.

(**A–C**) Representative images of HVZ-derived neurospheres 5d in culture from Control (**A**), HFD (**B**) and HFD + LiPR (**C**) treated mice. Schematics of the experimental protocol shown above. (**D,F**) Quantification of diameter of neurospheres 5d (**D**) and 10d (**F**) in culture. (**E,G**) Kernel density plots of neurosphere diameter frequency distribution as a function of diameter for 5d (**E**) and 10d (**G**) in culture. (**H,I**) Relative mRNA fold change of Prlh (**H**) and Prlhr (**I**) compared to Gapdh in cDNA from MBH-derived neurospheres (10d in culture). (**J–L**) Example cell division trees from 4-day time-lapse imaging of aNSCs from HVZ of Control (**J**), HFD (**K**), HFD + LiPR (**L**) mice. (**M**) Quantification of the number of cell divisions per division tree clone. (**N**) Time-lapse quantification of active (dividing) clones per 20,000 plated cells. (**O**) Proportion of active clones containing at least one apoptotic cell. (**P**) Cell cycle length from the time-lapse imaging over observed cell divisions. Data information: Scale bars: 20 µm. In all panels, n = 3 mice for each data set. In panel **D**, number of neurospheres: $n = 26$ (Control), 20 (HFD), 30 (HFD+LiPR). In panel **E**, number of neurospheres: $n = 66$ (Control), 46 (HFD), 13 (HFD+LiPR). In panels **M–P**, number of traced clones: $n = 48$ (Control), 68 (HFD), 53 (HFD+LiPR). Data information: In panel **O**, Chi-square test. In panel **F**, Kruskal–Wallis test with Dunn's test ($H = 10.30$, $p = 0.0058$). In panels **H,N,O,P**, un-paired two-tailed *T*-Test. In other panels, One-way ANOVA with Bonferroni's test (**D**: $F(2,73) = 15.80$, $p < 0.0001$; **M**: $F(2,6) = 5.61$, $p = 0.042$). $^*p < 0.05$, $^{**}p < 0.01$, $^{***}p < 0.001$. Data are presented as median ± IQR (**F**) or mean ± SEM (all other panels). Source data are available online for this figure.

Appendix Figure 3. LiPrRP reduces cell activation and proliferation of htNSCs in vitro.

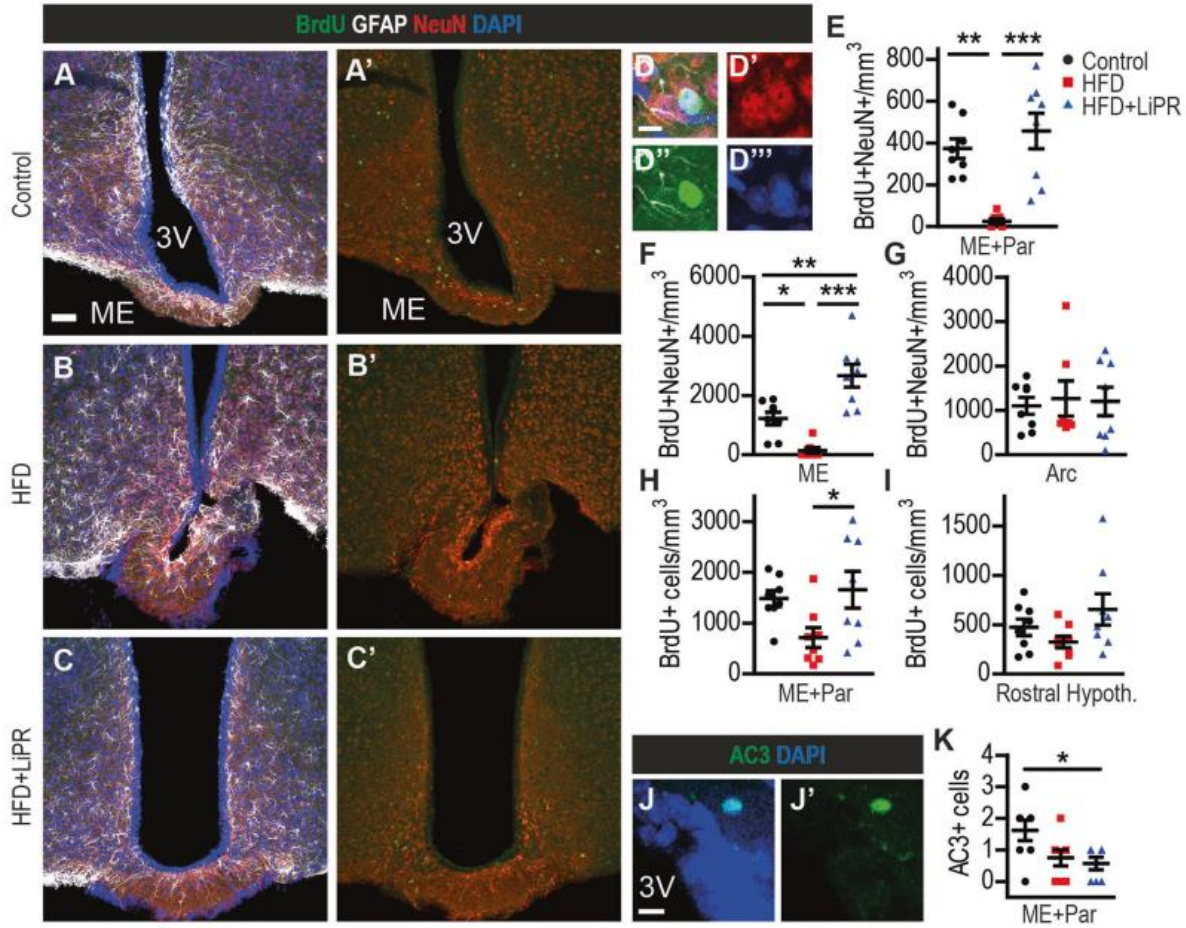

Figure 4. LiPR improves the survival of new neurons in the MBH.

(**A–C**) Representative confocal images of HVZ stained as indicated in Control (**A**), HFD (**B**) and HFD + LiPR (**C**) of 4 mo HFD group. (**D**) An example of BrdU+ neuron in the MBH parenchyma. (**E–G**) Quantification of BrdU+ neurons in MBH parenchyma (**E**), ME (**F**) and Arcuate Nucleus (Arc, **G**). **H,I** Quantification of all BrdU+ cells in parenchyma of MBH (**H**) and rostral hypothalamus (**I**). (**J**) An example of Activated Caspase 3 (AC3) positive cell near 3 V wall. (**K**) Quantification of AC3+ cells in MBH. Data information: Scale bars: 50 µm (**A–C**), 10 µm (**D,J**). $n = 5$ mice per data set for 7d and 21d groups and $n = 8$ mice per data set for 4mo group. Data information: In all panels, One-way ANOVA with Bonferroni's test (**E**: $F(2,20) = 14.21$, $p < 0.0001$; **F**: $F(2,20) = 21.37$, $p < 0.0001$; **H**: $F(2,21) = 3.87$, $p = 0.037$; **K**: $F(2, 22) = 2.46$, $p = 0.025$). $^*p < 0.05$, $^{**}p < 0.01$, $^{***}p < 0.001$. Data are presented as mean ± SEM. Source data are available online for this figure.

Appendix Figure 4. LiPrRP improves the survival of new neurons in the MBH.

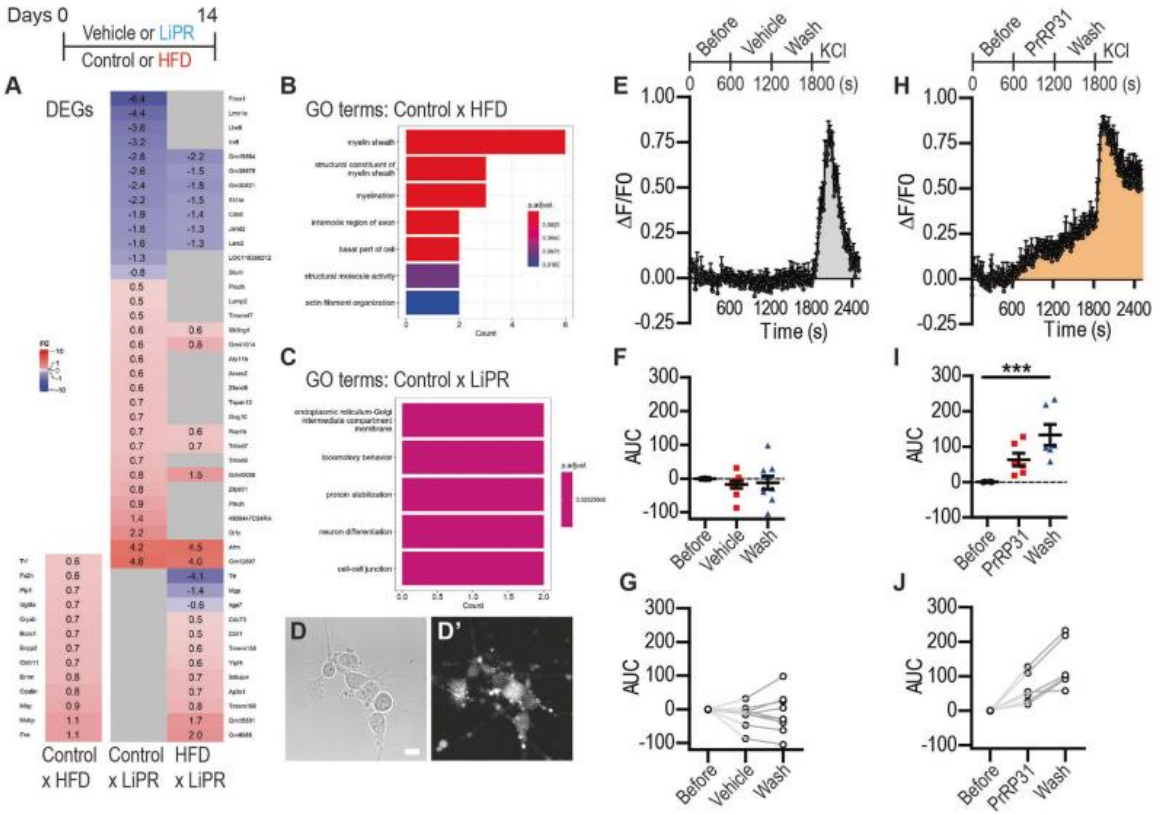

Figure 5. Effects of LiPR on gene expression in the MBH and human iPSC-derived hypothalamic neurons.

(A) A table of Differentially Expressed Genes (DEGs) in three different pair-wise comparisons of bulk RNAseq data. Experimental protocol is depicted above. **(B)** Bulk RNAseq Gene Ontology (GO) terms for the Control Diet vs HFD comparison. **(C)** Bulk RNAseq GO terms for Control Diet vs Control Diet+LiPR comparison. **(D)** A representative image in the bright field **(D)** and fluorescence **(D')** of hiPSC-derived hypothalamic neurons loaded with the Rhod-3 AM dye and used in calcium imaging. **(E,H)** A graph of the relative fluorescence change (ΔF/F0) of Rhod-3 as a function of time before and during hPrRP31 (or Vehicle) application in medium, wash-out and KCl positive control. **(E)** Neurons exposed to Vehicle. **(H)** Neurons responding to hPrRP31. **(F,I)** A summary of fluorescence before (0–600 s), during hPrRP31 **(F)** or Vehicle **(I,** 600–1200 s) or wash-out (1200–1800 s) in area under curve (AUC). **(G,J)** Individual neurons from calcium imaging in the before-after plot from the Vehicle **(G)** and hPrRP31-responsive **(J)** groups. Data information: Scale bar: 10 µm. In panels **A–C**, $n = 3$–4 mice per data set. In panels **E–G**, $n = 9$ recorded cells. In panels **H–J**, $n = 6$ recorded cells. Data information: One-way ANOVA (**I**: $F(2,15) = 10.90$, $p = 0.0012$). ***$p < 0.001$ (Bonferroni's test). Data are presented as mean ± SEM. Source data are available online for this figure.

Appendix Figure 5. Effects of LiPrRP on gene expression in the MBH and human iPSC-derived hypothalamic neurons.

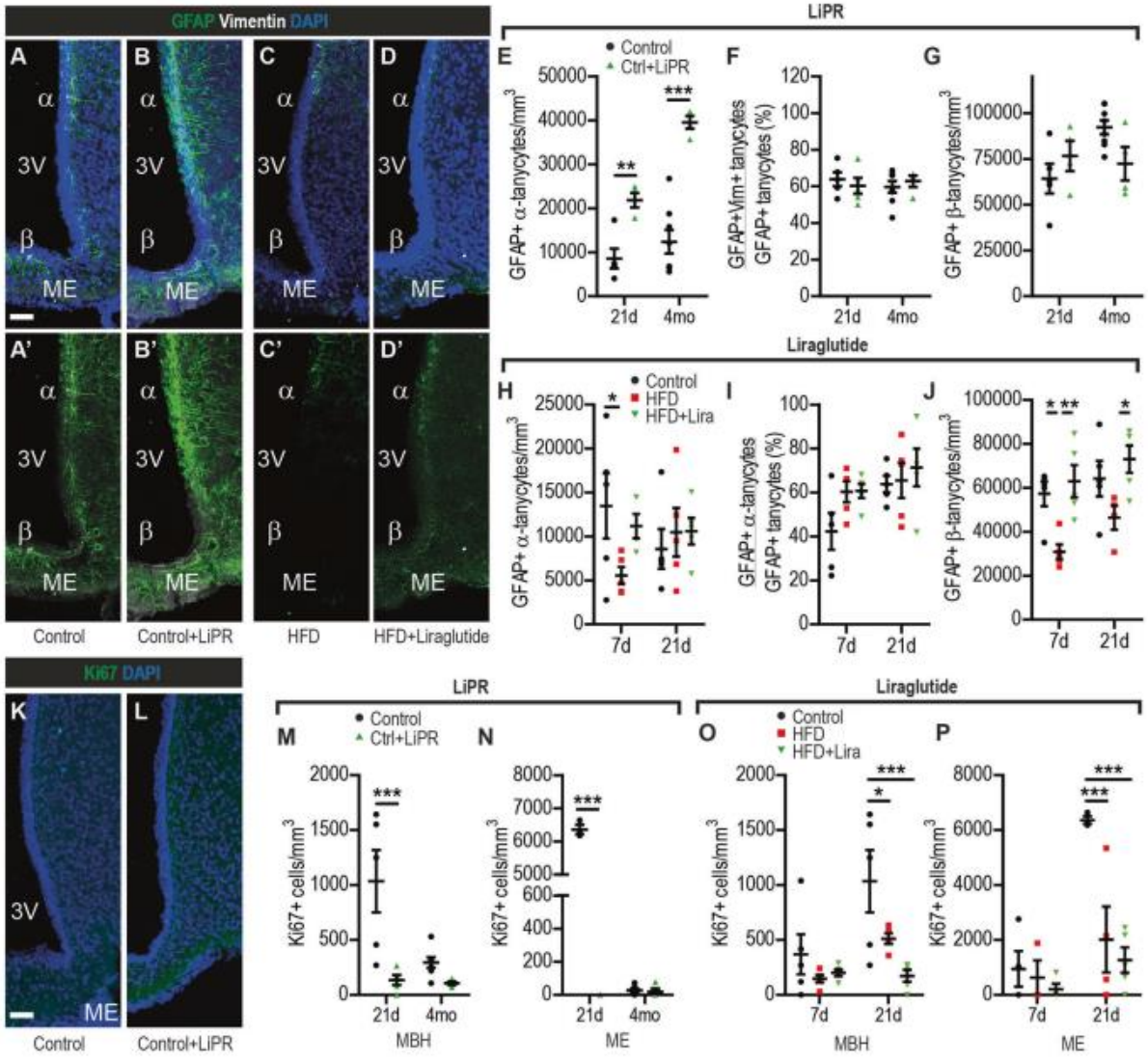

Figure EV1. Effects of LiPR in Control Diet and Liraglutide on tanycytes and proliferating cells in the MBH.

(**A–D**) Representative confocal images of HVZ stained as indicated in Control (**A**), Control+LiPR (**B**), HFD (**C**) and HFD + Liraglutide (Lira) (**D**) of 21d HFD group. Images in panels **A** and **C** are identical with representative confocal images in Fig. 2A and B and are shown for direct comparison with the control in both figures. (**E–G**) Effects of LiPR on number of GFAP+ α-tanycytes per volume of MBH (**E**), the proportion of GFAP+Vimentin+ tanycytes (**F**) and the number of GFAP+ β-tanycytes in MBH (**G**). (**H–J**) Effects of Liraglutide on GFAP+ α-tanycytes (**H**), the proportion of GFAP+Vimentin+ tanycytes (**I**) and the number of GFAP+ β-tanycytes in MBH (**J**). (**K,L**) Representative confocal images of MBH stained for Ki67 in Control (**K**) and Control+LiPR (**L**) of 4mo treatment group. (**M,N**) Quantification of Ki67+ cells in the MBH (M) and in the ME (**N**) from Control+LiPR mice. (**O,P**) Quantification of Ki67+ (**O**) and PCNA+ cells (**P**) in the MBH of Liraglutide-treated mice. Data information: Scale bars: 50 µm. $n = 5$ mice (7d and 21d), $n = 8$ mice (4mo Control), $n = 4$ mice (4mo Control + LiPR). In panel **P**, One-Way ANOVA. In all other panels, Two-Way ANOVA (**E**: treatment $F(1,17) = 59.74$, $p < 0.0001$, duration $F(1,17) = 16.87$, $p = 0.0007$, interaction $F(1,17) = 7.04$, $p = 0.017$; **J**: treatment $F(2,23) = 11.36$, $p = 0.0004$, duration $F(1,23) = 4.42$, $p = 0.047$; **M**: treatment $F(1,17) = 14.52$, $p = 0.0014$, duration $F(1,17) = 7.24$, $p = 0.016$, interaction $F(1,17) = 6.2$, $p = 0.023$; **N**: treatment $F(1,14) = 4481$, $p < 0.0001$, duration $F(1,14) = 4404$, $p < 0.0001$, interaction $F(1,14) = 6.2$, $p < 0.0001$; **O**: treatment $F(2,24) = 7.04$, $p < 0.0039$, duration $F(1,24) = 8.35$, $p < 0.0081$, interaction $F(2,24) = 3.01$, $p < 0.068$; **P**: treatment $F(2,17) = 10.11$, $p < 0.0013$, duration $F(1,17) = 21.99$, $p < 0.0002$, interaction $F(2,17) = 6.1$, $p < 0.01$). $^*p < 0.05$, $^{**}p < 0.01$, $^{***}p < 0.001$ (Bonferroni's test). Data are presented as mean ± SEM.

Appendix Figure EV1. Effects of LiPrRP in Control Diet and Liraglutide on tanycytes and proliferating cells in the MBH.

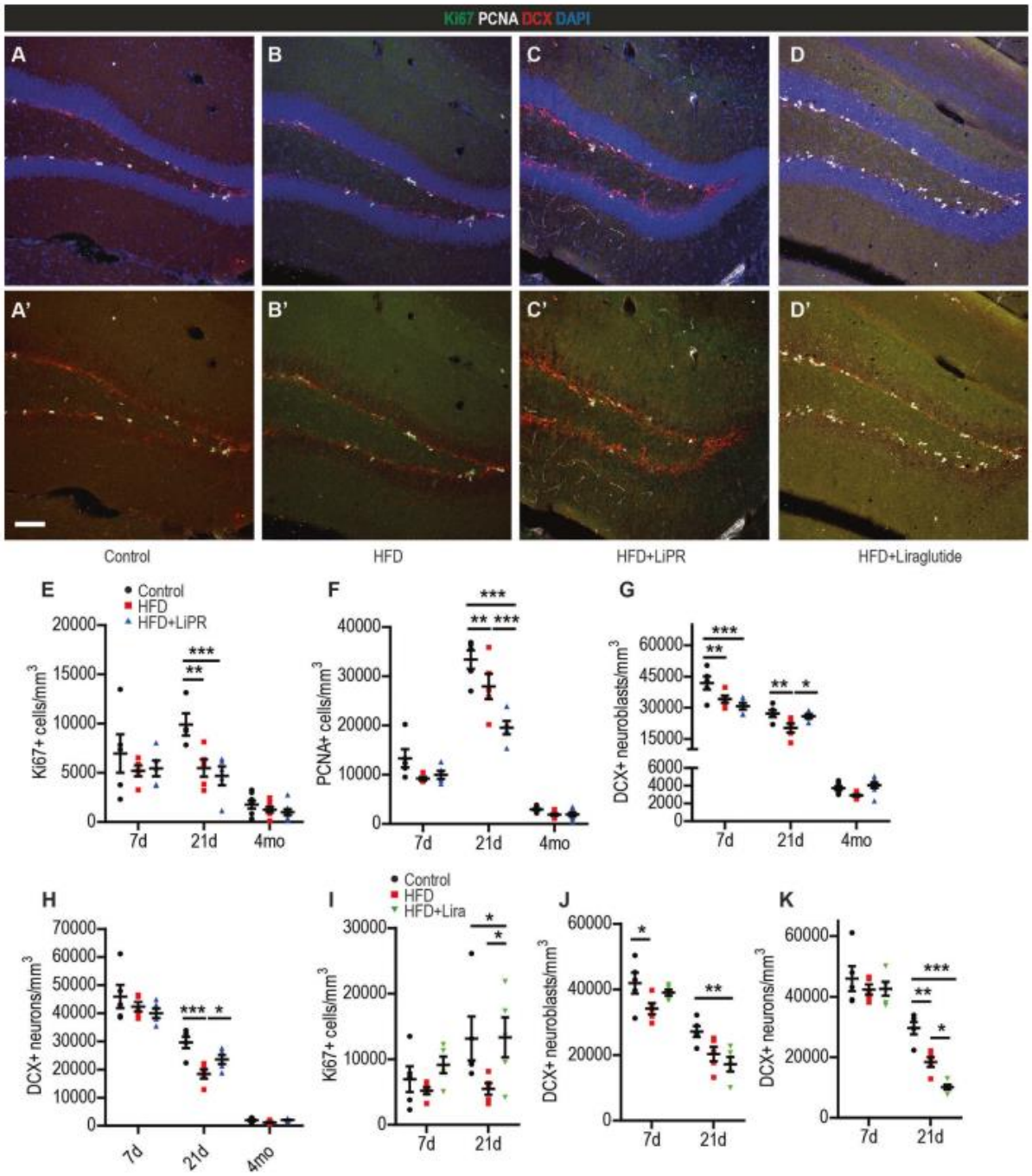

Figure EV2. LiPR promotes neurogenesis in the SGZ.

(**A–D**) Representative confocal images of the Dentate Gyrus (DG) of the hippocampus showing the Subgranular Zone (SGZ) stained as indicated in Control (**A**), HFD (**B**), HFD + LiPR (**C**) and HFD + Lira of 21d HFD group. (**E–H**) Quantification of Ki67+ (**E**), PCNA+ cells (**F**), DCX+ neuroblasts (**G**) and DCX+ neurons (**H**) in SGZ for Control, HFD and HFD + LiPR. (**I–K**) Cell quantification in SGZ as described for Control, HFD and HFD + Liraglutide. Data information: Scale bars: 50 µm. $n = 5$ mice per data set for 7d and 21d groups, $n = 8$ mice per data set for 4mo group. All panels, Two-Way ANOVA (**E**: treatment $F(2,44) = 9.88$, $p = 0.0003$, duration $F(2,44) = 6.86$, $p = 0.0002$, interaction $F(4,44) = 9.88$, $p = 0.0003$; **F**: treatment $F(2,45) = 21.19$, $p < 0.0001$, duration $F(2,45) = 374.3$, interaction $F(4,45) = 9.88$, $p < 0.0001$; **G**: treatment $F(2,45) = 11.38$, $p < 0.0001$, duration $F(2,45) = 463.03$, $p < 0.0001$; interaction $F(4,45) = 6.25$, $p = 0.0004$; **H**: treatment $F(2,45) = 8.77$, $p = 0.0006$, duration $F(2,54) = 552.73$, $p < 0.0001$, interaction $F(4,45) = 3.78$, $p = 0.011$; **I**: treatment $F(2,24) = 4.3$, $p = 0.025$,duration $F(1,24) = 4.22$, $p = 0.05$; **J**: treatment $F(2,24) = 7.21$, $p = 0.0035$, duration $F(1,24) = 95.86$, $p < 0.0001$; **K** treatment $F(2,24) = 12.29$, $p = 0.0002$, duration $F(1,24) = 161.57$, $p < 0.0001$, interaction $F(2,24) = 5.96$, $p = 0.0079$). $^*p < 0.05$, $^{**}p < 0.01$, $^{***}p < 0.001$ (Bonferroni's test). Data are presented as mean ± SEM.

Appendix Figure EV2. LiPrRP promotes neurogenesis in the SGZ.

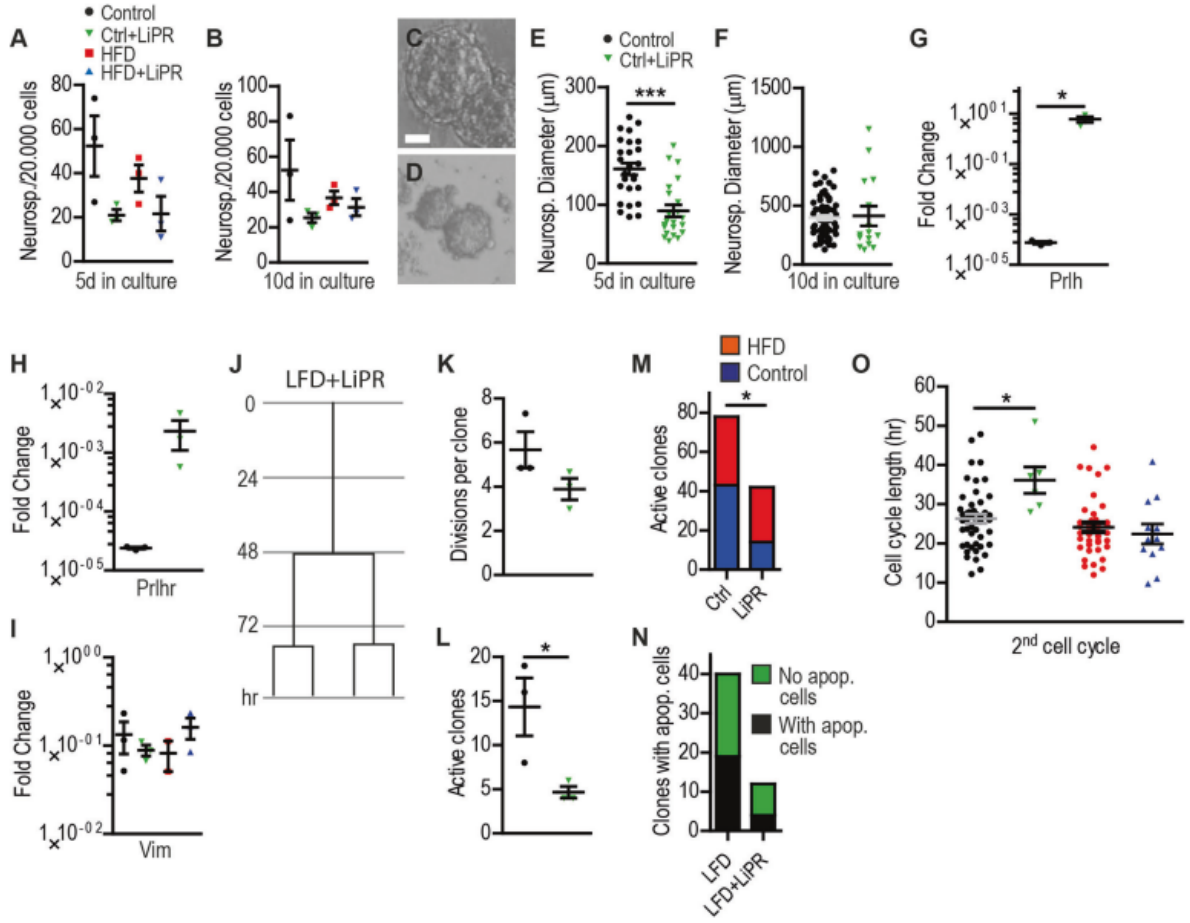

Figure EV3. LiPR reduces proliferation of naïve neurospheres.

(**A**,**B**) Quantification of number of HVZ-derived neurospheres per 20.000 plated cells after 5d (**A**) and 10d (**B**) in culture. (**C**,**D**) Representative images of HVZ-derived neurospheres 5d in culture from Control (**C**) and Control + LiPR (**D**) treated mice. The Image in panel **C** is identical with the image in Fig. 3A and is shown for direct comparison with the control in both figures. (**E**,**F**) Quantification of diameter of neurospheres 5d (**E**) and 10d (**F**) in culture. (**G-I**) Relative mRNA fold change of Prlh (**G**), Prlhr (**H**) and Vimentin (**I**) compared to Gapdh in cDNA from MBH-derived neurospheres (10d in culture). (**J**) An example cell division tree from 4-day time-lapse imaging of aNSCs from HVZ of Control + LiPR treated mouse. (**K**) Quantification of the number of cell divisions per division tree. (**L**) Time-lapse quantification of active (dividing) clones per 20.000 plated cells. (**M**) Number of all active clones of HVZ aNSCs from Control or LiPR-treated mice exposed to Control or HFD. Active clones pooled from all observed time-lapse imaging regions of interests per given treatment group. (**N**) Proportion of active clones containing at least one apoptotic cell. (**O**) Cell cycle length from the time-lapse imaging in the 2nd observed cell division. Data information: Scale bar: 20 µm. In all panels, $n = 3$ mice per data set. In panel **E**, number of neurospheres: $n = 26$ (Control), 22 (Control+LiPR). In panel **F**, number of neurospheres: $n = 66$ (Control), 15 (Control+LiPR). For panel **K**,**L**, number of traced cells: $n = 25$ per data set. In panel **O**, number of traced cells: $n = 47$ (Control), 6 (Control+LiPR), 35 (HFD), 12 (HFD+LiPR). Fisher's exact test (**M**,**N**), Un-paired two-tailed T-Test (**E-H**,**K**,**L**,**O**) and Two-Way ANOVA with Bonferroni's test (**A**,**B**,**I**). $^{*}p < 0.05$, $^{***}p < 0.001$. Data are presented as mean ± SEM.

Appendix Figure EV3. LiPrRP reduces proliferation of naïve neurospheres.

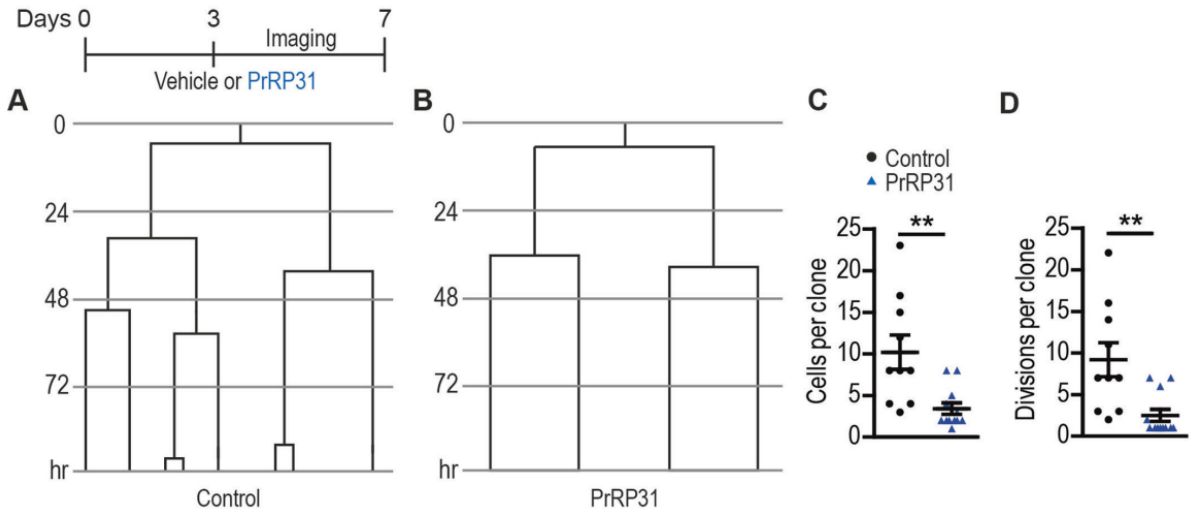

Figure EV4. LiPR reduces proliferation of naïve htNSCs.

(**A**,**B**) Example cell division trees from 4-day time-lapse imaging of aNSCs from HVZ of Control (**A**) and hPrRP31-treated (**B**) cells. A schematic of the experimental protocol shown above. (**C**,**D**) Quantification of cells per clone (**C**) and divisions per clone (**D**). Data information: In all panels, $n = 3$ mice per data set. In panels **C**,**D**, number of traced clones: $n = 10$ (Control), 12 (Control+LiPR). Un-paired two-tailed T-Test. $^{**}p < 0.01$. Data are presented as mean ± SEM.

Appendix Figure EV4. LiPrRP reduces proliferation of naïve htNSCs.

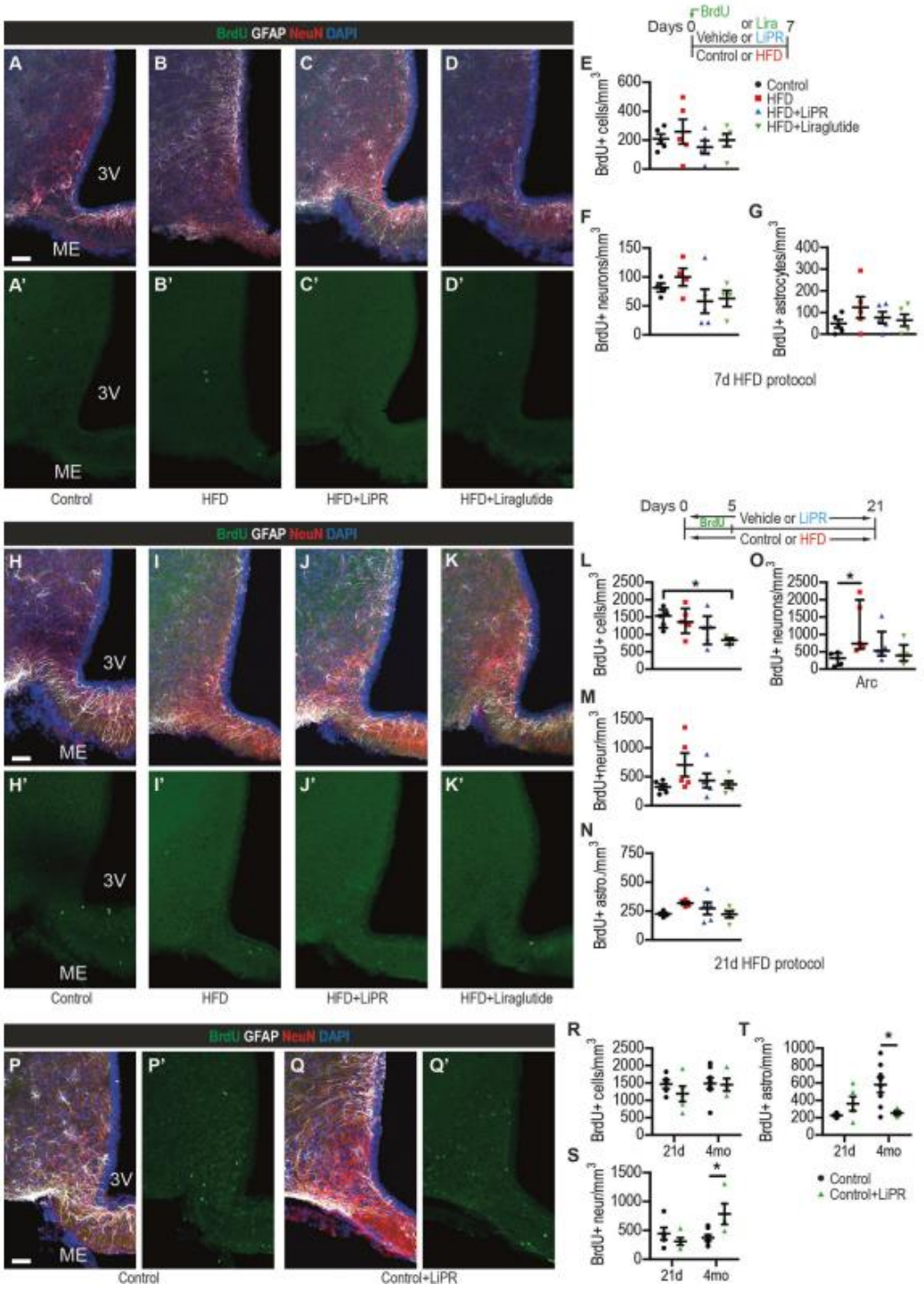

Figure EV5. Effects of LiPR on new adult-generated cells in shorter HFD protocols and in the context of Control Diet.

(**A–D**, **H–K**) Representative confocal images of HVZ and MBH stained as indicated in Control (**A**,**H**,**P**), HFD (**B**,**I**), HFD + LiPR (**C**,**J**), HFD + Liraglutide (Lira) (**D**,**K**) and Control Diet + LiPR (**Q**) of 7d (**A–D**), 21d (**H–K**) and 4mo (**P**,**Q**) groups. (**E–G**) Quantification of BrdU+ cells (**E**), BrdU+ neurons (**F**) and BrdU+ astrocytes (**G**) in the MBH of 7d HFD group. (**L–N**) Quantification of BrdU+ cells (**L**), BrdU+ neurons (**M**) and BrdU+ astrocytes (**N**) in the MBH parenchyma and BrdU+ neurons in the Arc (**O**) of 21d HFD group. (**R–T**) Quantification of BrdU+ cells (**R**), BrdU+ neurons (**S**) and BrdU+ astrocytes (**T**) in MBH parenchyma of Control and Control Diet + LiPR treated mice of 21d and 4mo groups. Data information: Scale bars: 50 µm. $n = 5$ mice per data set (7d, 21d), $n = 8$ mice (Control 4mo), $n = 4$ mice (Control + LiPR 4mo) per data set. In panel **O**, Kruskal–Wallis test with Dunn's test ($H = 9.88$, $p = 0.02$). In panels **E**-G and **L**-N, One-Way ANOVA with Tukey's test (**L**: $F(3,19) = 3.58$, $p = 0.038$) or Bonferroni's test (**N**: $F(3,19) = 4.3$, $p = 0.021$). In panels **R**-**T**, Two-Way ANOVA with Bonferroni's test (**S**: treatment $F(1,18) = 5.71$, $p = 0.021$; duration $F(1,18) = 9.9$, $p = 0.0056$; interaction $F(1,18) = 6.43$, $p = 0.02$; **T**: treatment $F(1,17) = 1.32$, $p = 0.27$; duration $F(1,17) = 2.2$, $p = 0.15$; interaction $F(1,17) = 7.75$, $p = 0.013$). $^*p < 0.05$, $^{***}p < 0.001$. Data are presented as median ± SEM (**O**) or mean ± SEM (all other).

Appendix Figure EV5. Effects of LiPrRP on new adult-generated cells in shorter HFD protocols and in the context of Control diet.

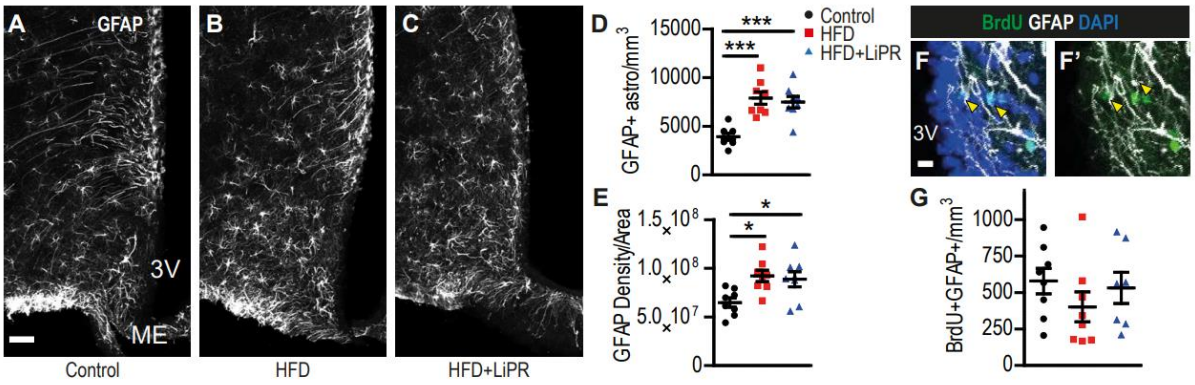

Appendix Figure S1 – LiPR does not affect astrogliogenesis in the MBH
(A-C) Representative confocal images of HVZ stained for GFAP in Control (A), HFD (B) nd HFD + LiPR (C) of 4mo HFD group.
(D-E) Quantification of GFAP+ astrocytes (D) and GFAP density (E) in MBH parenchyma of 4mo HFD group.
(F) Representative confocal image of BrdU+ astrocytes in MBH parenchyma.
(G) Quantification of BrdU+ astrocytes in MBH parenchyma.
Scale bars: 50 µm (A-C), 20 µm (F). n = 8.
Data information: One-Way ANOVA (panel D: $F(2,21) = 16.22$, $p < 0.0001$; panel E: $F(2,21) = 5.67$, $p = 0.011$).
*$p < 0.05$, ***$p < 0.001$ (Bonferroni's test). Data are presented as mean ± SEM.

Appendix Figure S1 – LiPrRP does not affect astrogliogenesis in the MBH.

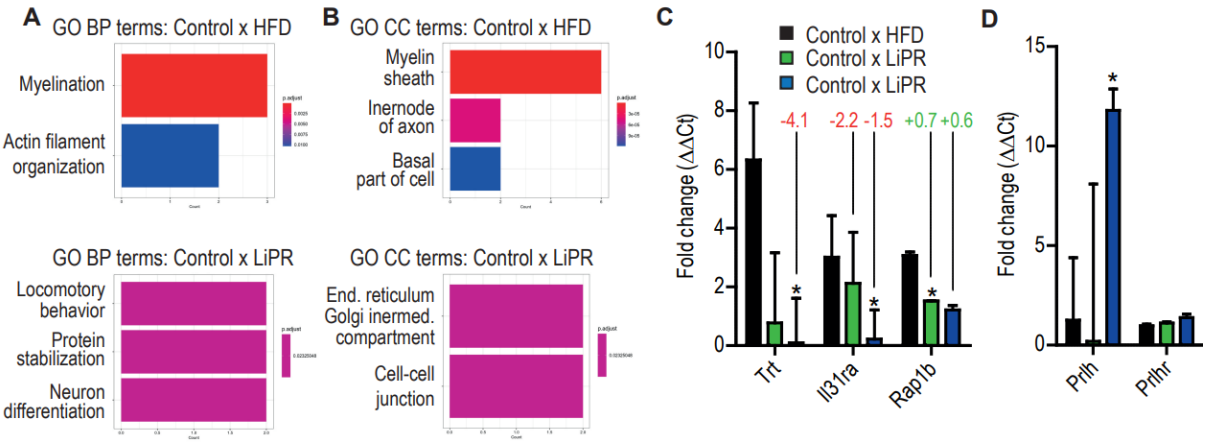

Appendix Figure S2 – Additional RNAseq data and confirmation of RNAseq by RT-qPCR
(A) Bulk MBH RNAseq GO terms for Biological Processes (BP) for Control Diet vs HFD (top graph) and Control Diet vs Control Diet+LiPR (bottom graph).
(B) Bulk MBH RNAseq GO terms for Cell Compartments (CC).
(C) Relative mRNA fold change of Trt, Il31ra and Rap1b compared to Gapdh in cDNA used for the bulk RNAseq of the MBH. Numbers above the bar graphs represent expression change values for a given gene from the RNAseq data.
(D) Relative mRNA fold change of Prlh and Prlhr compared to Gapdh in cDNA used for the bulk RNAseq of the MBH. Data information: un-paired two-tailed T-Test, *$p < 0.05$. Data are presented as mean ± SEM.

Appendix Figure S2 – Additional RNAseq data and confirmation of RNAseq by RT-qPCR

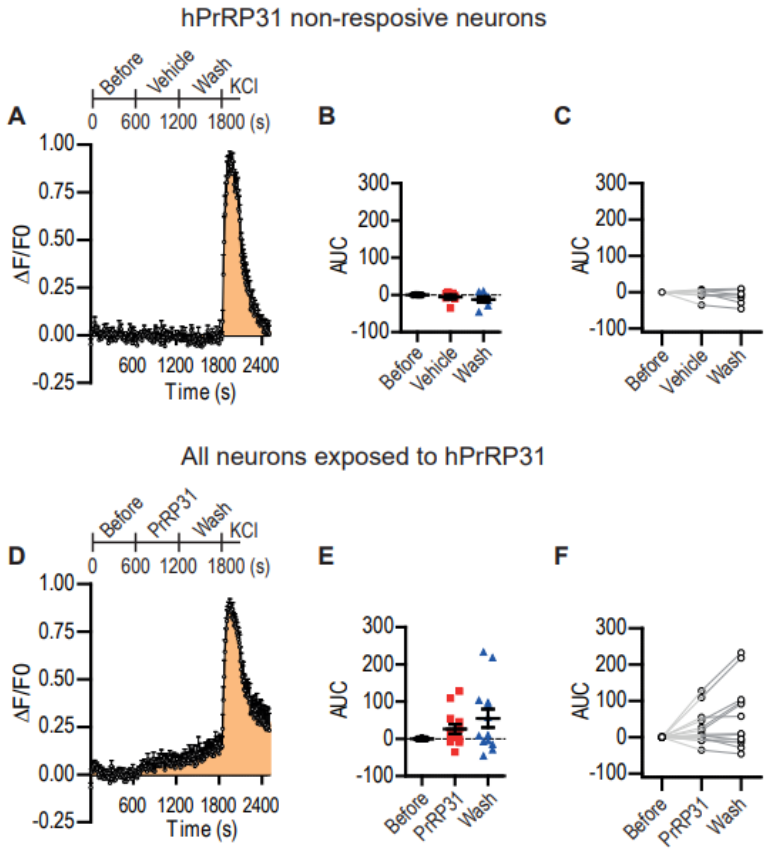

Appendix Figure S3 – Additional data from calcium imaging of hiPSC-derived hypothalamic neurons
(A,D) A graph of the relative fluorescence change (ΔF/F0) of Rhod-3 as a function of time before and during hPrRP31 application in medium, wash-out and KCl positive control in hiPSC-derived neurons non-responsive to hPrRP31 (A) and all neurons exposed to hPrRP31.
(B,E) A summary of fluorescence before (0-600 s), during hPrRP31 (600-1200 s) or wash-out (1200-1800 s) in Area Under Curve (AUC) for hPrRP31 non-responsive (B) and all neurons exposed to hPrRP31 (E).
(C,F) Individual neurons from calcium imaging in the before-after plot from the non-responsive (C) and all exposed neurons (F).
n = 7 for non-responsive, n =13 all neurons. Data are presented as mean ± SEM.

Appendix Figure S3 – Additional data from calcium imaging of hiPSC – derived hypothalamic neurons

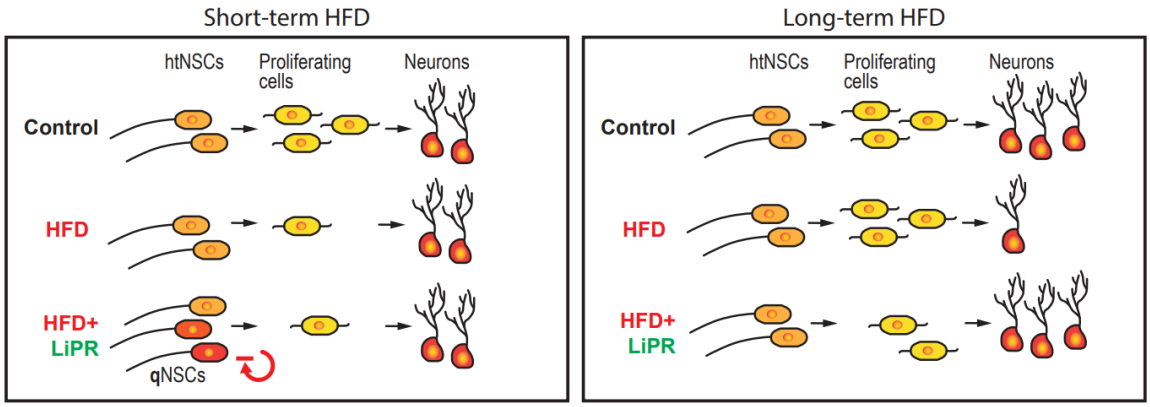

Appendix Figure S4 – A schematic of LiPR effects on hypothalamic adult neurogenesis
(Left) LiPR decreases proliferation and activation of htNSCs during short and intermediate HFD protocols. (Right) LiPR increases survival of new hypothalamic neurons during long-term HFD and obesity.

Appendix Figure S4 – A schematic of LiPrRP effects on hypothalamic adult neurogenesis

Appendix 2

Other work by the author of this thesis, also referenced in this work, has been published:

Singular Adult Neural Stem Cells Do Not Exist

Petrik, D., Jörgensen, S., Eftychidis, V., & Siebzehnrübl, F A. (2022, February 18). Singular Adult Neural Stem Cells Do Not Exist. Multidisciplinary Digital Publishing Institute, 11(4), 722-722. https://doi.org/10.3390/cells11040722